NOVEL IMMUNOTHERAPIES TO TREAT GASTROINTESTINAL SOLID TUMOR CANCERS

EDITED BY: Vita Golubovskaya and Sripathi Sureban
PUBLISHED IN: Frontiers in Oncology

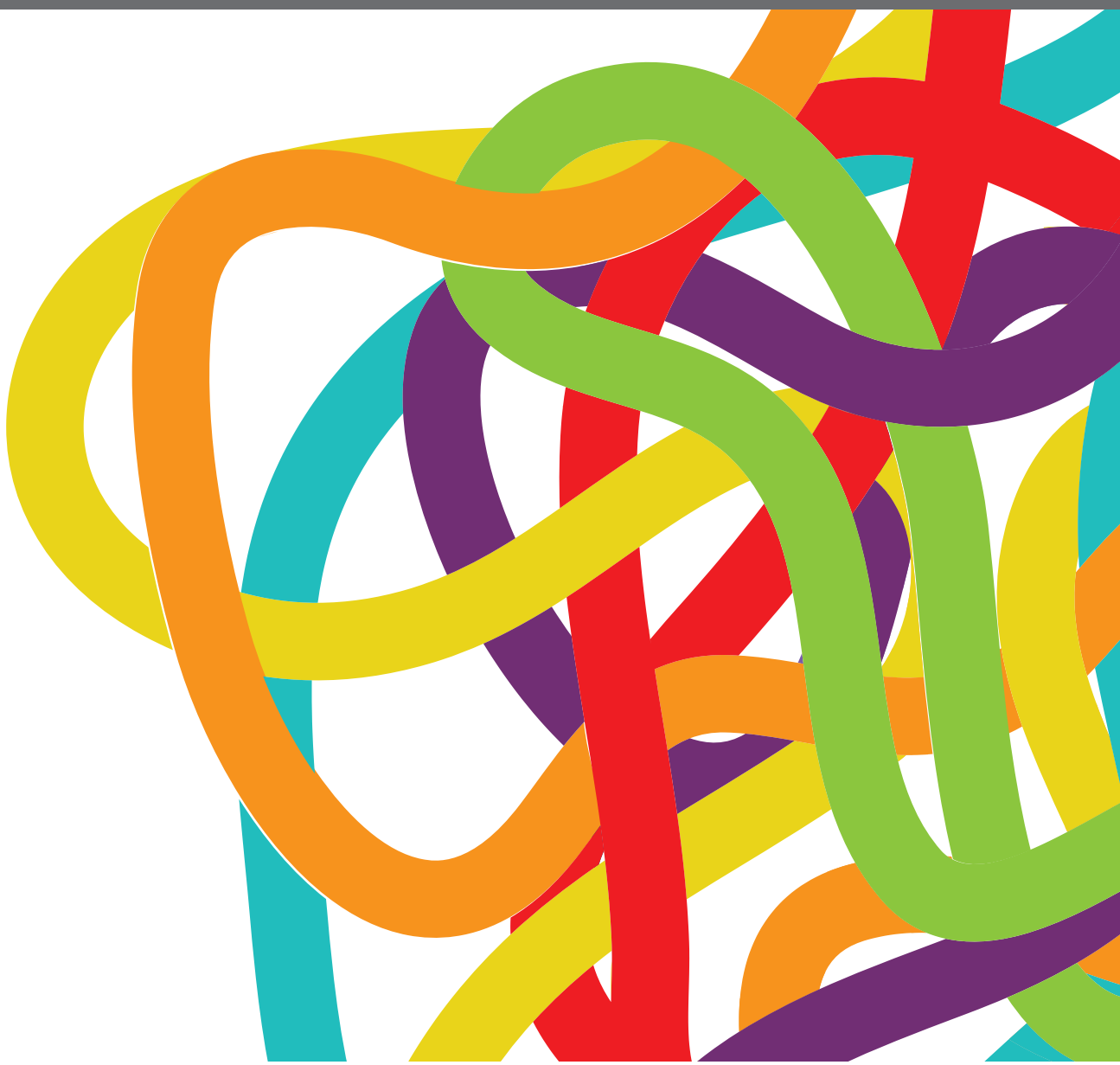

frontiers Research Topics

frontiers

ISSN 1664-8714
ISBN 978-2-83250-730-8
DOI 10.3389/978-2-83250-730-8

About Frontiers

Frontiers is more than just an open-access publisher of scholarly articles: it is a pioneering approach to the world of academia, radically improving the way scholarly research is managed. The grand vision of Frontiers is a world where all people have an equal opportunity to seek, share and generate knowledge. Frontiers provides immediate and permanent online open access to all its publications, but this alone is not enough to realize our grand goals.

Frontiers Journal Series

The Frontiers Journal Series is a multi-tier and interdisciplinary set of open-access, online journals, promising a paradigm shift from the current review, selection and dissemination processes in academic publishing. All Frontiers journals are driven by researchers for researchers; therefore, they constitute a service to the scholarly community. At the same time, the Frontiers Journal Series operates on a revolutionary invention, the tiered publishing system, initially addressing specific communities of scholars, and gradually climbing up to broader public understanding, thus serving the interests of the lay society, too.

Dedication to Quality

Each Frontiers article is a landmark of the highest quality, thanks to genuinely collaborative interactions between authors and review editors, who include some of the world's best academicians. Research must be certified by peers before entering a stream of knowledge that may eventually reach the public - and shape society; therefore, Frontiers only applies the most rigorous and unbiased reviews.
Frontiers revolutionizes research publishing by freely delivering the most outstanding research, evaluated with no bias from both the academic and social point of view. By applying the most advanced information technologies, Frontiers is catapulting scholarly publishing into a new generation.

What are Frontiers Research Topics?

Frontiers Research Topics are very popular trademarks of the Frontiers Journals Series: they are collections of at least ten articles, all centered on a particular subject. With their unique mix of varied contributions from Original Research to Review Articles, Frontiers Research Topics unify the most influential researchers, the latest key findings and historical advances in a hot research area! Find out more on how to host your own Frontiers Research Topic or contribute to one as an author by contacting the Frontiers Editorial Office: frontiersin.org/about/contact

NOVEL IMMUNOTHERAPIES TO TREAT GASTROINTESTINAL SOLID TUMOR CANCERS

Topic Editors:
Vita Golubovskaya, ProMab Biotechnologies, United States
Sripathi Sureban, University of Oklahoma Health Sciences Center, United States

Citation: Golubovskaya, V., Sureban, S., eds. (2022). Novel Immunotherapies to Treat Gastrointestinal Solid Tumor Cancers. Lausanne: Frontiers Media SA.
doi: 10.3389/978-2-83250-730-8

Table of Contents

frontiers | Frontiers in Oncology

TYPE Editorial
PUBLISHED 24 October 2022
DOI 10.3389/fonc.2022.1043615

OPEN ACCESS

EDITED AND REVIEWED BY
Dunfa Peng,
University of Miami, United States

*CORRESPONDENCE
Sripathi M. Sureban
sripathi.sureban@gmail.com

SPECIALTY SECTION
This article was submitted to Gastrointestinal Cancers: Gastric and Esophageal Cancers, a section of the journal Frontiers in Oncology

RECEIVED 13 September 2022
ACCEPTED 10 October 2022
PUBLISHED 24 October 2022

CITATION
Sureban SM and Golubovskaya V (2022) Editorial: Novel immunotherapies to treat gastrointestinal solid tumor cancers. *Front. Oncol.* 12:1043615. doi: 10.3389/fonc.2022.1043615

Editorial: Novel immunotherapies to treat gastrointestinal solid tumor cancers

Sripathi M. Sureban[1]* and Vita Golubovskaya[2]

[1]Department of Internal Medicine, The University of Oklahoma Health Sciences, Oklahoma City, OK, United States, [2]Promab Biotechnologies, Richmond, CA, United States

KEYWORDS

gastrointestinal cancer (GI cancer), immunotherapies and vaccines, clinical trials, PD-1 - PD-L1 axis, solid tumors

Editorial on the Research Topic
Novel immunotherapies to treat gastrointestinal solid tumor cancers

Gastrointestinal (GI) solid tumor cancers include cancers of the colorectal, liver, pancreas, gastric, and esophagus. There is an unmet medical need to treat GI cancers as they are the leading cause of cancer-related deaths worldwide (1). Traditional therapies include chemo and radiotherapy, and targeted therapies that do not eliminate GI cancers (2). Novel immunotherapies that target checkpoint inhibitors and reactivation of the host's anti-tumor immunity to target and treat cancers have been gaining importance (3). Immunotherapies to treat GI cancers are an emerging field of research and are of utmost importance (1, 3). These data taken together provide the strongest rationale to initiate and complete a special issue entitled: Novel Immunotherapies to Treat Gastrointestinal Solid Tumor Cancers

The special issue was focused on identifying novel immunotherapies that are effective against GI cancers. Immunotherapies to treat GI cancers present challenges due to resistance to immune checkpoints and hostile tumor microenvironments. We aimed to provide a spotlight on research involving research-related immunotherapies to treat GI tumors. This special issue includes 12 articles on this topic.

Original non-clinical research studies

This Research Topic within the Frontiers in Oncology journal has an accumulation of various interesting original research articles. Some of them are so unique that they provide a strong focus on novel and interesting topics.

Wang et al., have focused on a novel approach of conjugating PD-L1 polypeptide (PPA1) with Doxorubicin (DOX) that alleviated resistance to chemotherapy thereby enhancing an anti-colon cancer immune response. This study for the first time provided a dual-functional

conjugate of PD-L1 peptide and DOX for cancer cell-targeted drug delivery and inhibition of PD-1 and PD-L1 immune checkpoint and DOX-induced cancer cell death with reduced toxicity. The novelty of this study seems the demonstration of a combined anti-cancer immune response and reduced drug resistance following the treatment with PPA1-DOX.

Wang et al., provided novel evidence that loss of hyaluronan and proteoglycan link protein-1 (HAPLN1), a component of the tumor microenvironment within the extracellular matrix, induces tumorigenesis in colorectal cancers (CRC). Earlier studies have suggested that HAPLN1 plays an important role in cancer tumor stem/progenitor cells under the control of the Wnt signaling pathway (4). In this article, the authors found that expression HAPLN1 was downregulated in CRC tissues when compared with the normal adjacent tissues. HAPLN1 expression was downregulated following TGF-b stimulation and overexpression of HAPLN1 resulted in reduced tumor growth and cancer cell migration *via* inhibition of collagen alpha-1 protein. Their findings suggest that HAPLN1 controls the TGF-β signaling pathway and collagen deposition *via* the TGF-β signaling pathway. This mediates E-adhesion to control tumor growth. The outcome of this study indicates that treatments involving the induction of HAPLN1 levels may represent a novel approach to treating CRC. (Wang et al.) This is study provides novel and compelling evidence of the role of HAPLN1 that is against the current norm. It is unique as the emerging new roles can play a vital role in devising strategies targeting HAPLN1. Also, this study demonstrates that HAPLN1 regulates collagen which is known to regulate immune cell motility (5) providing novel avenues to further investigate the effect of overexpression of HAPLN1 on immune modulation in CRC.

Another important study within this special issue is an efficacy study by Smith et al., where they have demonstrated that the gastrin vaccine treatment alone and with an immune checkpoint antibody inhibits gastric cancer growth and metastases. They have used an immunocompetent syngeneic mouse model of gastric cancer to demonstrate the efficacy of the gastrin vaccine (polyclonal antibody stimulator – PAS) with or without PD-1 antibody. Tumor growth and metastases were significantly inhibited following treatment either with PDS alone or in combination with PD-1 antibody and increased tumor CD8+ T-lymphocytes and decreased immunosuppressive M2-polarized tumor-associated macrophages *via* a gastrin-CCK-BR (cholecystokinin-B receptor) signaling pathway. This compelling study is further validation of the use of the gastrin vaccine as a treatment strategy against gastric cancer.

Original clinical and retrospect studies

Pan et al., has provided a comprehensive study demonstrating derived neutrophil-lymphocyte ratio (dNLR) with platelet-lymphocyte ratio (PLR) as a potential composite biomarker to identify or correlate the outcomes following the treatment of advanced gastric cancer patient with anti-PD-1 antibodies. Based on the retrospective data from 238 patients with advanced gastric cancer and a significant correlation between the dNLR and PLR, they concluded that their study demonstrates that the combination of dNLR and PLR is a composite biomarker and an independent prognostic factor to evaluate the survival of gastric cancer patients treated with anti-PD-1. They also conclude that the patients with intermediate/poor dNLR/PLR may not benefit from anti-PD-1 treatments. Furthermore, these outcomes need to be further investigated in a larger study. These findings taken together provide novel insights into the predictive efficacy and potentially personalizing immunotherapy for advanced gastric cancer patients. This study provides novel insights into the use of dNLR/PLR as a predictive biomarker to evaluate the efficacy of anti-PD-1 or perhaps other immune therapies.

Cho et al., provided strong clinical evidence of the cost-effectiveness way to treat hepatocellular carcinoma (HCC) with adjuvant immunotherapy using cytokine-induced killer cells.They built a partitioned survival model comparing the expected costs, life-year, and quality of life-year of a hypothetical population of 10,000 patients between cytokine-induced killer (CIK) cell treatments and controls (no adjuvant therapy groups). They concluded that, based on their extensive analysis, HCC patients treated with adjuvant CIK cell was more cost-effective than controls.A further extensive evaluation of other types of immunotherapy needs to be compared to validate this comprehensive study.

In another retrospective study by Sun et al., evidence of the safety and efficacy of treatments with Fruquintinib and PD-1 inhibitors (FP) versus Regorafenib and PD-1 inhibitors (RP) in metastatic colorectal cancer (mCRC). According to their study, the disease control rate and progression-free survival (PFS) were better in the FP group, however, the overall response rate was better in the RP group. Benefits from the FP treatment were observed in patients with no liver metastasis, KRAS wild type, and left colon tumor. Finally, they conclude that their study indicates that better PFS time of patients with mCRC was observed following FP when compared with RP treatments. Though the PFS is merely 2.5 months more than the RP, this study provides insight into the possible treatment strategies that can be considered for patients with no liver metastasis and KRAS wildtype and further validation of this study should be conducted with increasing the number of patients and from various geographical locations.

A meta-analysis by Gu et al., showcased the safety and efficacy of immune checkpoint inhibitors in advanced esophageal squamous cell carcinoma (ESCC). Seven clinical trials with 1733 patients were included in this analysis. The authors conclude that treatment schedules with immune checkpoint inhibitors as second and beyond second-line therapy can improve response and overall survival of esophageal adenocarcinoma patients with locally advanced or metastatic disease. Although, the authors make a summary that not all oncological outcomes for patients can be improved. This

correlative study is a pilot study and provides novel insights into the benefits of certain immunotherapies for treating ESCC.

Nie et al. demonstrated the clinical effect of Sintilimab in patients with advanced gastric cancer. The authors concluded that Sintilimab monotherapy or combination therapy had a median PFS of 2.5 months and provides a feasible therapeutic strategy for gastric cancer patients. The study provided the basis for future development therapy of Sintilimab for gastric cancer. This is a good retrospective study that evaluated the clinical efficacy and potential avenue to use Sintilimab in combination with other immunotherapies.

Zhou et al. showed the safety and efficacy of Camrelizumab along with XELOX with bevacizumab or regorafenib in patients with mCRC. This study is based on the study populations with microsatellite-stable mCRC. This is a pilot study and further evaluation with a larger patient population from a diverse geographical location is warranted.

Zhang et al. demonstrated an analysis of the cost-effectiveness of treatments between Cambrelizumab vs placebo added to chemotherapy as primary/first-line therapy in patients with metastatic ESCC. This analysis suggests that the addition of Camrelizumab to chemotherapy is not cost-effective in patients with advanced ESCC in China.

Hong et al. showed data on neoadjuvant immunotherapy combined with chemotherapy followed by surgery versus surgery alone for advanced esophageal squamous carcinoma patients. The authors conclude that this therapy is safe and effective. Further validation of this study is needed with multicentered prospective trials.

Review article

The review of Huang et al., summarizes data on neoadjuvant therapy for locally advanced esophageal cancers. The authors describe research combining immunotherapy with adjuvant therapy and conclude that for the best synergistic effect future research should be focused on the sequence of immunotherapy and radio(chemo)therapy and biomarkers. This is a very good review article showcasing the development of neoadjuvant therapy for locally advanced esophageal cancers and unsolved clinical problems.

Conclusions

We tried to provide a comprehensive and diverse type of original research articles in the field of immunotherapies to treat gastrointestinal cancers. This issue provides the current trend of ongoing animal-based research and cost-effective clinical studies and provides novel insights into the potential personalized immunotherapies. The combination of these articles also provides the best strategies for overcoming challenges in treating cold and metastatic GI cancers. Some of the studies also provide novel pathways and future directions in successfully planning to treat GI cancers.

Author contributions

All authors listed have made a substantial, direct, and intellectual contribution to the work and approved it for publication.

Conflict of interest

SS has ownership interests in COARE Biotechnology Inc., and is an inventor on multiple patents.

The remaining author declares that the research was conducted in the absence of any commercial or financial relationships that could be construed as a potential conflict of interest.

Publisher's note

References

1. Arnold M, Abnet CC, Neale RE, Vignat J, Giovannucci EL, McGlynn KA, et al. Global burden of 5 major types of gastrointestinal cancer. *Gastroenterology* (2020) 159:335–349.e15. doi: 10.1053/j.gastro.2020.02.068

2. Smyth EC, Moehler M. Late-line treatment in metastatic gastric cancer: Today and tomorrow. *Ther Adv Med Oncol* (2019) 11:1758835919867522. doi: 10.1177/1758835919867522

3. Wang DK, Zuo Q, He QY, Li B. Targeted immunotherapies in gastrointestinal cancer: From molecular mechanisms to implications. *Front Immunol* (2021) 12:705999. doi: 10.3389/fimmu.2021.705999

4. Mebarki S, Desert R, Sulpice L, Sicard M, Desille M, Canal F, et al. *De novo* HAPLN1 expression hallmarks wnt-induced stem cell and fibrogenic networks leading to aggressive human hepatocellular carcinomas. *Oncotarget* (2016) 7:39026–43. doi: doi.org/10.18632/oncotarget.9346

5. Kaur A, Ecker BL, Douglass SM, Kugel CH 3rd, Webster MR, Almeida FV, et al. Remodeling of the collagen matrix in aging skin promotes melanoma metastasis and affects immune cell motility. *Cancer Discov* (2019) 9:64–81. doi: 10.1158/2159-8290.CD-18-0193

frontiers in Oncology

ORIGINAL RESEARCH
published: 22 September 2021
doi: 10.3389/fonc.2021.741865

Clinical Study of Sintilimab as Second-Line or Above Therapy in Patients With Advanced or Metastatic Gastric Cancer: A Retrospective Study

Caiyun Nie[1,2], *Huifang Lv*[1,2], *Yingjun Liu*[3], *Beibei Chen*[1,2], *Weifeng Xu*[1,2], *Jianzheng Wang*[1,2] *and Xiaobing Chen*[1,2*]

[1] Department of Medical Oncology, Affiliated Cancer Hospital of Zhengzhou University, Henan Cancer Hospital, Zhengzhou, China, [2] State Key Laboratory of Esophageal Cancer Prevention & Treatment, Zhengzhou University, Zhengzhou, China, [3] Department of General Surgery, Affiliated Cancer Hospital of Zhengzhou University, Henan Cancer Hospital, Zhengzhou, China

OPEN ACCESS

Edited by:
Sripathi Sureban, University of Oklahoma Health Sciences Center, United States

Reviewed by:
Wafaa M. Rashed, Children's Cancer Hospital, Egypt
Christian Cotsoglou, Ospedale di Vimercate - ASST Brianza, Italy

***Correspondence:**
Xiaobing Chen
zlyychenxb0807@zzu.edu.cn

Specialty section:
This article was submitted to Gastrointestinal Cancers: Gastric Esophageal Cancers, a section of the journal Frontiers in Oncology

Received: *15 July 2021*
Accepted: *03 September 2021*
Published: *22 September 2021*

Citation:
Nie C, Lv H, Liu Y, Chen B, Xu W, Wang J and Chen X (2021) Clinical Study of Sintilimab as Second-Line or Above Therapy in Patients With Advanced or Metastatic Gastric Cancer: A Retrospective Study. Front. Oncol. 11:741865. doi: 10.3389/fonc.2021.741865

Background: The present study was conducted to analyze the clinical efficacy and safety of sintilimab as second-line or above therapy for patients with advanced or metastatic gastric cancer.

Methods: Patients with advanced or metastatic gastric cancer that progressed after prior systemic therapies and treated with sintilimab from March 2019 to July 2020 were retrospectively analyzed in this study. The primary end point was progression-free survival (PFS). Secondary end points included objective response rate (ORR), disease control rate (DCR), overall survival (OS), and safety.

Results: Fifty-two patients with advanced or metastatic gastric cancer received sintilimab monotherapy or combination therapy after they failed from prior systemic therapies. Eight patients achieved partial response (PR), 26 patients had stable disease (SD), and 18 patients had progressive disease (PD). The ORR and DCR were 15.4% (8/52) and 65.4% (34/52), respectively. Median PFS was 2.5 months (95% CI = 2.0–3.0), and median OS was 5.8 months (95% CI = 4.9–6.7). The ORR and DCR were 30.0% (6/20) and 80.0% (16/20), respectively, in intestinal subtype, which were superior than in non-intestinal subtype (ORR: 6.3%, DCR: 56.3%). Patients with intestinal subtype obtained longer PFS (4.0 *vs.* 1.9) and OS (9.0 *vs.* 4.1) than those with non-intestinal subtype. The incidence of grade 3–4 adverse events was 44.2%.

Conclusions: Sintilimab monotherapy or combination therapy provides a feasible therapeutic strategy for patients with advanced or metastatic gastric cancer who failed from prior systemic therapies. The efficacy of sintilimab in intestinal subtype was superior than that in non-intestinal subtype.

Keywords: gastric/gastroesophageal junction adenocarcinoma, sintilimab, immunotherapy, efficacy, Lauren classification

INTRODUCTION

Most cases of gastric cancer are advanced at diagnosis, the prognosis is extremely poor, and there is a lack of effective treatment. For some strictly selected cases, local treatment, including surgical resection and hyperthermic intraperitoneal chemotherapy, may be able to improve the prognosis of patients (1, 2). Medical treatment, including chemotherapy and targeted therapy, is currently the main treatment for advanced or metastatic gastric cancer. However, the efficacy of chemotherapy drugs seems to have reached a plateau, and the progress of traditional targeted therapy drugs is relatively slow (3, 4). As an emerging treatment method, immunotherapy is the current research hotspot, and it is hoped that it can further improve the curative effect of advanced gastric cancer (5). Based on the ATTRACTION-02 and KEYNOTE-059 studies, nivolumab and pembrolizumab have been approved in advanced gastric cancer in Japan and the United States as third-line treatment, respectively (6, 7).

Sintilimab is a fully human IgG4 monoclonal antibody that acts on PD-1 and its ligands. It is the second approved Chinese PD-1 inhibitor in China (8). In 2018, sintilimab received indications for relapsed/refractory Hodgkin's lymphoma in China. Clinical trials on other tumor types are also underway, including lymphoma (9), non-small cell lung cancer (10), liver cancer (11), esophageal cancer (12), and gastric cancer (13). Compared with other PD-1 inhibitors, sintilimab has similar anti-tumor effects, better safety, and economic advantages. A phase IB study evaluating sintilimab combined with XELOX as first-line treatment for HER-2 negative gastric and gastroesophageal junction (GEJ) adenocarcinoma showed that the objective response rate (ORR) of sintilimab treatment was 85%, and the disease control rate (DCR) was 100% (13).

Although many advances have been made in immunotherapy of gastric cancer, there are still many problems. Arranging the troops, optimizing the treatment strategy, and better targeting the patients who will benefit from immunotherapy based on biomarkers have become an urgent clinical goal (14). Gastric cancer is highly heterogeneous. In the classical Lauren classification, gastric cancer can be divided into intestinal, diffuse, and mixed types. Previous studies have shown that immunotherapy is not effective in diffuse gastric cancer (6, 15). The present study was performed to evaluate the efficacy and safety of sintilimab for patients with advanced or metastatic gastric cancer as second-line or above therapy.

METHODS

Patient Population

From March 2019 to July 2020, patients with advanced or metastatic gastric cancer who failed from prior systemic therapies at Henan Cancer Hospital were retrospectively analyzed. Eligibility criteria were as follows: 1) patients with gastric cancer that progressed after first-line chemotherapy and treated with sintilimab as second-line or above therapy; 2) Eastern Cooperative Oncology Group (ECOG) performance status 0/1; 3) measurable disease per Response Evaluation Criteria in Solid Tumors version 1.1 (RECIST v1.1), at least one lesion can be measured by imaging examination, and the lesion measured by spiral CT or MRI is ≥10 mm; and 4) adequate organ function.

Study Treatment

Sintilimab was administered *via* intravenous infusion at a dose of 200 mg once every 3 weeks until disease progression, unacceptable toxicity, or death. In this study, sintilimab monotherapy and combination therapy were the two regimens. In the combination therapy regimen, sintilimab was given with concurrent chemotherapy or targeted therapy, including apatinib, trastuzumab, or nab-paclitaxel.

Efficacy and Safety Assessments

The primary end point was progression-free survival (PFS). Secondary end points included ORR, DCR, overall survival (OS), and safety. After treatment, all patients underwent imaging examination every two cycles to evaluate the clinical efficacy. The efficacy evaluation criteria are RECIST version 1.1 response evaluation criteria in solid tumors, including complete response (CR), partial response (PR), stable disease (SD), and progressive disease (PD). The ORR was CR + PR, and the DCR was CR+ PR and SD. Adverse events (AEs) were assessed according to the Common Terminology Criteria for Adverse Events, version 4.0.

Statistical Analysis

Survival curves were estimated using the Kaplan–Meier method and compared by log-rank test. PFS was defined as the period from the time of treatment with sintilimab to disease progression or patient death due to any cause. OS was defined as the period from the time of treatment with sintilimab to patient death from any cause or last follow-up. ORR and DCR with 95% CI were calculated using the exact method based on binomial distribution. Safety and efficacy were analyzed in all patients who received ≥1 dose of study treatment. Safety was analyzed using descriptive statistics. All the statistical and descriptive analyses were conducted using SPSS software version 17.0 (SPSS, Chicago, IL). $p < 0.05$ was considered significant.

RESULTS

Patient and Treatment Characteristics

A total of 52 patients with advanced or metastatic gastric cancer who progressed after first-line treatment were retrospectively analyzed. **Table 1** summarizes patient and treatment characteristics. The median age was 64 years (range 30–80), with 17 female patients and 35 male patients. Twenty-three patients had advanced gastric cancer, and the other 29 patients had GEJ adenocarcinoma. All the patients were diagnosed as advanced or recurrent; the metastatic sites included the intra-abdominal lymph node (65.4%), liver (42.3%), peritoneum (28.8%), and lung (25%). In this study, 19 patients (36.5%) received sintilimab as second-line treatment and the other

TABLE 1 | Patient and treatment characteristics.

Characteristic	Total (n = 52) n (%)	Monotherapy (n = 8) n (%)	Combination therapy (n = 44) n (%)
Age (years, median)	64 (30–80)	67.5 (62–75)	61 (30–80)
Gender			
Female	17 (32.7%)	4 (50%)	13 (29.5%)
Male	35 (67.3%)	4 (50%)	31 (70.5%)
ECOG			
0–1	40 (76.9%)	5 (62.5%)	35 (79.5%)
2	12 (23.1%)	3 (37.5%)	9 (20.5%)
Primary tumor site			
Gastric	23 (44.2%)	0 (0%)	23 (52.3%)
GEJ	29 (55.8%)	8 (100%)	21 (47.7%)
Histopathology			
Intestinal	20 (38.5%)	1 (12.5%)	19 (43.2%)
Diffuse	22 (42.3%)	6 (75%)	16 (36.4%)
Mixed	10 (19.2%)	1 (12.5%)	9 (20.4%)
MSI			
dMMR	1 (1.9%)	0 (0%)	1 (2.3%)
MSS	51 (98.1%)	8 (100%)	43 (97.7%)
Metastatic site			
Lymph node	34 (65.4%)	5 (62.5%)	29 (65.9%)
Peritoneum	15 (28.8%)	3 (37.5%)	12 (27.3%)
Liver	22 (42.3%)	3 (37.5%)	19 (43.2%)
Lung	13 (25%)	4 (50%)	9 (20.5%)
Others	9 (17.3%)	0 (%)	9 (20.5%)
Number of metastatic sites			
1–2	41 (78.8%)	6 (75%)	35 (79.5%)
≥3	11 (21.2%)	2 (25%)	9 (20.5%)
Treatment line			
2	19 (36.5%)	2 (25%)	17 (38.6%)
3–5	33 (63.5%)	6 (75%)	27 (61.4%)

ECOG, Eastern Cooperative Oncology Group performance status; GEJ, gastroesophageal junction tumors; MSI, microsatellite instability; dMMR, deficient mismatch repair; MSS, microsatellite stability.

33 patients (63.5%) as third or above treatment. Eight patients received sintilimab as monotherapy, and 44 patients received sintilimab combination therapy. In the 44 patients who received sintilimab combination therapy, 24 patients received sintilimab combined with apatinib, and the other 20 patients received sintilimab combined with nab-paclitaxel or irinotecan. In the early days, due to the limitation of testing reagents, PD-L1 was not a routine test item in the pathology department of our center. Among the 52 patients in this study, there were 21 patients with PD-L1 expression results, of which seven were PD-L1 positive and 14 were PD-L1 negative.

Efficacy

In the general population, CR was not observed, eight patients achieved PR, 26 patients had SD, and 18 patients had PD. The ORR and DCR were 15.4% (8/52) and 65.4% (34/52), respectively. In the intestinal subtype population, six patients achieved PR, 10 patients had SD, and four patients had PD; the ORR and DCR were 30.0% (6/20) and 80.0% (16/20), respectively. In the non-intestinal subtype population, two patients achieved PR, 16 patients had SD, and 14 patients had PD; the ORR and DCR were 6.3% (2/32) and 56.3% (18/32), respectively. In the PD-L1-positive population, four patients achieved PR, three patients had SD, and no patients had PD; the ORR and DCR were 57.1% (4/7) and 100% (7/7), respectively. In the PD-L1-negative population, one patient achieved PR, eight patients had SD, and five patients had PD; the ORR and DCR were 7.1% (1/14) and 64.3% (9/14), respectively. In the sintilimab monotherapy population, one patient achieved PR, three patients had SD, and four patients had PD; the ORR and DCR were 12.5% (1/8) and 50.0% (4/8), respectively. In the combination therapy population, seven patients achieved PR, 23 patients had SD, and 14 patients had PD; the ORR and DCR were 15.9% (7/44) and 68.2% (30/44), respectively (**Table 2**).

Median PFS and OS were 2.5 months (95% CI = 2.0–3.0) (**Figure 1A**) and 5.8 (95% CI = 4.9–6.7) months (**Figure 1B**), respectively. The median PFS in patients who received mono- and combo-regimens was 1.5 (95% CI = 0.3–2.7) and 2.9 (95% CI = 2.3–3.5) months, respectively ($p = 0.088$) (**Figure 2A**); and OS was 4.0 (95% CI = 0–8.7) and 6.0 (95% CI = 5.0–7.0) months, respectively ($p = 0.133$) (**Figure 2B**). Twenty-four patients who received sintilimab combined with apatinib obtained 2.4 (95% CI = 1.7–3.1) months' PFS and 6.0 (95% CI = 2.1–9.9) months' OS. Twenty patients who received sintilimab combined with nab-paclitaxel or irinotecan obtained 2.9 (95% CI = 1.9–3.9) months' PFS and 5.8 (95% CI = 4.7–6.9) months' OS (for PFS, $p = 0.818$; for OS, $p = 0.883$) (**Figures 2C, D**). For Lauren classification, the median PFS in intestinal and non-intestinal subtypes was 4.0 (95% CI = 3.1–4.8) months and 1.9 (95% CI = 1.2–2.6) months, respectively ($p = 0.000$) (**Figure 3A**). The median OS in intestinal and non-intestinal subtypes was 9.0 (95% CI = 6.7–11.3) months and 4.1 (95% CI = 2.7–5.4) months, respectively ($p = 0.000$) (**Figure 3B**). The median PFS in PD-L1-positive and

TABLE 2 | Efficacy of sintilimab in patients with advanced or metastatic gastric cancer.

Parameter	Best response				ORR	DCR	Median PFS (95% CI)	Median OS (95% CI)
	CR	PR	SD	PD				
Total	0	8	26	18	15.4% (8/52)	65.4% (34/52)	2.5 (2.0–3.0)	5.8 (4.9–6.7)
Lauren classification								
Intestinal	0	6	10	4	30.0% (6/20)	80.0% (16/20)	4.0 (3.1–4.8)	9.0 (6.7–11.3)
Non-intestinal	0	2	16	14	6.3% (2/32)	56.3% (18/32)	1.9 (1.2–2.6)	4.1 (2.7–5.4)
Treatment programs								
Monotherapy	0	1	3	4	12.5% (1/8)	50.0% (4/8)	1.5 (0.3–2.7)	4.0 (0–8.7)
Combination	0	7	23	14	15.9% (7/44)	68.2% (30/44)	2.9 (2.3–3.5)	6.0 (5.0–7.0)
PD-L1								
Positive	0	4	3	0	57.1% (4/7)	100.0% (7/7)	5.0 (4.0–6.0)	12.1 (6.4–17.8)
Negative	0	1	8	5	7.1% (1/14)	64.3% (9/14)	2.0 (1.1–2.9)	4.1 (2.0–6.2)
Combination type								
Apatinib	0	3	13	8	12.5% (3/24)	66.7% (16/24)	2.4 (1.7–3.1)	6.0 (2.1–9.9)
Chemotherapy	0	4	10	6	20.0% (4/20)	70.0% (14/20)	2.9 (1.9–3.9)	5.8 (4.7–6.9)

CR, complete response; PR, partial response; SD, stable disease; PD, progressive disease; ORR, overall response rate; DCR, disease control rate; PFS, progression-free survival; OS, overall survival.

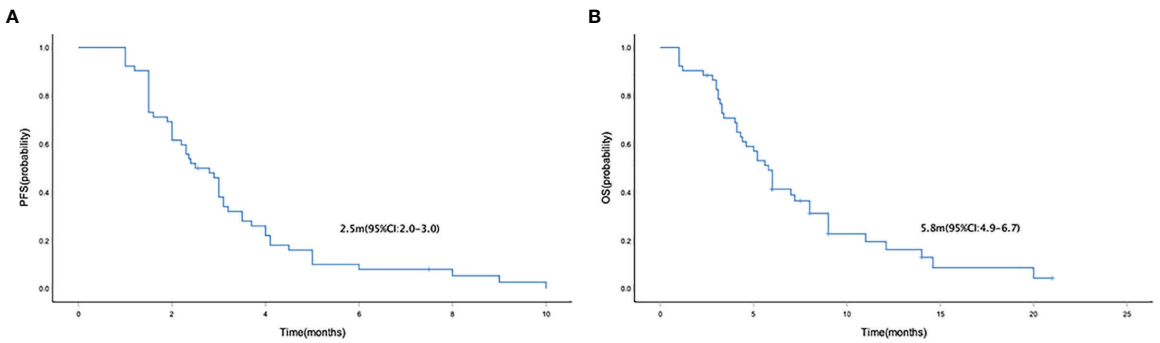

FIGURE 1 | Kaplan–Meier curve of PFS **(A)** and OS **(B)** in the general population. PFS, progression-free survival; OS, overall survival.

PD-L1-negative patients was 5.0 (95% CI = 4.0–6.0) months and 2.0 (95% CI = 1.1–2.9) months, respectively (p = 0.000) (**Figure 3C**). The median OS in PD-L1-positive and PD-L1-negative patients was 12.1 (95% CI = 6.4–17.8) months and 4.1 (95% CI = 2.0–6.2) months, respectively (p = 0.027) (**Figure 3D**).

Safety

In terms of safety, all of the 52 patients reported at least one treatment-related AE (TRAE). In general, sintilimab treatment was well tolerated, and only two patients discontinued treatment due to intolerable toxicity. Most of the AEs were grade 1–2 (**Table 3**). Grade 3–4 adverse reactions occurred in 23 (44.2%) patients. No unexpected side effects or treatment-related death were observed. The most common sintilimab-related AEs were hematological toxicity, including anemia (n = 32, 61.5%), decreased neutrophil count (n = 42, 80.8%), decreased platelet (n = 31, 59.6%), and decreased white blood count (n = 41, 78.9%). Other common sintilimab-related AEs were pyrexia (n = 15, 28.8%), increased aspartate aminotransferase and alanine aminotransferase (n = 16, 30.8%), hypothyroidism (n = 12, 23.1%), rash (n = 18, 34.6%), and pneumonitis (n = 7, 13.5%). Grade 3–4 AE rash occurred in two patients. Apatinib-related AEs were secondary hypertension (n = 11, 21.2%), hand and foot syndrome (n = 8, 15.4%), and proteinuria (n = 6, 11.5%).

DISCUSSION

In the present study, the results from this retrospective study demonstrated favorable anti-tumor activity and manageable safety of sintilimab as second-line or above therapy for advanced or metastatic gastric cancer.

Immune checkpoint inhibitors have been approved in gastric cancer worldwide as a third-line treatment option. The results of the ATTRACTION-02 study in the Asian population showed that nivolumab treatment significantly reduced the risk of death of advanced or metastatic gastric cancer patients (6). The 1-year OS rates reached 26.2%. The National Medical Products Administration has approved the use of nivolumab in the treatment of patients with advanced or metastatic gastric cancer or GEJ adenocarcinoma who failed from two or more systemic treatment regimens. In the KEYNOTE-059 study, pembrolizumab was confirmed to be effective in the treatment

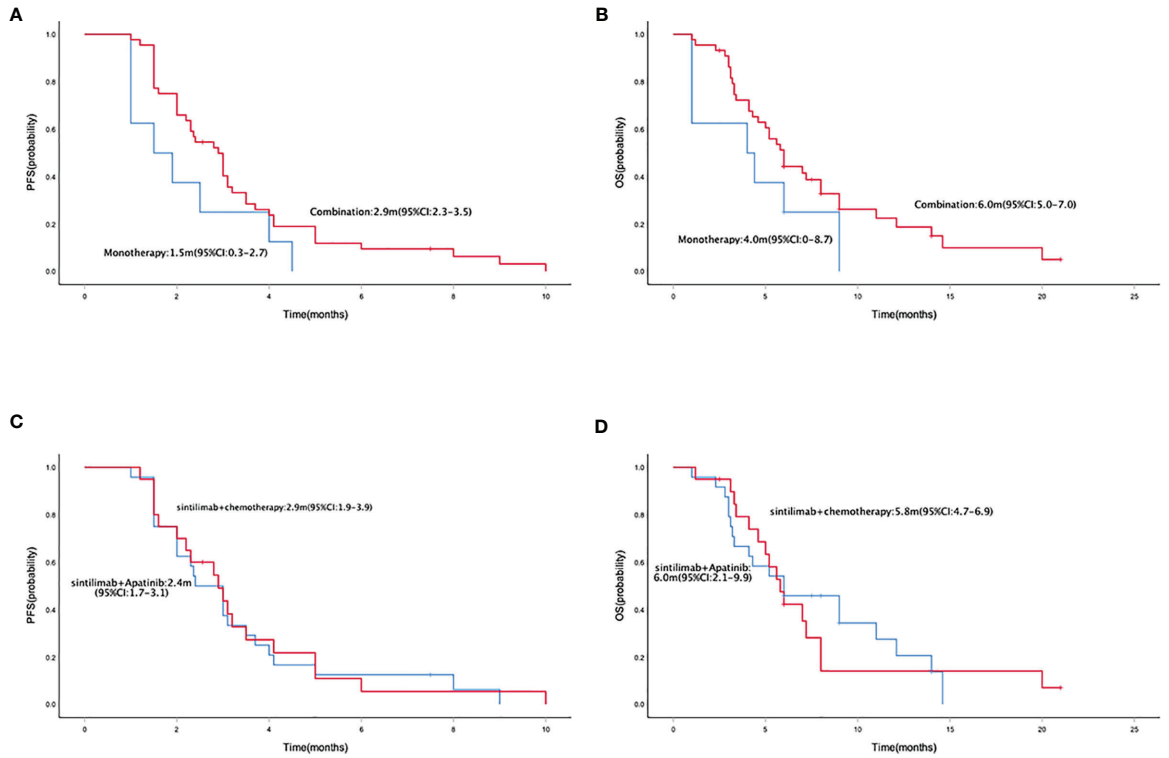

FIGURE 2 | Kaplan–Meier curve of PFS **(A)** and OS **(B)** in sintilimab monotherapy and combination therapy population. Kaplan–Meier curve of PFS **(C)** and OS **(D)** in sintilimab combination therapy population. PFS, progression-free survival; OS, overall survival.

of advanced or metastatic gastric cancer (7). But unfortunately, in the subsequent clinical trials where immunotherapy was moved to the second line before the treatment of advanced gastric cancer, the results of KEYNOTE-061 brought confusion to clinicians (15). The role of immune checkpoint inhibitors in the second-line treatment of advanced gastric cancer has not been established. However, data on second-line immunotherapy for gastric cancer are also accumulating. In this study, 19 patients (36.5%) received sintilimab as second-line treatment and the other 33 patients (63.5%) as third or above treatment. Whether in second-line or third to fifth-line treatment, sintilimab demonstrated encouraging results. The results of this present study substantiate evidence for gastric cancer immunotherapy, especially in the second-line immunotherapy of gastric cancer.

The optimal drug treatment model of immunotherapy for gastric cancer is still inconclusive. In this study, eight patients received sintilimab monotherapy, and another 44 patients received sintilimab combination therapy. In terms of efficacy, the ORR and DCR of the combined treatment group were higher than those of the monotherapy group, and the PFS and OS were also superior. For drug safety, sintilimab monotherapy had a lower incidence of TRAEs and superior tolerability. Most patients with gastric cancer cannot tolerate chemotherapy for a long time because of disease progression. For patients with poor ECOG scores, immunotherapy like sintilimab monotherapy could an optional strategy in terms of safety profile.

In this study, 24 patients received sintilimab combined with apatinib, and the other 20 patients received sintilimab combined with nab-paclitaxel or irinotecan. In terms of efficacy, no significant difference was found. Currently, clinical trials are exploring the combination manner of immunotherapy. In addition to the traditional immunotherapy combined with chemotherapy, immunotherapy combined with targeted therapy has been proved to be an effective combination mode. HER-2 and VEGF are two vital targets (16, 17). Trastuzumab combined with pembrolizumab has achieved good results in patients with HER2-positive second-line and above treatment of gastric cancer. In this study, sintilimab combined with apatinib achieved significant efficacy. Studies had shown that antiangiogenic drugs can change the tumor immune microenvironment and enhance the efficacy of immunotherapy, which has become a new therapeutic strategy (18–20).

There are still no effective biomarkers to predict the efficacy of immunotherapy for gastric cancer. Some studies suggest that PD-L1 expression level, tumor mutational burden (TMB), Epstein–Barr virus (EBV) positive, and POLE gene mutation may be potential biomarkers to predict the efficacy of immunotherapy, but it has not been proved to be specific and effective enough, which is still controversial (21). At present, deficient mismatch repair/microsatellite instability-high (dMMR/MSI-H) is the only effective marker for anti-PD-1 treatment (22, 23). However, in gastric cancer, MSI-H accounted for only 20%, and 80% of gastric cancer patients had microsatellite stability (MSS) (24). In this study, only one

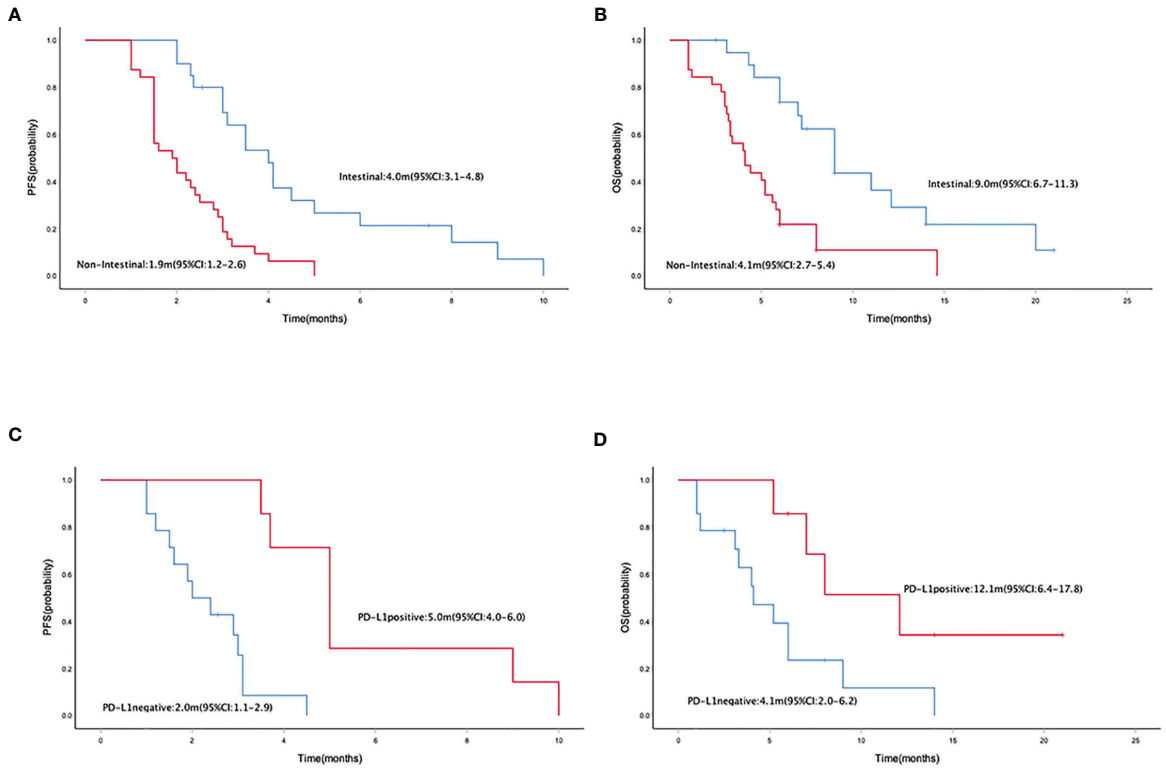

FIGURE 3 | Kaplan–Meier curve of PFS **(A)** and OS **(B)** in intestinal and non-intestinal subtype populations. Kaplan–Meier curve of PFS **(C)** and OS **(D)** in PD-L1-positive and PD-L1-negative populations. PFS, progression-free survival; OS, overall survival.

TABLE 3 | Treatment-related adverse events (TRAEs).

Adverse event	All grade n (%)	≥Grade 3 n (%)
Any event	52 (100.0)	23 (44.2)
AE led to any treatment discontinuation	4 (7.7)	3 (5.8)
AE led to death	0 (0.0)	0 (0.0)
Event occurring in ≥10% patients		
Pyrexia	15 (28.8)	0 (0.0)
Anemia	32 (61.5)	4 (7.7)
Decreased neutrophil count	42 (80.8)	8 (15.4)
Decreased platelet	31 (59.6)	12 (23.1)
Decreased white blood count	41 (78.9)	6 (11.5)
Fatigue	20 (38.5)	0 (0.0)
Nausea	15 (28.8)	0 (0.0)
Vomiting	8 (15.4)	0 (0.0)
Increased aspartate aminotransferase	16 (30.8)	0 (0.0)
Increased alanine aminotransferase	16 (30.8)	0 (0.0)
Proteinuria	6 (11.5)	0 (0.0)
Hypothyroidism	12 (23.1)	0 (0.0)
Hand and foot syndrome	8 (15.4)	2 (3.8)
Rash	18 (34.6)	2 (3.8)
Pneumonitis	7 (13.5)	0 (0.0)
Sensory neurotoxicity	10 (19.2)	1 (1.9)
Diarrhea	7 (13.5)	0 (0.0)
Secondary hypertension	11 (21.2)	3 (5.8)

AE, adverse event.

patient was diagnosed as dMMR, and the others were MSS. In the 21 patients with PD-L1 expression results, PD-L1-positive patients exhibited better anti-tumor immune response and longer PFS and OS. Since only some patients have PD-L1 results, the predictive value of PD-L1 in the immunotherapy of sintilimab for gastric cancer still needs to be further explored.

Previous studies suggested that the expression level of PD-L1 in diffuse gastric cancer may be lower than that in intestinal type. ONO-4538 study and KEYNOTE-061 study demonstrated that immunotherapy with nivolumab or pembrolizumab was not effective in diffuse gastric cancer. Our present study showed the ORR and DCR in the intestinal subtype population were significantly higher than in the non-intestinal subtype population; meanwhile, the intestinal subtype gastric cancer population has achieved better prognosis. The relationship between the efficacy of sintilimab immunotherapy and Lauren classification has not been reported. Our research suggests that the Lauren classification may affect the effect of sintilimab immunotherapy.

For safety, sintilimab treatment was well tolerated, and only two patients discontinued treatment due to intolerable toxicity. The most common sintilimab-related AEs were consistent with previous studies (25, 26). Among all levels of AEs, hematological toxicity is most common, including decreased neutrophil count, decreased white blood count, decreased platelet, and anemia. Rash was one of the most frequent grade 3 or 4 AEs. Other ≥grade 3 AEs were hand and foot syndrome, sensory neurotoxicity, and secondary hypertension, which were similar to previous data of chemotherapy and apatinib treatment.

A retrospective study obtained from a single center with not sufficiently large patient cases is the limitation of our study. Thus, we should design and conduct large randomized and prospective trials to confirm the clinical value of sintilimab monotherapy or combination therapy in advanced or metastatic gastric cancer.

CONCLUSION

Sintilimab monotherapy or combination therapy provides a feasible therapeutic strategy in patients with advanced or metastatic gastric cancer who progressed after prior systemic therapies, and a median PFS of 2.5 months was obtained with well-tolerated toxicity. The efficacy of sintilimab in intestinal subtype was superior than in non-intestinal subtype.

DATA AVAILABILITY STATEMENT

The raw data supporting the conclusions of this article will be made available by the authors, without undue reservation.

ETHICS STATEMENT

The studies involving human participants were reviewed and approved by the ethics committee of the Affiliated Cancer Hospital of Zhengzhou University. The patients/participants provided their written informed consent to participate in this study.

AUTHOR CONTRIBUTIONS

CN and XC designed the research, analyzed the data, and drafted the paper. CN, HL, YL, BC, and WX were mainly responsible for data collection and analysis. CN, XC, and JW were primarily responsible for statistical analysis. CN, HL, and XC contributed to the study design and revised the manuscript. All authors contributed to the article and approved the submitted version.

FUNDING

This work was supported by the National Natural Science Foundation of China (No. 81472714), Medical Science and Technique Foundation of Henan Province (No. 212102310623) and 1000 Talents Program of Central plains (No. 204200510023).

REFERENCES

1. Granieri S, Altomare M, Bruno F, Paleino S, Bonomi A, Germini A, et al. Surgical Treatment of Gastric Cancer Liver Metastases: Systematic Review and Meta-Analysis of Long-Term Outcomes and Prognostic Factors. *Crit Rev Oncol Hematol* (2021) 163:103313. doi: 10.1016/j.critrevonc.2021.103313
2. Granieri S, Bonomi A, Frassini S, Chierici AP, Bruno F, Paleino S, et al. Prognostic Impact of Cytoreductive Surgery (CRS) With Hyperthermic Intraperitoneal Chemotherapy (HIPEC) in Gastric Cancer Patients: A Meta-Analysis of Randomized Controlled Trials. *Eur J Surg Oncol* (2021) S0748-7983(21)00492-3. doi: 10.1016/j.ejso.2021.05.016
3. Pellino A, Riello E, Nappo F, Brignola S, Murgioni S, Djaballah SA, et al. Targeted Therapies in Metastatic Gastric Cancer: Current Knowledge and Future Perspectives. *World J Gastroenterol* (2019) 25(38):5773–88. doi: 10.3748/wjg.v25.i38.5773
4. Yamada Y. Present Status and Perspective of Chemotherapy for Patients With Unresectable Advanced or Metastatic Gastric Cancer in Japan. *Glob Health Med* (2020) 2(3):156–63. doi: 10.35772/ghm.2019.01025
5. Joshi SS, Badgwell BD. Current Treatment and Recent Progress in Gastric Cancer. *CA Cancer J Clin* (2021) 71(3):264–79. doi: 10.3322/caac.21657
6. Kang YK, Boku N, Satoh T, Ryu MH, Chao Y, Kato K, et al. Nivolumab in Patients With Advanced Gastric or Gastro-Oesophageal Junction Cancer Refractory to, or Intolerant of, at Least Two Previous Chemotherapy Regimens (ONO-4538-12, ATTRACTION-2): A Randomised, Double-Blind, Placebo-Controlled, Phase 3 Trial. *Lancet* (2017) 390(10111):2461–71. doi: 10.1016/S0140-6736(17)31827-5
7. Fuchs CS, Doi T, Jang RW, Muro K, Satoh T, Machado M, et al. Safety and Efficacy of Pembrolizumab Monotherapy in Patients With Previously Treated Advanced Gastric and Gastroesophageal Junction Cancer: Phase 2 Clinical KEYNOTE-059 Trial. *JAMA Oncol* (2018) 4(5):e180013. doi: 10.1001/jamaoncol.2018.0013
8. Hoy SM. Sintilimab: First Global Approval. *Drugs* (2019) 79(3):341–6. doi: 10.1007/s40265-019-1066-z
9. Shi Y, Su H, Song Y, Jiang W, Sun X, Qian W, et al. Safety and Activity of Sintilimab in Patients With Relapsed or Refractory Classical Hodgkin

Lymphoma (ORIENT-1): A Multicentre, Single-Arm, Phase 2 Trial. *Lancet Haematol* (2019) 6(1):e12–9. doi: 10.1016/S2352-3026(18)30192-3
10. Zhou C, Wu L, Fan Y, Wang Z, Liu L, Chen G, et al. Sintilimab Plus Platinum and Gemcitabine as First-Line Treatment for Advanced or Metastatic Squamous NSCLC: Results From a Randomized, Double-Blind, Phase 3 Trial (ORIENT-12). *J Thorac Oncol* (2021) 16(9):1501–11. doi: 10.1016/j.jtho.2021.04.011
11. Duan X, Zhang H, Zhou L, Jiang B, Mao X. Complete Response to the Combination of Sintilimab and IBI305 for a Patient With HBV-Associated Hepatocellular Carcinoma With Multiple Lung Metastasis. *Dig Liver Dis* (2020) 52(7):794–6. doi: 10.1016/j.dld.2020.04.005
12. Shah MA, Kojima T, Hochhauser D, Enzinger P, Raimbourg J, Hollebecque A, et al. Efficacy and Safety of Pembrolizumab for Heavily Pretreated Patients With Advanced, Metastatic Adenocarcinoma or Squamous Cell Carcinoma of the Esophagus: The Phase 2 KEYNOTE-180 Study. *JAMA Oncol* (2019) 5 (4):546–50. doi: 10.1001/jamaoncol.2018.5441
13. Jiang H, Zheng Y, Qian J, Mao C, Xu X, Li N, et al. Safety and Efficacy of Sintilimab Combined With Oxaliplatin/Capecitabine as First-Line Treatment in Patients With Locally Advanced or Metastatic Gastric/Gastroesophageal Junction Adenocarcinoma in a Phase Ib Clinical Trial. *BMC Cancer* (2020) 20 (1):760. doi: 10.1186/s12885-020-07251-z
14. Fumet JD, Truntzer C, Yarchoan M, Ghiringhelli F. Tumour Mutational Burden as a Biomarker for Immunotherapy: Current Data and Emerging Concepts. *Eur J Cancer* (2020) 131:40–50. doi: 10.1016/j.ejca.2020.02.038
15. Shitara K, Ozguroglu M, Bang YJ, Di Bartolomeo M, Mandala M, Ryu MH, et al. Pembrolizumab *Versus* Paclitaxel for Previously Treated, Advanced Gastric or Gastro-Oesophageal Junction Cancer (KEYNOTE-061): A Randomised, Open-Label, Controlled, Phase 3 Trial. *Lancet* (2018) 392 (10142):123–33. doi: 10.1016/S0140-6736(18)31257-1
16. Bang YJ, Van Cutsem E, Feyereislova A, Chung HC, Shen L, Sawaki A, et al. Trastuzumab in Combination With Chemotherapy *Versus* Chemotherapy Alone for Treatment of HER2-Positive Advanced Gastric or Gastro-Oesophageal Junction Cancer (ToGA): A Phase 3, Open-Label, Randomised Controlled Trial. *Lancet* (2010) 376(9742):687–97. doi: 10.1016/S0140-6736(10)61121-X
17. Mawalla B, Yuan X, Luo X, Chalya PL. Treatment Outcome of Anti-Angiogenesis Through VEGF-Pathway in the Management of Gastric Cancer: A Systematic Review of Phase II and III Clinical Trials. *BMC Res Notes* (2018) 11(1):21. doi: 10.1186/s13104-018-3137-8
18. Leong A, Kim M. The Angiopoietin-2 and TIE Pathway as a Therapeutic Target for Enhancing Antiangiogenic Therapy and Immunotherapy in Patients With Advanced Cancer. *Int J Mol Sci* (2020) 21(22):1–20. doi: 10.3390/ijms21228689
19. Zhou S, Zhang H. Synergies of Targeting Angiogenesis and Immune Checkpoints in Cancer: From Mechanism to Clinical Applications. *Anticancer Agents Med Chem* (2020) 20(7):768–76. doi: 10.2174/1871520620666200207091653
20. Zhu N, Weng S, Wang J, Chen J, Yu L, Fang X, et al. Preclinical Rationale and Clinical Efficacy of Antiangiogenic Therapy and Immune Checkpoint Blockade Combination Therapy in Urogenital Tumors. *J Cancer Res Clin Oncol* (2019) 145(12):3021–36. doi: 10.1007/s00432-019-03044-5
21. Zeng Z, Yang B, Liao Z. Biomarkers in Immunotherapy-Based Precision Treatments of Digestive System Tumors. *Front Oncol* (2021) 11:650481. doi: 10.3389/fonc.2021.650481
22. Cui G. The Mechanisms Leading to Distinct Responses to PD-1/PD-L1 Blockades in Colorectal Cancers With Different MSI Statuses. *Front Oncol* (2021) 11:573547. doi: 10.3389/fonc.2021.573547
23. Le DT, Durham JN, Smith KN, Wang H, Bartlett BR, Aulakh LK, et al. Mismatch Repair Deficiency Predicts Response of Solid Tumors to PD-1 Blockade. *Science* (2017) 357(6349):409–13. doi: 10.1126/science.aan6733
24. Dhakras P, Uboha N, Horner V, Reinig E, Matkowskyj KA. Gastrointestinal Cancers: Current Biomarkers in Esophageal and Gastric Adenocarcinoma. *Transl Gastroenterol Hepatol* (2020) 5:55. doi: 10.21037/tgh.2020.01.08
25. Zhang L, Mai W, Jiang W, Geng Q. Sintilimab: A Promising Anti-Tumor PD-1 Antibody. *Front Oncol* (2020) 10:594558. doi: 10.3389/fonc.2020.594558
26. Gao S, Li N, Gao S, Xue Q, Ying J, Wang S, et al. Neoadjuvant PD-1 Inhibitor (Sintilimab) in NSCLC. *J Thorac Oncol* (2020) 15(5):816–26. doi: 10.1016/j.jtho.2020.01.017

Conflict of Interest: The authors declare that the research was conducted in the absence of any commercial or financial relationships that could be construed as a potential conflict of interest.

frontiers in Oncology

ORIGINAL RESEARCH
published: 06 October 2021
doi: 10.3389/fonc.2021.754881

Efficacy and Safety of Fruquintinib Plus PD-1 Inhibitors Versus Regorafenib Plus PD-1 Inhibitors in Refractory Microsatellite Stable Metastatic Colorectal Cancer

Liying Sun[1,2], *Shenglan Huang*[1,2], *Dan Li*[1,2], *Ye Mao*[1,2], *Yurou Wang*[3] *and Jianbing Wu*[1,2]*

[1] Department of Digestive Oncology, The Second Affiliated Hospital of Nanchang University, Nanchang, China, [2] Jiangxi Key Laboratory of Clinical and Translational Cancer Research, Nanchang, China, [3] Department of Oncology, The First Affiliated Hospital of Nanchang University, Nanchang, China

OPEN ACCESS

Edited by:
Vita Golubovskaya,
ProMab Biotechnologies,
United States

Reviewed by:
Yoon Sun Choi,
Inje University Busan Paik Hospital,
South Korea
Zixu Yuan,
The Sixth Affiliated Hospital of
Sun Yat-sen University, China

***Correspondence:**
Jianbing Wu
hhgwjb@163.com

Specialty section:
This article was submitted to
Gastrointestinal Cancers:
Colorectal Cancer,
a section of the journal
Frontiers in Oncology

Received: 07 August 2021
Accepted: 14 September 2021
Published: 06 October 2021

Citation:
Sun L, Huang S, Li D, Mao Y, Wang Y and Wu J (2021) Efficacy and Safety of Fruquintinib Plus PD-1 Inhibitors Versus Regorafenib Plus PD-1 Inhibitors in Refractory Microsatellite Stable Metastatic Colorectal Cancer. Front. Oncol. 11:754881. doi: 10.3389/fonc.2021.754881

Background: Microsatellite stability (MSS) or mismatch repair proficient (pMMR) metastatic colorectal cancer (mCRC) is resistant to immune checkpoint inhibitors. Studies have shown that antiangiogenic drugs combined with programmed death receptor-1 (PD-1) inhibitors can improve immunosuppression. The purpose of this study was to compare the efficacy of fruquintinib combined with PD-1 inhibitor (FP) and regorafenib combined with PD-1 inhibitor (RP) in the treatment of advanced mCRC with MSS or pMMR.

Materials and Methods: We retrospectively collected advanced MSS or pMMR mCRC patient data from The Second Affiliated Hospital of Nanchang, China, from June 2019 to March 2021. Then, we analyzed and compared the efficacy and safety of FP and RP.

Results: A total of 51 patients who met the criteria were divided into FP (n = 28) and RP groups (n = 23). The overall response rate of the FP and RP groups was 7.1% and 8.7% and the disease control rate was 89.3% and 56.5%, respectively. The median progression-free survival (PFS) time was higher in the FP group than in the RP group (6.4 vs. 3.9 months, respectively; P = 0.0209). Patients with no liver metastasis, KRAS wild type, and left colon tumor may benefit from FP. Eight patients (15.7%) had grade 3 toxicity related to treatment. Cox multivariate regression analysis showed that the treatment method was an independent risk factor for median PFS time.

Conclusion: Our study indicates that FP could improve PFS time of patients with advanced mCRC compared with RP.

Keywords: colorectal cancer, immunotherapy, microsatellite stable, fruquintinib, regorafenib, PD-1

INTRODUCTION

Global colorectal cancer (CRC) ranks third in morbidity and second in mortality (1). For patients with advanced CRC who have failed to receive standard first-line and second-line treatment, the third-line treatment consists of regorafenib, fruquintinib, and TAS-102 (2), but the effects are not suitable (3). In recent years, the application of immune checkpoint inhibitor (ICI) has brought new hope for improving the therapeutic effect of metastatic CRC (mCRC) treatment (4–6).

As monoclonal antibodies (mAb) to programmed death receptor-1 (PD-1), pembrolizumab and nivolumab have shown considerable activity in advanced CRC patients with high microsatellite instability (MSI-H) or DNA mismatch repair defects (dMMR) tumors (7–9). However, MSI-H or dMMR mCRC patients account for only 5% of all CRC patients. Ninety-five percent of CRC patients with microsatellite stability (MSS) or mismatch repair proficient (pMMR) CRC do not respond to immunotherapy (10), which is a key clinical problem related to PD-1 inhibitors. Zelenay et al. found that immunotherapy combined with antivascular endothelial growth factor therapy can improve the immunosuppressive state in a CRC mouse model (11, 12). Clinical studies have shown that antiangiogenic drugs combined with immune checkpoint blocking can significantly improve the effectiveness of malignant tumor treatment (13–16). Therefore, ICI combined with antiangiogenesis therapy may overcome the resistance of MSS or pMMR mCRC to immunotherapy.

Fruquintinib is an effective and highly selective oral inhibitor of vascular endothelial growth factor receptor (VEGFR) 1, 2, 3 tyrosine kinase (17, 18). The FRESCO trial—a multicenter, randomized, double-blind, placebo-controlled phase III trial—compared fruquintinib with placebo in patients with mCRC who failed to receive standard chemotherapy (19). The results showed that the median overall survival (OS) and the median progression-free survival (PFS) of the patients receiving fruquintinib were 9.3 and 3.71 months, respectively, which were significantly longer than those of patients in the placebo control group. Clinical studies have shown that fruquintinib has the advantages of low off-target toxicity, good drug resistance, and strong curative effect. Regorafenib is a new type of multitarget tyrosine kinase inhibitor, which can inhibit the activation of VEGFR-1, VEGFR-2, VEGFR-3, FGFR, PDGFR, KIT, RET, TIE2, and BRAF (20). The results of CORRECT—an international, multicenter, phase III clinical study—showed that the median OS of the regorafenib group was 6.4 months, which was significantly longer than that of the placebo group (21). A subsequent CONCUR study conducted in Asia showed that regorafenib significantly prolonged the median OS to 8.8 months in patients with advanced CRC (22), thus indicating that regorafenib can improve the survival of patients with refractory mCRC. Fruquintinib and regorafenib are both third-line drugs for advanced CRC; indirect comparison by meta-analysis showed no significant difference in their efficacy and safety in advanced CRC (23–28).

In a phase Ib clinical study from Japan, the objective response rate (ORR) of regorafenib combined with nivolumab in patients with refractory mCRC was 36% and the median PFS was 7.9 months (29). The results of this early trial gave hope to patients and oncologists worldwide and provided additional options for patients with refractory mCRC. However, a retrospective study of 18 patients at the American Cancer Center failed to reveal comparable clinical activity of regorafenib plus nivolumab (30). In a retrospective clinical study of regorafenib combined with anti-PD-1 antibody in the treatment of MSS or pMMR mCRC patients in China, some potential benefits in disease control rate (DCR) and PFS were observed, albeit the results showed no objective effect (31). Therefore, additional evidence is needed to evaluate this joint strategy. Reportedly, a patient with advanced MSS CRC showed a rapid response after the failure of multiline therapy when fruquintinib was combined with anti-PD-1; then, the effect of fruquintinib combined with anti-PD-1 was verified in a CT26 cell (MSS) mouse co-gene model (32). Studies have shown that fruquintinib combined with PD-1 inhibitors can synergistically inhibit the progression of CRC, change the tumor microenvironment, and contribute to antitumor immune response. In a study conducted in China, the ORR and DCR of regorafenib or fruquintinib combined with camrelizumab in the treatment of MSS or pMMR mCRC patients were 25.0% and 62.5%, respectively, reflecting the good efficacy of regorafenib or fruquintinib plus camrelizumab in MSS or pMMR mCRC patients and thereby indicating the potential of ICI combined therapy (33).

There are no studies comparing the efficacy and safety of fruquintinib combined with PD-1 inhibitors against those of regorafenib and PD-1 inhibitors in the treatment of advanced CRC. Therefore, in this study, we retrospectively analyzed the treatment of refractory mCRC patients in the second affiliated Hospital of Nanchang University in China and compared the efficacy and safety of fruquintinib combined with PD-1 inhibitors against those of regorafenib combined with PD-1 inhibitors in the treatment of advanced CRC.

Abbreviations: PD-1, programmed death receptor-1; mCRC, metastatic colorectal cancer; MSS, microsatellite stability; pMMR, effective mismatch repair; FP, fruquintinib combined with PD-1 inhibitors; RP, regorafenib combined with PD-1 inhibitors; ICI, immune checkpoint inhibitor; ECOG PS, Eastern Cooperative Oncology Group performance status; mAb, monoclonal antibodies; dMMR, DNA mismatch repair defects; MSI-H, high microsatellite instability; CR, complete remission; PR, partial remission; SD, stable disease; PD, progression of disease; ORR, objective response rate; DCR, disease control rate; PFS, progression-free survival; OS, overall survival; CTC5.0, toxicity standard version 5.0; SE, standard deviation; HR, hazard ratio; CI, confidence interval; IQR, interquartile range; AE, adverse events; RCCEP, capillary endothelial hyperplasia; TAMs, tumor-associated macrophages; VEGF, vascular endothelial growth factor; EGFR, epidermal growth factor receptor.

PATIENTS AND METHODS

Patients

We conducted a retrospective study of patients with advanced MSS or pMMR CRC treated in the second affiliated Hospital of Nanchang University. The patients received fruquintinib or regorafenib combined with PD-1 inhibitors as third-line or

above posterior line therapy for a compassionate purpose. Formalin-fixed paraffin-embedded tissue specimens were used to detect the protein expression deletion of four kinds of MMR (MLH1/MSH2/MSH6/PMS2) by immunohistochemistry (IHC), or five tumor microsatellite sites [five single nucleotide sites (BAT25, BAT26, NR21, NR24, Mono27)] were analyzed by polymerase chain reaction (PCR) to determine the MMR/MSI status of the tumor. The main selection criteria included 1) advanced or mCRC that was histologically or cytologically confirmed to be at least refractory to second-line system treatment or could not tolerate standard treatment, 2) age 18–79 years (3), performance status of (ECOG PS) 0–2 in the Eastern Cancer Cooperation group, 4) adequate bone marrow reserve, 5) adequate liver and kidney function, and 6) at least one measurable lesion based on RECIST v1.1. The main exclusion criteria included 1) history of active, chronic, or recurrent autoimmune diseases and 2) severe complications. This study was conducted in accordance with the Helsinki Declaration and approved by the Ethics Review Committee of the Second Affiliated Hospital of Nanchang University.

Treatment Methods

Patients in the FP group took 3–5 mg oral fruquintinib, and patients in the RP group took 80–160 mg oral regorafenib once a day for 21 consecutive days in 28-day cycles. In order to control the side effects associated with treatment, some patients had adjusted dosages. Regarding immunotherapy, the patients were injected intravenously with PD-1 inhibitors at the recommended dose from the first day of taking molecular targeted drugs: toripalimab (240 mg) every 3 weeks, nivolumab (200 mg) every 2 weeks, and sintilimab or camrelizumab (200 mg) every 3 weeks.

Efficacy and Toxicities

The tumor was measured by computed tomography every 2–3 cycles of immunotherapy, and the tumor response was evaluated according to RECIST version 1.1 until the disease progressed or subsequent treatment began. Tumor remission was defined as complete remission (CR), partial remission (PR), stable disease (SD), or progression of disease (PD). ORR is defined as the best percentage of patients with total remission in either CR or PR. DCR was defined as the proportion of patients with the best overall response to CR, PR, or SD. PFS was calculated from the beginning of treatment to the time of disease progression or death from any cause. The toxicity assessment was based on the National Cancer Institute General Toxicity Standard version 5.0 (CTC5.0). The deadline for data was June 20, 2021.

Statistical Analysis

A Pearson chi-square test or Fisher exact test was used to compare the classification variables in the baseline features. The mean standard deviation (SE) was used to describe the variable distribution in the normal distribution, and the median and range were used to describe the variable distribution in the non-normal distribution. The Kaplan–Meier method was used for survival analysis, and the logarithmic rank test was used for the difference of survival curve. The Cox regression model was used to analyze the variables with P <0.05 in univariate analysis. The hazard ratio (HR) and confidence interval (CI) were calculated. P <0.05 was considered to be statistically significant. All data were analyzed using SPSS 26.0 software and GraphPad Prism 8.0.

RESULTS

Patient Characteristics

We included 653 patients who were diagnosed with mCRC from June 2019 to March 2021 at the Second Affiliated Hospital of Nanchang University. Among them, 268 mCRC patients were selected according to the inclusion criteria. Finally, 51 mCRC patients treated with fruquintinib or regorafenib combined with PD-1 inhibitors were enrolled in the present study (**Figure 1**). The deadline for data was June 20, 2021, with a median follow-up period of 6.2 months (IQR 3.9–8.43).

Table 1 shows the baseline characteristics of patients. Among them, 28 mCRC patients received FP, and the other 23 mCRC patients received RP. In this study, these patients were treated with FP or RP as the third line (56.9%) or more than third line (43.1%) of mCRC treatment. All patients experienced tumor progression after standard chemotherapy. Thirty-nine patients (76.5%) had left primary tumor, 12 patients (23.5%) had right primary tumor, and 38 patients (74.5%) had liver metastasis. As for primary tumor gene mutations, 14 patients had a RAS mutation, 1 patient had a BRAF mutation, and 18 patients had RAS/BRAF wild type. In the combined therapy, the initial doses of fruquintinib were 3 mg (20 patients), 4 mg (5 patients), and 5 mg (3 patients); as for regorafenib, 17 patients started with 80 mg, 5 patients started with 120 mg, and 1 patient started with 160 mg. The types of PD-1 inhibitors used were sintilimab, camrelizumab, toripalimab, and nivolumab. PD-1 inhibitors sintilimab (53.6%) and camrelizumab (46.4%) were used in the FP group, and camrelizumab (52.2%) was the most common PD-1 inhibitor in the RP group. In the FP group, the cycles of PD-1 inhibitors plus fruquintinib ranged from 3 to 8, with a median of 6. In the RP group, the cycles of PD-1 inhibitor plus regorafenib were 3 to 5, with a median of 4.

Clinical Efficacy

The treatment effect is summarized in **Table 2**. PR was the best response, and an objective response was observed in two patients in the FP group and two patients in the RP group. The SD of the FP group was significantly higher than that of the RP group (82.1% vs. 47.8%, P = 0.01). The ORR of the whole population was 7.8% (4/51), the ORR of the FP group was 7.1% (2/28), and the ORR of the RP group was 8.7% (2/23). The DCR of the FP group (89.3%) was higher than that of the RP group (56.5%), and the DCR of the whole population was 74.5%. The median PFS of the FP group was 6.4 months (HR = 0.445; 95% CI: 5.527–7.273), and that of RP group was 3.9 months (HR = 0.594; 95% CI: 2.736–5.064). The difference was statistically significant (P = 0.0209, **Figure 2**).

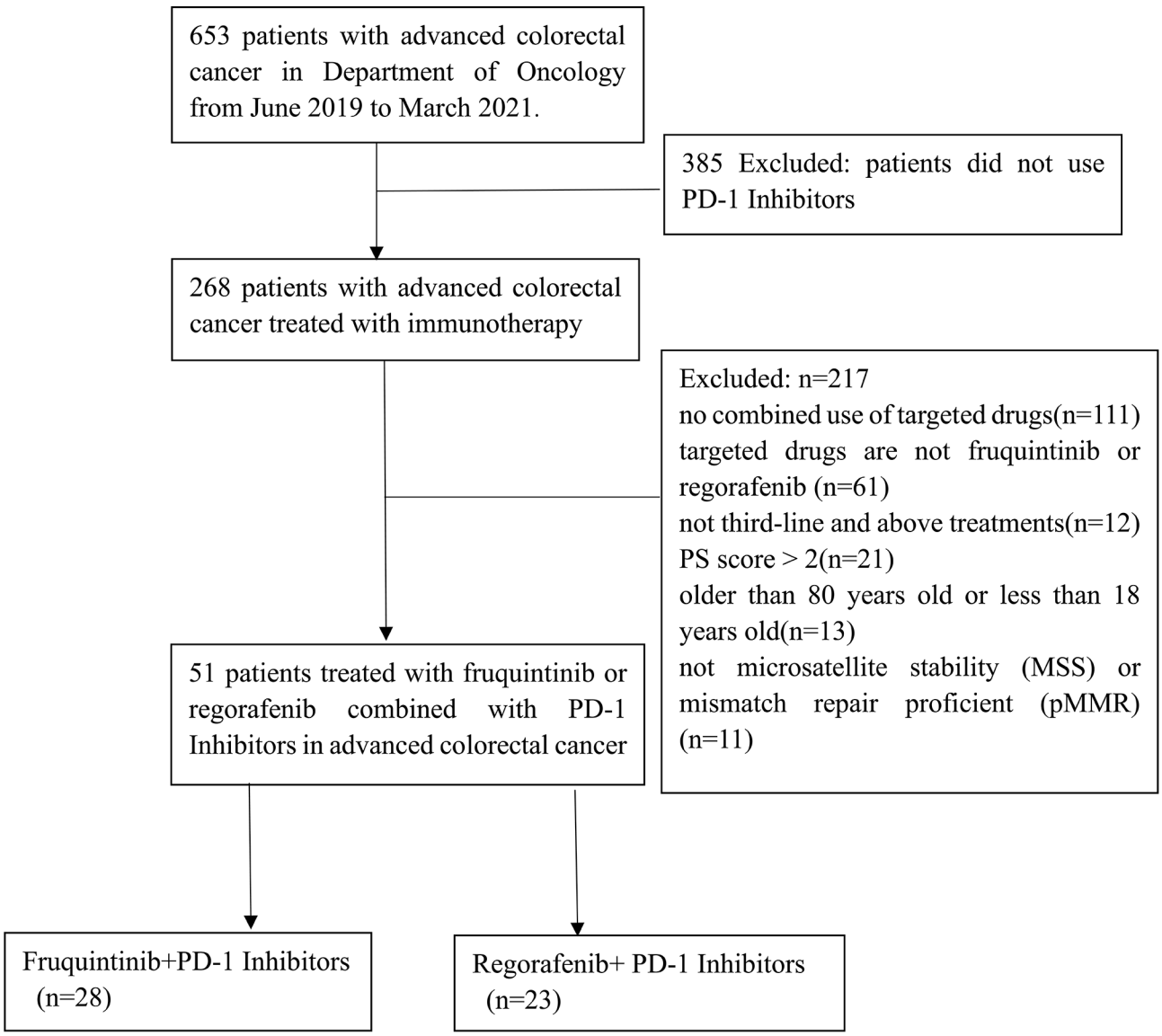

FIGURE 1 | Flowchart of the patient queue.

In order to analyze the beneficiaries of FP therapy compared with those of RP therapy, we performed Kaplan–Meier survival analysis and log-rank tests. In terms of patients with liver metastasis, there was a significant difference in median PFS between the FP and RP groups without liver metastasis ($P < 0.0001$, **Figure 3A**), but there was no significant difference in patients with liver metastasis ($P > 0.05$, **Figure 3B**). For patients with the wild type of KRAS, there was a significant difference in median PFS between the FP and RP groups ($P = 0.0288$, **Figure 3C**). For patients with the KRAS mutant, there was no significant difference between the two groups ($P = 0.1836$, **Figure 3D**). Based on the primary location of the tumor, there was a significant difference in median PFS between the FP and RP groups with the left colon as the primary location ($P = 0.0105$, **Figure 3E**) but not in the groups with the right colon as the primary location ($P = 0.8538$, **Figure 3**). In addition, there was no significant difference in median PFS between the FP and RP groups with or without peritoneal metastasis ($P > 0.05$, **Figures S1A, B**).

Safety

Adverse events were evaluated in 28 patients in the FP group and 23 patients in the RP group. All patients experienced adverse events. The common treatment-related adverse events (AE) of any level in the FP group were liver dysfunction (42.8%), palmar–plantar erythrodysesthesia (39.3%), hypertension (35.7%), capillary endothelial hyperplasia (RCCEP) (39.3%), and proteinuria (32.1%). The common treatment-related AE of any level in the RP group were liver dysfunction (52.2%),

TABLE 1 | Baseline clinical characteristics of patients.

Characteristic	Total, *n* (%)	FP group, *n* (%)	RP group, *n* (%)	*P*-value
Patients, *N* (%)	51	28	23	
Median age (range)	54.2 ± 11.9	54.6 ± 11.7	53.0 ± 12.02	0.724
Age group				0.718
<65 years	41 (80.4)	22 (78.6)	19 (82.6)	
≥65 years	10 (19.6)	6 (21.4)	4 (17.4)	
Sex				0.304
Male	27 (52.9)	13 (46.4)	14 (60.9)	
Female	24 (47.1)	15 (53.6)	9 (39.1)	
Baseline ECOG PS				0.702
0	21 (41.2)	13 (46.4)	8 (34.8)	
1	22 (43.1)	11 (39.3)	11 (47.8)	
2	8 (15.7)	4 (14.3)	4 (17.4)	
Time from first diagnosis to randomization, median (range), months	24 (16.0–47.0)	22 (15.3–39.5)	26 (18.0–50.0)	0.35
Time from first metastatic diagnosis to randomization				0.276
<18 months	15 (29.4)	10 (35.7)	5 (21.7)	
≥18 months	36 (70.6)	18 (64.3)	18 (78.3)	
Primary disease site at first diagnosis				0.18
Colon	28 (54.9)	13 (46.4)	15 (65.2)	
Rectum	23 (45.1)	15 (53.6)	8 (34.8)	
Colon and rectum	51 (100.0)	28 (100.0)	23 (100.0)	
Primary tumor location at first diagnosis				0.11
Left	39 (76.5)	19 (67.9)	20 (87.0)	
Right	12 (23.5)	9 (32.1)	3 (13.0)	
Left and right	51 (100.0)	28 (100.0)	23 (100.0)	
Multiple metastases				
Liver	38 (74.5)	18 (64.3)	20 (87.0)	0.065
Lung	43 (84.3)	24 (85.7)	19 (82.6)	0.762
Peritoneum	13 (25.5)	7 (25.0)	6 (26.1)	0.929
Previous treatment agents				
5-Fluorouracil	43 (84.3)	24 (85.7)	18 (78.3)	0.487
Oxaliplatin	47 (92.2)	26 (92.9)	21 (91.3)	0.837
Irinotecan	48 (94.1)	26 (92.9)	22 (95.7)	0.673
Bevacizumab	40 (78.4)	20 (71.4)	20 (87.0)	0.18
Cetuximab	20 (39.2)	14 (50.0)	6 (26.1)	0.082
Regorafenib	9 (17.6)	3 (10.7)	6 (26.1)	0.152
Fruquintinib	0	0	0	
Number of prior treatment lines on metastatic disease				0.964
3	29 (56.9)	16 (57.1)	13 (56.5)	
>3	22 (43.1)	12 (42.9)	10 (43.5)	
Prior antitumor treatment				
Chemotherapy and pharmacological treatment	51 (100.0)	28 (100.0)	23 (100.0)	1
Radiation therapy	9 (17.6)	5 (17.9)	4 (17.4)	0.965
Surgery	45 (88.2)	23 (82.1)	22 (95.7)	0.136
Gene mutation status				0.853
RAS/BRAF wild type	18 (35.3)	13 (46.4)	5 (21.7)	
RAS mutant	14 (27.5)	10 (35.7)	4 (17.4)	
BRAF mutant	1 (1.9)	0 (0.0)	1 (4.3)	
Unknown	18 (35.3)	5 (17.9)	13 (56.5)	
Prior chemotherapy with VEGF and EGFR inhibitors				0.348
Neither	2 (4.0)	1 (3.6)	1 (4.3)	
VEGF only	28 (54.9)	12 (42.9)	16 (69.6)	
EGFR only	8 (15.7)	6 (21.4)	2 (8.7)	
Both	12 (23.5)	8 (28.6)	4 (17.4)	
Unknown	1 (1.9)	1 (3.6)	0 (0.0)	
PD-1 cycles	5 (3–8)	6 (3–8)	4 (3–5)	0.105

PD-1, programmed death receptor-1; FP, fruquintinib combined with PD-1 inhibitors; RP, regorafenib combined with PD-1 inhibitors; ECOG PS, Eastern Cooperative Oncology Group performance status; VEGF, vascular endothelial growth factor; EGFR, epidermal growth factor receptor.

palmar–plantar erythrodysesthesia (43.5%), hypertension (39.1%), RCCEP (39.1%), proteinuria (30.4%), and fatigue (30.4%). The incidence of liver dysfunction, palmar–plantar erythrodysesthesia, and hypertension in the RP group was higher than that in the FP group, but the difference was not statistically significant (**Table 3**). Grade 3 adverse events in the FP group were diarrhea (n = 1) and liver dysfunction (n = 2); there were no deaths due to adverse events. The adverse events related to grade 3 treatment in the RP group were palmar–plantar erythrodysesthesia (n = 1), rash (n = 1), liver dysfunction

TABLE 2 | Curative effect evaluation.

Best overall response	Total, *n* (%)	FP (*n* = 28), *n* (%)	RP (*n* = 23), *n* (%)	*P*-value
Complete response	0	0	0	1
Partial response	4 (7.8)	2 (7.1)	2 (8.7)	0.709
Stable disease	34 (66.7)	23 (82.1)	11 (47.8)	**0.01**
Progressive disease	13 (25.5)	3 (10.7)	10 (43.5)	0.08
Objective response rate	4 (7.8)	2 (7.1)	2 (8.7)	0.709
Disease control rate	38 (74.5)	25 (89.3)	13 (56.5)	0.08

FP, fruquintinib combined with PD-1 inhibitors; RP, regorafenib combined with PD-1 inhibitors.
The bold values represent P < 0.05, and the difference is statistically significant.

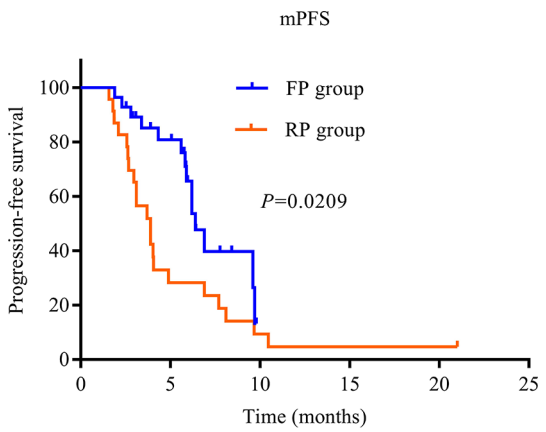

FIGURE 2 | Kaplan–Meier curves of median progression-free survival of patients in the two groups. PD-1, programmed death receptor-1; FP, fruquintinib combined with PD-1 inhibitors; RP, regorafenib combined with PD-1 inhibitors; PFS, progression-free survival.

(*n* = 1), colonic perforation (*n* = 1), and myocardial enzyme elevation (*n* = 1); one patient died of immune myocarditis.

Prognostic Factor Analysis

The prognostic factors affecting survival are shown in **Table 4**. Multivariate analyses showed that the comparison between fruquintinib and regorafenib was identified as an independent risk factor for two kinds of PFS (HR = 2.688; 95% CI: 1.246–5.797; *P* = 0.012).

DISCUSSION

Immunotherapy is a promising treatment method for patients with mCRC. Based on several large trials, ICIs, including anti-PD-1 and CTLA-4 antibodies, have been approved by the US Food and Drug Administration for the treatment of MSI-H or dMMR mCRC patients (7, 9). However, MSS and pMMR CRC have a low immune response, and most MSS CRC patients do not benefit from ICIs alone (8, 34, 35).

Many studies are exploring anti-VEGF therapy combined with ICIs to overcome the drug resistance of pMMR CRCs. First, VEGF-driven angiogenesis can lead to the expansion of tumor-suppressing immune cells (including Tregs and MDSCs) and increase the infiltration of tumor-associated macrophages (TAMs) in the tumor site (36–38). Secondly, VEGF also exerts immunosuppressive effects by inhibiting progenitor cells differentiated with CD4+ and CD8+ lymphocytes (39); T-cell proliferation is decreased, and cytotoxicity is weakened. In addition, VEGF has been shown to increase T-cell failure by increasing the expression of PD-1, CTLA-4, TIM3, and LAG3 on T cells. This provides a strong theoretical basis for the combination of angiogenesis inhibitors and ICIs.

Fruquintinib and regorafenib are both antiangiogenic drugs and third-line treatments for advanced CRC (19, 21), but there is a lack of head-to-head clinical research on their efficacy. Indirect comparison of fruquintinib and regorafenib by meta-analysis showed that there was no significant difference in efficacy and safety between them (23–28). Preclinical studies have shown that fruquintinib combined with PD-1 inhibitors and regorafenib combined with PD-1 inhibitors have synergistic effects in a CRC model (32, 40). At present, there is no research report comparing the efficacy of FP and RP. Our retrospective study shows that FP has better survival benefits than RP in late mCRC.

In the REGONIVO study, 24 Japanese MSS mCRC patients were treated with regorafenib + nivolumab, the ORR was 36%, and the median PFS time was 7.9 months (29). The preliminary results provided MSS patients with refractory mCRC and oncologists with hope. However, a retrospective study of 18 MSS CRC patients at the American Cancer Center in 2019 failed to reveal the comparable clinical activity of regorafenib plus nivolumab, with a median PFS of 2.0 months (30). In a retrospective study, 23 Asian patients with MSS or pMMR mCRC treated with regorafenib combined with anti-PD-1 antibody had an ORR of 0% and a median PFS of 3.1 months (31). In our study, 23 MSS mCRC patients treated with regorafenib combined with PD-1 inhibitors had an ORR of 8.7% and a median PFS of 3.9 months, similar to those in the Asian population. The PFS (3.9 months) in our study was not as long as the PFS (7.9 months) reported in the REGONIVO study, but there was one patient in the RP group who had been taking medication for as long as 21 months. The data at the cutoff time showed SD, and the patient was still using RP. We need to further analyze the clinical data of the patient. However, the PFS (3.9 months) of the RP group was much better than the PFS (2.0 months) of the group in the US study, probably because the US study included only five Asian patients (27.8%). Different ethnic characteristics may also lead to differences in the efficacy of the combination.

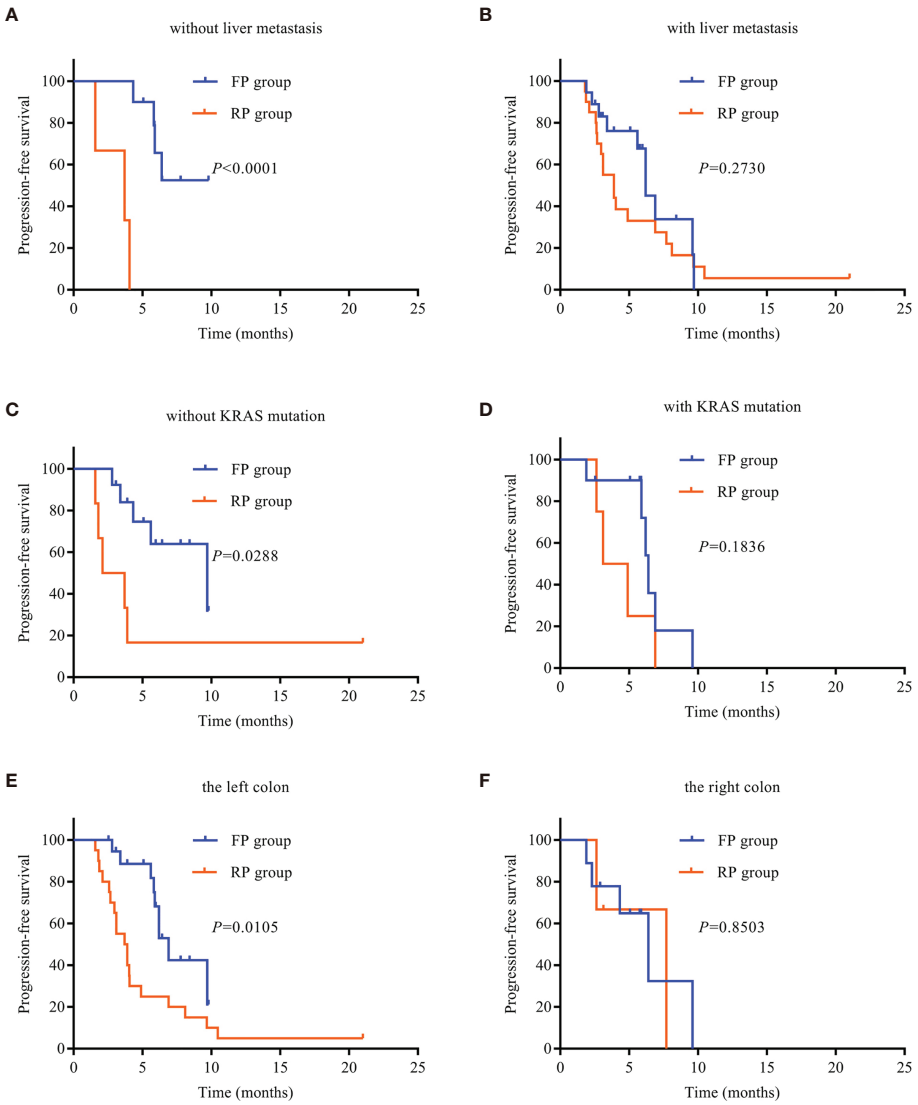

FIGURE 3 | Kaplan–Meier survival curves. **(A)** PFS in patients without liver metastasis. **(B)** PFS in patients with liver metastasis. **(C)** PFS in patients without KRAS mutation. **(D)** PFS in patients with KRAS mutation. **(E)** PFS of the left colon. **(F)** PFS of the right colon. PD-1, programmed death receptor-1; FP, fruquintinib combined with PD-1 inhibitors; RP, regorafenib combined with PD-1 inhibitors; PFS, progression-free survival.

The median PFS of the FP group was superior to that of the RP group in the treatment of MSS mCRC. The reasons may be as follows: first, fruquintinib belongs to a new generation of small molecular tyrosine kinase inhibitors with strong effects, which is highly selective to VEGFR-1, VEGFR-2, and VEGFR-3 but has no obvious inhibitory effect on other kinase activities; it is expected to maintain target inhibition and minimize toxicity (17, 18). Regorafenib is a multitarget kinase inhibitor (MKI), which inhibits the activation of VEGFR-1, VEGFR-2, VEGFR-3, FGFR, PDGFR, KIT, RET, TIE2, and BRAF (20). Second, the adverse reactions of inhibitors were more tolerable in the FP group than in the RP group. Although there was no significant difference in adverse reactions between the FP and RP groups, the adverse reactions in the FP group were generally lower than those in the RP group. Third, the proportion of liver metastasis in the FP group (64.3%) was lower than that in the RP group (87%). As an immunologically tolerant organ, the liver may reduce the intrahepatic and extrahepatic immune responses of tumor patients (41, 42). Fourth, the RP group was treated with regorafenib before the combined treatment, but the FP group was not treated with fruquintinib before the combined treatment. Notably, one patient in the FP group progressed 6.9 months after the use of regorafenib combined with sintilimab, and the regimen of fruquintinib combined with sintilimab still achieved good results. As of the data cutoff date, fruquintinib was used in combination with sintilimab for 5.06 months. Hence, in possible future trials, patients who have made progress when previously treated with regorafenib combined with immunosuppressants

TABLE 3 | Adverse events.

	All			Grade >3		
	FP group (*n* = 28)	**RP group (*n* = 23)**	***P*-value**	**FP group (*n* = 28)**	**RP group (*n* = 23)**	***P*-value**
n (%)	28 (100)	23 (100)	1	3 (10.7)	5 (21.7)	0.281
Palmar–plantar erythrodysesthesia	11 (39.3)	10 (43.5)	0.95	0	1 (4.3)	0.265
Hypertension	10 (35.7)	9 (39.1)	0.193	0	0	1
Fatigue	7 (25.0)	7 (30.4)	0.665	0	0	1
Rash	5 (17.8)	4 (17.30)	0.404	0	1 (4.3)	0.265
Capillary endothelial hyperplasia (RCCEP)	11 (39.3)	9 (39.1)	0.762	0	0	1
Proteinuria	9 (32.1)	7 (30.4)	0.358	0	0	1
Fever	2 (3.6)	1 (4.3)	0.673	0	0	1
Oral mucositis	2 (7.1)	1 (4.3)	0.238	0	0	1
Diarrhea	2 (7.1)	0	0.425	1 (3.6)	0	0.36
Decreased appetite	6 (21.4)	3 (13.0)	0.434	0	0	1
Liver dysfunction	12 (42.8)	12 (52.2)	0.575	2 (7.1)	1 (4.3)	0.673
Hyperthyroidism	1 (3.6)	0	0.36	0	0	1
Hypothyroidism	8 (28.5)	6 (26.1)	0.984	0	0	1
Platelet count decreased	5 (17.8)	2 (8.6)	0.493	0	0	1
Neutrophil count decreased	2 (7.1)	1 (4.3)	0.424	0	0	1
Hoarseness	1 (3.6)	0	0.36	0	0	1
Colonic perforation	1 (3.6)	2 (8.6)	0.529	0	1 (4.3)	0.265
Lipase elevated	0	0	1	0	0	1
Interstitial pneumonitis	0	0	1	0	0	1
Myocardial enzyme elevation	0	1 (4.3)	0.265	0	1 (4.3)	0.265

FP, fruquintinib combined with PD-1 inhibitors; RP, regorafenib combined with PD-1 inhibitors; RCCEP, capillary endothelial hyperplasia.

TABLE 4 | Univariate and multivariate analyses of risk factors for progression-free survival.

	Univariate analysis			Multivariate analysis		
	HR	**95% CI**	***P*-value**	**HR**	**95% CI**	***P*-value**
Age (years), (</≥65)	1.082	0.467–2.511	0.854			
Sex (female/male)	1.502	0.770–2.931	0.233			
Baseline ECOG PS (0/1/2)	**1.953**	**1.21–3.151**	**0.006**	2.17	1.259–3.74	0.05
First diagnosis time (months), (</≥18)	1.161	0.557–2.421	0.69			
Tumor location (left/right)	1.005	0.435–2.32	0.991			
Primary disease site at first diagnosis (colon/rectum)	0.763	0.393–1.478	0.422			
Liver metastasis (yes/no)	0.613	0.266–1.413	0.251			
Treatment lines (3/>3)	1.269	0.652–2.472	0.483			
Gene mutation status (RAS wild type/RAS mutant)	0.95	0.628–1.437	0.809			
Targeted drugs (fruquintinib/regorafenib)	**2.069**	**1.050–4.079**	**0.036**	**2.688**	**1.246–5.797**	**0.012**
Prior chemotherapy with VEGF (yes/no)	**2.999**	**1.052–8.545**	**0.04**	2.135	0.664–6.863	0.203
Prior chemotherapy with EGFR (yes/no)	**0.683**	**0.476–0.982**	**0.039**	0.962	0.632–1.464	0.856
PD-1 inhibitors	1.567	0.986–2.49	0.057			

ECOG PS, Eastern Cooperative Oncology Group performance status; HR, hazard ratio; CI, confidence interval; VEGF, vascular endothelial growth factor; EGFR, epidermal growth factor receptor. The bold values represent P < 0.05, and the difference is statistically significant.

should not necessarily be excluded from receiving the combination of fruquintinib and immunosuppressant therapy.

Owing to its evolving immune tolerance, the liver is thought to be associated with a high proportion of immunosuppressive cells (41). Both primary liver cancer and liver metastasis can use liver immune tolerance to suppress the anticancer responses and weaken the efficacy of ICIs (42). In this study, we observed that the curative effect in the FP group was better than that in the RP group in patients without liver metastasis; the difference was statistically significant, but there was no significant difference in the liver metastasis groups. This result suggests that the FP regimen is more effective in advanced CRC patients without liver metastasis than in those with metastasis. The KRAS oncogene is one of the most common mutation genes in cancer. KRAS mutation has been found in approximately half of mCRC patients. KRAS mutation results in highly invasive tumor biology and poor prognosis (43–45). In the right colon, KRAS mutations are common (46). In this study, we observed that there was no significant difference in KRAS mutant and right tumor between the FP and RP groups; however, the curative effect in the FP group was better than that in the RP group for mCRC patients harboring the KRAS wild type and having the left colon as the primary location. These findings suggest that the FP regimen is relatively effective in advanced CRC patients with KRAS wild type and left tumor, but this needs to be confirmed in large-sample randomized studies.

This study has some limitations. First, this study is a single-center retrospective study, which inevitably has selection bias. Second, four different PD-1 inhibitors were used in this study, which affected the uniformity of the treatment process. Third, the number of cases was relatively small. Fourth, because of the late market time of fruquintinib, patients in the FP group began its use later than those in the RP group, and there may be a time bias. Fifth, the doses of fruquintinib and regorafenib were not uniform in patients, which further increased the heterogeneity of this study. Sixth, not all patients were tested for RAS and BRAF genes, which limited the analysis of their effects on the efficacy of drug therapy. Finally, the PD-L1 CPS and TMB of this study are unknown and cannot be used to determine the best population for immunosuppressant use. Therefore, the results of this study should be further extended to large-scale prospective studies in order to obtain a higher level of medical evidence.

In summary, FP has better survival benefits than RP. Patients with no liver metastasis, KRAS wild type, and left colon tumor may be the beneficiaries of FP. FP may become a new treatment option for advanced mCRC with MSS or pMMR.

DATA AVAILABILITY STATEMENT

The original contributions presented in the study are included in the article/**Supplementary Material**. Further inquiries can be directed to the corresponding author.

ETHICS STATEMENT

Written informed consent was obtained from the individual(s) for the publication of any potentially identifiable images or data included in this article.

AUTHOR CONTRIBUTIONS

JW and YM designed the study. LS and YW collected the data. LS analyzed and interpreted the data. LS, SH, DL, YM, and JW carried out the clinical treatment and management of the patients. LS and JW prepared the final draft. All authors contributed to the article and approved the submitted version.

FUNDING

This work was supported by the National Natural Science Foundation of China (No. 82060435).

ACKNOWLEDGMENTS

The authors would like to thank ZQH for his useful comments. We thank our colleagues for their valuable efforts and comments on this manuscript. We also sincerely thank the editors and reviewers for their careful review and valuable opinions that helped to greatly improve the manuscript.

SUPPLEMENTARY MATERIAL

The Supplementary Material for this article can be found online at: https://www.frontiersin.org/articles/10.3389/fonc.2021.754881/full#supplementary-material

Supplementary Figure 1 | Kaplan-Meier survival curves. **(A)** PFS of patients without peritoneal metastasis. **(B)** PFS of patients with peritoneal metastasis.

REFERENCES

1. Siegel RL, Miller KD, Jemal A. Cancer Statistics, 2020. *CA: A Cancer J Clin* (2020) 70(1):7–30. doi: 10.3322/caac.21590
2. Dhillon S. Regorafenib: A Review in Metastatic Colorectal Cancer. *Drugs* (2018) 78(11):1133–44. doi: 10.1007/s40265-018-0938-y
3. Messersmith WA. NCCN Guidelines Updates: Management of Metastatic Colorectal Cancer. *J Natl Compr Cancer Network JNCCN* (2019) 17(5.5):599–601. doi: 10.6004/jnccn.2019.5014
4. Hirsch L, Zitvogel L, Eggermont A, Marabelle A. PD-Loma: A Cancer Entity With a Shared Sensitivity to the PD-1/PD-L1 Pathway Blockade. *Br J Cancer* (2019) 120(1):3–5. doi: 10.1038/s41416-018-0294-4
5. Jacquelot N, Yamazaki T, Roberti MP, Duong CPM, Andrews MC, Verlingue L, et al. Sustained Type I Interferon Signaling as a Mechanism of Resistance to PD-1 Blockade. *Cell Res* (2019) 29(10):846–61. doi: 10.1038/s41422-019-0224-x
6. Powles T, Durán I, van der Heijden MS, Loriot Y, Vogelzang NJ, De Giorgi U, et al. Atezolizumab Versus Chemotherapy in Patients With Platinum-Treated Locally Advanced or Metastatic Urothelial Carcinoma (IMvigor211): A Multicentre, Open-Label, Phase 3 Randomised Controlled Trial. *Lancet (London England)* (2018) 392(1402):748–57. doi: 10.1016/S0140-6736(17)33297-X
7. Le DT, Uram JN, Wang H, Bartlett BR, Kemberling H, Eyring AD, et al. PD-1 Blockade in Tumors With Mismatch-Repair Deficiency. *N Engl J Med* (2015) 372(26):2509–20. doi: 10.1056/NEJMoa1500596
8. Le DT, Durham JN, Smith KN, Wang H, Bartlett BR, Aulakh LK, et al. Mismatch Repair Deficiency Predicts Response of Solid Tumors to PD-1 Blockade. *Sci (New York NY)* (2017) 357(6349):409–13. doi: 10.1126/science.aan6733
9. Overman MJ, McDermott R, Leach JL, Lonardi S, Lenz H-J, Morse MA, et al. Nivolumab in Patients With Metastatic DNA Mismatch Repair-Deficient or Microsatellite Instability-High Colorectal Cancer (CheckMate 142): An Open-Label, Multicentre, Phase 2 Study. *Lancet Oncol* (2017) 18(9):1182–91. doi: 10.1016/S1470-2045(17)30422-9
10. DBK L. An Expanding Role for Immunotherapy in Colorectal Cancer. *J Natl Compr Cancer Network JNCCN* (2017) 15(3):401–10. doi: 10.6004/jnccn.2017.0037
11. Zelenay S, van der Veen AG, Bottcher JP, Snelgrove KJ, Rogers N, Acton SE, et al. Cyclooxygenase-Dependent Tumor Growth Through Evasion of Immunity. *Cell* (2015) 162(6):1257–70. doi: 10.1016/j.cell.2015.08.015
12. Ou D-L, Chen C-W, Hsu C-L, Chung C-H, Feng Z-R, Lee B-S, et al. Regorafenib Enhances Antitumor Immunity via Inhibition of P38 Kinase/Creb1/Klf4 Axis in Tumor-Associated Macrophages. *J ImmunoTher Cancer* (2021) 9(3):e001657. doi: 10.1136/jitc-2020-001657
13. Hodi FS, Lawrence D, Lezcano C, Wu X, Zhou J, Sasada T, et al. Bevacizumab Plus Ipilimumab in Patients With Metastatic Melanoma. *Cancer Immunol Res* (2014) 2(7):632–42. doi: 10.1158/2326-6066
14. Zhao S, Ren S, Jiang T, Zhu B, Li X, Zhao C, et al. Low-Dose Apatinib Optimizes Tumor Microenvironment and Potentiates Antitumor Effect of

PD-1/PD-L1 Blockade in Lung Cancer. *Cancer Immunol Res* (2019):630–43. doi: 10.1158/2326-6066
15. Shigeta K, Datta M, Hato T, Kitahara S, Chen IX, Matsui A, et al. Dual Programmed Death Receptor-1 and Vascular Endothelial Growth Factor Receptor-2 Blockade Promotes Vascular Normalization and Enhances Antitumor Immune Responses in Hepatocellular Carcinoma. *Hepatology* (2019) 71(4):1247–61. doi: 10.1002/hep.30889
16. Konecny GE. Inhibition of PD-1 and VEGF in Microsatellite-Stable Endometrial Cancer. *Lancet Oncol* (2019) 20(5):612–4. doi: 10.1016/S1470-2045(19)30079-8
17. Sun Q, Zhou J, Zhang Z, Guo M, Liang J, Zhou F, et al. Discovery of Fruquintinib, A Potent and Highly Selective Small Molecule Inhibitor of VEGFR 1, 2, 3 Tyrosine Kinases for Cancer Therapy. *Cancer Biol Ther* (2014) 15(12):1635–45. doi: 10.4161/15384047.2014.964087
18. Gu Y, Wang J, Li K, Zhang L, Ren H, Guo L, et al. Preclinical Pharmacokinetics and Disposition of a Novel Selective VEGFR Inhibitor Fruquintinib (HMPL-013) and the Prediction of Its Human Pharmacokinetics. *Cancer Chemother Pharmacol* (2014) 74(1):95–115. doi: 10.1007/s00280-014-2471-3
19. Li J, Qin S, Xu RH, Shen L, Xu J, Bai Y, et al. Effect of Fruquintinib vs Placebo on Overall Survival in Patients With Previously Treated Metastatic Colorectal Cancer: The FRESCO Randomized Clinical Trial. *JAMA* (2018) 319 (24):2486–96. doi: 10.1001/jama.2018.7855
20. Wilhelm SM, Dumas J, Adnane L, Lynch M, Carter CA, Schutz G, et al. Regorafenib (BAY 73-4506): A New Oral Multikinase Inhibitor of Angiogenic, Stromal and Oncogenic Receptor Tyrosine Kinases With Potent Preclinical Antitumor Activity. *Int J Cancer* (2011) 129(1):245–55. doi: 10.1002/ijc.25864
21. Grothey A, Van Cutsem E, Sobrero A, Siena S, Falcone A, Ychou M, et al. Regorafenib Monotherapy for Previously Treated Metastatic Colorectal Cancer (CORRECT): An International, Multicentre, Randomised, Placebo-Controlled, Phase 3 Trial. *Lancet (London England)* (2013) 381(9863):303–12. doi: 10.1016/S0140-6736(12)61900-X
22. Li J, Qin S, Xu R, Yau TC, Ma B, Pan H, et al. Regorafenib Plus Best Supportive Care Versus Placebo Plus Best Supportive Care in Asian Patients With Previously Treated Metastatic Colorectal Cancer (CONCUR): A Randomised, Double-Blind, Placebo-Controlled, Phase 3 Trial. *Lancet Oncol* (2015) 16(6):619–29. doi: 10.1016/S1470-2045(15)70156-7
23. Jing Z, Rui Z, Binglan Z. A Comparison of Regorafenib and Fruquintinib for Metastatic Colorectal Cancer: A Systematic Review and Network Meta-Analysis. *J Cancer Res Clin Oncol* (2019) 145(9):2313–23. doi: 10.1007/s00432-019-02964-6
24. Cao M, Zhou M, Zhang J. Comparison of Efficacy and Safety for Patients With Beyond Second Line Treated Metastatic Colorectal Cancer: A Network Meta-Analysis of Randomized Controlled Trials. *J chemother (Florence Italy)* (2020) 32(4):163–70. doi: 10.1080/1120009X.2020.1728860
25. Chen J, Wang J, Lin H, Peng Y. Comparison of Regorafenib, Fruquintinib, and TAS-102 in Previously Treated Patients With Metastatic Colorectal Cancer: A Systematic Review and Network Meta-Analysis of Five Clinical Trials. *Med Sci Monitor Int Med J Exp Clin Res* (2019) 25:9179–91. doi: 10.12659/MSM.918411
26. Gao Z, Cao C, Bao Y, Fan Y, Chen G, Fu P. Systematic Review and Meta-Analysis of Multitargeted Tyrosine Kinase Inhibitors in Patients With Intractable Metastatic Colorectal Cancer. *Technol Cancer Res Treat* (2020) 19:1533033820943241. doi: 10.1177/1533033820943241
27. Wu Y, Fan Y, Dong D, Dong X, Hu Y, Shi Y, et al. Efficacy and Safety of Regorafenib as Beyond Second-Line Therapy in Patients With Metastatic Colorectal Cancer: An Adjusted Indirect Meta-Analysis and Systematic Review. *Ther Adv Med Oncol* (2020) 12:1758835920940932. doi: 10.1177/1758835920940932
28. Zhang Q, Wang Q, Wang X, Li J, Shen L, Peng Z. Regorafenib, TAS-102, or Fruquintinib for Metastatic Colorectal Cancer: Any Difference in Randomized Trials? *Int J Colorectal Dis* (2020) 35(2):295–306. doi: 10.1007/s00384-019-03477-x
29. Fukuoka S HH, Hara H, Takahashi N, Kojima T, Kawazoe A, Asayama M, et al. Regorafenib Plus Nivolumab in Patients With Advanced Gastric or Colorectal Cancer: An Open-Label, Dose-Escalation, and Dose-Expansion Phase Ib Trial(Regonivo, Epoc1603). *J Clin Oncol* (2020) 38(18):2053–61. doi: 10.1200/JCO.19.03296
30. Wang C, Chevalier D, Saluja J, Sandhu J, Lau C, Fakih M. Regorafenib and Nivolumab or Pembrolizumab Combination and Circulating Tumor DNA Response Assessment in Refractory Microsatellite Stable Colorectal Cancer. *Oncology* (2020) 25(8):e1188–94. doi: 10.1634/theoncologist.2020-0161
31. Li J, Cong L, Liu J, Peng L, Wang J, Feng A, et al. The Efficacy and Safety of Regorafenib in Combination With Anti-PD-1 Antibody in Refractory Microsatellite Stable Metastatic Colorectal Cancer: A Retrospective Study. *Front Oncol* (2020) 10:594125. doi: 10.3389/fonc.2020.594125
32. Wang Y, Wei B, Gao J, Cai X, Xu L, Zhong H, et al. Combination of Fruquintinib and Anti-PD-1 for the Treatment of Colorectal Cancer. *J Immunol (Baltimore Md 1950)* (2020) 205(10):2905–15. doi: 10.4049/jimmunol.2000463
33. Jiang FE ZH, Yu CY, Liu AN. Efficacy and Safety of Regorafenib or Fruquintinib Plus Camrelizumab in Patients With Microsatellite Stable and/or Proficient Mismatch Repair Metastatic Colorectal Cancer: An Observational Pilot Study. *Neoplasma* (2021) 68(4):861–6. doi: 10.4149/neo_2021_201228N1415
34. Hermel DJ, Sigal D. The Emerging Role of Checkpoint Inhibition in Microsatellite Stable Colorectal Cancer. *J Pers Med* (2019) 9(1):5. doi: 10.3390/jpm9010005
35. Galon J, Bruni D. Approaches to Treat Immune Hot, Altered and Cold Tumours With Combination Immunotherapies. *Nat Rev Drug Discov* (2019) 18(3):197–218. doi: 10.1038/s41573-018-0007-y
36. Varney ML, Johansson SL, Singh RK. Tumour-Associated Macrophage Infiltration, Neovascularization and Aggressiveness in Malignant Melanoma: Role of Monocyte Chemotactic Protein-1 and Vascular Endothelial Growth Factor-A. *Melanoma Res* (2005) 15(5):417–25. doi: 10.1097/00008390-200510000-00010
37. Huang Y, Chen X, Dikov MM, Novitskiy SV, Mosse CA, Yang L, et al. Distinct Roles of VEGFR-1 and VEGFR-2 in the Aberrant Hematopoiesis Associated With Elevated Levels of VEGF. *Blood* (2007) 110(2):624–31. doi: 10.1182/blood-2007-01-065714
38. Wada J, Suzuki H, Fuchino R, Yamasaki A, Nagai S, Yanai K, et al. The Contribution of Vascular Endothelial Growth Factor to the Induction of Regulatory T-Cells in Malignant Effusions. *Anticancer Res* (2009) 29:881–8. doi: 10.1103/PhysRevLett.94.028701
39. Ohm JE, Gabrilovich DI, Sempowski GD, Kisseleva E, Parman KS, Nadaf S, et al. VEGF Inhibits T-Cell Development and may Contribute to Tumor-Induced Immune Suppression. *Blood* (2003) 101(12):4878–86. doi: 10.1182/blood-2002-07-1956
40. Hoff S, Röse S, Rse L, Zopf D. Immunomodulation by Regorafenib Alone and in Combination With Anti PD1 Antibody on Murine Models of Colorectal Cancer. *Ann Oncol Off J Eur Soc Med Oncol* (2017) 28(suppl 5):v403–27. doi: 10.1093/annonc/mdx376.060
41. Zheng M, Tian Z. Liver-Mediated Adaptive Immune Tolerance. *Front Immunol* (2019) 10:2525. doi: 10.3389/fimmu.2019.02525
42. Tumeh PC, Hellmann MD, Hamid O, Tsai KK, Loo KL, Gubens MA, et al. Liver Metastasis and Treatment Outcome With Anti-PD-1 Monoclonal Antibody in Patients With Melanoma and NSCLC. *Cancer Immunol Res* (2017) 5(5):417–24. doi: 10.1158/2326-6066.CIR-16-0325
43. Douillard JY, Oliner KS, Siena S, Tabernero J, Burkes R, Barugel M, et al. Panitumumab-FOLFOX4 Treatment and RAS Mutations in Colorectal Cancer. *N Engl J Med* (2013) 369(11):1023–34. doi: 10.1056/NEJMoa1305275
44. Stintzing S, Miller-Phillips L, Modest DP, Fischer von Weikersthal L, Decker T, Kiani A, et al. Impact of BRAF and RAS Mutations on First-Line Efficacy of FOLFIRI Plus Cetuximab Versus FOLFIRI Plus Bevacizumab: Analysis of the FIRE-3 (AIO KRK-0306) Study. *Eur J Cancer (Oxford Engl 1990)* (2017) 79:50–60. doi: 10.1016/j.ejca.2017.03.023
45. Taieb J, Le Malicot K, Shi Q, Penault-Llorca F, Bouche O, Tabernero J, et al. Prognostic Value of BRAF and KRAS Mutations in MSI and MSS Stage III Colon Cancer. *J Natl Cancer Inst* (2017) 109(5):djw272. doi: 10.1093/jnci/djw272
46. Baran B, Mert Ozupek N, Yerli Tetik N, Acar E, Bekcioglu O, Baskin Y. Difference Between Left-Sided and Right-Sided Colorectal Cancer: A Focused Review of Literature. *Gastroenterol Res* (2018) 11(4):264–73. doi: 10.14740/gr1062w

Conflict of Interest: The authors declare that the research was conducted in the absence of any commercial or financial relationships that could be construed as a potential conflict of interest.

this article, or claim that may be made by its manufacturer, is not guaranteed or endorsed by the publisher.

frontiers in Oncology

ORIGINAL RESEARCH
published: 10 November 2021
doi: 10.3389/fonc.2021.737323

A Novel Strategy Conjugating PD-L1 Polypeptide With Doxorubicin Alleviates Chemotherapeutic Resistance and Enhances Immune Response in Colon Cancer

Maolin Wang[1,2†], Xing-sheng Shu[1†], Meiqi Li[1], Yilin Zhang[1], Youli Yao[1], Xiaoyan Huang[1], Jianna Li[3], Pengfei Wei[4], Zhendan He[2], Jun Lu[5,6*] and Ying Ying[1*]*

[1] Department of Physiology, School of Basic Medical Sciences, Shenzhen University Health Science Center, Shenzhen, China, [2] College of Pharmacy, Shenzhen Technology University, Shenzhen, China, [3] Department of Pathogen Biology, School of Basic Medical Sciences, Shenzhen University Health Science Center, Shenzhen, China, [4] Shenzhen University General Hospital, Department of Endocrinology, Shenzhen, China, [5] School of Pharmacy, Chengdu University of Traditional Chinese Medicine, Chengdu, China, [6] Institute of Integrated Bioinfomedicine & Translational Science, Hong Kong Baptist University Shenzhen Research Institute and Continuing Education, Shenzhen, China

Background: Modifying the structure of anti-tumor chemotherapy drug is of significance to enhance the specificity and efficacy of drug-delivery. A novel proteolysis resistant PD-L1-targeted peptide (PPA1) has been reported to bind to PD-L1 and disrupt the PD-1/PD-L1 interaction, thus appearing as an outstanding tumor-targeting modification of synergistic drug conjugate for effective anti-tumor treatment. However, the combination regimen of coupling PD-L1 polypeptide with chemotherapeutic drug in tumoricidal treatment has not been reported thus far.

Methods: We developed a novel synergistic strategy by conjugating PPA1 to doxorubicin (DOX) with a pH sensitive linker that can trigger the release of DOX near acidic tumor tissues. The binding affinity of PPA1-DOX with PD-L1 and the acid-sensitive cleavage of PPA1-DOX were investigated. A mouse xenograft model of colon cancer was used to evaluate the biodistribution, cytotoxicity and anti-tumor activity of PPA1-DOX.

Results: PPA1-DOX construct showed high binding affinity with PD-L1 *in vitro* and specifically enriched within tumor when administered *in vivo*. PPA1-DOX exhibited a significantly lower toxicity and a remarkably higher antitumor activity *in vivo*, as compared with free PPA1, random polypeptide-DOX conjugate, DOX, or 5-FU, respectively. Moreover, increased infiltration of both $CD4^+$ and $CD8^+$ T cells was found in tumors from PPA1-DOX treated mice.

Conclusions: We describe here for the first time that the dual-functional conjugate PPA1-DOX, which consist of the PD-L1-targeted polypeptide that renders both the tumor-specific drug delivery and inhibitory PD-1/PD-L1 immune checkpoint inhibition, and a cytotoxic agent that is released and kills tumor cells once reaching tumor tissues, thus representing a promising therapeutic option for colon cancer with improved efficacy and reduced toxicity.

Keywords: target delivery system, colon cancer, PD-L1 targeting polypeptide, pH sensitive linker, chemotherapeutics drug release

OPEN ACCESS

Edited by:
Sripathi Sureban, University of Oklahoma Health Sciences Center, United States

Reviewed by:
Soudamani Singh, Marshall University, United States
Chao Liang, Southern University of Science and Technology, China
Jin Liu, Hong Kong Baptist University, Hong Kong, SAR China

***Correspondence:**
Ying Ying
yingying@szu.edu.cn
Jun Lu
ljaaalll@163.com
Zhendan He
hezhendan@szu.edu.cn

†These authors have contributed equally to this work

Specialty section:
This article was submitted to Gastrointestinal Cancers: Gastric Esophageal Cancers, a section of the journal Frontiers in Oncology

Received: *06 July 2021*
Accepted: *15 October 2021*
Published: *10 November 2021*

Citation:
Wang M, Shu X-s, Li M, Zhang Y, Yao Y, Huang X, Li J, Wei P, He Z, Lu J and Ying Y (2021) A Novel Strategy Conjugating PD-L1 Polypeptide With Doxorubicin Alleviates Chemotherapeutic Resistance and Enhances Immune Response in Colon Cancer. Front. Oncol. 11:737323. doi: 10.3389/fonc.2021.737323

1 INTRODUCTION

Chemotherapy is one of the major categories of the medical discipline specifically devoted to pharmacotherapy for variety of cancers, including colon cancer (1, 2). Since the anti-tumor drugs of chemotherapy do not distinguish tumor cells from normal tissue cells, chemotherapeutic techniques have a range of undesirable side effects (3). Modifying the structure of anti-tumor chemotherapy drug is of significance, which allows the drug to recognize tumor cells and reduce the lethality to normal tissue cells. There have been several techniques that attach the targeted recognition part to chemotherapy drugs. Antibody-drug conjugate (ADC) is a class of biopharmaceutical drugs combining antibodies with chemotherapy drugs, however, the risk of immunogenicity and the raising incidents of resistance still limit its clinical treatment (4–6). Aptamer drug conjugate (ApDC) is another class of molecule that binds to a specific target protein (7, 8). ApDCs are comprised of targeted component and drug component. Generally, the nucleic acid and polypeptide are utilized to bind to a specific target, such as nucleolin, EGFR and Vimentin for tumor cells (9–11). However, this approach has suffered from rapid elimination by systemic clearance. Therefore, it is urgently desirable to develop a tumor targeting modification method to enhance drug-delivery efficacy and reduce side effects.

Target polypeptides are artificial proteins selected or engineered to bind specific target molecules, which consist of a number of peptides forming loops of variable sequence and displaying unique protein scaffold (12). To prevent the degradation of proteolytic enzymes, D-polypeptide was chosen as the target polypeptide. Programmed death-ligand 1 (PD-L1) has been proven to play a major role in suppressing the activity of T cells of immune system and up-regulated in various types of cancers (13–15). The blockade of PD-L1 by target polypeptides could disrupt the inhibitory PD-1/PD-L1 immune checkpoint and provide a promising cancer treatment (16, 17). A novel polypeptide PPA1 has been reported that it can bind PD-L1 *in vitro* and inhibit the tumor growth in CT26 bearing mice by disrupting the PD-1/PD-L1 interaction. The D-peptide construct of PPA1 may prevent the degradation of proteolytic enzymes in serum (18). Therefore, PPA1 appears as an outstanding tumor-targeting modification of synergistic drug conjugate for effective anti-tumor treatment. However, the combination regimen of coupling PD-L1 polypeptide with chemotherapeutic drug in tumoricidal treatment has not been reported thus far.

Studies have shown that intracellular pH of solid tumors is maintained in a range of 7.0 to 7.2, whereas the extracellular pH demonstrates acidic microenvironment (19). The acidic microenvironment may be a significant factor that could trigger the release of the anti-tumor chemotherapeutic drug in tumor tissues (20), but to keep the chemotherapeutic construct steady in non-tumor tissues. Therefore, the polypeptide and drug can be conjugated by an acid-sensitive linker, forming a polypeptide-drug conjugate that is able to stay steady in normal tissue and be specifically delivered to tumor tissue by target polypeptide, then release chemotherapeutic drug due to the cleavage of acidic pH sensitive linker.

In this study, the proteolysis resistant PD-L1-targeted peptide, PPA1, was conjugated to doxorubicin (DOX) with a pH sensitive linker. The reason that we did not select 5-Fu as the conjugated drug was the lack of suitable synthetic site on 5-Fu. Although the development of resistance to DOX in colon cancer has been shown (21), DOX was selected as the candidate chemotherapeutic drug herein to verify the feasibility of reducing tumor drug-resistance by improving tumor-specific targeted drug delivery. We found that PPA1-DOX construct showed high binding affinity with PD-L1 *in vitro* and was specifically enriched within tumor when administered *in vivo*. Moreover, a significantly lower toxicity and higher antitumor activity was achieved by PPA1-DOX *in vivo*, as compared with the respective free PPA1, random polypeptide-DOX conjugate, DOX, or 5-FU. Thus, we believe that the dual-functional conjugates, which consist of the PD-L1-targeted polypeptide that renders both the tumor-specific drug delivery and inhibitory PD-1/PD-L1 immune checkpoint inhibition, and a cytotoxic agent that kills tumor cells once reaching tumor tissues, represents a promising therapeutic option for colon cancer.

Abbreviations: PD-L1, programmed death-ligand 1; ApDC, aptamer drug conjugate; DOX, doxorubicin; DMAP, 4-dimethylaminopyrid; TLC, thin-layer chromatography.

2 MATERIAL AND METHODS

2.1 Synthesis Information

The PPA1 (nyskptdrqyhfk) and RNA (rhtndysqfypk) were purchased from Chinapeptides Co.,Ltd., China. The polypeptides were both in D-form.

Methanol, ethanol, trifluoroethanoic acid (TFA) and N,N-dimethylformamid (DMF) were purchased from Sigma-Aldrich. N,N'-dicyclohexylcarbodimide (DCC), 4-dimethylaminopyrid (DMAP), hydrazine hydrate (N_2H_4, about 80% in H_2O), doxoriubicin, 4A molecular sieves, $CuSO_4.5H_2O$, sodium ascorbate, 1-(1-benzyltriazol-4-yl)-N,N-bis[(1-benzyltriazol-4-yl) methyl]- methanamine (TBTA) were purchased from TCI. DOX and 5-Fu were purchased from J&K Scientific Ltd. Those custom peptides of R(2-Azido) were synthesized by ChinaPeptides Co,. Ltd. All of the purchased chemicals were of at least reagent grade and were used without further purification. Reactions were monitored by analytical thin-layer chromatography (TLC) using silica gel 60 F254 pre-coated glass plates (0.25 mm thickness) and visualized using UV light.

The ^1H and ^{13}C NMR spectra were recorded on a Bruker Avance 400 MHz (^1H: 400 MHz, ^{13}C:101 MHz) spectrometer using tetramethylsilane (TMS) as internal standard at 25°C. Samples were prepared as solutions in deuterated solvent. Those following abbreviations were used to indicate the observed spin multiplicities on NMR spectra: s = singlet, d = doublet, t = triplet, q = quartet, dd = doublet of doublets, m = multiplet, and br = broad. High resolution mass spectra (HRMS) were recorded on Bruker Autoflex MALDI-TOF mass spectrometer. Purity of all final compounds was 95% or higher as determined by high performance liquid chromatography (HPLC) (SHIMADZU

Labsolutions) analysis on the Aglilent C18 column (4.6 × 250 mm, 5 μm) using gradient elution (Mobile Phase: A Phase = ACN, B Phase = 0.3% H_3PO_4 in H_2O) at a flow rate of 1.0 mL/min.

2.1.1 Synthesis of Methyl hex-5-ynoate (2)

To a solution of 5-hexynoic acid (2.00 g, 17.85 mmol) in MeOH (30 mL), DCC (3.67 g, 17.85 mmol) and DMAP (2.40 g,19.64 mmol) were added successively and the mixture was stirred at room temperature for 4 h, then filtrated and concentrated under reduced pressure. Weak acidic water was added and extracted with EtOAc (4 * 30 mL). The organic layers were dried over Na_2SO_4 and the solvent was removed under reduced pressure. The residue was purified by column chromatography to give **2** (1.98 g, yield 88%) as a colorless oil.

2.1.2 Synthesis of Hex-5-ynehydrazide (3)

To the solution of **2** (1.26 g, 10 mmol) in EtOH (30 mL) was added 80% hydrazine hydrate solution in H_2O (1 mL) at room temperature. Then the mixture was stirred at 80°C for 6 h and the solution was evaporated *in vacuo*. The residue was dissolved in EtOAc and washed with aqueous citric acid (*3) and brine (*2). The organic solution was dried over Na_2SO_4, filtered and evaporated *in vacuo*. The residue was purified by column chromatography to obtain **3** (1.02 g, yield 81%) as a yellow solid.

2.1.3 Synthesis of Hydrazine-DOX (4)

Doxorubicin hydrochloride (1.56 g, 2.7 mmol) and **3** (0.38 g, 3.0 mmol) was dissolved in MeOH (30 mL) and treated with 4A molecular sieves following a drop of TFA (20 μL). The resulting mixture was stirred at room temperature for 24 h. Then the solvent was evaporated and the crude product was purified by column chromatography to provide **4** (1.12 g, yield 64%) as a reddish-brown solid.

2.1.4 Synthesis of PPA1-DOX (5)

4 (65.1 mg, 0.1 mmol), azide end-functionalized peptide (PPA1) (102.8 mg, 0.11 mmol) and Tris(benzyltriazolylmethyl)amine (TATB) (10.6 mg, 0.02 mmol) were introduced in a Schlenk tube and 4 mL of DMF: H_2O (v: v = 3:1) were added. The solution was degassed by bubbling argon for 10 min. $CuSO_4.5H_2O$ (5.0 mg, 0.02 mmol) and sodium ascorbate (4.0 mg, 0.02 mmol) were added to the mixture contained in the Schlenk tube and the mixture was degassed once more by bubbling argon for 10 min. The Schlenk tube was filled with argon and stirred at room temperature for 4 h. The solution was filtered and concentrated under vacuum. The resulting crude mixture was purified by HPLC to offer **5** (95.9 mg, yield 43%) as a reddish-brown solid.

2.1.5 Synthesis of RNA-DOX (6), RhB-PPA1-DOX (7) and RhB-RNA-DOX (8)

The conjugates of **6**, **7** and **8** were prepared as the synthetic procedure of conjugate **5**.

2.2 Cell Culture

Mouse colorectal cancer cell line CT26 was purchased from Shanghai Cell Bank of Chinese Academy of Sciences. The cells were maintained in RPMI-1640 medium, supplemented with 10% fetal bovine serum, 1% penicillin-streptomycin, and incubated at 37°C with 5% CO_2 and 95% humidity. The cells were cultured in T75 culture flask and the cell density up to 80% was used in experiments. The cell line was negative for mycoplasma.

2.3 Simulation of Docking Calculation and Molecular Dynamics

The three-dimensional models of PD-L1 were downloaded from Protein Data Bank (PDB) (PDB ID: 3BIK). The structure of the peptides was generated by Chimera 1.14. The molecular dynamic for the coarse structures were implemented for energy minimization and optimization in amber force field. Molecular docking was performed to generate the initial complex of PPA1-DOX or PPA1 and PD-L1 by using Cluspro 2.0 web server. The binding free energy was calculated with MM-PBSA algorithm.

2.4 PD1/PD-L1 Binding Assay

The interaction between Tag1-PD-L1 and Tag2-PD1 is detected by using anti-Tag1-Europium (HTRF donor) and anti-Tag2-XL665 (HTRF acceptor). When the donor and acceptor antibodies are brought into close proximity due to PD-L1 and PD1 binding, excitation of the donor antibody triggers fluorescent resonance energy transfer (FRET) towards the acceptor antibody, which in turn emits specifically at 665 nm. This specific signal is directly proportional to the extent of PD1/PD-L1 interaction. Thus, compound or antibody blocking PD1/PD-L1 interaction will cause a reduction in HTRF signal. The HTRF PD1/PD-L1 binding assay kit was from Cisbio. The IC_{50} is calculated by fitting the dose-response data to a sigmoidal curve, typically using the Hill equation. The calculation is performed by using ECCpy (https://github.com/teese/eccpy).

2.5 The Cleavage Assay for the PPA1-DOX

To verify the acid sensitivity of hydrazone bond linking the PPA1 to DOX, a series of PPA1-DOX and DOX solutions with different concentrations were configured in the sodium phosphate buffer (pH= 9.0), respectively. A 5 μL aliquot of each sample was injected onto an HPLC system with ultraviolet detector wavelength to determine 254 nm absorbance values, using hydrophilic interaction chromatography (HILIC) column separation (Waters, XBridge BEH HILIC XP Column, 2.1 mm, 50 mm, 2.5 μm). Through simulating the linearity fitting from disposed concentrations and detected absorbance values, standard curves of PPA1-DOX and DOX were obtained, respectively.

Preparing two partials of PPA1-DOX (1 mg/mol) were dissolved into the 2 mL sodium phosphate buffer (pH = 5.0) and 2 mL mouse serum (pH = 7.4), respectively, and the vials were capped and kept 37°C under nitrogen with continuously slight oscillaation. Samples (20 μL) were spiked and analyzed by HPLC under the 254 nm absorbance value after incubating

0.5 h, 1 h, 2 h, 4 h, 12 h and 24 h. For evaluation of hydrazone bond cleavage data was considered the disappearance of the major peak related to the standard curves of PPA1-DOX and DOX.

2.6 Immunohistochemistry

The tumor tissues were fixed in 4% paraformaldehyde, gradually dehydrated, embedded in paraffin, cut into 4um sections, and subjected for hematoxylin/eosin staining. For immunohistochemical staining of CD4/CD8 positive cells, tissue sections processed through deparaffinage, rehydration and antigen plerosised, and endogenous peroxidase activity blockade, were incubated with mouse anti-human CD4(1:300, Proteintech, USA), mouse anti-human CD8(1:200, Proteintech, USA) at 4°C overnight, respectively. The secrions were then washed and incubated with a HRP-labeled secondary antibody at RT for 40 min. After color development through incubation with diaminobenzidine, the sections were counterstained with hematoxylin. The stained sections were observed and imaged under a light microscope.

2.7 Ethics Committee Approval

Animal experiments and maintenance were approved by the Laboratory Animal Ethics Committee of Shenzhen University.

2.8 Animal Model

Currently the institute does not provide approval or accreditation number. Six-week-old female Balb/c mice were inoculated subcutaneously with 5×10^6 CT26 cells in the left armpit. The mice were randomly divided into groups with 7 mice in each group after the tumor reached about 100 mm^3. The mice were housed in animal house of Shenzhen University. For the survival experiment, the mice were killed when the tumor reached about 1500 mm^3. The tumor size and body weight were monitored every day after the injection of the drugs. At the end of the experiment, the tumors and major organs (heart, liver, spleen, lung, and kidney) were collected for immunohistochemistry and/or histological tests. For the PPA1-DOX distribution experiment, the tumors and major organs were subsequently analyzed with an *in vivo* imaging system (IVIS Spectrum, PerkinElmer).

2.9 Dosage of the Injection to Mice

DOX at 5 mg/kg, 5-Fu at 10 mg/kg, PPA1 and RAN at 15mg/kg, PPA1-DOX and RAN-DOX at 20 mg/kg were injected intraperitoneally to mice twice a week for two weeks. From the fifteen day, no further injections of the drugs were given because mice injected with 5-Fu and DOX became very sick due to toxicity. For the PPA1-DOX distribution experiment, RhB-PPA1-DOX and RhB-RAN-DOX at 20mg/kg were injected into the tail vein of the mice.

2.10 Statistical Analysis

All the variables were expressed as mean ± standard deviation. Student's t-test or one-way analyses of variance (ANOVA) were performed in statistical evaluation. A p-value <0.05 was considered to be significant.

3 RESULTS

3.1 Design of the Polypeptide-Drug Conjugate

A tumor-specific targeted synergistic strategy was designed by coupling anti-PD-L1 polypeptide with chemotherapy for colon cancer, where a proteolysis resistant PD-L1-targeted peptide PPA1 was conjugated to DOX with a pH sensitive linker (**Figure 1A**). To verify the binding mode of PD-L1 and PD-1, we downloaded and visualized the crystal complex of PD-L1 and PD-1. PD-L1 is composed of one N-terminal V domain and one C-terminal C domain, which are joined by a short linker (22). The complex shows that PD-1 binds to the V domain of PD-L1 (**Figure 1B**). The PD-1/PD-L1 interaction could then halt or limit the development of the T cell response (23). Polypeptide PPA1 was reported to show the potential of targeting PD-L1 in colorectal cancer cell. In order to ensure the binding mode of PD-L1 and polypeptide PPA1, we performed a protein-peptide docking simulation. The results show that PPA1 possesses the PD-1 binding position, which could competitively bind to the V domain of PD-L1 (**Figure 1C**). Thus, we designed the polypeptide-drug conjugate by linking the C terminal (tail) of PPA1 and the carboxylic acid group of DOX with a linker (**Figure 1D**). Quantitatively, further binding free energy of PPA1 and PPA1-DOX showed no significant difference when binding to PD-L1.

3.2 Synthesis of the PD-L1-Targeted Peptide-DOX Conjugate (PPA1-DOX)

For the synthesis of acid-sensitive PPA1-DOX (**Figure 2**), the carboxylic acid group of 5-hexynoic acid **1** was reacted with methanol under the condensation reagent of DCC and catalysis reagent of DMAP to effectively provide the methyl 5-hexynoate **2**. Ester **2** was treated with 80% aqueous hydrazine hydrate in ethanol at 80°C for 6 hours to smoothly give acyl hydrazide **3**. The desired compound **4** with an acid-sensitive hydrazone was afforded by compound **3** coupling to commercially available doxorubicin in methanol. Compound **4** was allowed to undergo cycloaddition reaction with various peptide azides under sharpless click chemistry condition to offer the target compound **5** (PPA1-DOX) in good to excellent yields. Compound **6** (RAN-DOX) was synthesized in the similar routine by using a random polypeptides. Compound **7** and **8** with rhodamine (RhB) were designed and synthesized to verify the distribution of the compounds. The intermediates were characterized by Nuclear Magnetic Resonance (NMR), including 1H-NMR, 13C-NMR, and high resolution mass spectrometry (HRMS), and the conjugates were confirmed by high performance liquid chromatography (HPLC) and HRMS. (**Supplementary Figures S1**–**S7**).

3.3 PPA1-DOX Conjugate Cleavages Around Tumor-Like Environment

We designed an acidic pH sensitive linker to link the polypeptide and drug. To test whether the acidic pH sensitive linker can enable the split of PPA1-DOX construct into two components around the

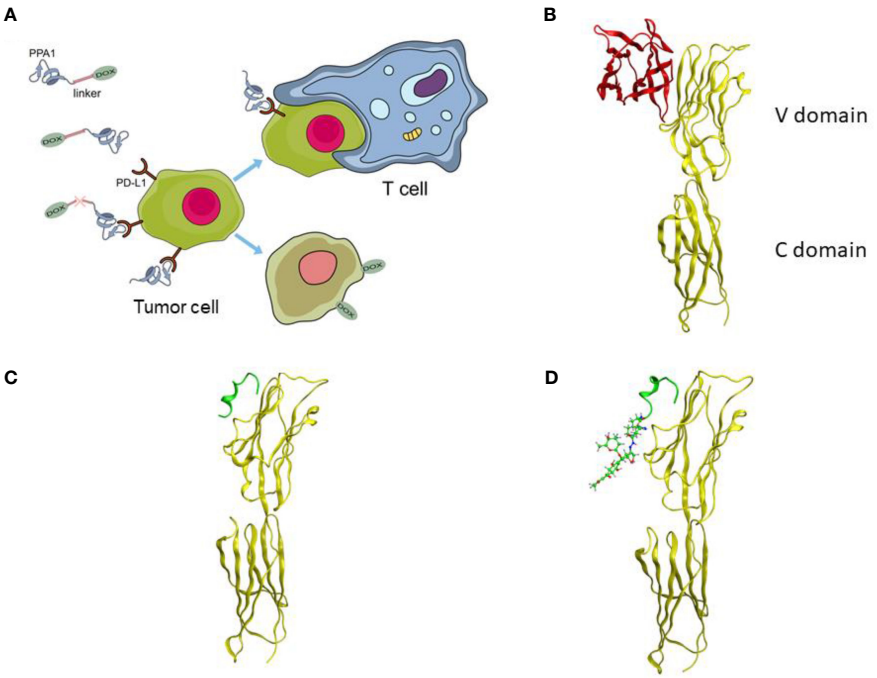

FIGURE 1 | The design of the polypeptide-drug conjugate (PPA1-DOX). **(A)** The mechanism of tumor inhibition by PPA1-DOX. **(B)** The crystal structure of the PD-1/PD-L1 complex from Protein Data Bank (PDB ID: 3BIK). **(C)** The structure of PD-L1/PPA1 from molecular dynamic simulation. **(D)** The structure of PD-L1/PPA1-DOX from molecular dynamic simulation. The yellow ribbon structure stands for PD-L1; The red ribbon structure stands for PD-1; The green ribbon structure stands for PPA1; The green stick and ball molecule stands for DOX.

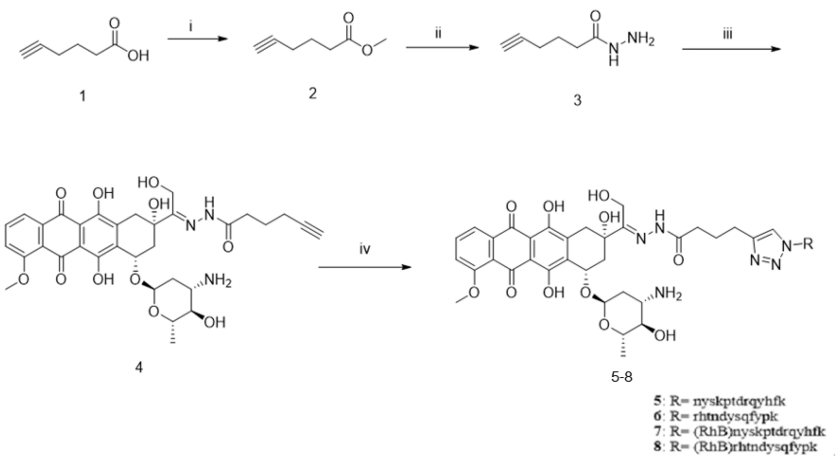

FIGURE 2 | The synthesis of PPA1-DOX conjugate with an acid-labile linker. Reagents and conditions: (i) MeOH, DCC, DMAP, r.t., 4h; (ii) NH_2-NH_2 80% in H_2O, EtOH, 80°C, 6h; (iii) doxoriubicin, TFA, MeOH, 4A molecular sieves, r.t., 24h, (iv) nyskptdrqyhf-Lys(N_3), $CuSO_4.5H_2O$, sodium ascorbate, TBTA, DMF/H_2O, r.t., 4h, N_2.

tumor tissue, the HPLC experiment was performed (**Figures 3A, B**). When PPA1-DOX conjugate was incubated in the mouse serum (pH=7.4) at 37°C for 24 h, the HPLC result showed little change on peaks, suggesting that PPA1-DOX conjugate existed stable in nearly neutral solution. In contrast, in an acidic environment (pH=5.0), HPLC results implied that PPA1-DOX conjugate rapidly cleaved into PPA1 and DOX (**Supplementary Figure S8**). Given the neutral physiological environment around normal tissue and the acidic microenvironment around solid tumor tissues, these results thus indicate that PPA1-DOX conjugate is able to stay steady in normal tissue, while release DOX to tumor tissues due to the cleavage of acidic pH sensitive linker.

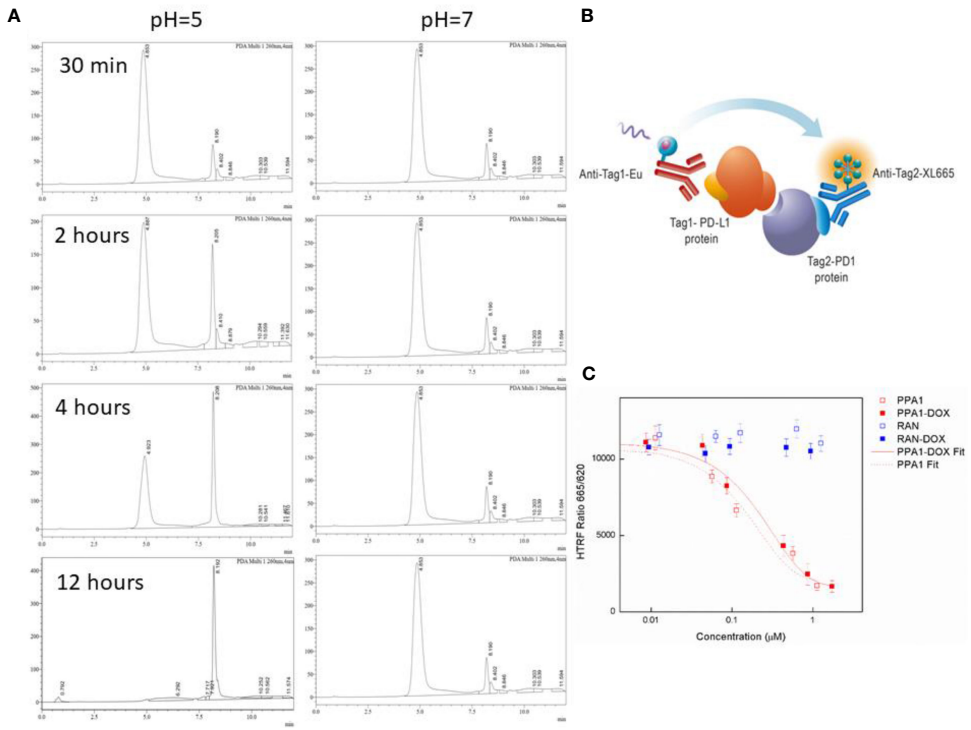

FIGURE 3 | The cleavage and binding affinity of the PPA1-DOX conjugate. **(A)** Representative HPLC chromatograms of PPA1-DOX in mouse serum (pH = 7.4) upon time. Representative HPLC chromaograms of PPA1-DOX and free DOX in the weak-acid PBS buffer (pH = 5) upon time. **(B)** The mechanism of HTRF assay to test the blocking of PD-1 and PD-L1. **(C)** The result of HTRF assay of 4 kinds of drugs. Error bars indicate mean± standard deviation. n = 3.

3.4 PPA1-DOX Conjugate Exhibits High Binding Affinity With PD-L1

The HTRF (Homogeneous Time-resolved Fluorescence) PD1/PD-L1 binding assay is designed to measure the interaction between PD1 and PD-L1 proteins. By utilizing HTRF technology, the assay enables simple and rapid characterization of compound and antibody blockers in a high throughput format (**Figure 3C**). The detailed information is listed in Material and Methods section. The HTRF data showed no significant difference in the binding affinity between free PPA1 and PPA1-DOX with PD-L1. The inhibition effect of compounds and PD-L1 was shown in **Figure 3D**, with the IC_{50} = 0.174 μM of PPA1 and IC_{50} = 0.281 μM of PPA1-DOX, respectively. The results suggested that the PPA1-DOX conjugate did not affect the interaction between PPA1 and PD-L1, which is consistent with the calculated results. Of note, both of the random polypeptide (RAN) and RAN-DOX conjugate exhibited low binding affinity with PD-L1.

3.5 PPA1-DOX Conjugate Shows Low Toxicity *In Vivo*

Since DOX can cause multi-organ toxicities in various patients, including cumulative and dose-dependent cardiotoxicity (24), we evaluated the toxicity of PPA1-DOX conjugate *in vivo*. Firstly, we measured the body weight of the tumor-bearing mice every day after 10 days of CT26 subcutaneous injection. The DOX and 5-Fu treated group showed significant weight loss after day 7, suggesting that the chemotherapeutic reagents could cause the potential systematic toxicity. In contrast, no remarkable body weight loss was observed in PPA1 and PPA1-DOX groups (**Figure 4A**). Then, the histology analysis with H&E staining was performed to evaluate the *in vivo* toxicity to major organs. The chemotherapy treated groups (DOX and 5-Fu) showed severe damages in the H&E stained sections of heart, liver and kidney, respectively (**Figure 4B**). The cytoplasmic vacuolation and loss of myofibrillar were observed in heart damage. For liver damage, hepatic cords loss, mild steatosis, and dilatation of blood sinus were observed. By contrast, PPA1-DOX and free PPA1 exhibit rather low toxicity to major organs of tumor-bearing mice.

3.6 PPA1-DOX Conjugate Improves Tumor-Specific Drug Delivery and Enhances Immune Response *In Vivo*

Firstly, to test the specificity of tumor targeting by the PPA1-DOX conjugate, we synthesized RhB-PPA1-DOX (fluorescence of PPA1-DOX) and RhB-RAN-DOX (fluorescence of a random polypeptides-DOX) and evaluated the biodistribution of the compound in the CT26-bearing mice after 24h intravenous injection by collecting major organs for *ex vivo* fluorescence imaging. We found that the RhB signals in the tumor tissues of RhB-PPA1-DOX group were remarkably higher than those of

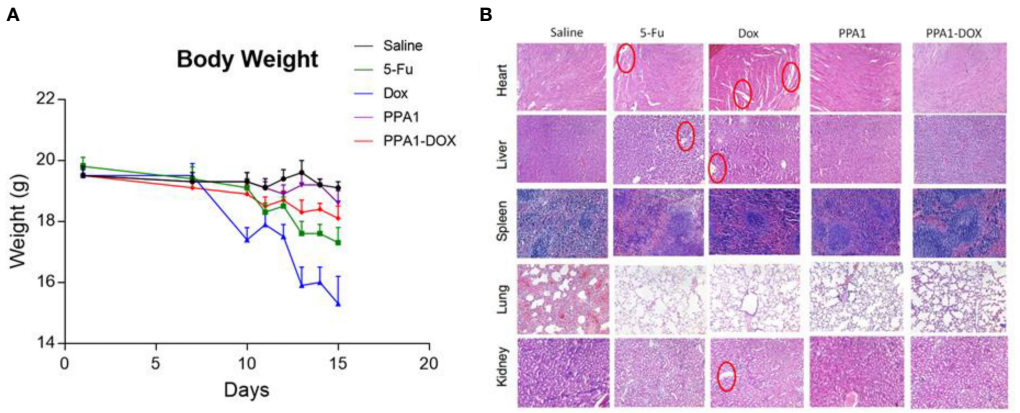

FIGURE 4 | The toxicity of PPA1-DOX for treating CT26-bearing mice. **(A)** The body weight analysis of 5 groups of treatment at a dosing frequency of twice a week *via* intraperitoneal injection. **(B)** H&E staining analysis of individual tissues from 5 respective treatment groups. The cytoplasmic vacuolation and loss of myofibrillar were observed in heart damage in 5-Fu and Dox groups. For liver damage, hepatic cords loss, mild steatosis, and dilatation of blood sinus were observed in 5-Fu and Dox groups. All the damages were highlighted in red circles. Scale bars, 100 μm. The data were represented by means ± SEM. n = 7.

RhB-RAN-DOX group (**Figure 5A**), while the one in liver tissues of RhB-PPA1-DOX group were significant lower than those of RhB-RAN-DOX group (**Figure 5A**), suggesting that a tumor-specific targeting was achieved by the PPA1-DOX construct. Accordingly, the improved specificity of tumor-targeted drug delivery by PPA1-DOX renders itself a significantly increased antitumor activity, as demonstrated by improved tumor growth inhibition and prolonged survival time in PPA-DOX-treated CT26 bearing mice, in comparison with RAN-DOX-treated group (**Figures 5B, C**). Interestingly, despite that PPA1-DOX and PPA1 are expected to harbour similar targeting ability in principle, the PPA1-DOX treatment led to effective suppression of tumor growth and longer survival time superior to free PPA1 treatment, most probably benefited from the cytotoxic effect of DOX once released into tumor tissues (**Figures 5B, C**).

Last but not least, to evaluate the functional reinvigoration of tumor-infiltrating lymphocytes, a sign for successful immune checkpoint blockage, we examined the functional effect of PPA1-

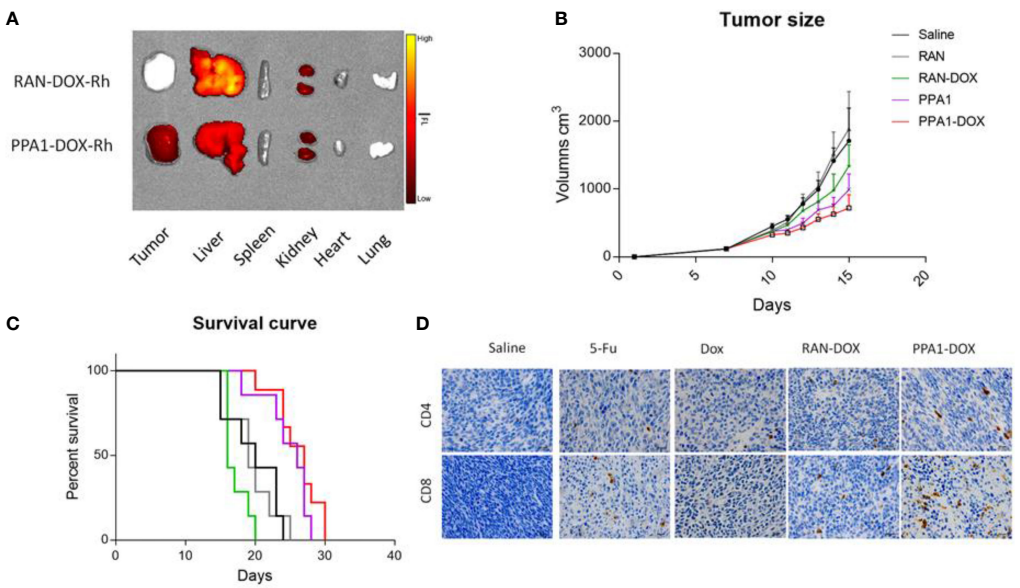

FIGURE 5 | The antitumor activity of PPA1-DOX in CT26-bearing mice. **(A)** The distribution of PPA1-DOX-RhB and RAN-DOX-RhB in tumor and major tissues at 24h post-intravenous injection. **(B)** Analysis of tumor sizes from 5 respective treatment group at a dosing frequency of twice a week *via* intraperitoneal injection. **(C)** The survival curve of 5 groups of treatment at a dosing frequency of twice a week *via* intraperitoneal injection. **(D)** CD4 and CD8 immunohistochemical staining of tumor tissues from the respective treatment group. Scale bars, 50 μm. The data were represented by means ± SEM. n = 7.

DOX on restoring intratumoral $CD4^+$ and $CD8^+$ T cells by immunohistochemistry staining. We found that tumors from PPA1-DOX-treated mice showed obviously increased infiltration of both $CD4^+$ and $CD8^+$ T cells, as compared with RNA-DOX-, DOX-, or 5-FU-treated mice, respectively (**Figure 5D**), suggesting that PPA1-DOX can enhance immune response in colon cancer due to disruption of the inhibitory PD-1/PD-L1 immune checkpoint by the PD-L1 targeted polypeptide PPA1. The positive cell number of different groups for CD4 and CD8 were provided in **Supplementary Figure S9**.

4 DISCUSSION

Severe toxic side effects and developed drug resistance are the major drawbacks of DOX in its clinical use in treating colon cancer (21, 25). Modifying the structure of DOX offers the opportunity to overcome these limitations. Recently, a novel proteolysis resistant PD-L1-targeted polypeptide, PPA1, has appeared as an outstanding tumor-targeting modification of synergistic drug conjugate for effective anti-tumor treatment (18). However, the combination regimen of coupling PD-L1 polypeptide with DOX in anti-tumor treatment has not been reported so far. In this study, we developed a novel synergistic strategy in which PPA1 was conjugated to DOX with a pH sensitive linker. Such sophisticated design could enable a tumor-specific targeted delivery of the conjugate to PD-L1 expressing tumor cells with the guidance of PPA1, as well as the controlled release of DOX to acidic tumor tissues due to the cleavage of acid-sensitive linker, thus reducing the toxicity of DOX to non-tumor tissues. In addition, given that the antitumor mechanism of DOX is its action as a topoisomerase II poison by intercalating DNA *via* its anthracycline structure (26–28) (**Supplementary Figure S10**) to inhibit DNA replication, the pH sensitive linker was designed to be connected to the azide part of DOX to reduce the steric hindrance from PPA1 (**Figure 2**). As a result, PPA1-DOX conjugate was found to exhibit a significantly lower toxicity to non-tumor cells, in particular for cardiomyocytes and hepatocytes that are major toxic targets of DOX (28, 29), and a remarkably higher antitumor activity *in vivo*, as compared with DOX and free PPA1, respectively. Of note, despite that PPA1-DOX and PPA1 are expected to harbor similar targeting ability in principle, the superiority of PPA1-DOX in tumor treatment is most likely benefited from the cytotoxic effect of DOX once released into tumor tissues, demonstrating that the combination regimen of coupling PD-L1 polypeptide with DOX represents a potential targeted treatment strategy of colon cancer.

In order to verify that the improved therapeutic efficacy and reduced toxicity of the PPA1-DOX conjugate is attributed to the tumor-targeted delivery offered by the PPA1 polypeptide, but not to the random changes in the surface modification of DOX, a random polypeptide (RAN) was conjugated to DOX as a control and the biodistribution of the fluorescence labelled compound was evaluated in the CT26-bearing mice after intravenous injection. As expected, a remarkably higher tumor-specific enrichment and lower distribution in other non-tumor major tissues was achieved by the PPA1-DOX construct, as compared with the RAN-DOX construct. Accordingly, PPA-DOX conjugate demonstrated a significantly increased antitumor activity and remarkably reduced off-target toxicity, in comparison with RAN-DOX construct, which even though showed a weak tumor inhibition effect, probably due to a few of DOX released from RAN-DOX conjugate. Thus, delivery of DOX guided by PD-L1-targeted polypeptide contributes to the improved anti-tumor effect of PPA1-DOX conjugate.

It is worth to note that the traditional drug delivery system, including DNA aptamers (11), RNA aptamers (30), peptide aptamers (12) *etc.*, could only deliver the drugs to specific target cells or proteins with little activity itself. Compared to the traditional drug delivery system, PPA1 not only acts as a targeting navigator for the drug, but also binds with PD-L1 to improve the antitumor activity of immune cells. It is well known that when PD-L1 is bound to PD-1, these 'coinhibitory' receptors function as breaks for the adaptive immune response to protect the host from being attacked by its own adaptive immune system, serving as immune checkpoints that effector T cells must pass to exert their functions (31). However, some cancers, including colon cancer, exploit this negative feedback loop by expressing PD-L1 to avoid being killed by T cells. Recently, antagonizing the PD-1/PD-L1 interaction has been shown to revert the exhausted phenotype of T cells and allow efficient killing of tumor cells (32, 33). In this study, binding of PD-1 by PPA1-DOX was approved *in vitro* and increased infiltration of both $CD4^+$ and $CD8^+$ T cells was found in tumors from PPA1-DOX treated mice. $CD4^+$ and $CD8^+$ T cell responses are part of the cancer immune cycle, which significantly influence the clinical treatment outcome, while the phenotype of T cell exhaustion usually occurs in both CD4+ and CD8+ T cell populations (34). Therefore, the increased $CD4^+$ and $CD8^+$ T cell frequencies by PPA1-DOX indicates that this conjugate is able to restore T cell function and enhance immune response in colon cancer.

The antimetabolite 5-FU remains a mainstay of standard therapy in colon cancer and is effective as a part of combination therapies that induce remissions (35). However, the chemical structure of 5-FU lacks the active synthetic site for PPA1 linker conjugation. We are working on PPA1 targeting nanoparticles, which could deliver various kinds of drugs to tumor tissues.

5 CONCLUSION

To summarize, we have designed and synthesized a novel strategy of coupling PD-L1 polypeptide with cytotoxic agent for tumor-targeted therapy in colon cancer, in which a proteolysis resistant PD-L1 targeting peptide PPA1 is conjugated with DOX by a pH sensitive linker, which could trigger the release of drugs near tumor tissues. Our data demonstrate that PPA1-DOX harbour high binding affinity with PD-L1 *in vitro* and specifically enriched within tumor when administered *in vivo*. Importantly, PPA1-DOX exhibits a significantly improved antitumor activity *in vivo*, most likely by

alleviating chemotherapeutic resistance of DOX and enhancing immune response in colon cancer. Thus, targeted delivery of chemotherapeutic reagent to tumor tissues by PD-L1 polypeptide represents a potential treatment strategy of colon cancer with improved efficacy and reduced toxicity.

DATA AVAILABILITY STATEMENT

The original contributions presented in the study are included in the article/**Supplementary Material**. Further inquiries can be directed to the corresponding authors.

ETHICS STATEMENT

The animal study was reviewed and approved by Laboratory Animal Ethics Committee of Shenzhen University.

AUTHOR CONTRIBUTIONS

MW, X-sS, and YY conceived the study and wrote the manuscript. ML and YZ performed experiments. YoY and XH: Data Curation. PW: Validation. ZH and JiL: Writing – Review & Editing. JuL and YiY: Supervision and Funding Acquisition. All authors contributed to the article and approved the submitted version.

FUNDING

This work was supported by Shenzhen Commission of Science and Innovation programs (JCYJ20200109105613463; JCYJ20190808145211234; JCYJ20190808165003697; JCYJ20180302174121208), National Science Foundation of China (81803374; 82070978; 21807090; 81973293), Natural Science Foundation of Guangdong Province, China (Grant No. 2021A1515012436; 2020A1515010196; 2020A1515010125), SZU Medical Young Scientist Program (71201-000001), SZU Top Ranking Project (86000000210) and Medical science foundation of Guangdong province (A2017072).

ACKNOWLEDGMENTS

We thank Mr. Junbo Yi from Instrumental Analysis Center of Shenzhen University (Xili Campus) for his technical support. We also thank the College of Pharmacy, Shenzhen Technology University for the publication fee support.

SUPPLEMENTARY MATERIAL

The Supplementary Material for this article can be found online at: https://www.frontiersin.org/articles/10.3389/fonc.2021.737323/full#supplementary-material

REFERENCES

1. Gustavsson B, Carlsson G, Machover D, Petrelli N, Roth A, Schmoll H-J, et al. A Review of the Evolution of Systemic Chemotherapy in the Management of Colorectal Cancer. *Clin Colorectal Cancer* (2015) 14:1–10. doi: 10.1016/j.clcc.2014.11.002
2. Breugom AJ, Swets M, Bosset J-F, Collette L, Sainato A, Cionini L, et al. Adjuvant Chemotherapy After Preoperative (Chemo)Radiotherapy and Surgery for Patients With Rectal Cancer: A Systematic Review and Meta-Analysis of Individual Patient Data. *Lancet Oncol* (2015) 16:200–7. doi: 10.1016/S1470-2045(14)71199-4
3. Hutchinson AD, Hosking JR, Kichenadasse G, Mattiske JK, Wilson C. Objective and Subjective Cognitive Impairment Following Chemotherapy for Cancer: A Systematic Review. *Cancer Treat Rev* (2012) 38:926–34. doi: 10.1016/j.ctrv.2012.05.002
4. Flygare JA, Pillow TH, Aristoff P. Antibody-Drug Conjugates for the Treatment of Cancer. *Chem Biol Drug Design* (2013) 81:113–21. doi: 10.1111/cbdd.12085
5. Sievers EL, Senter PD. Antibody-Drug Conjugates in Cancer Therapy. *Annu Rev Med* (2013) 64:15–29. doi: 10.1146/annurev-med-050311-201823
6. Alley SC, Okeley NM, Senter PD. Antibody–Drug Conjugates: Targeted Drug Delivery for Cancer. *Curr Opin Chem Biol* (2010) 14:529–37. doi: 10.1016/j.cbpa.2010.06.170
7. Cerchia L, de Franciscis V. Targeting Cancer Cells With Nucleic Acid Aptamers. *Trends Biotechnol* (2010) 28:517–25. doi: 10.1016/j.tibtech.2010.07.005
8. Xiang D, Shigdar S, Qiao G, Wang T, Kouzani AZ, Zhou S-F, et al. Nucleic Acid Aptamer-Guided Cancer Therapeutics and Diagnostics: The Next Generation of Cancer Medicine. *Theranostics* (2015) 5:23–42. doi: 10.7150/thno.10202
9. Xuan W, Peng Y, Deng Z, Peng T, Kuai H, Li Y, et al. A Basic Insight Into Aptamer-Drug Conjugates (Apdcs). *Biomaterials* (2018) 182:216–26. doi: 10.1016/j.biomaterials.2018.08.021
10. Zhang Y, Lai BS, Juhas M. Recent Advances in Aptamer Discovery and Applications. *Molecules* (2019) 24:941–5. doi: 10.3390/molecules24050941
11. Li F, Lu J, Liu J, Liang C, Wang M, Wang L, et al. A Water-Soluble Nucleolin Aptamer-Paclitaxel Conjugate for Tumor-Specific Targeting in Ovarian Cancer. *Nat Commun* (2017) 8:1390. doi: 10.1038/s41467-017-01565-6
12. Reverdatto S, Burz DS, Shekhtman A. Peptide Aptamers: Development and Applications. *Curr Top Med Chem* (2015) 15:1082–101. doi: 10.2174/1568026615666150413153143
13. Powles T, Eder JP, Fine GD, Braiteh FS, Loriot Y, Cruz C, et al. MPDL3280A (Anti-PD-L1) Treatment Leads to Clinical Activity in Metastatic Bladder Cancer. *Nature* (2014) 515:558–62. doi: 10.1038/nature13904
14. Topalian SL, Drake CG, Pardoll DM. Targeting the PD-1/B7-H1(PD-L1) Pathway to Activate Anti-Tumor Immunity. *Curr Opin Immunol* (2012) 24:207–12. doi: 10.1016/j.coi.2011.12.009
15. Reck M, Rodríguez-Abreu D, Robinson AG, Hui R, Csőszi T, Fülöp A, et al. Pembrolizumab Versus Chemotherapy for PD-L1–Positive Non–Small-Cell Lung Cancer. *New Engl J Med* (2016) 375:1823–33. doi: 10.1056/NEJMoa1606774
16. Mittendorf EA, Philips AV, Meric-Bernstam F, Qiao N, Wu Y, Harrington S, et al. PD-L1 Expression in Triple-Negative Breast Cancer. *Cancer Immunol Res* (2014) 2:361–70. doi: 10.1158/2326-6066.CIR-13-0127
17. Zou W, Wolchok JD, Chen L. PD-L1 (B7-H1) and PD-1 Pathway Blockade for Cancer Therapy: Mechanisms, Response Biomarkers, and Combinations. *Sci Trans Med* (2016) 8:328rv4–4. doi: 10.1126/scitranslmed.aad7118
18. Chang H-N, Liu B-Y, Qi Y-K, Zhou Y, Chen Y-P, Pan K-M, et al. Blocking of the PD-1/PD-L1 Interaction by a D-Peptide Antagonist for Cancer Immunotherapy. *Angewandte Chemie Int Edition* (2015) 54:11760–4. doi: 10.1002/anie.201506225
19. Zhang X, Lin Y, Gillies RJ. Tumor Ph and Its Measurement. *J Nucl Med* (2010) 51:1167–70. doi: 10.2967/jnumed.109.068981
20. Lu J, Wang M, Wang Z, Fu Z, Lu A, Zhang G. Advances in the Discovery of Cathepsin K Inhibitors on Bone Resorption. *J Enzyme Inhib Med Chem* (2018) 33:890–904. doi: 10.1080/14756366.2018.1465417

21. Xiong S, Xiao G-W. Reverting Doxorubicin Resistance in Colon Cancer by Targeting a Key Signaling Protein, Steroid Receptor Coactivator. *Exp Ther Med* (2018) 15:3751–8. doi: 10.3892/etm.2018.5912
22. Lin DY, Tanaka Y, Iwasaki M, Gittis AG, Su H-P, Mikami B, et al. The PD-1/PD-L1 Complex Resembles the Antigen-Binding Fv Domains of Antibodies and T Cell Receptors. *Proc Natl Acad Sci USA* (2008) 105:3011–6. doi: 10.1073/pnas.0712278105
23. Salmaninejad A, Valilou SF, Shabgah AG, Aslani S, Alimardani M, Pasdar A, et al. PD-1/PD-L1 Pathway: Basic Biology and Role in Cancer Immunotherapy. *J Cell Physiol* (2019) 234:16824–37. doi: 10.1002/jcp.28358
24. Pugazhendhi A, Edison TNJI, Velmurugan BK, Jacob JA, Karuppusamy I. Toxicity of Doxorubicin (Dox) to Different Experimental Organ Systems. *Life Sci* (2018) 200:26–30. doi: 10.1016/j.lfs.2018.03.023
25. Rivankar S. An Overview of Doxorubicin Formulations in Cancer Therapy. *J Cancer Res Ther* (2014) 10:853–8. doi: 10.4103/0973-1482.139267
26. Frederick CA, Williams LD, Ughetto G, van der Marel GA, Van Boom JH, Rich A, et al. Structural Comparison of Anticancer Drug-DNA Complexes: Adriamycin and Daunomycin. *Biochemistry* (1990) 29:2538–49. doi: 10.1021/bi00462a016
27. Fornari FA, Randolph JK, Yalowich JC, Ritke MK, Gewirtz DA. Interference by Doxorubicin With DNA Unwinding in MCF-7 Breast Tumor Cells. *Mol Pharmacol* (1994) 45:649–56.
28. Pommier Y, Leo E, Zhang H, Marchand C. DNA Topoisomerases and Their Poisoning by Anticancer and Antibacterial Drugs. *Chem Biol* (2010) 17:421–33. doi: 10.1016/j.chembiol.2010.04.012
29. Zhao X, Jin Y, Li L, Xu L, Tang Z, Qi Y, et al. Microrna-128-3p Aggravates Doxorubicin-Induced Liver Injury by Promoting Oxidative Stress *via* Targeting Sirtuin-1. *Pharmacol Res* (2019) 146:104276. doi: 10.1016/j.phrs.2019.104276
30. Bell DR, Weber JK, Yin W, Huynh T, Duan W, Zhou R. *In Silico* Design and Validation of High-Affinity RNA Aptamers Targeting Epithelial Cellular Adhesion Molecule Dimers. *PNAS* (2020) 117:8486–93. doi: 10.1073/pnas.1913242117
31. Chen L, Han X. Anti-PD-1/PD-L1 Therapy of Human Cancer: Past, Present, and Future. *J Clin Invest* (2015) 125:3384–91. doi: 10.1172/JCI80011
32. Pauken KE, Wherry EJ. Overcoming T Cell Exhaustion in Infection and Cancer. *Trends Immunol* (2015) 36:265–76. doi: 10.1016/j.it.2015.02.008
33. Topalian SL, Drake CG, Pardoll DM. Immune Checkpoint Blockade: A Common Denominator Approach to Cancer Therapy. *Cancer Cell* (2015) 27:450–61. doi: 10.1016/j.ccell.2015.03.001
34. Shankaran V, Ikeda H, Bruce AT, White JM, Swanson PE, Old LJ, et al. IFNγ and Lymphocytes Prevent Primary Tumour Development and Shape Tumour Immunogenicity. *Nature* (2001) 410:1107–11. doi: 10.1038/35074122
35. Das D, Preet R, Mohapatra P, Satapathy SR, Siddharth S, Tamir T, et al. 5-Fluorouracil Mediated Anti-Cancer Activity in Colon Cancer Cells Is Through the Induction of Adenomatous Polyposis Coli: Implication of the Long-Patch Base Excision Repair Pathway. *DNA Repair (Amst)* (2014) 24:15–25. doi: 10.1016/j.dnarep.2014.10.006

Conflict of Interest: The authors declare that the research was conducted in the absence of any commercial or financial relationships that could be construed as a potential conflict of interest.

Publisher's Note: All claims expressed in this article are solely those of the authors and do not necessarily represent those of their affiliated organizations, or those of the publisher, the editors and the reviewers. Any product that may be evaluated in this article, or claim that may be made by its manufacturer, is not guaranteed or endorsed by the publisher.

frontiers in Oncology

ORIGINAL RESEARCH
published: 25 November 2021
doi: 10.3389/fonc.2021.774445

Preliminary Efficacy and Safety of Camrelizumab in Combination With XELOX Plus Bevacizumab or Regorafenib in Patients With Metastatic Colorectal Cancer: A Retrospective Study

*Hong Zhou[1], Yuehui Wang[2], Yanfang Lin[1], Wenjie Cai[3], Xiaofeng Li[4] and Xiaomeng He[5]**

[1] Department of Pharmacy, First Hospital of Quanzhou Affiliated to Fujian Medical University, Quanzhou, China, [2] Department of Radiology, First Hospital of Quanzhou Affiliated to Fujian Medical University, Quanzhou, China, [3] Department of Radiation Oncology, First Hospital of Quanzhou Affiliated to Fujian Medical University, Quanzhou, China, [4] Department of Medical Oncology, First Hospital of Quanzhou Affiliated to Fujian Medical University, Quanzhou, China, [5] Department of Pharmacy, The First Affiliated Hospital of Dalian Medical University, Dalian, China

Background: For a majority of patients with metastatic colorectal cancer (mCRC) with MS stable (MSS) or mismatch repair proficient (pMMR), the role of immunotherapy is undetermined. This study investigated the efficacy and safety of camrelizumab when added to XELOX chemotherapy plus bevacizumab or regorafenib as first-line therapy for mCRC.

Materials and Methods: Medical records of mCRC patients who received camrelizumab and XELOX plus bevacizumab or regorafenib at the First Hospital of Quanzhou Affiliated to Fujian Medical University between June 1, 2019, and April 30, 2021, were retrospectively collected. The objective response rate (ORR), disease control rate (DCR), progression-free survival (PFS), overall survival (OS), and side effects of the drug were recorded and reviewed.

Results: Twenty-five eligible patients received combination therapy, including bevacizumab in 19 patients and regorafenib in 6. Twenty-one patients had pMMR/MSS and one MSI-H. Of the 25 patients who could be evaluated for efficacy, 18 (72%) achieved PR, 6 (24%) achieved SD, and 1 (4%) achieved PD. The ORR and DCR were 72% (18/25) and 96% (24/25), respectively. The median progression-free survival (PFS) was 11.2 months (95% CI 8.9–13.9), and OS had not yet been reached. The combination regimen of regorafenib in six (24%) patients was unassociated with treatment outcomes. Most AEs were either grade 1 or 2, and treatment-related grade 3 toxicities were observed in 8/25 (32%) patients.

OPEN ACCESS

Edited by:
Vita Golubovskaya, ProMab Biotechnologies, United States

Reviewed by:
Ravindra Deshpande, Wake Forest School of Medicine, United States
Louise Catherine Connell, Cornell University, United States

***Correspondence:**
Xiaomeng He
hxm1987@alumni.hust.edu.cn

Specialty section:
This article was submitted to Gastrointestinal Cancers: Colorectal Cancer, a section of the journal Frontiers in Oncology

Received: *12 September 2021*
Accepted: *08 November 2021*
Published: *25 November 2021*

Citation:
Zhou H, Wang Y, Lin Y, Cai W, Li X and He X (2021) Preliminary Efficacy and Safety of Camrelizumab in Combination With XELOX Plus Bevacizumab or Regorafenib in Patients With Metastatic Colorectal Cancer: A Retrospective Study. Front. Oncol. 11:774445. doi: 10.3389/fonc.2021.774445

Conclusion: Camrelizumab combined with XELOX plus bevacizumab or regorafenib was feasible, producing high rates of responses as first-line therapy in unselected Chinese patients with MSS mCRC. The toxicities were generally tolerable and manageable. Prospective randomized trials with large sample sizes are needed to evaluate these findings.

Keywords: colorectal cancer, camrelizumab, immune checkpoint inhibitor, microsatellite stable, bevacizumab, regorafenib

INTRODUCTION

Immune checkpoint inhibitors (ICIs) have been shown to benefit patients with metastatic colorectal cancer (mCRC) with mismatch repair deficiency (dMMR) or high microsatellite instability (MSI-H) (1, 2). However, PD-1/PDL1 blockade immunotherapy is not effective in pMMR/MSS, which constitutes a large population of patients (3). Ongoing clinical trials are evaluating the efficacy of immunotherapy-based strategies, including chemotherapy, radiotherapy, MEK inhibitors, or other agents in pMMR/MSS mCRC (4). In the REGONIVO study (5), regorafenib combined with nivolumab produced an ORR of 33% (95% CI, 15.6% to 55.3%) in 24 patients with pMMR/MSS refractory mCRC, indicating that anti-angiogenic drugs may enhance the efficacy of immune checkpoint inhibitors. In addition, a single-arm phase II AVETUX trial produced a high ORR of 79.5% in 39 patients, showing the feasibility and early efficacy of avelumab and cetuximab combined with FOLFOX as first-line therapy in RAS/BRAF wildtype MCRC patients (6).

Camrelizumab (SHR-1210) a high-affinity, humanized immunoglobulin and selective IgG4-anti-PD-1 monoclonal antibody, has been approved for the treatment of classical Hodgkin's lymphoma, advanced hepatic cancer, advanced esophageal cancer, and advanced non-small-cell lung cancer in China (7). Camrelizumab is one of the most widely used anti-PD-1 antibodies for various solid tumors in real-time practice owing to drug accessibility and economic pressure for patients in China. It has shown promising clinical efficacy in several kinds of solid tumors, based on positive efficacy results in clinical trials (8–11), and has also been shown to be effective in MSI-H/dMMR solid tumors (12). The combination of regorafenib and camrelizumab achieved an ORR of 25% in 16 patients with MSS refractory mCRC, indicating the potential benefit of immunotherapy under an appropriately combined therapeutic strategy (13). Hence, we evaluated the efficacy and safety of camrelizumab when added to the first-line XELOX chemotherapy with bevacizumab or regorafenib in patients with metastatic colorectal cancer.

MATERIALS AND METHODS

Patients

The medical records of patients with mCRC who were treated with camrelizumab combined with XELOX plus bevacizumab or regorafenib at the First Hospital of Quanzhou Affiliated to Fujian Medical University between June 1, 2019, and April 30, 2021, were retrieved. The data cutoff date was October 15, 2021. Eligibility for inclusion included histologically-confirmed metastatic colorectal cancer, treated with camrelizumab combined with XELOX plus bevacizumab or regorafenib and no prior systemic therapy, and one or more uni-dimensional measurable lesions according to Response Evaluation Criteria in Solid Tumors (RECIST) version 1.1. Prior adjuvant therapy and radiotherapy or surgery for mCRC were allowed. There were no exclusion criteria. This study was performed in accordance with the Declaration of Helsinki and was approved by the Ethics Review Board of the First Hospital of Quanzhou Affiliated to Fujian Medical University (Fujian Province, China).

Treatment Methods

Camrelizumab was intravenously administered at a dose of 200 mg on day 1 every 3 weeks. XELOX consisted of oxaliplatin 130 mg/m^2 on day 1, followed by oral capecitabine 1,000 mg/m^2 twice daily on days 1 through 14 (28 doses) of a 21-day cycle. Bevacizumab was administered before oxaliplatin at a dose of 7.5 mg/kg on day 1 every 3 weeks. Regorafenib was orally administered 80 mg once per day on day 1 through 21 in a 28-day cycle. Camrelizumab was administered prior to bevacizumab and chemotherapy.

Efficacy and Toxicities

Tumor responses were evaluated after every two or three cycles of the combination therapy according to the RECIST 1.1 by computed tomography (CT) scan. The objective response rate (ORR) was calculated by pooling the complete response (CR) and partial response (PR) rates. The disease control rate (DCR) was defined as the proportion of patients with a CR, PR, or stable disease (SD). Progression-free survival (PFS) was defined as the time from the beginning of treatment to the first documentation of disease progression, or final follow-up. Overall survival (OS) was defined as the time from the beginning of treatment to the point of death or final follow-up. Toxicities were graded according to the National Cancer Institute Common Toxicity Criteria for Adverse Events, version 5. The data cutoff date was October 15, 2021.

Statistical Analysis

Statistical analysis was performed using SPSS version 19.0(SPSS, Inc., Chicago, IL, USA). The Kaplan–Meier method was used for PFS and OS. Median follow-up times were computed by the reverse Kaplan-Meier method. Log-Rank test was performed to compare the different groups for PFS univariate analysis. A two-tailed $p<0.05$ was considered statistically significant in all tests.

RESULTS

Patient Characteristics

The baseline characteristics of the 25 patients with mCRC are shown in **Table 1**. The median age was 64 years (range 43-86 years). Among all patients, 13 (52%) were male and 12 (48%) female. Fifteen (60%) were ECOG PS 0 and 8 (32%) ECOG PS 1. In total, 18 (72%) patients were left-sided primary colorectal cancer, and seven (28%) patients right-sided primary colon cancer. Fourteen (56%) patients had Liver metastases. Twenty-one (84%) patients were confirmed as pMMR/MSS. Among the 25 patients, 19 (76%) patients received combination immunotherapy of bevacizumab, and 6 (24%) of regorafenib (**Table 2**).

Efficacy

Of the 25 patients, none achieved CR; 18(72%) experienced partial responses and 6(24%) experienced stable disease as best responses, while one (4%) patient had progressive disease. The ORR and DCR were 72% (18/25) and 96% (24/25), respectively (**Table 3**). The median follow-up for overall survival was 11.5months (95% CI10.3–12.7). The median progression-free survival(mPFS) was 11.2 months (95% CI 8.9–13.9) (**Figure 1A**). The OS was still immature and one-year OS rates were 70.4% (95% CI 43.7–86.1) (**Figure 1B**). In addition, the mPFS of the regorafenib-containing regimen was 9.6 months and PFS of bevacizumab-containing regimen has not yet been reached, although the difference was considered not statistically significant (p = 0.08, **Figure 1C**). The difference in patients with liver metastasis did not reach statistical significance compared with patients without liver metastasis (11.2 *vs.* 10.9months, p = 0.81, **Figure 1D**).

TABLE 1 | Baseline Characteristics.

Characteristics	Patients N (%)
Age (year)	
Median age (range)	64 (43–86)
≥60	15 (60)
<60	10 (40)
Sex	
Male	13 (52)
Female	12 (48)
ECOG PS	
0	15 (60)
1	8 (32)
2	2 (8)
Primary tumor location	
Colon	14 (56)
Right-side	7 (28)
Left-side	7 (28)
Rectum	11 (44)
Type of metastasis	
With liver metastasis	14 (56)
Without liver metastasis	11 (44)
Site of distant metastasis	
Liver	14 (56)
Lung	7 (28)
Lymph nodes	6 (24)
Peritoneum	6 (24)
Peritoneal cavity	8 (32)
Other	5 (20)
MMR or MSI status	
pMMR or MSS	21 (84)
dMMR or MSI-H	1 (4)
Unknown	3 (12)

ECOG PS, Eastern Cooperative Oncology Group performance score.

Safety

All 25 patients were assessed for toxicities. The overall incidence of any grade toxicity was 72% (18/25). Common treatment-related adverse events (AEs) of any grade were neutropenia (36%) reactive cutaneous capillary endothelial proliferation (32%), decreased platelet count (28%), hand-foot syndrome (28%), and liver dysfunction (16%). Grade ≥3 treatment-related AEs occurred in 8(32%) patients. They included neutropenia, gastric hemorrhage, hand-foot syndrome, hyperglycemia, and elevated ALT. A fatal event of gastrointestinal perforation complicated by febrile neutropenia occurred in a patient treated with regorafenib. Treatment was switched from capecitabine to raltitrexed due to intolerable grade 3 hand-foot syndrome in three (12%) patients. The most common camrelizumab-related adverse events were reactive cutaneous capillary endothelial proliferation (32%) and thyroid dysfunction (24.0%), and all of them were either grade 1 or 2. A new camrelizumab-related adverse event, mild bilateral optic disc disease, was observed. Details of the adverse events are presented in **Table 4**.

DISCUSSION

Although recently, rapid development has been made in the field of immunotherapy (14, 15), the first-line standard treatment for metastatic colorectal cancer (mCRC) is 5FU-based chemotherapies, with or without anti-angiogenic agents. ICI monotherapy is efficacious in the treatment of mCRC with dMMR/MSI-H. The role of the combination of PD-1 blockade with VEGF inhibition has been investigated in MSS mCRC. Adding atezolizumab to FP/BEV (standard of care) as first-line maintenance treatment for patients with BRAF wild-type mCRC did not lead to improvement in the outcomes for efficacy (16). However, in the AVETUX trial, avelumab and cetuximab in combination with FOLFOX in patients with previously untreated mCRC produced a high response rate of 79.5%, disease control rate of 92.3% and mPFS of 11.1months in 39 patients with RAS/BRAF wild-type MSS mCRC (6). In this study, a high ORR of 72% and a DCR of 96% were recorded. The mPFS of 11.2 months is as long as that of the AVETUX trial (11.1 months), which is much better than that of bevacizumab plus XELOX chemotherapy (9.4 months) as first-line therapy in patients with mCRC (17). The main factors leading to different efficacies may be that populations in the AVETUX trial included more patients with left-sided tumors (91%) compared to our study (68.8%), and all patients were RAS/BRAF wild-type. Patients with RAS with left-sided mCRC had significantly superior PFS, OS, and ORR compared with patients with

TABLE 2 | Characteristics of individual patients.

No.	Age (year)	Sex	ECOG PS	Cancer type	Sites of metastasis when on treatment	KRAS/ BRAF mutation status	MMR or MSI status	Combining regimen	No. of cycles	Response
1	62	F	0	Rectum	Abdomino-pelvic cavity	Wt	pMMR/MSS	Cam+Rego+ XELOX	17	PR
2	68	F	1	Rectum	Liver, lung, kidney, peritoneal cavity, RPLN	Wt	pMMR/MSS	Cam+Rego+ XELOX	4	PD
3	45	F	1	Right-sided colon	Peritoneal cavity, RPLN, abdominal aortic LN	KRAS Mt	pMMR/MSS	Cam+Rego+ XELOX	8	SD
4	70	M	0	Right-sided colon	Liver, lung, peritoneal cavity	KRAS Mt	pMMR/MSS	Cam+Rego+ XELOX	15	PR
5	58	M	0	Right-sided colon	Liver	Wt	pMMR/MSS	Cam+Rego+ XELOX	14	PR
6	55	M	0	Rectum	Lung	Wt	pMMR/MSS	Cam+Rego+ XELOX	15	PR
7	53	F	0	Rectum	Liver	KRAS Mt	pMMR/MSS	Cam+Bev+ XELOX	4	PR
8	64	M	0	Right-sided colon	Liver, lung, peritoneal cavity	Unknown	Unknown	Cam+Bev+ XELOX	18	PR
9	86	F	2	Right-sided colon	Abdomino-pelvic cavity	Unknown	Unknown	Cam+Bev+ XELOX	2	SD
10	78	M	0	Left-sided colon	Liver	Wt	pMMR/MSS	Cam+Bev+ XELOX	4	PR
11	65	M	0	Left-sided colon	Liver	Wt	pMMR/MSS	Cam+Bev+ XELOX	7	PR
12	64	M	0	Rectum	Lung	Wt	pMMR/MSS	Cam+Bev+ XELOX	8	PR
13	69	M	0	Left-sided colon	Peritoneum	KRAS Mt	pMMR/MSS	Cam+Bev+ XELOX	6	PR
14	70	M	1	Rectum	Pelvic cavity	Unknown	pMMR/MSS	Cam+Bev+ XELOX	10	SD
15	66	F	0	Left-sided colon	Liver	KRAS Mt	dMMR/MSI-H	Cam+Bev+ XELOX	14	PR
16	62	F	0	Right-sided colon	Adrenal gland, peritoneal cavity, peritoneum, lymph nodes	Unknown	pMMR/MSS	Cam+Bev+ XELOX	6	SD
17	43	F	0	Left-sided colon	Liver	Wt	pMMR/MSS	Cam+Bev+ XELOX	8	PR
18	55	F	1	Right-sided colon	Liver, peritoneum, peritoneal cavity	Unknown	pMMR/MSS	Cam+Bev+ XELOX	12	PR
19	52	M	0	Rectum	Lung	KRAS Mt	pMMR/MSS	Cam+Bev+ XELOX	8	SD
20	57	F	1	Rectum	Liver, peritoneal cavity, bilateral ovarian	KRAS Mt	pMMR/MSS	Cam+Bev+ XELOX	11	PR
21	67	M	2	Rectum	Liver, peritoneum	Unknown	Unknown	Cam+Bev+ XELOX	5	PR
22	63	M	0	Left-sided colon	Liver, lymph nodes	KRAS Mt	pMMR/MSS	Cam+Bev+ XELOX	5	PR
23	54	F	1	Rectum	Liver	Wt	pMMR/MSS	Cam+Bev+ XELOX	4	PR
24	77	F	1	Rectum	Lung, bone, cervical and pelvic wall	Wt	pMMR/MSS	Cam+Bev+ XELOX	3	PR
25	76	M	1	Left-sided colon	Abdominal wall, abdomino-pelvic cavity	Wt	pMMR/MSS	Cam+Bev+ XELOX	8	SD

ECOG PS, Eastern Cooperative Oncology Group performance status; F, female; M, male; Mt, mutant; Wt, wild-type; Cam, camrelizumab; Bev, bevacizumab; Rego, regorafenib; XELOX, capecitabine and oxaliplatin; PR, partial response; SD, stable disease; PD, progression of disease; RPLN, retroperitoneal lymph node.

right-sided tumors (18), and cetuximab plus FOLFIRI versus bevacizumab as first-line treatment clearly benefitted patients with left-sided tumors (18, 19).

Several studies have suggested that liver metastases are predictive of a lack of benefit from PD-1/PD-L1 inhibitors in MSS mCRC (5, 20). The liver is considered an immunologically-tolerant organ that is characterized by a much higher proportion of immunosuppressive cells (21). In the present study, the difference in patients with liver metastasis was considered not statistically significant compared with those without liver metastasis, probably due to the small sample size.

Recently, in the REGONIVO trial, the combination of regorafenib and nivolumab achieved a robust response rate of 33% in pMMR/MSS refractory mCRC (5). More and more

TABLE 3 | Tumor response.

Response	Patients N (%)
CR	0
PR	18 (72)
SD	6 (24)
PD	1 (4)
ORR	18 (72)
DCR	24 (96)

CR, complete response; PR, partial response; SD-stable disease; PD, progression of disease; ORR, objective response rate; DCR, disease control rate.

TABLE 4 | Adverse events.

Adverse event	Grade 1-2, N (%)	Grade ≥3, N (%)	Any grade, N (%)
Neutropenia	8 (32)	1 (4)	9 (36)
Decreased platelet count	6 (24)	1 (4)	7 (28)
Nausea and Vomiting	1 (4)	1 (4)	2 (8)
Liver dysfunction	2 (8)	2 (8)	4 (16)
Hand-foot syndrome	4 (16)	3 (12)	7 (28)
Gastric hemorrhage	0	1 (4)	1 (4)
Diarrhea	1 (4)	1 (4)	2 (8)
Fever	2 (8)	1 (4)	3 (12)
Hyperthyroidism	4 (16)	0	4 (16)
Hypothyroidism	2 (8)	0	2 (8)
Hyperglycemia	1 (4)	1 (4)	2 (8)
RCCEP	8 (32)	0	8 (32)
Vision changes	1 (4)	0	1 (4)
Myocarditis	2 (8)	0	2 (8)
Infusion-related reactions	2 (8)	0	2 (8)
ALL	16 (64)	8 (32)	18 (72)

RCCEP, reactive cutaneous capillary endothelial proliferation.

research focused on the regorafenib plus ICIs in MSS refractory mCRC, the current conclusion is controversial due to the small sample size and inconsistency (5, 13, 22–24). In this study, we observed that the mPFS of regorafenib-containing therapies was not as long as that of bevacizumab-containing therapies. Moreover, capecitabine-related hand-foot syndrome (HFS), one of the causes of the switch in three treatments, was in a regorafenib-containing regimen. HFS is a common skin reaction to capecitabine with rates of any grade, of 22%–77% (25). Similarly, regorafenib-associated hand-foot skin reactions occurred at a rate of 61% overall and 20% at grade 3 (26, 27). Regorafenib combined with capecitabine treatment should be used cautiously due to the risk of overlapping skin toxicity. Therefore, this might suggest that as first-line therapy for mCRC, regorafenib may not be a suitable choice for combination with XELOX chemotherapy in future trials.

The combination strategy indicated a potential benefit in terms of ORR and PFS with a acceptable safety profile. Despite its strengths, there are some limitations to consider. First, this is a retrospective pilot study with a small sample size, reflecting its preliminary nature. Second, although antitumor response was observed in mCRC in spite of RAS mutations, a small number of patients had unknown RAS or BRAF status before the beginning

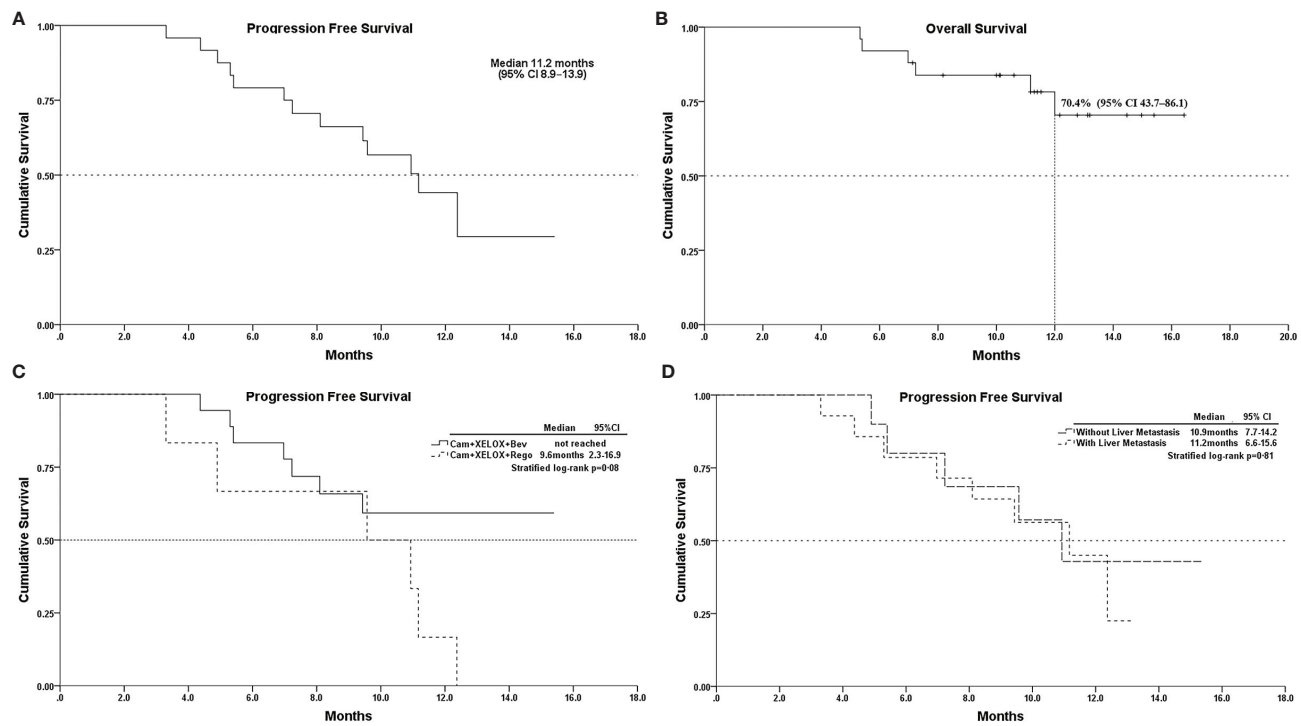

FIGURE 1 | **(A)**, Kaplan–Meier survival curves of progression-free survival; **(B)**, overall survival; **(C)**, PFS of Cam+XELOX+Bev *vs* Cam+XELOX+Rego ($p > 0.05$); and **(D)**, PFS in patients with or without liver metastasis ($p > 0.05$); Cam, camrelizumab; Bev, bevacizumab; Rego, regorafenib; XELOX, capecitabine and oxaliplatin.

of the combination treatment. Besides, the MMR or MSI status of three patients was unknown. Finally, even if the same chemotherapy regimen was adopted, different courses of treatment and varying follow-up intervals may have increased the heterogeneity. Thus, the findings need to be further assessed in a large prospective study.

In conclusion, our study differs from previous immunotherapy study in MSS mCRC based on the study populations and the novel combination regimen. In present study showed the addition of camrelizumab to the first-line XELOX chemotherapy with bevacizumab have demonstrated high response rates, and this immunotherapy combination was practical and helpful in unselected patients with mCRC. Further randomized trials with large sample sizes for this combination strategy are warranted.

DATA AVAILABILITY STATEMENT

The raw data supporting the conclusions of this article will be made available by the authors, without undue reservation.

ETHICS STATEMENT

This study was approved by the Ethics Review Board of the First Hospital of Quanzhou Affiliated to Fujian Medical University, East Road 250, Quanzhou 362000, Fujian Province, China. Written informed consent for participation was not required for this study, in accordance with the national legislation and institutional requirements.

AUTHOR CONTRIBUTIONS

WC, XL, and XH designed the project. HZ, YL, and XH collected patients' information and wrote the manuscript. WC and XL provided study material or patient. YW evaluated tumor responses. All authors contributed to the article and approved the submitted version.

ACKNOWLEDGMENTS

We sincerely thank Hongyue Lin, Zhiqiang Lin, Zhihang Lin, Lili Cai, Lei Hong, and Zede Ye who offered their assistance in preparing the manuscript.

SUPPLEMENTARY MATERIAL

The Supplementary Material for this article can be found online at: https://www.frontiersin.org/articles/10.3389/fonc.2021.774445/full#supplementary-material

REFERENCES

1. Le DT, Uram JN, Wang H, Bartlett BR, Kemberling H, Eyring AD, et al. PD-1 Blockade in Tumors With Mismatch-Repair Deficiency. *N Engl J Med* (2015) 372(26):2509–20. doi: 10.1056/NEJMoa1500596
2. Overman MJ, McDermott R, Leach JL, Lonardi S, Lenz HJ, Morse MA, et al. Nivolumab in Patients With Metastatic DNA Mismatch Repair-Deficient or Microsatellite Instability-High Colorectal Cancer (Checkmate 142): An Open-Label, Multicentre, Phase 2 Study. *Lancet Oncol* (2017) 18(9):1182–91. doi: 10.1016/S1470-2045(17)30422-9
3. Overman MJ, Lonardi S, Wong KYM, Lenz HJ, Gelsomino F, Aglietta M, et al. Durable Clinical Benefit With Nivolumab Plus Ipilimumab in DNA Mismatch Repair-Deficient/Microsatellite Instability-High Metastatic Colorectal Cancer. *J Clin Oncol* (2018) 36(8):773–9. doi: 10.1200/JCO.2017.76.9901
4. Wei XL, Zhang Y, Zhao HY, Wang ZQ, Li YH, Wang F, et al. A Phase I Study of SHR7390 Plus Camrelizumab in Advanced/Metastatic Colorectal Cancer. *J Clin Oncol* (2021) 39(15_suppl):e15553. doi: 10.1200/JCO.2021.39.15_suppl.e15553
5. Fukuoka S, Hara H, Takahashi N, Kojima T, Kawazoe A, Asayama M, et al. Regorafenib Plus Nivolumab in Patients With Advanced Gastric or Colorectal Cancer: An Open-Label, Dose-Escalation, and Dose-Expansion Phase Ib Trial (Regonivo, Epoc1603). *J Clin Oncol* (2020) 38(18):2053–61. doi: 10.1200/JCO.19.03296
6. Stein A, Binder M, Goekkurt E, Lorenzen S, Riera-Knorrenschild J, Depenbusch R, et al. Avelumab and Cetuximab in Combination With Folfox in Patients With Previously Untreated Metastatic Colorectal Cancer (mCRC): Final Results of the Phase Ii Avetux Trial (Aio-Krk-0216). *J Clin Oncol* (2020) 38(4_suppl):96. doi: 10.1200/JCO.2020.38.4_suppl.96
7. Song H, Liu X, Jiang L, Li F, Zhang R, Wang P. Current Status and Prospects of Camrelizumab, a Humanized Antibody Against Programmed Cell Death Receptor 1. *Recent Pat Anticancer Drug Discov* (2021) 16(3):312–32. doi: 10.2174/1574892816666210208231744
8. Liu J, Liu Q, Li Y, Li Q, Su F, Yao H, et al. Efficacy and Safety of Camrelizumab Combined With Apatinib in Advanced Triple-Negative Breast Cancer: An Open-Label Phase Ii Trial. *J Immunother Cancer* (2020) 8(1):e000696. doi: 10.1136/jitc-2020-000696
9. Lan C, Huang X, Shen JX, Wang Y, Xiong Y, Li J, et al. Camrelizumab Plus Apatinib in Patients With Advanced Cervical Cancer: A Multicenter, Open-Label, Single-Arm, Phase Ii Trial. *J Clin Oncol* (2020) 38(15_suppl):6021. doi: 10.1200/JCO.2020.38.15_suppl.6021
10. Fan Y, Zhao J, Wang Q, Huang D, Li X, Chen J, et al. Camrelizumab Plus Apatinib in Extensive-Stage SCLC (PASSION): A Multicenter, Two-Stage, Phase 2 Trial. *J Thorac Oncol* (2021) 16(2):299–309. doi: 10.1016/j.jtho.2020.10.002
11. Chen X, Wu X, Wu H, Gu Y, Shao Y, Shao Q, et al. Camrelizumab Plus Gemcitabine and Oxaliplatin (Gemox) in Patients With Advanced Biliary Tract Cancer: A Single-Arm, Open-Label, Phase Ii Trial. *J Immunother Cancer* (2020) 8(2):e001240. doi: 10.1136/jitc-2020-001240
12. Chen J, Quan M, Chen Z, Zeng T, Li Y, Zhou Y, et al. Camrelizumab in Advanced or Metastatic Solid Tumour Patients With DNA Mismatch Repair Deficient or Microsatellite Instability High: An Open-Label Prospective Pivotal Trial. *J Cancer Res Clin Oncol* (2020) 146(10):2651–7. doi: 10.1007/s00432-020-03251-5
13. Jiang FE, Zhang HJ, Yu CY, Liu AN. Efficacy and Safety of Regorafenib or Fruquintinib Plus Camrelizumab in Patients With Microsatellite Stable and/or Proficient Mismatch Repair Metastatic Colorectal Cancer: An Observational Pilot Study. *Neoplasma* (2021) 68(4):861–6. doi: 10.4149/neo_2021_201228N1415
14. Benson AB, Venook AP, Al-Hawary MM, Arain MA, Chen YJ, Ciombor KK, et al. Colon Cancer, Version 2.2021, NCCN Clinical Practice Guidelines in Oncology. *J Natl Compr Canc Netw* (2021) 19(3):329–59. doi: 10.6004/jnccn.2021.0012
15. Damilakis E, Mavroudis D, Sfakianaki M, Souglakos J. Immunotherapy in Metastatic Colorectal Cancer: Could the Latest Developments Hold the Key to Improving Patient Survival? *Cancers (Basel)* (2020) 12(4):889. doi: 10.3390/cancers12040889

16. Grothey A, Tabernero J, Arnold D, De Gramont A, Ducreux MP, O'Dwyer PJ, et al. Fluoropyrimidine (FP) + Bevacizumab (BEV) + Atezolizumab *vs* FP/BEV in BRAFwt Metastatic Colorectal Cancer (mCRC): Findings From Cohort 2 of MODUL – A Multicentre, Randomized Trial of Biomarker-Driven Maintenance Treatment Following First-Line Induction Therapy. *Ann Oncol* (2018) 29:viii714–5. doi: 10.1093/annonc/mdy424.020
17. Saltz LB, Clarke S, Díaz-Rubio E, Scheithauer W, Figer A, Wong R, et al. Bevacizumab in Combination With Oxaliplatin-Based Chemotherapy as First-Line Therapy in Metastatic Colorectal Cancer: A Randomized Phase Iii Study. *J Clin Oncol* (2008) 26(12):2013–9. doi: 10.1200/JCO.2007.14.9930
18. Tejpar S, Stintzing S, Ciardiello F, Tabernero J, Van Cutsem E, Beier F, et al. Prognostic and Predictive Relevance of Primary Tumor Location in Patients With Ras Wild-Type Metastatic Colorectal Cancer: Retrospective Analyses of the Crystal and Fire-3 Trials. *JAMA Oncol* (2017) 3(2):194–201. doi: 10.1001/jamaoncol.2016.3797
19. Heinemann V, Von Weikersthal LF, Decker T, Kiani A, Vehling-Kaiser U, Al-Batran SE, et al. Folfiri Plus Cetuximab Versus Folfiri Plus Bevacizumab as First-Line Treatment for Patients With Metastatic Colorectal Cancer (Fire-3): A Randomised, Open-Label, Phase 3 Trial. *Lancet Oncol* (2014) 15(10):1065–75. doi: 10.1016/S1470-2045(14)70330-4
20. Fakih M, Sandhu J, Wang C, Ouyang C. Response to PD-1 and PD-L1 Based Immunotherapy in MSS Advanced Colorectal Cancer is Impacted by Metastatic Disease Sites. *J Clin Oncol* (2021) 39(3_suppl):72. doi: 10.1200/JCO.2021.39.3_suppl.72
21. Kubes P, Jenne C. Immune Responses in the Liver. *Annu Rev Immunol* (2018) 36:247–77. doi: 10.1146/annurev-immunol-051116-052415
22. Wang C, Chevalier D, Saluja J, Sandhu J, Lau C, Fakih M. Regorafenib and Nivolumab or Pembrolizumab Combination and Circulating Tumor DNA Response Assessment in Refractory Microsatellite Stable Colorectal Cancer. *Oncologist* (2020) 25(8):e1188–94. doi: 10.1634/theoncologist.2020-0161
23. Li J, Cong L, Liu J, Peng L, Wang J, Feng A, et al. The Efficacy and Safety of Regorafenib in Combination With Anti-Pd-1 Antibody in Refractory Microsatellite Stable Metastatic Colorectal Cancer: A Retrospective Study. *Front Oncol* (2020) 10:594125. doi: 10.3389/fonc.2020.594125
24. Wang F, He MM, Yao YC, Zhao X, Wang ZQ, Jin Y, et al. Regorafenib Plus Toripalimab in Patients With Metastatic Colorectal Cancer: A Phase Ib/II Clinical Trial and Gut Microbiome Analysis. *Cell Rep Med* (2021) 2(9):100383. doi: 10.1016/j.xcrm.2021.100383
25. Kwakman JJM, Elshot YS, Punt CJA, Koopman M. Management of Cytotoxic Chemotherapy-Induced Hand-Foot Syndrome. *Oncol Rev* (2020) 14(1):442–2. doi: 10.4081/oncol.2020.442
26. Belum VR, Wu S, Lacouture ME. Risk of Hand-Foot Skin Reaction With the Novel Multikinase Inhibitor Regorafenib: A Meta-Analysis. *Inves New Drugs* (2013) 31(4):1078–86. doi: 10.1007/s10637-013-9977-0
27. McLellan B, Ciardiello F, Lacouture ME, Segaert S, Van Cutsem E. Regorafenib-Associated Hand-Foot Skin Reaction: Practical Advice on Diagnosis, Prevention, and Management. *Ann Oncol* (2015) 26(10):2017–26. doi: 10.1093/annonc/mdv244

Conflict of Interest: The authors declare that the research was conducted in the absence of any commercial or financial relationships that could be construed as a potential conflict of interest.

Publisher's Note: All claims expressed in this article are solely those of the authors and do not necessarily represent those of their affiliated organizations, or those of the publisher, the editors and the reviewers. Any product that may be evaluated in this article, or claim that may be made by its manufacturer, is not guaranteed or endorsed by the publisher.

frontiers in Oncology

ORIGINAL RESEARCH
published: 01 December 2021
doi: 10.3389/fonc.2021.790373

Cost-Effectiveness Analysis of Camrelizumab *vs.* Placebo Added to Chemotherapy as First-Line Therapy for Advanced or Metastatic Esophageal Squamous Cell Carcinoma in China

Qilin Zhang[1], *Pan Wu*[2], *Xucheng He*[3], *Yufeng Ding*[4] *and Yamin Shu*[4]*

[1] Department of Pharmacy, Union Hospital, Tongji Medical College, Huazhong University of Science and Technology, Wuhan, China, [2] Department of Pharmacy, Qionglai Maternal & Child Health and Family Planning Service Center, Qionglai, China, [3] Department of Pharmacy, Pengzhou Second People's Hospital, Pengzhou, China, [4] Department of Pharmacy, Tongji Hospital, Tongji Medical College, Huazhong University of Science and Technology, Wuhan, China

OPEN ACCESS

Edited by:
Sripathi Sureban,
University of Oklahoma Health Sciences Center, United States

Reviewed by:
Azin Nahvijou,
Tehran University of Medical Science, Iran
Wenbin Liu,
Second Military Medical University, China

***Correspondence:**
Yamin Shu
shuyamin1990hust@163.com

Specialty section:
This article was submitted to Gastrointestinal Cancers: Gastric and Esophageal Cancers, a section of the journal Frontiers in Oncology

Received: 06 October 2021
Accepted: 16 November 2021
Published: 01 December 2021

Citation:
Zhang Q, Wu P, He X, Ding Y and Shu Y (2021) Cost-Effectiveness Analysis of Camrelizumab vs. Placebo Added to Chemotherapy as First-Line Therapy for Advanced or Metastatic Esophageal Squamous Cell Carcinoma in China. Front. Oncol. 11:790373. doi: 10.3389/fonc.2021.790373

Objective: The purpose of this cost-effectiveness analysis was to estimate the effects of adding camrelizumab to standard chemotherapy as the first-line treatment in patients with advanced or metastatic esophageal squamous cell carcinoma (ESCC) on health and economic outcomes in China.

Methods: A Markov model was developed to simulate the clinical course of typical patients with advanced or metastatic ESCC in the ESCORT-1st trial. Weibull survival model was employed to fit the Kaplan-Meier progression-free survival and overall survival probabilities of the camrelizumab-chemotherapy and placebo-chemotherapy strategy, respectively. Quality-adjusted life-years (QALYs) and incremental cost-effectiveness ratios (ICER) were estimated over a 5-year lifetime horizon. Meanwhile, one-way and probabilistic sensitivity analyses were conducted to test the uncertainty in the model.

Results: On baseline analysis, the incremental effectiveness and cost of camrelizumab-chemotherapy versus placebo-chemotherapy were 0.15 QALYs and $7,110.56, resulting in an ICER of $46,671.10/QALY, higher than the willingness-to-pay (WTP) threshold of China ($31,498.70/QALY). The results were sensitive to the utility of PFS and cost of camrelizumab.

Conclusion: The findings from the present analysis suggest that the addition of camrelizumab to chemotherapy might not be cost-effective in patients with advanced or metastatic ESCC in China.

Keywords: cost-effectiveness analysis, ESCORT-1st trial, esophageal squamous cell carcinoma, camrelizumab, first-line treatment

INTRODUCTION

Esophageal cancer is the seventh most frequently diagnosed malignant cancer and ranks sixth in mortality worldwide (1). China has a high incidence of esophageal cancer, accounting for more than 50% of the global morbidity and mortality (2). Esophageal squamous cell carcinoma (ESCC) and esophageal adenocarcinoma (EAC) are the two major histological types of esophageal cancer. In China, approximately 90% of esophageal cancer patients are diagnosed with ESCC (3). Palliative chemotherapy regiments, including fluorouracil plus platinum, and paclitaxel plus platinum, are the current recommended standard first-line therapy for patients with unresectable advanced, relapsed or metastatic ESCC (4). However, the prognosis of patients with advanced ESCC is still poor. The 5-year survival rate is only 12.4% in Europe and 20.9% in China (5, 6). Therefore, new treatment options for patients with advanced or metastatic ESCC are urgently needed.

In recent years, immune checkpoint inhibitors (ICIs) have made exciting breakthroughs in cancer therapy by blocking CTLA-4 or PD-1 pathways to enhance the antitumor activity of T cells, and have also shown outstanding performance in the treatment of esophageal cancer (7, 8). Among them, KEYNOTE-181, ATTRACTION-3 and ESCORT studies focusing on advanced or metastatic ESCC patients successfully presented excellent efficacy in the second-line treatment, indicating the arrival of the era of esophageal cancer immunotherapy (7, 9, 10). The Chinese Society of Clinical Oncology (CSCO) Guidelines for the Diagnosis and Treatment of Esophageal Cancer in the 2021 edition have recommended camrelizumab combined with paclitaxel and cisplatin chemotherapy as the first-line treatment of advance or metastatic ESCC.

The world's first phase III clinical trial of the first-line immunotherapy combined with chemotherapy for the advanced ESCC was the ESCORT-1st trial conducted in China, and we performed a cost-effectiveness analysis based on ESCORT-1st trial (11). The ESCORT-1st trial was conducted to evaluate the efficacy and adverse events of camrelizumab combined with paclitaxel and cisplatin compared with placebo combined with paclitaxel and cisplatin for the first-line treatment of advanced ESCC (11). Results demonstrated that camrelizumab combined with chemotherapy significantly prolonged median OS (mOS, 15.3 months *vs.* 12.0 months) and median PFS (mPFS, 6.9 months *vs.* 5.6 months) compared with placebo plus chemotherapy. The objective response rate was higher (ORR, 72.1% *vs.* 62.1%) and the duration of response was longer (DOR, 7.0 months *vs.* 4.6 months) with patients in the camrelizumab plus chemotherapy group. In terms of safety, the incidence of grade ≥3 treatment-related adverse events were similar in both groups (63.4% *vs.* 67.7%), with the most common grade ≥3 treatment-related adverse event being neutrophil count reduction (39.9% *vs.* 43.4%).

The statistically significant improvements in PFS and OS demonstrated the apparent benefit of camrelizumab in the treatment of advanced ESCC. However, the high cost of camrilizumab may have profound economic consequences. Hence, this study aims to assess the economics of camrelizumab plus chemotherapy for the first-line treatment of advanced or metastatic ESCC based on the ESCORT-1st trial from the perspective of the Chinese healthcare system.

METHODS

Model Structure

A state-transition Markov model was established to integrate clinical and economic outcomes of camrelizumab-chemotherapy versus placebo-chemotherapy as first-line therapy for patients with advanced or metastatic ESCC in China. The model comprised three mutually exclusive health states: progression-free survival (PFS), progressive disease (PD) and death (**Figure 1**). The initial health state for all patients was PFS and patients either remained in their assigned health state or progressed to a new health state

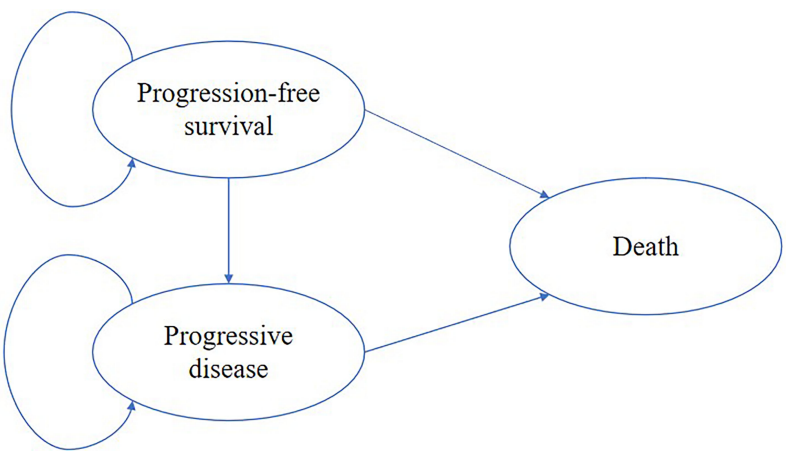

FIGURE 1 | The Markov model simulated three health states: progression-free survival, progressive disease and death.

during each Markov cycle (12). The tracked time horizon of the model was 5 years and the Markov cycle in the model was 1 month. The primary outcomes were quality-adjusted life-years (QALYs) and cost in the study. The future costs and benefits were discounted using a 3% annual discount rate according to the WHO guidelines for pharmacoeconomic evaluations (13). All costs had been adjusted to 2020 prices according to the local Consumer Price Index and were presented in US dollars ($1 = ¥6.9). A cost-effectiveness analysis was conducted to evaluate the outcomes of the two strategies and presented as incremental cost-effectiveness ratios (ICERs). The formula used to calculate the ICER as following: ICER = [Cost (camrelizumab)-Cost (placebo)]/[QALY (camrelizumab)-QALY (placebo)]. We used 3×the per capita gross domestic product (GDP) of China in 2020 ($31,498.70) as the willingness-to-pay (WTP) threshold according to the WHO recommendations. Model development and outcomes analysis were performed in the TreeAge Pro 2019 software (Williamstown, MA, USA) and R software (version 4.0.5, Vienna, Austria). This economic analysis was based on a randomized clinical trial and an experimental model and did not require approval from an institutional review board or ethics committee.

Clinical Data

The clinical efficacy and safety data were based on the patients in the ESCORT-1st trial, a randomized, double-blind, placebo-controlled, multicenter, phase 3 trial enrolled patients from 60 hospitals in China (11). Patients were eligible if they conformed to the following conditions: 1. 18-75 years old and had adequate organ function; 2. cytologically or histologically confirmed ESCC; 3. unresectable, locally advanced, or recurrent disease that precluded esophagectomy or definitive chemoradiation, or distant metastatic disease; 4. received no previous systemic therapy (patients who had progressed ≥6 months after definitive chemoradiation were eligible); 5. an Eastern Cooperative Oncology Group performance status score of 0 or 1, and had at least 1 measurable lesion according to the Response Evaluation Criteria in Solid Tumors (RECIST) version 1.1; 6. a life expectancy of at least 12 weeks. Eligible patients were randomly assigned in a 1:1 ratio to either the camrelizumab-chemotherapy group (n = 298) or the placebo-chemotherapy group (n = 298). Camrelizumab (200 mg) or placebo were given every 3 weeks until disease progression or unacceptable toxicity. Paclitaxel (175 mg/m^2) and cisplatin (75 mg/m^2) were given every 3 weeks up to 6 cycles after randomization. The median OS was 15.3 months (95% CI:12.8-17.3) in the camrelizumab-chemotherapy group and 12.0 months (95% CI: 11.0-13.3) in the placebo-chemotherapy group. The median PFS was 6.9 months (95% CI: 5.8-7.4) in the camrelizumab-chemotherapy group and 5.6 months (95% CI:5.5-5.7) in the placebo-chemotherapy group.

Transition probabilities between the different health states were estimated from Kaplan-Meier survival curves which obtained from the ESCORT-1st trial. As individual patient data were not available, the Kaplan-Meier curves of PFS and OS for the two groups were read by GetData Graph Digitizer software (Version 2.26), which digitized data points from an image file. To extrapolate the probability of survival beyond the observation period, the Weibull distribution was fitted to the data for PFS and OS curves using R statistical software (version 4.0.5, Vienna, Austria). The estimated scale (λ) and shape (γ) parameters, standard error, and 95% confidence interval were presented in **Table 1**. Formula $S(t)=\exp(-\lambda t^{\gamma})$ was used to calculate the survival probability at time t and we used formula $P(t)=1-\exp[\lambda(t-1)^{\gamma}-\lambda t^{\gamma}]$ to estimate the transition probability at a given cycle t (14, 15). The transition probability from PFS to death state is derived from the natural death rate of Chinese population in 2020 (0.707%) (16). The survival curve simulation results were shown in **Figure 2**.

Costs and Utilities

Costs were estimated from the perspective of the Chinese healthcare system. Only direct medical costs, including the costs of camrelizumab and chemotherapy, laboratory tests and radiological examinations, management of treatment-related grade 3-4 serious adverse events (SAEs), best supportive care (BSC), cost of salvage therapy per cycle, routine follow-up and terminal care in end-of-life, were included in the model (**Table 2**). To estimate the dosage of chemotherapeutic agents (17), it was assumed that a typical patient weighed 65 kg and had a height of 1.64 m, resulting in a body surface area (BSA) of 1.72 m^2. The costs related to SAEs were calculated by multiplying the incidence of the SAEs by the costs of managing the SAEs per event. The most common adverse events, including anemia, white blood cell count decreased, neutrophil count decreased, and the incidence rates of adverse events that occurred with two groups were obtained from the ESCORT-1st trial (11). Once the

TABLE 1 | Weibull parameters of model estimated for progression-free and overall survival curves.

Group		Parameter	Mean	SE	95% CI	
					Low	Up
CTP	PFS	scale (λ)	0.035843	0.007191	0.024190	0.053110
		shape (γ)	1.440454	0.082920	1.286766	1.612498
	OS	scale (λ)	0.005274	0.001911	0.002593	0.010729
		shape (γ)	1.798021	0.135765	1.550680	2.084815
PTP	PFS	scale (λ)	0.030222	0.005986	0.020499	0.044558
		shape (γ)	1.824045	0.092109	1.652161	2.013811
	OS	scale (λ)	0.006991	0.002212	0.003760	0.013000
		shape (γ)	1.818036	0.120060	1.597315	2.069258

CTP, camrelizumab-chemotherapy; PTP, placebo-chemotherapy; PFS, progression-free survival; OS, overall survival; SE, standard error; 95% CI, 95% confidence interval.

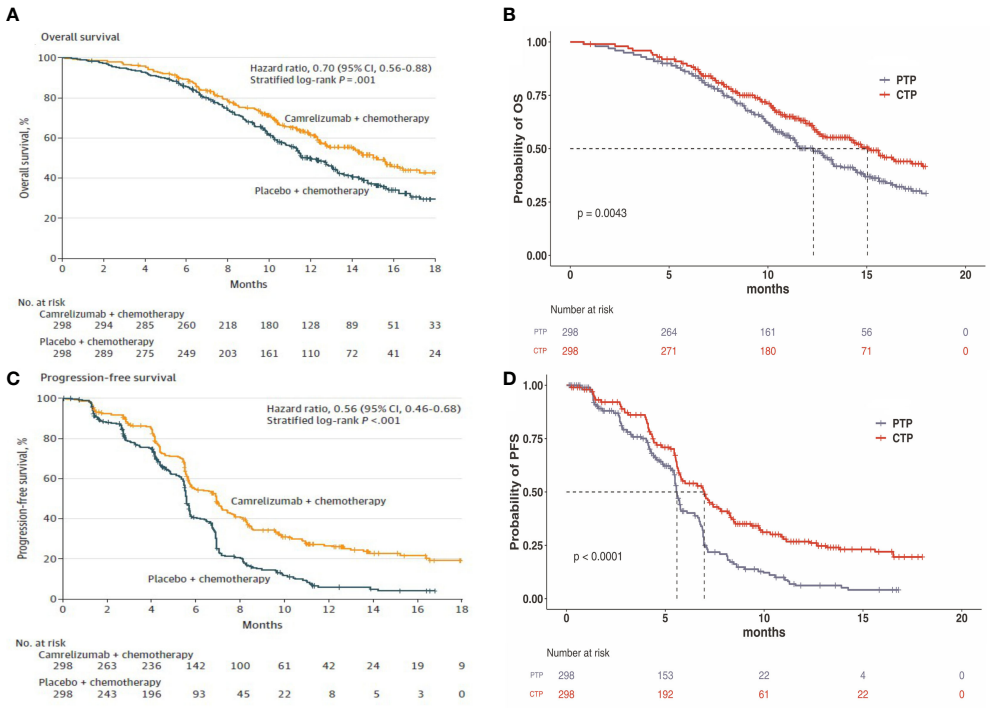

FIGURE 2 | **(A)** Kaplan–Meier curve of the overall survival from the ESCORT-1st trial. **(B)** Simulate overall survival curve for the CTP group and the PTP group. **(C)** Kaplan-Meier curve of progression-free survival from the ESCORT-1st trial. **(D)** Simulate progression-free survival curve for the CTP group and the PTP group. CTP, camrelizumab-chemotherapy; PTP, placebo-chemotherapy; OS, overall survival; PFS, progression-free survival.

TABLE 2 | Model economic parameters and the range of the sensitivity analysis.

Variables	Base Case (Rang)	Distribution	Source
Costs ($)			
Camrelizumab (200 mg)	424.35 (339.40-509.10)	Triangle	Local charge
Paclitaxel (100 mg)	108.26 (86.61-129.91)	Triangle	Local charge
Cisplatin (100 mg)	10.97 (8.78-13.16)	Triangle	Local charge
Routine follow-up cost per cycle	73.57 (58.86-88.28)	Triangle	(17)
Cost of laboratory tests and radiological examinations	356.60 (285.28-427.92)	Triangle	(17)
Cost of salvage therapy per cycle	638.43 (510.74-766.12)	Triangle	Local charge
Cost of supportive care per cycle	167.29 (133.83-200.75)	Triangle	(17)
Cost of terminal care in end-of-life	1,460.30 (1,168.24-1,752.36)	Triangle	(18)
Costs of serious adverse events ($)			
Anemia	508.2 (381.2-635.3)	Triangle	(17)
White blood cell count decreased	466.00 (372.80-559.20)	Triangle	(17)
Neutrophil count decreased	534.40 (427.52-641.28)	Triangle	(19)
Risks of serious adverse events in CTP group (grade 3 or 4) %			
Anemia	17.40 (13.92-20.88)	Beta	(11)
White blood cell count decreased	24.20 (19.36-29.04)	Beta	(11)
Neutrophil count decreased	39.90 (31.92-47.88)	Beta	(11)
Risks of serious adverse events in PTP group (grade 3 or 4) %			
Anemia	13.50 (10.80-16.20)	Beta	(11)
White blood cell count decreased	26.60 (21.28-31.92)	Beta	(11)
Neutrophil count decreased	43.40 (34.72-52.08)	Beta	(11)
Utility value			
PFS	0.68 (0.54-0.82)	Beta	(19)
PD	0.42 (0.34-0.50)	Beta	(19)
Body surface area (m^2)	1.72 (1.38-2.06)	Triangle	(17)
Discount rate (%)	3 (0–8)	Fixed in PSA	(13)

CTP, camrelizumab-chemotherapy; PTP, placebo-chemotherapy; PFS, progression-free survival; PD, progressive disease; PSA, probabilistic sensitivity analyses.

disease progressed, salvage chemotherapy and best supportive care were prescribed. All costs were derived from local hospitals or previously published studies (17–19). As no data on quality of life were estimated in the ESCORT-1st trial, the utility scores of PFS and survival after progression were obtained from the literature (19). Furthermore, terminal cost and a half-cycle correction were implemented, according to the TreeAge Pro 2019 manual.

Sensitivity Analyses

To assess the impact of uncertainty in model inputs on the outcomes, one-way and probabilistic sensitivity analyses (PSA) were performed in this research. In the one-way sensitivity analysis, relevant parameters were changed one-by-one to their respective upper and lower boundaries, with a range of ± 20% of the base case value, in order to identify the parameters that most significantly influenced the economic outcomes. The result of the one-way sensitivity analysis was presented in a Tornado diagram. The PSA was performed to assess the effects of uncertainty in all model parameters simultaneously. The model was run 1000 times, in which the parameters were changed with a specific pattern of distribution (triangle distribution for costs, beta distribution for the probability parameters and utilities). The results of the PSA were presented as cost-effectiveness acceptability curve and probabilistic scatter plot, to estimate the WTP threshold for an incremental unit of effectiveness.

TABLE 3 | The cost and outcome results of the cost-effectiveness analysis.

Parameters	CTP group	PTP group
Costs ($)		
PFS state	13,518.28	6,180.97
PD state	6,942.32	7,169.07
Total Cost	20,460.60	13,350.04
Incremental costs ($)	7,110.56	/
Effectiveness (QALYs)		
PFS state	0.55	0.39
PD state	0.24	0.25
Total effectiveness	0.79	0.64
Incremental effectiveness (QALYs)	0.15	/
ICER ($/QALY)	46,671.10	/

CTP, camrelizumab-chemotherapy; PTP, placebo-chemotherapy; PFS, progression-free survival; PD, progressive disease; QALYs, Quality-adjusted life-years; ICER, incremental cost-effectiveness ratios.

RESULTS

Base Case Analysis

The base case analysis showed that over 5-year time horizon, camrelizumab-chemotherapy group gained 0.79 QALYs at a cost of $20,460.60. In the placebo-chemotherapy group, the effectiveness was 0.64 QALYs while the cost was $13,350.04. Compared with placebo-chemotherapy, the mean incremental effect and cost were 0.15 QALYs and $7,110.56 for the camrelizumab-chemotherapy group. The ICER for camrelizumab-chemotherapy versus placebo-chemotherapy was $46,671.10/QALY (**Table 3**). At the Chinese cost-effectiveness WTP threshold of $31,498.70/QALY, camrelizumab-chemotherapy was not a cost-effective treatment strategy compared with placebo-chemotherapy.

Sensitivity Analyses

In the tornado diagram of one-way sensitivity analysis (**Figure 3**), the most influential variables were the utility of PFS and the cost of camrelizumab per 200 mg. However, altering these parameters could not yield substantial changes in the ICER, $38,293.88-$59,739.88/QALY and $38,999.36-$54,342.85/

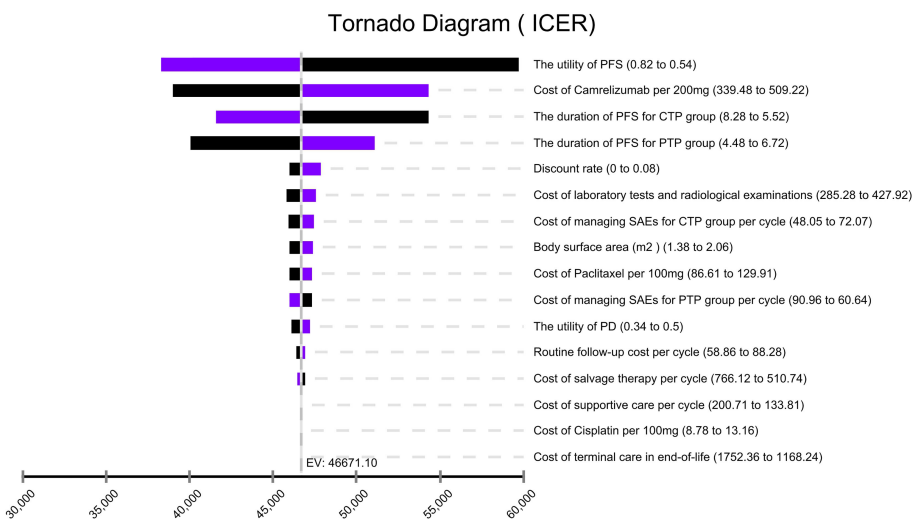

FIGURE 3 | Tornado diagram of one-way sensitivity analysis. It summarized the results of one-way sensitivity analysis, which listed influential parameters in descending order according to their effect on the ICER over the variation of each parameter value. ICER, incremental cost-effectiveness ratios; CTP, camrelizumab-chemotherapy; PTP, placebo-chemotherapy; PFS, progression-free survival; PD, progressive disease; SAEs, serious adverse events.

QALY, respectively. Other parameters influencing the model were the duration of PFS, discount rate, cost of laboratory tests and radiological examinations, cost of managing SAEs, body surface area, cost of paclitaxel per 100 mg. Changes in parameters, the utility of PD, routine follow-up cost per cycle, and the costs of salvage therapy per cycle, supportive care per cycle, cisplatin per 100 mg, terminal care in end-of-life had a mild impact on economic outcomes. Nevertheless, none of the variables could reduce the ICERs below the thresholds. The cost-effectiveness acceptability curve and probabilistic scatter plot were shown in **Figures 4**, **5**. Regardless of the scenarios, the camrelizumab-chemotherapy group was cost-effective in approximately less than 1% of the simulations compared with placebo-chemotherapy group, with a cost-effectiveness threshold of $31,498.70 in China.

DISCUSSION

ESCC is one of the most commonly malignant gastrointestinal tumors globally. Palliative chemotherapy as the first-line treatment for advanced/refractory ESCC, which not only had limited survival benefits, but also had poor prognosis and relatively high adverse reactions. ICIs significantly improved

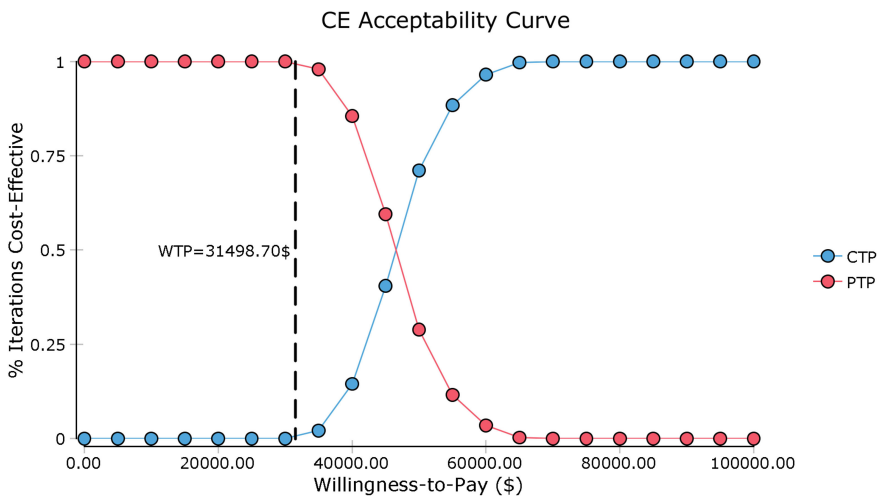

FIGURE 4 | Cost-effectiveness acceptability curve. CE, cost-effectiveness; CTP, camrelizumab-chemotherapy; PTP, placebo-chemotherapy; WTP, willingness-to-pay.

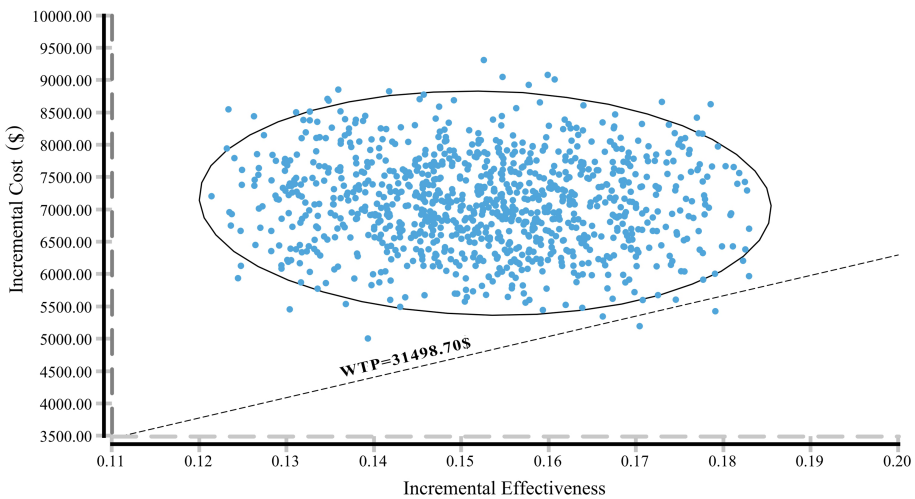

FIGURE 5 | A probabilistic scatter plot of the ICER between the CTP and PTP group. Each dot represents the ICER for 1 simulation. An ellipse means 95% confidence interval. Dots that are located below the ICER threshold represent cost-effective simulations. CTP, camrelizumab-chemotherapy; PTP, placebo-chemotherapy; WTP, willingness-to-pay, ICER, incremental cost-effectiveness ratios.

survival and quality of life in a range of malignancies by inhibiting the CTLA-4 or PD-1 pathway (20, 21). On September 14, 2021, the ESCORT-1st trial, the world's first phase III clinical trial using immunotherapy combined with chemotherapy as first-line treatment for advanced ESCC, was completed at more than 60 hospitals in China and published in ⟪JAMA⟫, comparing the efficacy and safety of camrelizumab combined with paclitaxel and cisplatin versus placebo combined with paclitaxel and cisplatin (11). As compared to standard chemotherapy, camrilizumab-chemotherapy significantly prolonged patients' median OS and median PFS, reducing the risk of death by 30% and the risk of disease progression by 44%. It has achieved the longest OS (15.3 months) and the highest response rate (72.1%) in the field of first-line treatment for esophageal cancer, which provided a novel first-line treatment option for patients with ESCC.

However, the price of ICIs is usually high, which may significantly increase the healthcare expenditures. Hence, it is important to evaluate the effect of ICIs from the perspective of pharmacoeconomics. In choosing a phase III trial for cost-effectiveness analysis, ESCORT-1st trial was the best choice. In this study, our analysis showed that the ICER of camrelizumab-chemotherapy for first-line treatment of advanced ESCC in China was $46,671.10/QALY and the WTP threshold was $31,498.70/QALY, revealing that camrelizumab-chemotherapy strategy may not be a cost-effective treatment option compared with chemotherapy.

In the one-way sensitivity analysis, the utility of PFS and the cost of camrelizumab per 200 mg had the highest impacts on the ICER. Probabilistic sensitivity analysis of 1000 Monte Carlo simulations was adopted to alter the cost of camrelizumab. Only about 1% of simulations in the camrelizumab-chemotherapy group are cost-effective at the WTP threshold ($31,498.70/QALY). The ICER ($31,362.86/QALY) approached the WTP threshold with cost-effectiveness when the price of camrilizumab was reduced to $255/200 mg in China. However, different regions have different cost-effectiveness WTP threshold value. The ICER in the camrelizumab-chemotherapy group was higher than the threshold recommended by wealthier developed countries, such as £20,000-30,000 per QALY proposed by the UK's National Institute for Health and Care Excellence (NICE) (22). Assuming that the prices of camrelizumab and chemotherapy remain constant, camrelizumab-chemotherapy may not be cost-effective as a first-line treatment for patients with advanced or metastatic ESCC in other countries as well. Particularly, camrelizumab-chemotherapy strategy might be the optimal alternative option in developed cities and provinces of China, such as Beijing (WTP = $72,886.96/QALY), Shanghai (WTP = $69,297.83/QALY), Jiangsu (WTP = $55,341.30/QALY), Fujian (WTP = $48,046.09/QALY) and Zhejiang (WTP = $48,021.74/QALY), which had over 50% chance to be cost-effective. In addition, the utility of PFS had a higher impact on the model outcomes, but even if the utility of PFS varied from 0.42 to 1, the ICER ranged from $78,606.77/QALY to $31,513.53/QALY, which was still higher than the WTP.

Currently, pharmacoeconomic studies on ESCC were limited, with only 10 articles been searched in PubMed, and most of them focused on screening, surgical techniques or chemoradiation (23–25). There were only two economic analyses of immunotherapy for ESCC. A recent study was the cost-effectiveness analysis of nivolumab in the second-line treatment for advanced ESCC. Their study included 419 advanced ESCC patients and showed an ICER of $136,709.35/QALY for nivolumab versus chemotherapy at a $29,306.43/QALY WTP threshold (17). From the perspective of Chinese society, nivolumab is not a cost-effective treatment option compared with chemotherapy, which were basically consistent with our results. Another study compared the economics of camrelizumab versus chemotherapy as second-line therapy for advanced ESCC (26). The study included 457 advanced ESCC patients at 43 hospitals, demonstrating that camrelizumab had higher QALYs (0.782 *vs.* 0.499) and higher cost ($31,537 *vs.* $6,998) than chemotherapy. The ICER of camrilizumab versus chemotherapy was $86,745/QALY, which was far above the WTP threshold ($30,094/QALY gained). Therefore, camrelizumab is not cost-effective in China compared with chemotherapy as second-line treatment for advanced or metastatic ESCC. Generally, the prices of PD-1 inhibitors in China are higher than those of conventional chemotherapy (17, 26). Based on previous studies and our results, it is demonstrated that camrelizumab was not cost-effective compared with chemotherapy, whether it is first-line treatment or second-line treatment for advanced or metastatic ESCC in China. Consequently, from the perspective of policy, the price of camrelizumab needs to be reduced to reduce the financial burden on the healthcare system and provide more access to Chinese patients.

In our study, higher QALYs (0.79 *vs.* 0.64) are obtained in camrelizumab- chemotherapy as first-line treatment for advanced or metastatic ESCC compared with chemotherapy. The ICER is $46,671.10/QALY. Although it is not economical, the ICER value is lower compared with second-line treatment. One possible reason is that the cost of camrelizumab per 200 mg has fallen from $2,802 in 2020 to $424 in 2021 (26). The second may be the effect of camrelizumab as first-line treatment is better than second-line treatment and it also could be the different utility values of PFS and PD in different studies. In recent years, China has formulated a series of preferential policies for antitumor drugs. In addition, with the continuous improvement of national medical insurance policies and the unique price advantage brought by volume-based procurement, the prices of PD-1 inhibitors may be further reduced, and this treatment could help ESCC patients obtain a first-line treatment that is safer and has a longer overall survival rate than traditional chemotherapy.

This study has several advantages. First, this is the first cost-effectiveness analysis of camrelizumab combine with chemotherapy as first-line treatment for advanced or metastatic ESCC in China and the world. In addition, it is also the largest ESCC immunotherapy trial with the largest sample size, longest overall survival and highest response rate among first-line therapies. Therefore, the results of this analysis could be taken into consideration by the National Healthcare Security Administration in its annual price negotiations. Our study

inevitably had some limitations that warrant discussion. First, due to lack of long-term (>5 years) survival data, we used a two-parameter Weibull survival model to extrapolate the tails of survival beyond the follow-up time horizon, which may not accurately reflect the real world condition (27). The current cost-effective analysis must be updated when long-term survival data are reported. Second, we assumed patients received paclitaxel after disease progression, which may not reflect the current Chinese clinical practice situation precisely because patients might switch to subsequent therapy upon the further progression. However, the result of the sensitivity analysis supported that the costs associated with disease progression did not have an important impact on economic outcomes. Third, we only considered the most common grade 3/4 SAEs in the model. We hypothesized that low-probability adverse events would not change the final conclusions of the study, and the sensitivity analysis showed that the result was not sensitive to SAEs-related parameters. Fourth, although all patients in the ESCORT-1st trial were from China, the utility values in this study were derived from western countries, which might lead to bias in the model outcomes. Finally, due to the strict eligible conditions of clinical trials and the unbalanced economic development in various regions of China, the applicability of this study may be limited. Despite these limitations, this study might be a valuable reference for decision makers about camrelizumab as a first-line treatment for advanced or metastatic ESCC in China.

CONCLUSION

In conclusion, camrelizumab combined with chemotherapy treatment is unlikely to be considered cost-effective as compared to conventional chemotherapy as a first-line treatment for advanced or metastatic ESCC from the perspective of the Chinese healthcare system. However, if the price is reduced, camrelizumab may be a cost-effective treatment option. Our results are potentially helpful to healthcare systems decision-making, but real-world studies are further needed to verify the efficacy, safety and economics of these regimens for first-line therapy of ESCC.

DATA AVAILABILITY STATEMENT

The raw data supporting the conclusions of this article will be made available by the authors, without undue reservation.

AUTHOR CONTRIBUTIONS

Conceptualization, QZ, YD, and YS. Data curation, YS. Formal analysis, QZ, YD, and YS. Funding acquisition, QZ. Methodology, PW, XH, and YS. Project administration, QZ and YS. Software, YS. Supervision, QZ, YD, and YS. Validation, QZ. Writing – original draft, QZ, PW, XH, YD, and YS. Writing – review & editing, QZ, YD, and YS. All authors contributed to the article and approved the submitted version.

FUNDING

This work was supported by the National Natural Science Foundation of China (No. 82104476) and National Key R&D Program of China (No. 2017YFC0909900).

REFERENCES

1. Bray F, Ferlay J, Soerjomataram I, Siegel RL, Torre LA, Jemal A. Global Cancer Statistics 2018: GLOBOCAN Estimates of Incidence and Mortality Worldwide for 36 Cancers in 185 Countries. *CA: Cancer J Clin* (2018) 68 (6):394–424. doi: 10.3322/caac.21492
2. Chen W, Zheng R, Baade PD, Zhang S, Zeng H, Bray F, et al. Cancer Statistics in China, 2015. *CA: Cancer J Clin* (2016) 66(2):115–32. doi: 10.3322/caac.21338
3. Abnet CC, Arnold M, Wei WQ. Epidemiology of Esophageal Squamous Cell Carcinoma. *Gastroenterology* (2018) 154(2):360–73. doi: 10.1053/j.gastro.2017.08.023
4. Kitagawa Y, Uno T, Oyama T, Kato K, Kato H, Kawakubo H, et al. Esophageal Cancer Practice Guidelines 2017 Edited by the Japan Esophageal Society: Part 2. *Esophagus Off J Japan Esophageal Soc* (2019) 16(1):25–43. doi: 10.1007/s10388-018-0642-8
5. Anderson LA, Tavilla A, Brenner H, Luttmann S, Navarro C, Gavin AT, et al. Survival for Oesophageal, Stomach and Small Intestine Cancers in Europe 1999-2007: Results From EUROCARE-5. *Eur J Cancer (Oxford Engl 1990)* (2015) 51(15):2144–57. doi: 10.1016/j.ejca.2015.07.026
6. Zeng H, Zheng R, Guo Y, Zhang S, Zou X, Wang N, et al. Cancer Survival in China, 2003-2005: A Population-Based Study. *Int J Cancer* (2015) 136 (8):1921–30. doi: 10.1002/ijc.29227
7. Huang J, Xu J, Chen Y, Zhuang W, Zhang Y, Chen Z, et al. Camrelizumab Versus Investigator's Choice of Chemotherapy as Second-Line Therapy for Advanced or Metastatic Oesophageal Squamous Cell Carcinoma (ESCORT): A Multicentre, Randomised, Open-Label, Phase 3 Study. *Lancet Oncol* (2020) 21(6):832–42. doi: 10.1016/s1470-2045(20)30110-8
8. Gandhi L, Rodríguez-Abreu D, Gadgeel S, Esteban E, Felip E, De Angelis F, et al. Pembrolizumab Plus Chemotherapy in Metastatic Non-Small-Cell Lung Cancer. *N Engl J Med* (2018) 378(22):2078–92. doi: 10.1056/NEJMoa1801005
9. Kojima T, Shah MA, Muro K, Francois E, Adenis A, Hsu CH, et al. Randomized Phase III KEYNOTE-181 Study of Pembrolizumab Versus Chemotherapy in Advanced Esophageal Cancer. *J Clin Oncol Off J Am Soc Clin Oncol* (2020) 38(35):4138–48. doi: 10.1200/jco.20.01888
10. Kato K, Cho BC, Takahashi M, Okada M, Lin CY, Chin K, et al. Nivolumab Versus Chemotherapy in Patients With Advanced Oesophageal Squamous Cell Carcinoma Refractory or Intolerant to Previous Chemotherapy (ATTRACTION-3): A Multicentre, Randomised, Open-Label, Phase 3 Trial. *Lancet Oncol* (2019) 20(11):1506–17. doi: 10.1016/s1470-2045(19)30626-6
11. Luo H, Lu J, Bai Y, Mao T, Wang J, Fan Q, et al. Effect of Camrelizumab *vs.* Placebo Added to Chemotherapy on Survival and Progression-Free Survival in Patients With Advanced or Metastatic Esophageal Squamous Cell Carcinoma: The ESCORT-1st Randomized Clinical Trial. *Jama* (2021) 326 (10):916–25. doi: 10.1001/jama.2021.12836
12. Wu B, Gu X, Zhang Q. Cost-Effectiveness of Osimertinib for EGFR Mutation-Positive Non-Small Cell Lung Cancer After Progression Following First-Line EGFR TKI Therapy. *J Thorac Oncol Off Publ Int Assoc Study Lung Cancer* (2018) 13(2):184–93. doi: 10.1016/j.jtho.2017.10.012

13. Murray CJ, Evans DB, Acharya A, Baltussen RM. Development of WHO Guidelines on Generalized Cost-Effectiveness Analysis. *Health Economics* (2000) 9(3):235–51. doi: 10.1002/(sici)1099-1050(200004)9:3<235::aid-hec502>3.0.co;2-o
14. Diaby V, Adunlin G, Montero AJ. Survival Modeling for the Estimation of Transition Probabilities in Model-Based Economic Evaluations in the Absence of Individual Patient Data: A Tutorial. *PharmacoEconomics* (2014) 32(2):101–8. doi: 10.1007/s40273-013-0123-9
15. Liu M, Zhang L, Huang Q, Li N, Zheng B, Cai H. Cost-Effectiveness Analysis Of Ceritinib And Alectinib Versus Crizotinib In The Treatment of Anaplastic Lymphoma Kinase-Positive Advanced Non-Small Cell Lung Cancer. *Cancer Manage Res* (2019) 11:9195–202. doi: 10.2147/cmar.S223441
16. National Bureau of Statistics. National Data of National Bureau of Statistics in 2020. Available at: https://datastatsgovcn/tablequeryhtm?code=AD02.
17. Zhang PF, Xie D, Li Q. Cost-Effectiveness Analysis of Nivolumab in the Second-Line Treatment for Advanced Esophageal Squamous Cell Carcinoma. *Future Oncol (London England)* (2020) 16(17):1189–98. doi: 10.2217/fon-2019-0821
18. Wu B, Li T, Cai J, Xu Y, Zhao G. Cost-Effectiveness Analysis of Adjuvant Chemotherapies in Patients Presenting With Gastric Cancer After D2 Gastrectomy. *BMC Cancer* (2014) 14:984. doi: 10.1186/1471-2407-14-984
19. Li S, Peng L, Tan C, Zeng X, Wan X, Luo X, et al. Cost-Effectiveness of Ramucirumab Plus Paclitaxel as a Second-Line Therapy for Advanced Gastric or Gastro-Oesophageal Cancer in China. *PloS One* (2020) 15(5):e0232240. doi: 10.1371/journal.pone.0232240
20. Bagchi S, Yuan R, Engleman EG. Immune Checkpoint Inhibitors for the Treatment of Cancer: Clinical Impact and Mechanisms of Response and Resistance. *Annu Rev Pathol* (2021) 16:223–49. doi: 10.1146/annurev-pathol-042020-042741
21. Galluzzi L, Humeau J, Buqué A, Zitvogel L, Kroemer G. Immunostimulation With Chemotherapy in the Era of Immune Checkpoint Inhibitors. *Nat Rev Clin Oncol* (2020) 17(12):725–41. doi: 10.1038/s41571-020-0413-z
22. National Institute for Health and Care Excellence. *Guide to the Methods of Technological Appraisal*. London: NICE (2013).
23. Wu B, Wang Z, Zhang Q. Age at Initiation and Frequency of Screening to Prevent Esophageal Squamous Cell Carcinoma in High-Risk Regions: An Economic Evaluation. *Cancer Prev Res (Philadelphia Pa)* (2020) 13(6):543–50. doi: 10.1158/1940-6207.Capr-19-0477
24. Liu CY, Lin CS, Shih CS, Huang YA, Liu CC, Cheng CT. Cost-Effectiveness of Minimally Invasive Esophagectomy for Esophageal Squamous Cell Carcinoma. *World J Surg* (2018) 42(8):2522–9. doi: 10.1007/s00268-018-4501-5
25. Zhan M, Zheng H, Yang Y, Xu T, Li Q. Cost-Effectiveness Analysis of Neoadjuvant Chemoradiotherapy Followed by Surgery Versus Surgery Alone for Locally Advanced Esophageal Squamous Cell Carcinoma Based on the NEOCRTEC5010 Trial. *Radiother Oncol J Eur Soc Ther Radiol Oncol* (2019) 141:27–32. doi: 10.1016/j.radonc.2019.07.031
26. Yang F, Fu Y, Kumar A, Chen M, Si L, Rojanasarot S. Cost-Effectiveness Analysis of Camrelizumab in the Second-Line Treatment for Advanced or Metastatic Esophageal Squamous Cell Carcinoma in China. *Ann Trans Med* (2021) 9(15):1226. doi: 10.21037/atm-21-1803
27. Wilson DL. The Analysis of Survival (Mortality) Data: Fitting Gompertz, Weibull, and Logistic Functions. *Mech Ageing Dev* (1994) 74(1-2):15–33. doi: 10.1016/0047-6374(94)90095-7

Conflict of Interest: The authors declare that the research was conducted in the absence of any commercial or financial relationships that could be construed as a potential conflict of interest.

Publisher's Note: All claims expressed in this article are solely those of the authors and do not necessarily represent those of their affiliated organizations, or those of the publisher, the editors and the reviewers. Any product that may be evaluated in this article, or claim that may be made by its manufacturer, is not guaranteed or endorsed by the publisher.

frontiers in Oncology

ORIGINAL RESEARCH
published: 01 December 2021
doi: 10.3389/fonc.2021.788875

Gastrin Vaccine Alone and in Combination With an Immune Checkpoint Antibody Inhibits Growth and Metastases of Gastric Cancer

Jill P. Smith[1], Hong Cao[1], Wenqiang Chen[1], Kanwal Mahmood[1], Teresa Phillips[2], Lynda Sutton[2] and Allen Cato[2]*

[1] Department of Medicine, Georgetown University, Washington, DC, United States, [2] Cancer Advances, Inc., Durham, NC, United States

OPEN ACCESS

Edited by:
Sripathi Sureban, University of Oklahoma Health Sciences Center, United States

Reviewed by:
Dipongkor Saha, Texas Tech University Health Sciences Center, Abilene, United States
Haruhiko Sugimura, Hamamatsu University School of Medicine, Japan

***Correspondence:**
Jill P. Smith
jps261@georgetown.edu

Specialty section:
This article was submitted to Gastrointestinal Cancers: Gastric & Esophageal Cancers, a section of the journal Frontiers in Oncology

Received: *03 October 2021*
Accepted: *10 November 2021*
Published: *01 December 2021*

Citation:
Smith JP, Cao H, Chen W, Mahmood K, Phillips T, Sutton L and Cato A (2021) Gastrin Vaccine Alone and in Combination With an Immune Checkpoint Antibody Inhibits Growth and Metastases of Gastric Cancer. Front. Oncol. 11:788875. doi: 10.3389/fonc.2021.788875

Gastric cancer is a leading cause of cancer-related deaths worldwide. Recently, clinical studies have demonstrated that many of those with advanced gastric cancer are responsive to immune checkpoint antibody therapy, although the median survival even with these new agents is less than 12 months for advanced disease. The gastrointestinal peptide gastrin has been shown to stimulate growth of gastric cancer in a paracrine and autocrine fashion through the cholecystokinin-B receptor (CCK-BR), a receptor that is expressed in at least 56.6% of human gastric cancers. In the current investigation, we studied the role of the gastrin-CCK-BR pathway *in vitro* and *in vivo* as well as the expression of the CCK-BR in a human gastric cancer tissue array. CCK-BR and PD-L1 receptor expression and gastrin peptide was found in two murine gastric cancer cells (NCC-S1 and YTN-16) by qRT-PCR and immunocytochemistry. Treatment of NCC-S1 cells with gastrin resulted in increased growth. *In vivo*, the effects of a cancer vaccine that targets gastrin peptide (polyclonal antibody stimulator—PAS) alone or in combination with a Programed Death-1 antibody (PD-1 Ab) was evaluated in immune competent mice (N = 40) bearing YTN-16 gastric tumors. Mice were treated with PBS, PD-1 Ab (50 µg), PAS (250 µg), or the combination of PD-1 Ab with PAS. Tumor growth was significantly slower than controls in PAS-treated mice, and tumor growth was decreased even more in combination-treated mice. There were no metastases in any of the mice treated with PAS either alone or in combination with PD-1 Ab. Tumor proliferation by the Ki67 staining was significantly decreased in mice treated with PAS monotherapy or the combination therapy. PAS monotherapy or combined with PD-1 Ab increased tumor CD8+ T-lymphocytes and decreased the number of immunosuppressive M2-polarized tumor-associated macrophages. CCK-BR expression was identified in samples from a human tissue

array by immunohistochemistry confirming the clinical relevance of this study. These results confirm the significance of the gastrin-CCK-BR signaling pathway in gastric cancer and suggest that the addition of a gastrin vaccine, PAS, to therapy with an immune checkpoint antibody may decrease growth and metastases of gastric cancer by altering the tumor microenvironment.

Keywords: gastric cancer, immune checkpoint, tumor microenvironment, metastases, gastrin, fibrosis, PAS, G17DT

INTRODUCTION

Gastric adenocarcinoma (gastric cancer) is a common malignancy and is the world's second leading cause of cancer mortality worldwide (1). Novel therapeutic targets are desperately needed because the meager improvement in the cure rate of about 10% realized by adjunctive treatments to surgery is unacceptable as >50% patients with localized gastric cancer succumb to their disease (2). The prognosis of those with advanced gastric cancer is poor with a five-year survival of only 20–30% (3, 4). The current standard of care for advanced gastric cancer in the first line setting remains a combination of a fluoropyrimidine (e.g., 5-fluorouracil; 5FU) and a platinum (e.g., cis-platinum) containing chemotherapeutic agent. Targeted therapy may offer new possibilities for the treatment of gastric cancer. Since HER2 receptors are found in approximately 20% of gastric cancers, the addition of a HER2 receptor antibody to standard chemotherapy may be beneficial as demonstrated in the ToGA study where Trastuzumab (Herceptin) was beneficial in subjects with HER2-positive gastric cancer (5). The Cancer Genome Atlas (TCGA) Research Network described four groups of gastric cancer based upon molecular classifications including: EBV (Epstein–Barr virus), MSI (microsatellite instability), GS (genomically stable), and CIN (chromosomal instability) (6). The immune response to the tumor could play an important role within the EBV and MSI subgroups (7). With the recent use of immune checkpoint antibodies, investigators have been exploring whether this immunotherapy would be beneficial for gastric cancer (7). The KEYNOTE-012 study tested 39 subjects in a Phase 1 trial that were PD-L1 positive with pembrolizumab and found an overall survival of 11.4 months (8). The KEYNOTE-059 trial showed that pembrolizumab monotherapy was effective treating those with previously treated gastric or gastroesophageal cancer (9). Another PD-1 antibody, nivolumab, has been approved for first line therapy in gastric cancer in combination with chemotherapy after the results of the CheckMate-649 clinical trial (10). A number of clinical trials have been conducted now with various immune checkpoint antibodies (11) and although these agents have provided additional therapeutic options for those with gastric cancer, unfortunately the median overall survival still remains less than 12 months (12). For these reasons novel strategies are needed to improve response of those with gastric cancer to immunotherapy. One possible reason for the still low response to immune checkpoint antibodies may be related to the paucity of tumor infiltrating CD8+ lymphocytes in the tumor (13). Another possible reason for the low response rate may be due to the fibrosis of the tumor microenvironment that prevents penetration of therapies and immune cells (14). Therapeutic agents that target cancer cell receptors such as HER2 (5) have been shown to improve survival and yet most chemotherapy agents used in gastric cancer are not target-specific.

The gastrointestinal (GI) peptide gastrin is responsible for gastric acid secretion and growth of the GI tract, and gastrin mediates its effects through the cholecystokinin-B receptor or CCK-BR (**Figure 1**) (16). Unlike the physiologic expression of gastrin in the G cells of the stomach antrum (17), the gastrin gene also becomes overexpressed *de novo* in non-endocrine epithelial cells of gastric cancer (18) where it can stimulate growth in an autocrine fashion. Likewise, the CCK-BR also becomes over-expressed in cancer cells (19) and this receptor is responsive to both paracrine and autocrine stimulation by gastrin. Investigators have studied the expression of gastrin and the CCK-BR from resected human gastric cancers and found that most expressed CCK-BRs and gastrin (20–22). Gastrin may also stimulate growth of gastric cancer when blood gastrin levels are increased from chronic use of high dose proton pump inhibits (PPIs), achlorhydria or *Helicobacter pylori* infection (**Figure 1**) (15). Since gastrin has been shown to stimulate growth of human gastric cancer (19), researchers have been studying means to block gastrin's actions in gastric cancer using CCK-BR antagonists (23, 24) and their use in human trials reviewed (25–27).

Polyclonal Antibody Stimulator (PAS) is a therapeutic immunogen cancer vaccine comprised of a nine amino acid epitope derived from the amino-terminal sequence of gastrin-17 that is conjugated to diphtheria toxoid. PAS exerts an immunomodulatory effect by activating both B (28–30) and T cells (31). PAS stimulates the production of antibodies to different epitopes of the G17 and precursor G17-Gly gastrin peptides. These antibodies can bind to gastrin peptides to prevent their interaction with the CCK-BRs on the surface of tumor cells. Preclinical studies were performed in several animal models that have CCK-BRs including gastric cancer (32). In animal models, PAS-generated anti-gastrin antibodies have been shown to reduce the growth and metastases (28, 29, 33). Passive immunization with PAS antibodies raised in rabbits improved survival of SCID mice bearing gastric cancers compared to diluent treated controls (32).

To date 22 clinical studies have been conducted with PAS. Of these, 840 patients have been enrolled in five clinical trials for the

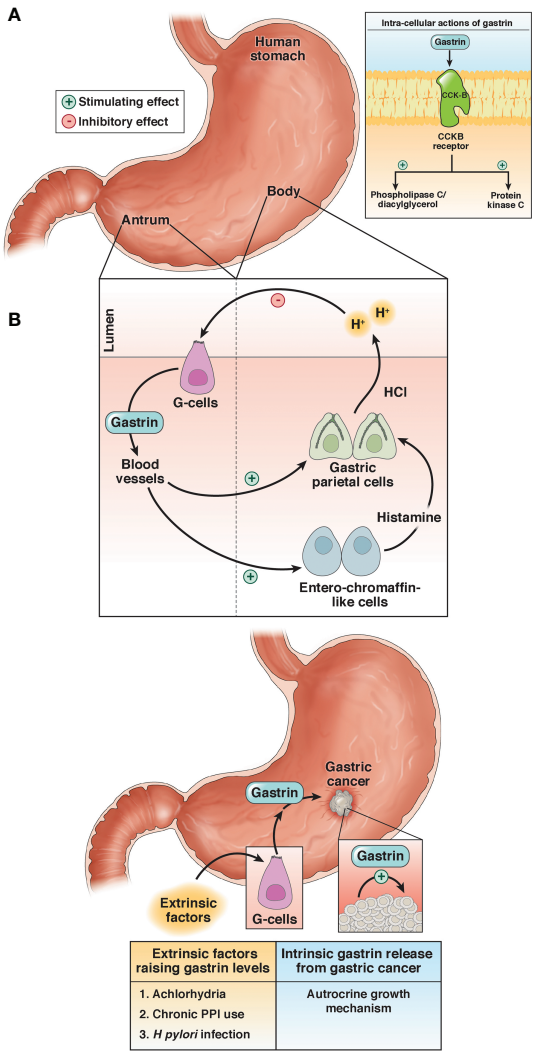

FIGURE 1 | Physiologic and pathologic roles of gastrin. **(A)** Under physiologic conditions, gastrin is released from the G-cells in the antrum of the stomach and stimulates the release of acid (HCl) by activation of the enterochromaffin-like cells and gastric parietal cells. **(B)** Gastrin stimulates growth of gastric cancer by activating the CCK-BR by an autocrine mechanism or exogenous stimulation by high gastrin blood levels induced by achlorhydria, chronic use of proton pump inhibitors (PPI), or infection with *Helicobacter pylori (H. pylori)*. Reproduced with permission from the Cell Mol Gastroenterol Hepatol (15).

treatment of pancreatic cancer; 234 subjects enrolled in five clinic studies in gastric cancer (34, 35); and 475 subjects enrolled in 10 clinical studies with advanced colon cancer. In the gastric cancer clinical trial (designated GC4 Study), the median survival of those with advanced gastric cancer treated with PAS plus cisplatin and 5FU was significantly prolonged (10.8 months) in subjects that mounted a protective antibody titer against gastrin compared to subjects treated with PAS plus cisplatin and 5FU that failed to generate an antibody response (4.8 months). The only notable PAS-related adverse events in all 22 studies were injection-site reaction and pyrexia. The purpose of the current study is to evaluate the effect of PAS and PD-1 antibody therapy alone or in combination in a murine model of gastric cancer.

MATERIALS AND METHODS

Cell Lines

Two murine cell lines were evaluated in this investigation. Murine gastric cancer cell line NCC-S1 (NCC) (36) was provided by Dr. Kim through his collaborator Dr. Timothy Wang of Columbia University, NY. The second gastric cancer cell line YTN-16 (YTN), was established and provided by Professor Sachiyo Nomura (37) through her collaborator Dr. James R. Goldenring of Vanderbilt University School of Medicine, TN. The YTN cells are known to be invasive and metastatic even after subcutaneous injection in mice. Before the cells were used in animals, they were tested by IMPACT II PCR Profile and were negative for all pathogens. YTN cells were grown in culture using DMEM and NCC cells were grown in RPMI media; both with 10% fetal bovine serum in a humidified 5% CO2 incubator at 37°C.

CCK-BR and PD-L1 Receptor Characterization in Gastric Cancer Cells by Quantitative PCR

Total RNA was extracted from cells (Qiagen) and subjected to quantitative PCR (qRT-PCR) in the fast cycling mode using a thermal cycler (Applied Biosystems) to examine the expression of the CCK-BR and PD-L1 expression. Primers used included: CCK-BR: F-5'GATGGCTGCTACGT-GCAACT-3'and R-5'CGCACCACCCGCTTCTTAG-3'; and PD-L1: F-5'TGCGGA CTACAAGCG-AATCACG-3' and R-5'-CTCAGCTTCTGGA TAACCC-TCG-3'. PCR was performed with 40 cycles and an annealing temperature at 60°C. HPRT was used as a normalizer control gene. Control RNA was extracted from normal mouse liver because it does not express either CCK-BR or PD-L1. Each reaction was performed in triplicate and each PCR test was performed three times for each receptor.

Effects of Gastrin Administration on *In Vitro* Growth of Gastric Cancer Cells

In order to determine if exogenous administration of gastrin could stimulate growth of gastric cancer cells, murine NCC cells (10,000) were plated into each well of a 96-well plate. After an overnight incubation, wells were exposed to gastrin 10 nM (N = 12 each) or media alone (control, N = 12). After an additional 24 h, the growth of the cells was evaluated with the MTT (3-[4,5-dimethylthiazol-2-yl]-2,5-diphenyltetrazolium bromide; thiazolyl blue) cell proliferation assay and differences analyzed by a colorimetric assay in a plate reader at 450 nm.

Gastrin Peptide Expression by Immunocytochemistry in Gastric Cancer Cells

NCC and YTN gastric cancer cells were plated onto glass coverslips in 4 cm^2 petri dishes. When cells reached log-phase

growth, the cells were fixed and reacted to a rabbit polyclonal antibody (Peninsula Laboratories, Belmont, CA; cat#: T4347) with a titer 1:50 overnight at 4°C, followed by incubation with one to three drops of Biotinylated Secondary Antibody (Vial A, Novus Biologicals; Centennial, CO) for 60 min. The slides were treated with one to three drops of HSS-HRP (Vial B, Novus) for 30 min, washed and DAB Chromogen was added for 3 min. Control cells were reacted with secondary antibody only. Images were taken of each sample from the slides using an Olympus BX61 microscope with a DP73 camera.

In Vivo Animal Studies

All animal studies were done in an ethical fashion and under the approval of the IACUC from Georgetown University. Several attempts were made to establish tumors in C57BL/6 mice using the NCC cells unsuccessfully. The first attempt included the injection of luciferase tagged 5×10^5 NCC cancer cells orthotopically into the stomach subserosa (N = 40). After imaging with luciferin and dissecting mice, no tumors were found. The NCC cells were then injected subcutaneously on the right flank with a total of 0.1 ml volume of 1.5×10^6 NCC cancer cells, but after 33 days, no tumors formed. It appears that the NCC cells will only form tumors in SCID mice or *Villin-Cre*, *Smad4*$^{F/F}$, *Trp53F/F*, *Cdh1*$^{F/wt}$ mice according to Park et al. (36). The YTN gastric cancer cells are known to be invasive and metastatic even after subcutaneous injection in C57BL/6 mice (37). Therefore, YTN were used for the *in vivo* studies by injecting (5×10^6) cells into each of 40 female C57BL/6 mice in 0.2 ml volume. Tumor growth was measured weekly with calipers and volume calculated by $L \times W^2 \times 0.5$.

Treatments

Mice bearing YTN tumors were divided into four treatment groups (N = 10 each). Control mice were treated with PBS in 0.1 ml ip injection given at the same time as the other treatments. PD-1 antibody 50 μg ip (PD-1 Ab; Clone RMPI-14 was purchased from Bio X Cell, West Lebanon, NH) was administered at baseline (one week after tumor inoculation; week 0) and at weeks 1, 3, and 6. PAS 250 μg was administered subcutaneously in 0.1 ml volume at the same time as PD-1 Ab and also at week 9. After 10 weeks of growth the control mice were appearing moribund so the mice were ethically euthanized, tumors removed and weighed and metastases counted.

Tissue Analysis

All observed metastases counted were dissected and formalin fixed and paraffin embedded for confirmation by hematoxylin and eosin (H&E) staining. Tumors were reacted with Masson's trichrome stain for analysis of fibrosis in the tumor microenvironment. To determine the proliferation index of the tumors, tissue sections (5 μm) were reacted with a rabbit monoclonal antibody for Ki67 (Biocare, cat# CRM325; 1:80). Immunohistochemical staining was also performed of tumor tissue sections (5 μm) to evaluate tumor infiltrating lymphocytes with CD8, (1:25, Cell Signaling, cat # 98941) and with rabbit polyclonal antibody against arginase-1 (ThermoFisher, cat # PA5-29645) at a dilution 1:1,800 to examine M2-polarized tumor associated macrophages.

CCK-BR Expression in Human Gastric Cancer

A human tissue microarray containing 24 cases/72 cores of human gastric cancer and samples from normal stomach was obtained from US Biomax (Rockville, MD; Cat#BC01011). After antigen retrieval, the array was incubated with the primary goat polyclonal antibody CCK-BR (#Ab77077, Abcam) at 1:200 titer overnight at 4°C. After rinsing, the slide was incubated with one to three drops of Biotinylated Secondary Antibody (Vial A, Novus) for 60 min. The slide was then treated with one to three drops of HSS-HRP (Vial B, Novus) for 30 min, washed and DAB Chromogen was added for 3 min. Images were scanned using an Aperio GT450 machine and images captured with software from Aperio Image Scope. CCK-BR staining was analyzed by densitometry with Image-J software corrected for area of tissue examined.

Statistical Analysis

Tumor growth rates were analyzed using linear regression analysis to compare slopes of the growth curves between each treatment group. Slides were scanned using an Aperio GT450 machine and images analyzed with software from Aperio Image Scope for the number of immunoreactive cells per high powered field (for Ki67 and CD8 cells). Images at the same magnification and identical surface area were taken (up to N = 10 per slide) for each tumor using the Aperio software. Slides for fibrosis and M2 polarized macrophage were quantitatively analyzed for integrated density with ImageJ computer software. Raw data results from images were analyzed using ANOVA and T-Test (with Bonferroni correction for multiple comparisons to controls) with GraphPad Prism version 9.

RESULTS

Characterization of Gastric Cancer Cells *In Vitro*

Two separate murine gastric cancer cells were evaluated for expression of CCK-BR, PD-L1 receptors and gastrin peptide *in vitro*. Gene expression of CCK-BR and PD-L1 were increased in both NCC and YTN gastric cancer cells compared to noncancerous mouse tissues (**Figure 2**). CCK-BR expression was increased greater than 60-fold in mouse YTN and NCC gastric cancer cells compared to normal mouse tissues (**Figure 2A**). PD-L1 mRNA expression was increased 52-fold in YTN cells and 24-fold in NCC cells over normal tissues (**Figure 2B**). Growth of NCC cells increased significantly (P = 0.004) when exposed to exogenous gastrin (**Figure 2C**). Immunocytochemistry revealed endogenous gastrin peptide expression in both NCC (**Figure 2D**) and YTN (**Figure 2E**) gastric cancer cells suggesting that these gastric cancer cells produce their own gastrin peptide to stimulate growth *via* the CCK-BR in an autocrine fashion. Control cells that reacted with the secondary antibody alone were negative for staining (**Figure 2F**).

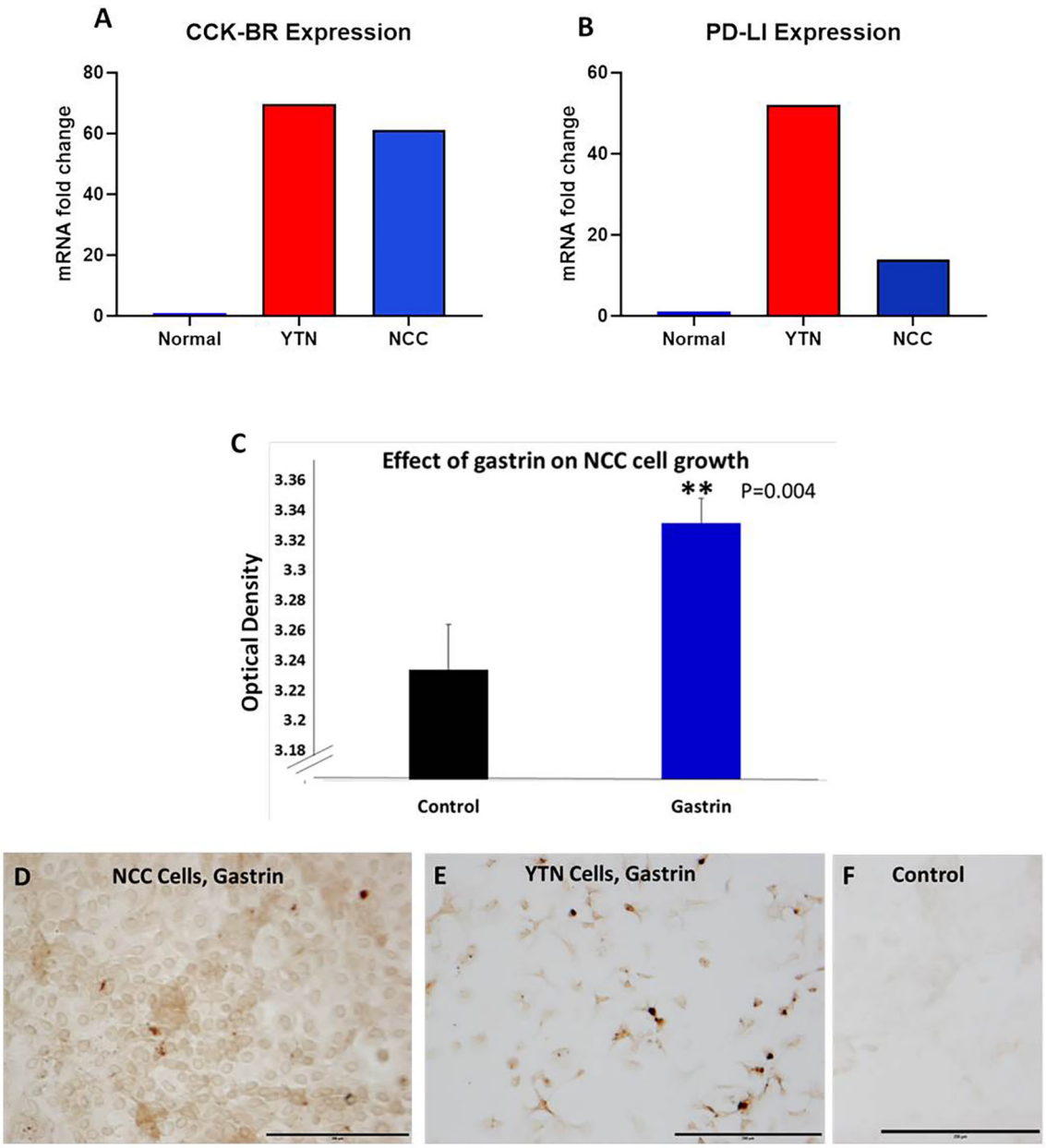

FIGURE 2 | Characterization of murine gastric cancer cells *in vitro*. **(A)** mRNA expression of CCK-BR is increased greater than 60-fold in YTN and NCC gastric cancer cells compared to normal mouse tissue. **(B)** mRNA expression by qRT-PCR of PD-L1 is markedly increased in gastric cancer YTN and NCC cells compared to normal tissues. **(C)** Exogenous gastrin stimulates growth of murine NCC gastric cancer cells *in vitro* (P = 0.004). **Significantly different from control. **(D)** Gastrin peptide expression is detected in NCC gastric cancer cells. **(E)** Gastrin peptide expression is detected in YTN gastric cancer cells. **(F)** Control cells stained with the secondary antibody only show no evidence of nonspecific immunoreactivity. Scale bar 200 μm.

Effects of PAS and PD-1 on Growth and Metastases of YTN Tumors

YTN gastric cancer tumor volumes measured over time are shown in **Figure 3A**. Therapy with PD-1 Ab monotherapy had no effect on tumor growth compared to controls. In contrast, mice treated with PAS monotherapy or PAS in combination with PD-1 Ab had significantly slowed tumor growth over time. PAS monotherapy slowed tumor growth by 31% compared to PBS-treated controls (P = 0.023). When PAS was given in combination with the PD-1 Ab the tumor growth was slowed by 59% compared to tumors of PBS-treated controls (P = 0.0003). When the growth rate of tumors from PAS-vaccinated mice was compared to that of the tumors of mice treated with the combination therapy, the difference was statistically significant (P = 0.0018). These results would suggest that the combination therapy is

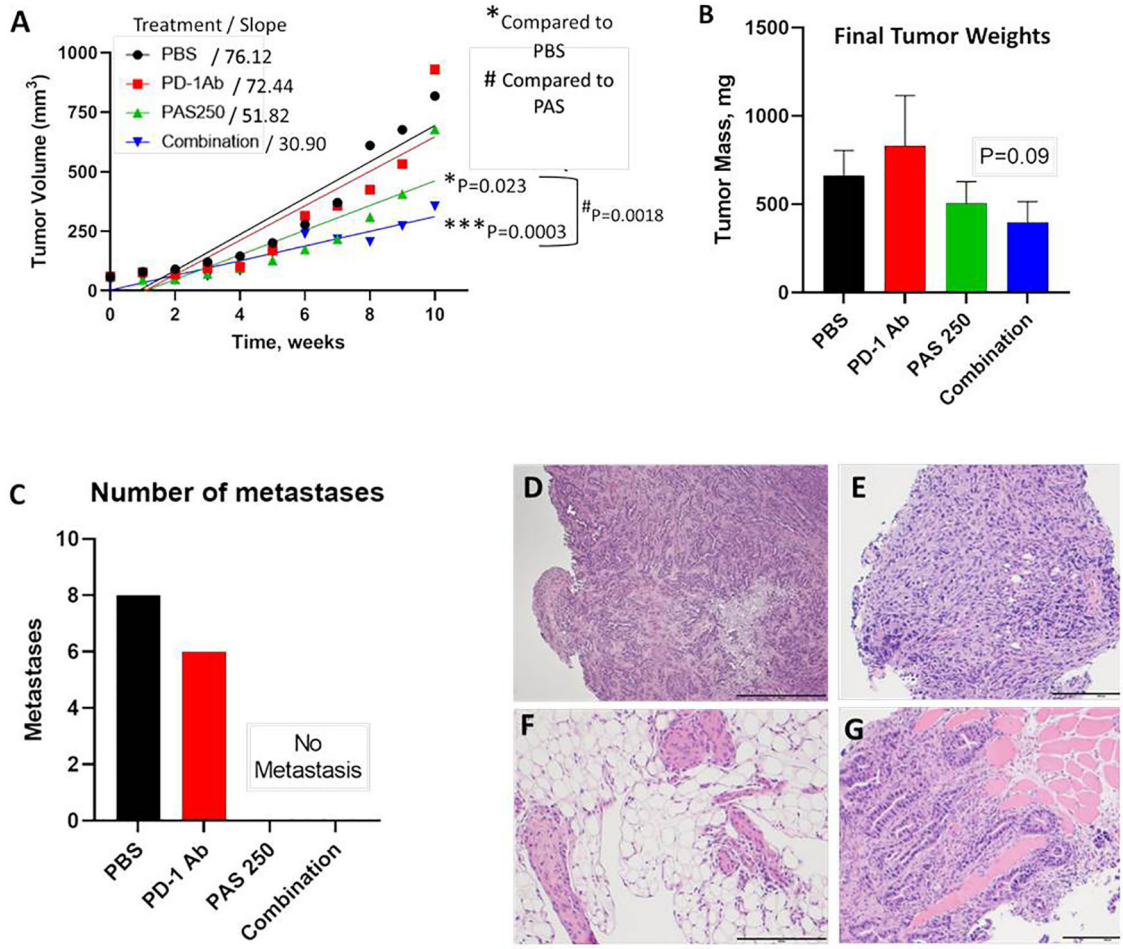

FIGURE 3 | PAS vaccination alone or in combination with PD-1 Ab inhibits growth and metastases of YTN gastric cancer tumors in mice. **(A)** YTN tumor volumes over time for each treatment group and respective slope of the line are shown. PD-1 Ab monotherapy did not alter rate of YTN tumor growth compared to PBS-treated controls. Tumors of mice treated with PAS monotherapy (P = 0.023) or in combination with PD-1 Ab (P = 0.0003) significantly reduced tumor growth in mice compared to PBS control treated mice. Tumors of mice treated with both PAS and the PD-1 Ab exhibited significantly smaller tumors compared to PAS monotherapy (P = 0.0018). **(B)** Final tumor mass *ex vivo* showed a reduction in size in mice treated with PAS in combination with the PD-1 Ab (P = 0.09). **(C)** Number of metastases for each treatment group demonstrates that metastases were only observed in Control (PBS-treated) mice and in mice treated with PD-1 Ab. No metastases were found in mice treated with PAS monotherapy or PAS in combination with the PD-1 Ab. **(D–G)** Metastases were confirmed histologically by H&E stain. **(D)** Invasive YTN tumor invading the stomach wall. **(E)** Peritoneal seeding with metastases. **(F)** Invasion of YTN tumor cells in the mesentery fat. **(G)** YTN cancer invading the abdominal wall skeletal muscle.

better than PAS monotherapy. The mass of the tumors when excised was less in the PAS- and combination-treated mice, but this difference did not reach significance (**Figure 3B**). The total number of metastases in each group were counted at autopsy and confirmed by histology. **Figure 3C** shows the remarkable finding that there were no metastases in the mice treated with PAS monotherapy or PAS combined with the PD-1 Ab. Hematoxylin & eosin staining confirmed that the tissues dissected from control mice and PD-1 Ab treated mice were metastases. **Figures 3D–G** show representative histology of YTN metastases from the stomach wall, mesentery, peritoneum, and abdominal wall, respectively.

Another demonstration of the effects on tumor growth is the measurement of the Ki67 proliferation index. Ki67 immunoreactivity is increased in the tumors of PBS and PD-1 Ab treated mice (**Figure 4A**). The proliferation index is significantly decreased in tumors of mice treated with PAS monotherapy or in combination with PD-1 Ab (**Figure 4A**). A low power (magnification 2×) representative image from each treatment group is shown in **Figure 4B** with a higher magnification (40×) insert image for each tumor. Marked Ki67 immunoreactivity is identified in tumors from PBS and PD-1 Ab treated mice. In contrast, the Ki67 staining is markedly decreased in tumors of mice treated with PAS with or without PD-1 Ab. These histologic sections confirm tumors of the PAS and combination-treated mice had decreased proliferation or growth rate.

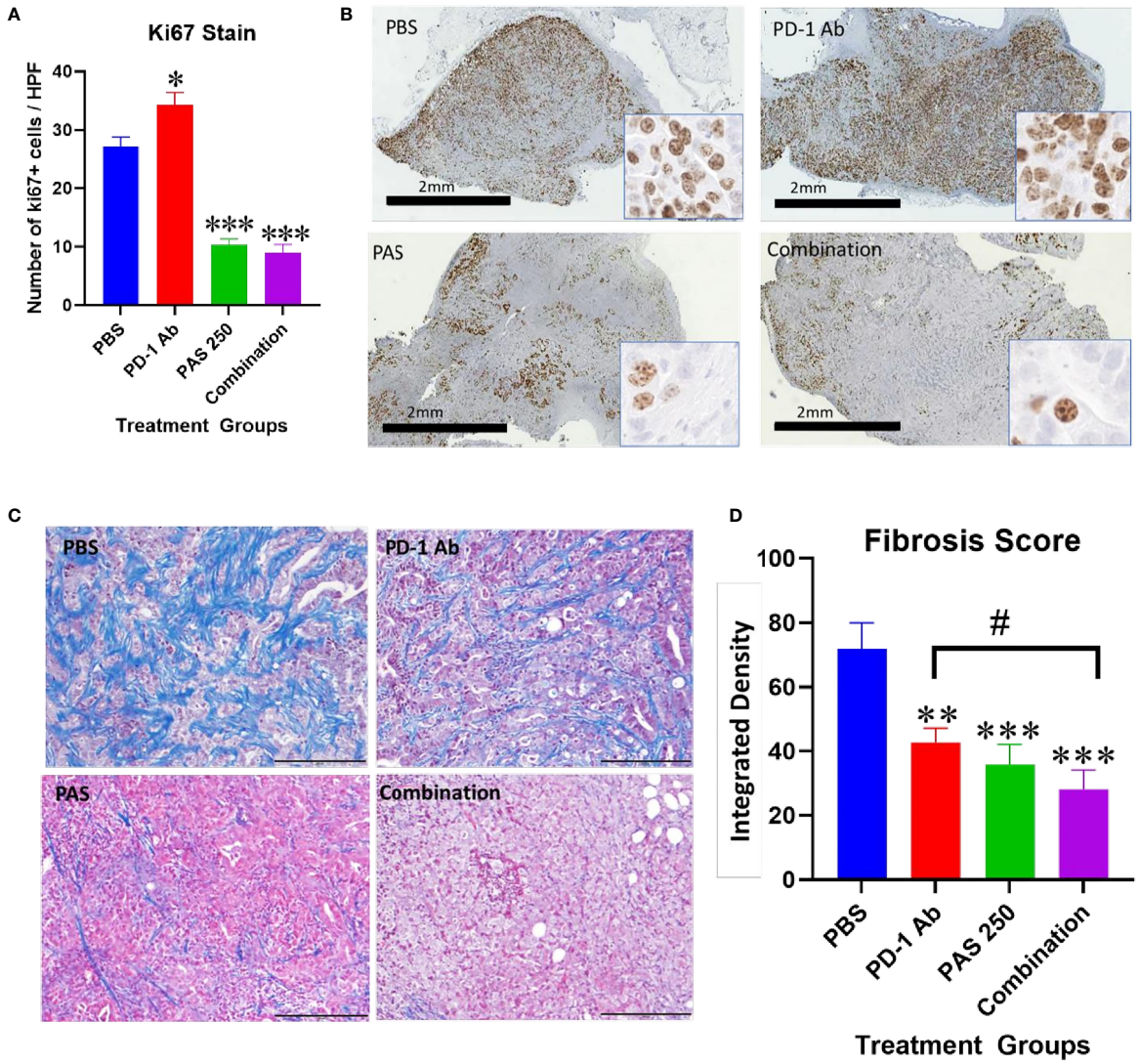

FIGURE 4 | Effects of PAS and PD-1 Ab treatment on tumor proliferation and fibrosis. **(A)** The mean number ± SEM of Ki67 stained cells is shown for each cohort of YTN tumors. Ki67 immunoreactivity in PD-1 Ab tumors increased compared to PBS-treated controls ($P < 0.05$). * Significantly different from control. Ki67 staining was significantly reduced in tumors of mice treated with PAS monotherapy or in combination with the PD-1 Ab ($P < 0.0001$). **(B)** Representative images from tumors reacted with Ki67 antibody for each treatment group is show at low magnification (2×, bar scale, 2 mm) and at a higher magnification (40×, Box insert). **(C)** Representative images of tumors from each treatment group stained for fibrosis with Masson's trichrome stain (scale bar = 200 μm). **(D)** Mean values ± SEM for fibrosis staining is shown for each treatment as analyzed by integrated density. Intratumoral fibrosis was decreased in all treatment groups compared to PBS-treated control tumors. Tumors of the combination therapy group also exhibited less fibrosis than tumors of the mice treated with PD-1 Ab monotherapy. (Compared to PBS $^{**}P < 0.01$; $^{***}P < 0.001$; compared to PD-1 Ab $^{\#}<0.05$).

PAS and PD-1 Ab Therapy Decrease Fibrosis in the Gastric Cancer

Tumor fibrosis is thought to impede the penetration of chemotherapeutic agents into cancers and also restrict the influx of T-lymphocytes. YTN gastric tumors demonstrate characteristic dense fibrosis as seen in tumors of PBS-treated control mice with the Masson's trichrome stain of **Figure 4C**. There is visibly less fibrosis noted in the tumors of mice treated with PAS monotherapy or PAS in combination with PD-1 Ab. Computerized analysis and quantification of the integrated density of fibrosis is shown for each treatment group in **Figure 4D**. Although there was modest decrease in fibrosis in tumors of PD-1 Ab treated mice, when combined with PAS therapy, the amount of fibrosis was significantly further decreased.

PAS and PD-1 Ab Therapy Change the Immune Cell Signature of Gastric Cancer

One reason for the lack of effect of immune checkpoint therapy in cancers is thought to be due to the paucity of tumor infiltrating T-cells. Tumors from each treatment group were stained for

CD8+ T-lymphocytes and the number of immunoreactive cells compared between groups. **Figure 5A** shows the lack of CD8+ T cells in gastric tumors of PBS control mice and in PD-1 Ab-treated mice. The number of CD8+ immunoreactive cells is visibly increased in tumors of PAS-treated mice and mice treated with the combination therapy (**Figure 5A**). Computer analysis of the YTN tumors stained with the CD8+ antibody show marked increase in CD8+ T-lymphocytes in tumors of PAS-treated mice and even a significantly greater increase of CD8+ T cells in mice treated with the combination therapy (**Figure 5B**).

Tumors from each group also underwent immunohistochemical staining with an antibody for arginase to detect M2-polarized tumor-associated macrophages (TAMs). These immunosuppressive TAMs are abundant in the tumors of control mice and PD-1 Ab-treated mice (**Figure 5C**). In contrast, there are noticeably fewer arginase+ TAMS in the gastric tumors of mice treated with PAS which confirms that the immunoreactivity is significantly decreased in tumors of PAS-treated mice. Tumors of mice treated with both PAS and the PD-1 Ab have even further decreased immunoreactivity of arginase positive TAMs (**Figure 5D**).

Human Gastric Cancer Expresses CCK-BR by Immunohistochemistry

Human gastric cancer epithelial cells were positive for CCK-BR immunoreactivity (**Figure 6**) implying that the administration of PAS to human subjects would also decrease activation of this

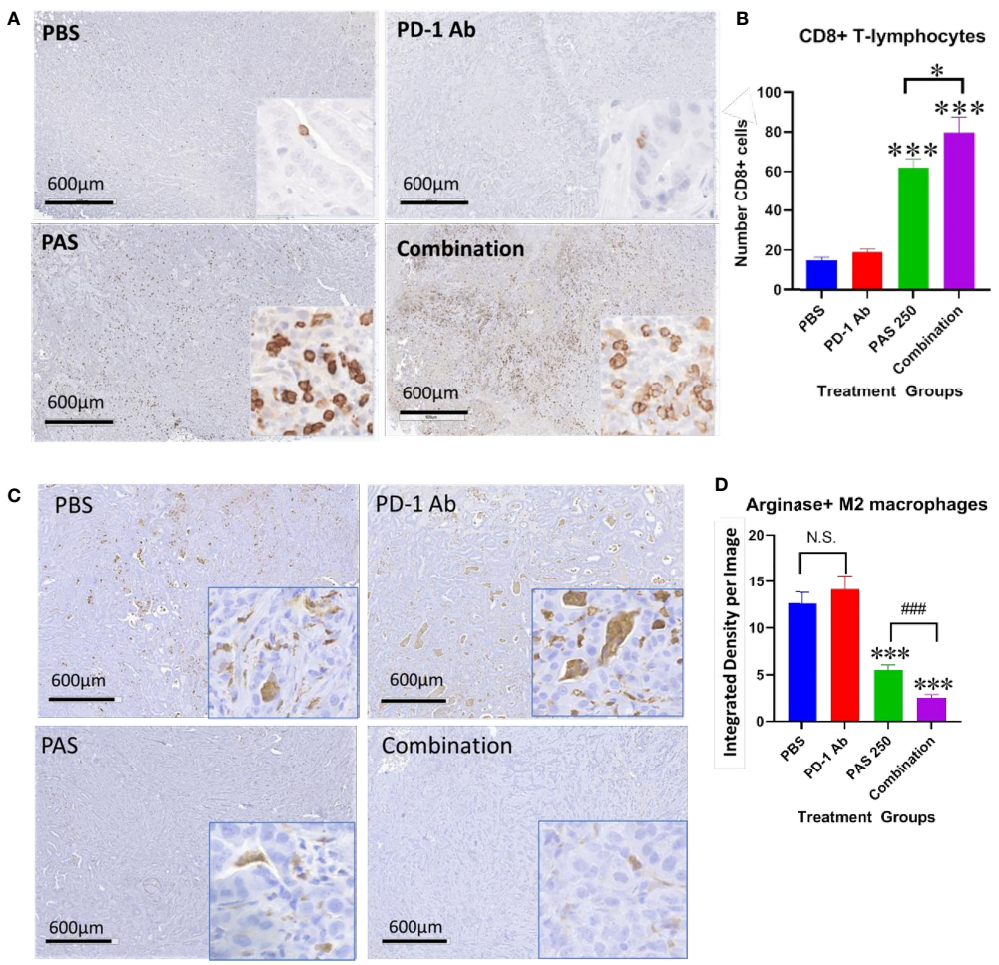

FIGURE 5 | PAS monotherapy and in combination with PD-1 Ab alter the tumor immune cell signature. **(A)** Representative low magnification tumor from each treatment or control group (scale bar 600µm) and a higher magnification (20×; Box insert) of tumors stained with an antibody for CD8+ T-lymphocytes. **(B)** Columns represent the mean ± SEM of the number of CD8+ immunoreactive cells in sections of YTN tumors from each group. PAS monotherapy and in combination with a PD-1 Ab significantly increase the number of CD8+ immunoreactive T-cells in the YTN tumors compared to tumors of PBS-treated mice. The combination of PAS with PD-1 Ab also markedly increased the number of CD8+ cells compared to PAS monotherapy. (***P <0.001 compared to PBS; $^{###}$P <0.001, compared to PAS). **(C)** Representative low magnification tumor from each treatment or control group (scale bar 600µm) and a higher magnification (20X; Box insert) of tumors stained with and antibody for M2-polarized tumor-associated macrophages (TAMs). **(D)** Columns represent the mean ± SEM of integrated density from ImageJ analysis for concentration of M2-polarized TAMs. The number of TAMs decreased significantly in tumors of mice treated with PAS monotherapy or in combination with the PD-1 Ab. Analysis showed that the combination therapy reduced TAMs significantly more than PAS alone. (***P<0.001 compared to PBS; ### P<0.001, compared to PAS). NS, not significant.

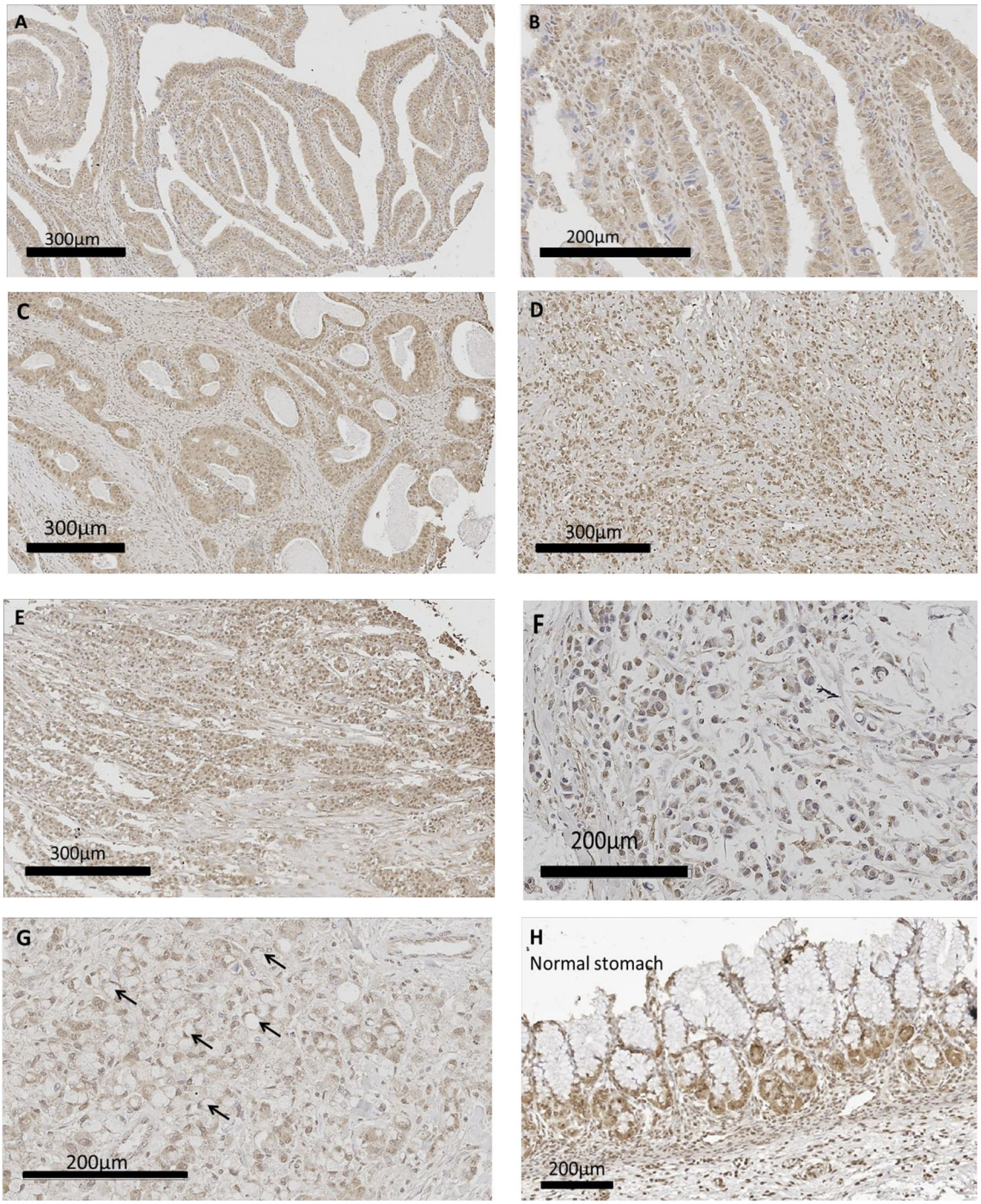

FIGURE 6 | CCK-BR protein expression by immunohistochemistry in human gastric cancer and normal tissues from a human gastric tissue array (US Biomax # BC01011). The array was stained with a CCK-BR antibody (Abcam 77077) at a titer of 1:200 overnight at 4°C. **(A–C)** Gastric cancer images representative of the intestinal type histology are shown. **(D, E)** Representative images of gastric cancers with the diffuse histologic type are shown. **(F)** Gastric carcinoma mucinous adenocarcinoma. **(G)** Gastric cancer signet ring histology; arrows point to signet ring cells. **(H)** Histology normal human stomach.

receptor by neutralizing gastrin. The most common histologic classification was described by Lauren (38) where cancers were categorized histologically into one of two types: intestinal or diffuse. **Figures 6A–C** show CCK-BR immunoreactivity in tissues from the human gastric cancer array with the intestinal-type histology showing the characteristic glands or tubules lines by epithelial cells. Histological diffuse gastric carcinoma cells lack cohesion and invade tissues independently

or in small clusters (39). Representative diffuse type gastric cancers also expressed CCK-BR expression and are shown in **Figures 6D–E**. Mucinous gastric cancer (**Figure 6F**) and signet ring gastric cancer (**Figure 6G**) are less common histologic types of gastric cancer. Characteristic staining of CCK-BR positive cells in the glands of the normal human stomach are seen in **Figure 6H**. There was not significant difference in the intensity of the CCK-BR staining according to the integrated density analyzed with ImageJ between tumors classified as Grade 1 (164.8 ± 1.4), Grade 2 (159.7 ± 1.4), and Grade 3 (162.8 ± 1.1).

DISCUSSION

In the current investigation, we demonstrated using two murine gastric cancer cell lines and a human tissue microarray that the gastrin: CCK-BR signaling pathway is important in stimulating growth of gastric cancer. CCK-BRs were expressed in both cell lines and exogenous gastrin stimulated cell growth *in vitro* confirming gastrin sensitivity. Immunocytochemistry revealed endogenous gastrin expression within the gastric cancer cells suggesting that gastric cancer may regulate its own growth by an autocrine mechanism. Since exogenously administered gastrin or endogenously produced gastrin from the cancer cells can activate the CCK-BR receptor resulting in cellular or tumor proliferation, strategies to interrupt the interaction of gastrin should inhibit growth. Indeed, we showed that a vaccine that targets gastrin can inhibit growth of gastric cancer in mice and prevent metastases. The PAS vaccine when administered as monotherapy decreased tumor growth in mice; however, the tumor inhibitory effect was significantly affected by co-administration of the PD-1 Ab with PAS. The advantage of having a therapy such as the PAS vaccine that shows efficacy with monotherapy is that when treating subjects with gastric cancer, not all subjects are eligible for immune checkpoint antibody treatment or some may have experienced adverse effects from the immune checkpoint therapy; hence, monotherapy may provide an alternative option to treat these subjects. However, in those subjects eligible for immune checkpoint therapy, the addition of PAS could significantly decrease tumor growth and prevent metastases. This vaccine, PAS, significantly decreased gastric cancer proliferation and this change was confirmed histologically with marked decreased in the number of Ki67 immunoreactive tumor cells. PAS therapy also decreased fibrosis in the tumor microenvironment. Vaccination with PAS also altered the tumor immune cell signature by increasing the number of CD8+ T-cells and decreasing the number of M2-polarized immunosuppressive macrophages rendering the tumor microenvironment more susceptible to other treatments, such as PD-1 Ab therapy.

Although the cancer cells expressed receptors for PD-L1, monotherapy with a PD-1 Ab did not significantly decrease gastric cancer growth or metastases. However, when PD-1 Ab therapy was administered in combination with PAS, there was a greater inhibitory effect on tumor growth rate than with PAS therapy alone. One explanation for the additive effect of PAS with the PD-1 Ab may be attributed to the marked increase in CD8+ T-cells when the two immune therapies are given together. Another beneficial finding of combined administration included the additive effect seen on the number of arginase positive M2-polarized macrophages. We previously described an additive effect on tumor inhibition in pancreatic cancer when PD-1 Ab therapy alone had no inhibitory effects but when combined with PAS, the combination therapy had a greater effect than PAS alone (31). In the prior study in pancreatic tumors, we also showed that PAS in combination with the PD-1 Ab decreased fibrosis in the tumor microenvironment. The decrease in fibrosis may perhaps allow for the influx of T cells.

Although this investigation was performed in immune competent mice with syngeneic murine tumors, the results of the CCK-BR immunoreactivity on the human gastric cancer array support the important translational and clinical relevance of this work. We found that both murine gastric cancers (YTN and NCC) expressed CCK-BRs and when YTN tumor bearing mice were treated with a gastrin vaccine, the tumor growth rate and metastases significantly decreased. Gastrin is the major ligand activating the CCK-BR and because PAS therapy induces neutralizing gastrin antibodies and gastrin-activated memory T cells (31), the ability to decrease signaling at this receptor is central to inhibiting cancer growth. Sheng et al. (40) demonstrated that that mature enterochromaffin-like cells (ECL) cells in the gastric corpus express CCK-BRs, and that that gastric isthmal progenitor cells also expressed CCK-BRs that responded to hypergastrinemia by supplying new ECL cells. Their elegant work supports the importance of gastrin as a trophic peptide activating the CCK-BR in the gastric mucosa. We previously showed that CCK-BRs are expressed on several human gastric cancer cell lines (19) and that gastrin-stimulated growth *in vitro* was only blocked by the selective CCK-BR antagonist, L265,260. The human gastric cancer tissue array immunoreactivity for the CCK-BR in numerous human gastric cancers in this current study suggests the importance of this receptor as a potential target for therapy in human subjects. The finding of CCK-BR staining in both the intestinal and diffuse histologic gastric cancer types suggests the broad implication of utilizing a therapy that targets this proliferative pathway. Although mucinous and signet ring histologic types occur less often, the prognosis with these histologic types is typically more severe (41). Tissues in the human gastric cancer array with these less frequent histologic types also stained positive for the CCK-BR suggesting the potential broad application of PAS therapy in gastric cancer.

Research on PAS was initiated by Dr. Susan Watson in the early 1990s (29, 32, 33). Although not popular at the time, Dr. Watson decided to take an immune approach to treating GI cancers by producing high-affinity anti-G17 antibodies that could neutralize serum gastrin and cell-associated gastrin. Since it had previously been reported that serum gastrin levels are elevated in colorectal tumors (42), she decided to begin her investigation in that tumor (28, 29). A wealth of clinical data was generated over the years that have been used to determine an appropriate adjuvant, dosing schedule, dose concentration and

boosters required to produce high affinity anti-G17 antibodies. It was discovered that as antibody titers rose, serum gastrin levels decreased (43). It was found that antibody titers could be followed and subjects with titers 1.2 units above baseline, on average, doubled their survival times in colon, pancreatic and gastric cancers. There were some surprising results along the way. PAS was synergistic with Gemcitabine, and unexpected long-term survivors were observed in several studies including in pancreatic cancer. These results led to discussions that perhaps something beyond neutralizing gastrin was occurring; however, the tools available today were not available then. Although there were positive studies in all three GI cancer indications and a well characterized safety profile of the product, the development of PAS took a major set-back when the company funding its development failed. The last subjects treated with PAS were in 2004.

In the last two years, a great deal has been learned about the mechanism of action of PAS. Not only does it produce high affinity anti-G17 antibodies, but PAS activates a cellular immune response that increases memory T-cells, NKT-cells and gamma-delta cells (31). Furthermore, it consistently changed the microenvironment in several animal models (pancreatic and gastric) leading to a synergistic effect with checkpoint inhibitors (31). The prevention of metastases in mice treated with PAS (44) was due to the inhibition of epithelial mesenchymal transition, and this mechanism of action may help explain the long-term survivors previously observed in the clinical program. The decreased fibrosis observed with PAS therapy may help to explain the synergy previously found with gemcitabine. PAS vaccination in a precancerous KRAS murine model demonstrated that PAS not only decreases pancreatic fibrosis and alters the immune cell signature of the tumor microenvironment but that it also decreases proliferation and progression on precancerous PanIN lesions preventing pancreatic cancer (45). The data are compelling for PAS to return to the clinic with a much better understanding of how to use the product.

DATA AVAILABILITY STATEMENT

The raw data supporting the conclusions of this article will be made available by the authors, without undue reservation.

ETHICS STATEMENT

The animal study was reviewed and approved by the Georgetown University IACUC.

AUTHOR CONTRIBUTIONS

Conception and design: JS, TP, LS, and AC. Acquisition of data: HC, JS, TP, KM, and WC. Analysis and interpretation of data: JS, HC, WC, KM, TP, LS, and AC. Writing, review and/or revision of manuscript: All authors. All authors contributed to the article and approved the submitted version.

FUNDING

The study was funded in part by a grant from Cancer Advances, Inc., and its subsidiary Vaccicure, and NIH CA051008 to the Georgetown Lombardi Cancer Center Core facilities.

ACKNOWLEDGMENTS

We appreciate the assistance of the animal technician from the Georgetown Department of Comparative Medicine. We also thank the researchers of the Lombardi Comprehensive Cancer Center Histology Core facility for assistance in preparing and staining tissues.

REFERENCES

1. Siegel R, Ma J, Zou Z, Jemal A. Cancer Statistics, 2014. *CA Cancer J Clin* (2014) 64:9–29. doi: 10.3322/caac.21208
2. Elimova E, Shiozaki H, Wadhwa R, Sudo K, Chen Q, Estrella JS, et al. Medical Management of Gastric Cancer: A 2014 Update. *World J Gastroenterol* (2014) 20:13637–47. doi: 10.3748/wjg.v20.i38.13637
3. Ferlay J, Steliarova-Foucher E, Lortet-Tieulent J, Rosso S, Coebergh JW, Comber H, et al. Cancer Incidence and Mortality Patterns in Europe: Estimates for 40 Countries in 2012. *Eur J Cancer* (2013) 49:1374–403. doi: 10.1016/j.ejca.2012.12.027
4. Howlader N, Ries LA, Stinchcomb DG, Edwards BK. The Impact of Underreported Veterans Affairs Data on National Cancer Statistics: Analysis Using Population-Based SEER Registries. *J Natl Cancer Inst* (2009) 101:533–6. doi: 10.1093/jnci/djn517
5. Bang YJ, Van CE, Feyereislova A, Chung HC, Shen L, Sawaki A, et al. Trastuzumab in Combination With Chemotherapy Versus Chemotherapy Alone for Treatment of HER2-Positive Advanced Gastric or Gastro-Oesophageal Junction Cancer (ToGA): A Phase 3, Open-Label, Randomised Controlled Trial. *Lancet* (2010) 376:687–97. doi: 10.1016/S0140-6736(10)61121-X
6. Bass AJ, Laird PW, Shmulevich I, Thorsson V. Comprehensive Molecular Characterization of Gastric Adenocarcinoma. *Nature* (2014) 513:202–9. doi: 10.1038/nature13480
7. Alsina M, Moehler M, Hierro C, Guardeno R, Tabernero J. Immunotherapy for Gastric Cancer: A Focus on Immune Checkpoints. *Target Oncol* (2016) 11:469–77. doi: 10.1007/s11523-016-0421-1
8. Muro K, Chung HC, Shankaran V, Geva R, Catenacci D, Gupta S, et al. Pembrolizumab for Patients With PD-L1-Positive Advanced Gastric Cancer (KEYNOTE-012): A Multicentre, Open-Label, Phase 1b Trial. *Lancet Oncol* (2016) 17:717–26. doi: 10.1016/S1470-2045(16)00175-3
9. Fuchs CS, Doi T, Jang RW, Muro K, Satoh T, Machado M, et al. Safety and Efficacy of Pembrolizumab Monotherapy in Patients With Previously Treated Advanced Gastric and Gastroesophageal Junction Cancer: Phase 2 Clinical KEYNOTE-059 Trial. *JAMA Oncol* (2018) 4:e180013. doi: 10.1001/jamaoncol.2018.0013
10. Janjigian YY, Shitara K, Moehler M, Garrido M, Salman P, Shen L, et al. First-Line Nivolumab Plus Chemotherapy Versus Chemotherapy Alone for Advanced Gastric, Gastro-Oesophageal Junction, and Oesophageal Adenocarcinoma (CheckMate 649): A Randomised, Open-Label, Phase 3 Trial. *Lancet* (2021) 398:27–40. doi: 10.1016/S0140-6736(21)00797-2
11. Brar G, Shah MA. The Role of Pembrolizumab in the Treatment of PD-L1 Expressing Gastric and Gastroesophageal Junction Adenocarcinoma. *Therap Adv Gastroenterol* (2019) 12:1756284819869767. doi: 10.1177/1756284819869767
12. Cronin KA, Lake AJ, Scott S, Sherman RL, Noone AM, Howlader N, et al. Annual Report to the Nation on the Status of Cancer, Part I: National Cancer Statistics. *Cancer* (2018) 124:2785–800. doi: 10.1002/cncr.31551

13. Svensson MC, Warfvinge CF, Fristedt R, Hedner C, Borg D, Eberhard J, et al. The Integrative Clinical Impact of Tumor-Infiltrating T Lymphocytes and NK Cells in Relation to B Lymphocyte and Plasma Cell Density in Esophageal and Gastric Adenocarcinoma. *Oncotarget* (2017) 8:72108–26. doi: 10.18632/oncotarget.19437
14. Saito H, Fushida S, Harada S, Miyashita T, Oyama K, Yamaguchi T, et al. Importance of Human Peritoneal Mesothelial Cells in the Progression, Fibrosis, and Control of Gastric Cancer: Inhibition of Growth and Fibrosis by Tranilast. *Gastric Cancer* (2018) 21:55–67. doi: 10.1007/s10120-017-0726-5
15. Smith JP, Nadella S, Osborne N. Gastrin and Gastric Cancer. *Cell Mol Gastroenterol Hepatol* (2017) 4:75–83. doi: 10.1016/j.jcmgh.2017.03.004
16. Dockray GJ, Moore A, Varro A, Pritchard DM. Gastrin Receptor Pharmacology. *Curr Gastroenterol Rep* (2012) 14:453–9. doi: 10.1007/s11894-012-0293-1
17. Watson SA, Grabowska AM, El-Zaatari M, Takhar A. Gastrin - Active Participant or Bystander in Gastric Carcinogenesis? *Nat Rev Cancer* (2006) 6:936–46. doi: 10.1038/nrc2014
18. Remy-Heintz N, Perrier-Meissonnier S, Nonotte I, Laliberte MF, Chevillard C, Laboisse C, et al. Evidence for Autocrine Growth Stimulation by a Gastrin/CCK-Like Peptide of the Gastric Cancer HGT-1 Cell Line. *Mol Cell Endocrinol* (1993) 93:23–9. doi: 10.1016/0303-7207(93)90135-7
19. Smith JP, Shih AH, Wotring MG, McLaughlin PJ, Zagon IS. Characterization of CCK-B/gastrin-Like Receptors in Human Gastric Carcinoma. *Int J Oncol* (1998) 12:411–9. doi: 10.3892/ijo.12.2.411
20. Goetze JP, Eiland S, Svendsen LB, Vainer B, Hannibal J, Rehfeld JF. Characterization of Gastrins and Their Receptor in Solid Human Gastric Adenocarcinomas. *Scand J Gastroenterol* (2013) 48:688–95. doi: 10.3109/00365521.2013.783101
21. Henwood M, Clarke PA, Smith AM, Watson SA. Expression of Gastrin in Developing Gastric Adenocarcinoma. *Br J Surg* (2001) 88:564–8. doi: 10.1046/j.1365-2168.2001.01716.x
22. Hur K, Kwak MK, Lee HJ, Park DJ, Lee HK, Lee HS, et al. Expression of Gastrin and its Receptor in Human Gastric Cancer Tissues. *J Cancer Res Clin Oncol* (2006) 132:85–91. doi: 10.1007/s00432-005-0043-y
23. Xu W, Chen GS, Shao Y, Li XL, Xu HC, Zhang H, et al. Gastrin Acting on the Cholecystokinin2 Receptor Induces Cyclooxygenase-2 Expression Through JAK2/STAT3/PI3K/Akt Pathway in Human Gastric Cancer Cells. *Cancer Lett* (2013) 332:11–8. doi: 10.1016/j.canlet.2012.12.030
24. Grabowska AM, Morris TM, McKenzie AJ, Kumari R, Hamano H, Emori Y, et al. Pre-Clinical Evaluation of a New Orally-Active CCK-2R Antagonist, Z-360, in Gastrointestinal Cancer Models. *Regul Pept* (2008) 146:46–57. doi: 10.1016/j.regpep.2007.08.007
25. Baldwin GS, Shulkes A. CCK Receptors and Cancer. *Curr Top Med Chem* (2007) 7:1232–8. doi: 10.2174/156802607780960492
26. Berna MJ, Jensen RT. Role of CCK/gastrin Receptors in Gastrointestinal/Metabolic Diseases and Results of Human Studies Using Gastrin/CCK Receptor Agonists/Antagonists in These Diseases. *Curr Top Med Chem* (2007) 7:1211–31. doi: 10.2174/156802607780960519
27. Rai R, Chandra V, Tewari M, Kumar M, Shukla HS. Cholecystokinin and Gastrin Receptors Targeting in Gastrointestinal Cancer. *Surg Oncol* (2012) 21:281–92. doi: 10.1016/j.suronc.2012.06.004
28. Watson SA, Michaeli D, Grimes S, Morris TM, Crosbee D, Wilkinson M, et al. Anti-Gastrin Antibodies Raised by Gastrimmune Inhibit Growth of the Human Colorectal Tumour AP5. *Int J Cancer* (1995) 61:233–40. doi: 10.1002/ijc.2910610216
29. Watson SA, Michaeli D, Grimes S, Morris TM, Robinson G, Varro A, et al. Gastrimmune Raises Antibodies That Neutralize Amidated and Glycine-Extended Gastrin-17 and Inhibit the Growth of Colon Cancer. *Cancer Res* (1996) 56:880–5. doi: 10.1002/ijc.2910610216
30. Watson SA, Michaeli D, Morris TM, Clarke P, Varro A, Griffin N, et al. Antibodies Raised by Gastrimmune Inhibit the Spontaneous Metastasis of a Human Colorectal Tumour, AP5LV. *Eur J Cancer* (1999) 35:1286–91. doi: 10.1016/S0959-8049(99)00115-X
31. Osborne N, Sundseth R, Burks J, Cao H, Liu X, Kroemer AH, et al. Gastrin Vaccine Improves Response to Immune Checkpoint Antibody in Murine Pancreatic Cancer by Altering the Tumor Microenvironment. *Cancer Immunol Immunother* (2019) 68:1635–48. doi: 10.1007/s00262-019-02398-6
32. Watson SA, Morris TM, Varro A, Michaeli D, Smith AM. A Comparison of the Therapeutic Effectiveness of Gastrin Neutralisation in Two Human Gastric Cancer Models: Relation to Endocrine and Autocrine/Paracrine Gastrin Mediated Growth. *Gut* (1999) 45:812–7. doi: 10.1136/gut.45.6.812
33. Watson SA, Michaeli D, Grimes S, Morris TM, Varro A, Clarke PA, et al. A Comparison of an Anti-Gastrin Antibody and Cytotoxic Drugs in the Therapy of Human Gastric Ascites in SCID Mice. *Int J Cancer* (1999) 81:248–54. doi: 10.1002/(SICI)1097-0215(19990412)81:2<248::AID-IJC14>3.0.CO;2-G
34. Ajani JA, Hecht JR, Ho L, Baker J, Oortgiesen M, Eduljee A, et al. An Open-Label, Multinational, Multicenter Study of G17DT Vaccination Combined With Cisplatin and 5-Fluorouracil in Patients With Untreated, Advanced Gastric or Gastroesophageal Cancer: The GC4 Study. *Cancer* (2006) 106:1908–16. doi: 10.1002/cncr.21814
35. Gilliam AD, Watson SA, Henwood M, McKenzie AJ, Humphreys JE, Elder J, et al. A Phase II Study of G17DT in Gastric Carcinoma. *Eur J Surg Oncol* (2004) 30:536–43. doi: 10.1016/j.ejso.2004.03.009
36. Park JW, Park DM, Choi BK, Kwon BS, Seong JK, Green JE, et al. Establishment and Characterization of Metastatic Gastric Cancer Cell Lines From Murine Gastric Adenocarcinoma Lacking Smad4, P53, and E-Cadherin. *Mol Carcinog* (2015) 54:1521–7. doi: 10.1002/mc.22226
37. Yamamoto M, Nomura S, Hosoi A, Nagaoka K, Iino T, Yasuda T, et al. Established Gastric Cancer Cell Lines Transplantable Into C57BL/6 Mice Show Fibroblast Growth Factor Receptor 4 Promotion of Tumor Growth. *Cancer Sci* (2018) 109:1480–92. doi: 10.1111/cas.13569
38. Lauren P. The Two Histological Main Types of Gastric Carcinoma: Diffuse and So-Called Intestinal-Type Carcinoma. An Attempt at a Histo-Clinical Classification. *Acta Pathol Microbiol Scand* (1965) 64:31–49. doi: 10.1111/apm.1965.64.1.31
39. Correa P. Gastric Cancer: Overview. *Gastroenterol Clin North Am* (2013) 42:211–7. doi: 10.1016/j.gtc.2013.01.002
40. Sheng W, Malagola E, Nienhuser H, Zhang Z, Kim W, Zamechek L, et al. Hypergastrinemia Expands Gastric ECL Cells Through CCK2R(+) Progenitor Cells *via* ERK Activation. *Cell Mol Gastroenterol Hepatol* (2020) 10:434–49. doi: 10.1016/j.jcmgh.2020.04.008
41. Taghavi S, Jayarajan SN, Davey A, Willis AI. Prognostic Significance of Signet Ring Gastric Cancer. *J Clin Oncol* (2012) 30:3493–8. doi: 10.1200/JCO.2012.42.6635
42. Smith JP, Wood JG, Solomon TE. Elevated Gastrin Levels in Patients With Colon Cancer or Adenomatous Polyps. *Dig Dis Sci* (1989) 34:171–4. doi: 10.1007/BF01536047
43. Rocha-Lima CM, de Queiroz Marques JE, Bayraktar S, Broome P, Weissman C, Nowacki M, et al. A Multicenter Phase II Study of G17DT Immunogen Plus Irinotecan in Pretreated Metastatic Colorectal Cancer Progressing on Irinotecan. *Cancer Chemother Pharmacol* (2014) 74:479–86. doi: 10.1007/s00280-014-2520-y
44. Osborne N, Sundseth R, Gay MD, Cao H, Tucker RD, Nadella S, et al. Vaccine Against Gastrin, a Polyclonal Antibody Stimulator, Decreases Pancreatic Cancer Metastases. *Am J Physiol Gastrointest Liver Physiol* (2019) 317:G682–93. doi: 10.1152/ajpgi.00145.2019
45. Smith JP, Cao H, Chen W, Kallakury B, Phillips T, Sutton L, et al. Vaccination With Polyclonal Antibody Stimulator (PAS) Prevents Pancreatic Carcinogenesis in the KRAS Mouse Model. *Cancer Prev Res (Phila)* (2021) 14:933–44. doi: 10.1158/1940-6207.CAPR-20-0650

Conflict of Interest: Authors TP, AC and LS are employees of Cancer Advances, Inc. and the company owns the patent rights to PAS.

The remaining authors declare that the research was conducted in the absence of any commercial or financial relationships that could be construed as a potential conflict of interest.

The authors declare that this study received funding from Cancer Advances, Inc. through a sponsored research agreement with Georgetown University. The funder had the following involvement with the study: Conception and design, Acquisition of data, Analysis and interpretation of data, and Writing, review and/ or revision of manuscript.

this article, or claim that may be made by its manufacturer, is not guaranteed or endorsed by the publisher.

frontiers in Oncology

ORIGINAL RESEARCH
published: 03 December 2021
doi: 10.3389/fonc.2021.728740

Cost-Effectiveness of Adjuvant Immunotherapy With Cytokine-Induced Killer Cell for Hepatocellular Carcinoma Based on a Randomized Controlled Trial and Real-World Data

Jeong-Yeon Cho[1†], *Sun-Hong Kwon*[1†], *Eui-Kyung Lee*[1], *Jeong-Hoon Lee*[2*] *and Hye-Lin Kim*[3*]

[1] School of Pharmacy, Sungkyunkwan University, Suwon, South Korea, [2] Department of Internal Medicine and Liver Research Institute, Seoul National University College of Medicine, Seoul, South Korea, [3] College of Pharmacy, Sahmyook University, Seoul, South Korea

OPEN ACCESS

Edited by:
Sripathi Sureban,
University of Oklahoma Health Sciences Center, United States

Reviewed by:
Ingo Schmidt-Wolf,
University Hospital Bonn, Germany
Hae Sun Suh,
Kyung Hee University, South Korea

***Correspondence:**
Hye-Lin Kim
maristella76@tistory.com
Jeong-Hoon Lee
pindra@empal.com;
JHLeeMD@snu.ac.kr

[†]These authors have contributed equally to this work and share first authorship

Specialty section:
This article was submitted to Gastrointestinal Cancers, a section of the journal Frontiers in Oncology

Received: 22 June 2021
Accepted: 16 November 2021
Published: 03 December 2021

Citation:
Cho J-Y, Kwon S-H, Lee E-K, Lee J-H and Kim H-L (2021) Cost-Effectiveness of Adjuvant Immunotherapy With Cytokine-Induced Killer Cell for Hepatocellular Carcinoma Based on a Randomized Controlled Trial and Real-World Data. Front. Oncol. 11:728740. doi: 10.3389/fonc.2021.728740

Background: Studies using data from randomized controlled trials (RCTs) and real-world data (RWD) have suggested that adjuvant cytokine-induced killer (CIK) cell immunotherapy after curative treatment for hepatocellular carcinoma (HCC) prolongs recurrence-free survival (RFS) and overall survival (OS). However, the cost-effectiveness of CIK cell immunotherapy as an adjuvant therapy for HCC compared to no adjuvant therapy is uncertain.

Methods: We constructed a partitioned survival model to compare the expected costs, life-year (LY), and quality-adjusted life-year (QALY) of a hypothetical population of 10,000 patients between CIK cell immunotherapy and no adjuvant therapy groups. Patients with HCC aged 55 years who underwent a potentially curative treatment were simulated with the model over a 20-year time horizon, from a healthcare system perspective. To model the effectiveness, we used OS and RFS data from RCTs and RWD. We estimated the incremental cost-effectiveness ratios (ICERs) and performed extensive sensitivity analyses.

Results: Based on the RCT data, the CIK cell immunotherapy incrementally incurred a cost of $61,813, 2.07 LYs, and 1.87 QALYs per patient compared to no adjuvant therapy, and the estimated ICER was $33,077/QALY. Being less than the willingness-to-pay threshold of $50,000/QALY, CIK cell immunotherapy was cost-effective. Using the RWD, the ICER was estimated as $25,107/QALY, which is lower than that obtained using RCT. The time horizon and cost of productivity loss were the most influential factors on the ICER.

Conclusion: We showed that receiving adjuvant CIK cell immunotherapy was more cost-effective than no adjuvant therapy in patients with HCC who underwent a potentially curative treatment, attributed to prolonged survival, reduced recurrence of HCC, and better prognosis of recurrence. Receiving CIK cell immunotherapy may be more cost-effective in real-world clinical practice.

Keywords: cost-effectiveness, immunotherapy, adjuvant therapy, cytokine-induced killer cell, economic evaluation, hepatocellular carcinoma

INTRODUCTION

Hepatocellular carcinoma (HCC) is an aggressive and frequently occurring cancer, with approximately 670,000 new cases and 625,000 deaths worldwide in 2018 (1). Interestingly, most HCC cases occur in individuals with well-known risk factors, such as chronic hepatitis B virus (HBV) or hepatitis C virus (HCV) infection, nonalcoholic steatohepatitis, chronic alcoholism, and liver cirrhosis. Thus, a regular surveillance program for populations with such risk factors is recommended to detect HCC at an early stage, and more than half of new HCC cases are now diagnosed at very early or early stages in Japan and Taiwan owing to the implementation of nationwide surveillance programs (2).

Generally, in the very early or early stages of HCC, potentially curative treatments, such as surgical resection or radiofrequency ablation (RFA), can be applied; however, even after successful resection, 50–70% of patients experience recurrence within 5 years (3, 4). The long-term prognosis of patients with recurrent HCC remains poor because of deterioration of liver function with repeated recurrences even after curative treatment following early detection of HCC and during a successful regular surveillance program (5). Therefore, in the treatment of HCC, recurrence after curative treatment is an important indicator that is negatively related to long-term survival (6). To improve recurrence-free survival (RFS) in patients with HCC, several studies on adjuvant therapy have been conducted; however, none of these studies provide sufficient evidence of improvement except for antiviral treatment for HBV- or HCV-related HCC (3).

Since the first report on the antitumor activity of cytokine-induced killer (CIK) cells, 106 clinical trials for various types of cancers have been registered in the international registry of CIK cells in the past decade (7, 8). Fortunately, recent phase III trials and real-world data (RWD) have shown that adjuvant CIK cell immunotherapy administered after curative treatment for HCC prolongs RFS, cancer-specific survival, and overall survival (OS) with minimum adverse effects. According to previous studies, patients who underwent repeated transfer of individualized autologous CIK cell agents had significantly longer RFS than the control group with a hazard ratio of 0.42 (95% confidence interval [CI], 0.22–0.80) to 0.63 (95% CI, 0.43–0.94) (9–11). These results have generated interest in the economic assessment of the benefits obtained and the input cost for adjuvant CIK immunotherapy. Nevertheless, there is limited data on the cost-effectiveness of immunotherapy in patients with HCC who have undergone potentially curative treatment.

Therefore, it is important for healthcare policymakers, providers, and patients to determine whether adjuvant CIK immunotherapy reflects an appreciable value in the current healthcare environment. We investigated the cost-effectiveness of CIK cell immunotherapy as an adjuvant therapy for patients with HCC using data from a recently reported phase III trial and RWD.

MATERIALS AND METHODS

Overview of Partitioned Survival Model

A cost-utility analysis was performed to evaluate the cost-effectiveness of receiving CIK cell immunotherapy compared with not receiving any adjuvant treatment (no adjuvant therapy) in patients with HCC who underwent a potentially curative treatment (surgical resection, RFA, or percutaneous ethanol injection [PEI]). Aligning with the phase III clinical study (the randomized controlled trial, hereafter referred to as RCT), its extended follow-up study (9, 10), and the phase IV clinical study (hereafter referred to as RWD) of CIK cell immunotherapy (11), we constructed a partitioned survival model, which has been widely used for the economic evaluation of oncology drugs, using Microsoft Excel (Microsoft, Redmond, Washington, USA) (12). The time horizon of the model was twenty years, and the cycle length was three months.

Our model included four conceptual health states: recurrence-free, curable recurrence, incurable recurrence, and death (**Figure 1A**). Because our population included patients with HCC who underwent a potentially curative treatment, all patients started from the recurrence-free state. RFS was defined as the time from randomization in RCT (in RWD, from curative treatment) to the first recurrence or death. Patients without recurrence remained in the recurrence-free state as the cycle went on. Otherwise, the patient experienced recurrence or death. Unlike a typical partitioned survival model, we divided the recurrence condition into two states according to the curability of treatment to consider the different treatments patients undergo. We assumed that patients received either curative or noncurative treatments once they demonstrated a recurrence. If patients remained in the curable recurrence state, they were treated with curative treatments, such as surgical resection, liver transplantation, RFA, or PEI. By contrast, patients staying in an incurable recurrence state would receive noncurative treatments including transarterial chemoembolization (TACE), external-

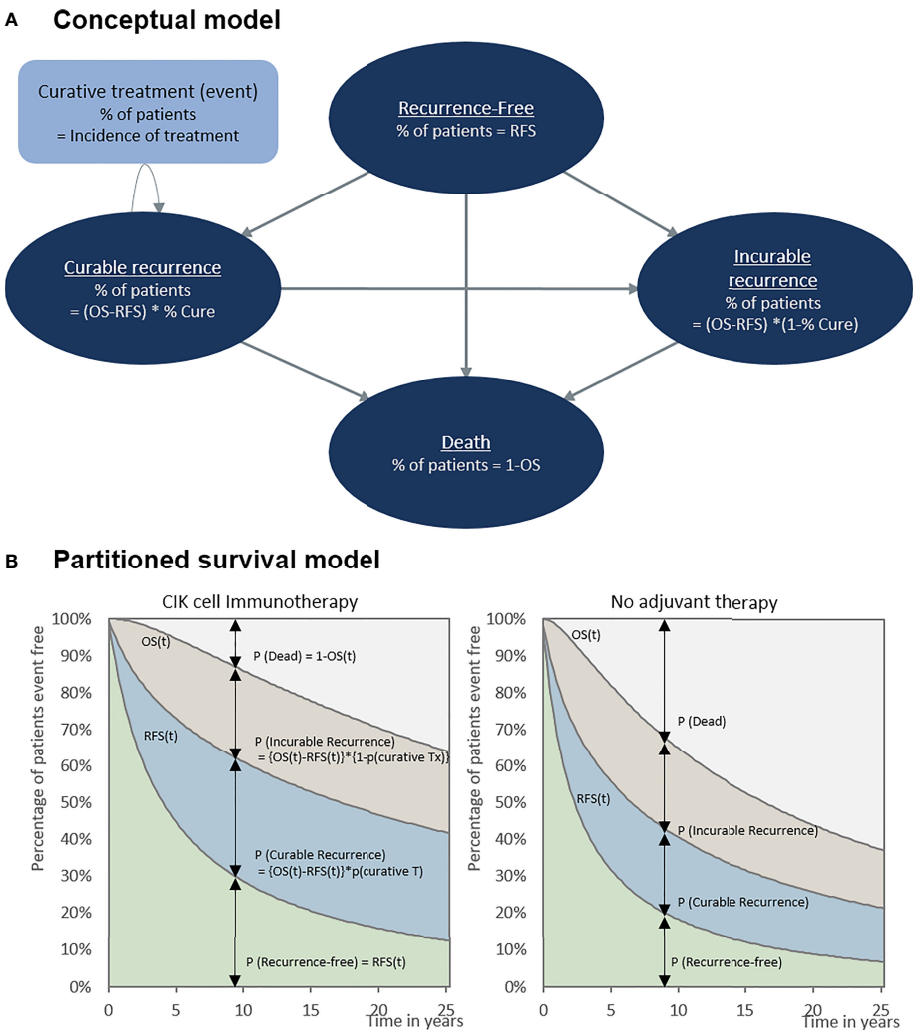

FIGURE 1 | Cost-effectiveness model. **(A)** Conceptual model and **(B)** partitioned survival model. OS, overall survival; RFS, recurrence-free survival.

beam radiation therapy, and systemic therapies including cytotoxic chemotherapy. We performed a *post-hoc* analysis of the records of individual patients on subsequent treatment and follow-up time after recurrences observed in phase III clinical trials to calculate the proportion of patients with curable recurrence and the incidence rates of each curative treatment applied in the curable recurrence state. For the treatment of HCC, liver transplantation, surgical resection, or RFA is considered as potentially curative treatment. In the base-case analysis, according to the international guideline, we assumed that once the patient received other non-curative therapy, such as TACE or systemic therapies including cytotoxic chemotherapy, the recurrence was classified as incurable (13). However, some of these patients might have received TACE for curative intent as curative treatment was not technically feasible; therefore, we adjusted the proportion of curative TACE to the calculation of curable recurrence in the sensitivity analysis. Our model simulated a cohort of 55-year-old patients, considering the mean age of patients in the RCT (9). To validate our model, clinical experts verified the key model assumptions.

The model estimated the costs, gained life-years (LYs), and quality-adjusted life-years (QALYs) for a 20-year time horizon. An annual discount rate of 5% was applied to the outcomes and costs, according to the pharmacoeconomic evaluation guideline from the Health Insurance Review & Assessment Service (HIRA) of the South Korean government (14). This economic evaluation was conducted and reported based on the Consolidated Health Economic Evaluation Reporting Standards (CHEERS) guidelines (15).

RFS and OS

Two survival curves of RFS and OS derived from the RCTs and RWD were applied in the model to estimate the distribution of patients in modeled health states following CIK cell immunotherapy or no adjuvant therapy (9–11). Using the effectiveness data from the RWD, we tried to reflect current

clinical practice for the early stage of HCC and to reduce the gap between the RCTs and the real-world setting Both RCT and RWD routine surveillance with CIK cell immunotherapy in an adjuvant setting for HCC were compared. At the median follow-up of 68.5 months for RCT and 28.0 months for RWD, investigators found statistically and clinically significant improvements in RFS (9–11). The patient characteristics and main results of both RCT and RWD were summarized in **Supplementary Table 1**.

RFS at a specific time was defined as the proportion of patients staying in the recurrence-free state (**Figure 1B**). The fraction of patients with recurrence was the difference between the OS and RFS (OS-RFS). The proportions of curable and incurable recurrence states were obtained from the RCTs to differentiate between patients receiving curative and noncurative treatment (**Table 1**). The incidence of curative treatment was estimated from the individual patient data reported in the RCTs. With regard to the distribution of patients who died, [1-OS] was adapted, as shown in **Figure 1B**.

To extrapolate patient survival beyond the duration of the clinical trial, parametric survival curves were fitted to our model: exponential, Weibull, generalized gamma, log-normal, and log-logistic. They were modeled jointly for each treatment group, and the best fit was determined using the Akaike information criterion, Bayesian information criterion, plausibility of the estimated long-term survival, and expert opinion (**Supplementary Table 2** and **Supplementary Figures 1, 2**) (12, 19). The parameter estimates for survival curves are presented in **Supplementary Table 3**.

Cost and Utility

We considered direct medical costs, which were represented in the model either as episodic costs for curative treatments and death (end-of-life) or state-based costs, in terms of the healthcare system perspective. The input costs, presented in USD in 2020 (1 USD = 1,166.51 KRW), are shown in **Table 1**. The cost data before 2020 were corrected for inflation using the national inflation calculator.

Treatment-specific costs in the recurrence-free state were estimated based on healthcare utilization from RCT and the unit cost from the reimbursement price list from HIRA. In accordance with the label of CIK cell immunotherapy,

TABLE 1 | Model input parameters.

Model input	Value	PSA distribution	Sources
Patient characteristics			
Starting age, years	55		Lee et al. (9)
Proportion of curable recurrence, %			Lee et al.[a] (10)
Treatment	56.6		
Control	47.8		
Incidence rate of curative treatments (/person-year), mean (95% CI)			Lee et al.[a] (10)
Resection	0.0888 (0.0385, 0.1390)	Normal	
Radiofrequency ablation	0.3033 (0.2105, 0.3962)	Normal	
Percutaneous ethanol injection	0.2071 (0.1304, 0.2839)	Normal	
Liver transplantation	0.0148 (0.0000, 0.0353)	Normal	
Utilities			
Health state utility (95% CI)			Pollom et al. (16)
Recurrence-free state	0.88 (0.85, 0.92)	Beta	
Curable recurrence	0.88 (0.85, 0.92)	Beta	
Incurable recurrence	0.40 (0.32, 0.48)	Beta	
Treatment-related disutility			Ock et al.[b] (17)
Resection	- 0.26		
Radiofrequency ablation	- 0.33		
Percutaneous ethanol injection	- 0.33		
Transplantation	- 0.21		
Costs (USD), mean (SD)[c]			
Treatment cost (per injection)	3,807		
Health state cost (per cycle)			
Recurrence-free state[d]	211 (21)	Gamma	Micro-costing
Curable recurrence[d]	211 (21)	Gamma	Micro-costing
Incurable recurrence	2,505 (711)	Gamma	HIRA data
Event cost for curative treatments			HIRA data
Resection	8,082 (3,015)	Gamma	
Radiofrequency ablation	2,085 (1,039)	Gamma	
Percutaneous ethanol injection	1,640 (1,282)	Gamma	
Liver transplantation	67,142 (23,888)	Gamma	
End-of-life cost[d]	6,798 (679)	Gamma	Yang, (18)

CI, confidence interval; HIRA, Health Insurance Review & Assessment Service of Korea; PSA, probabilistic sensitivity analysis; SD, standard deviation.

[a]*Derived from post-hoc analysis of recurrence data from phase III trial (Lee et al., 2015 & Lee et al., 2018).*

[b]*Converted to disutility from Ock et al., 2017.*

[c]*1 USD = 1,166.51 KRW.*

[d]*Standard deviation is assumed to be 10% of the mean value.*

treatment cost was considered for a total of 16 times at the price proposed by the manufacturer.

The medical costs for recurrence were obtained from the HIRA National Patient Sample (HIRA-NPS-2016-0106) data. The cost analysis of HIRA-NPS data was approved by the institutional review board of Sungkyunkwan University. The HIRA-NPS data are representative of the South Korean population, which includes approximately 3% of the total population (20, 21). From the HIRA-NPS data, we extracted the medical costs per episode of each curative treatments (i.e., resection, RFA, PEI, and transplantation) and noncurative treatments (i.e., TACE, external-beam radiation therapy, and systemic therapy with sorafenib or cytotoxic chemotherapy) from patients with the main diagnosis code of HCC (C22.0 of ICD-10, International Classifications of Disease 10th version) in 2016. The detailed procedure codes which were used to estimate the medical costs for each treatment were presented in **Supplementary Table 4**. For the curable recurrence state, the cost for each curative treatment was individually applied according to the incidence of curative treatment in the model. For the incurable recurrence state, the state-based cost was calculated by multiplying the cost of noncurative treatment by the frequency obtained from the RCT. The end-of-life costs were adapted from a previous study that observed end-of-life costs for patients with cancer (18).

We performed a systematic literature review using PubMed and the Cochrane library to obtain utility values for each health state in our model (16, 17). Utility is a number between 0 (death) and 1 (perfect health), which is used to calculate QALY by taking length and quality of life into consideration (22). A detailed list of the utilities and disutilities included in the model are shown in **Table 1**.

Analysis

The main output of this study was the incremental cost-effectiveness ratio (ICER), which was calculated by dividing the incremental costs by the incremental LYs and QALYs between the CIK cell immunotherapy group and no adjuvant therapy group. The cost-effectiveness was interpreted using ICER at the willingness-to-pay (WTP) threshold of $50,000/QALY.

Furthermore, one-way deterministic and probabilistic sensitivity analyses were performed to explore the robustness of the results by varying the parameter values and assumptions. For the one-way sensitivity analysis, clinical variables (parametric survival distribution to OS and RFS, and the proportion of patients receiving curative treatment), utility weights, medical costs, analytic perspective, time horizon, and discount rate were changed. Medical costs in other countries were also applied to the sensitivity analysis and are presented in **Supplementary Table 5** (23–25).

For the probabilistic sensitivity analysis, a comprehensive estimate of the uncertainty around the results was calculated using simultaneous random sampling of input parameters. The range and distribution of the parameters are listed in **Table 1** and **Supplementary Table 2**. The probabilistic sensitivity analysis consisted of 1,000 iterations with random values generated according to the range or distribution of each parameter included in the model. In addition, a cost-effectiveness acceptability curve (CEAC) was constructed to show the likelihood of the intervention being cost-effective according to the various WTP thresholds.

RESULTS

Based on the RCT data, the CIK cell immunotherapy resulted in 11.68 LYs and 8.80 QALYs per patient costing $115,002, whereas no adjuvant therapy resulted in 9.60 LYs and 6.94 QALYs per patient costing $53,190 (**Table 2**). Throughout the time horizon, the incremental LYs was 2.07 years, and the patients treated with CIK cell immunotherapy remained in the recurrence-free state longer than the patients without treatment (5.43 vs. 4.07 years, **Figure 2**). For treatment costs, a substantial difference between the two interventions was observed in the recurrence-free state. The incremental QALYs was 1.87 costing $61,813, and the ICER was $33,077/QALY.

Based on the RWD, the CIK cell immunotherapy resulted in 12.53 LYs and 9.76 QALYs per patient with a treatment cost of $110,670, whereas no adjuvant therapy resulted in 10.68 LYs and 7.66 QALYs per patient costing $57,959. The incremental life-years gained was 1.85, and the incremental QALY was 2.10, resulting in an ICER of $25,107/QALY. The ICERs estimated based on RCT data and RWD were both less than $50,000, which showed the cost-effectiveness of CIK cell immunotherapy.

The results of the deterministic sensitivity analysis are presented in **Supplementary Figure 3** and **Table 3**, showing the 10 most sensitive input parameters, given RCT data and RWD. The parameter that most influenced the ICER was the

TABLE 2 | Result of the cost-effectiveness analysis.

	CIK cell Immunotherapy	No adjuvant therapy	Incremental	ICER ($/LY or $/QALY)
Based on RCT data				
Cost	$115,002	$53,190	$61,813	
LY	11.68	9.60	2.07	$29,791
QALY	8.80	6.94	1.87	$33,077
Based on RWD				
Cost	$110,670	$57,959	$52,711	
LY	12.53	10.68	1.85	$28,437
QALY	9.76	7.66	2.10	$25,107

CIK, cytokine-induced killer cell; LY, life-year; QALY, quality-adjusted life-year; ICER, Incremental cost-effectiveness ratio; RCT, randomized controlled trial; RWD, real-world data.

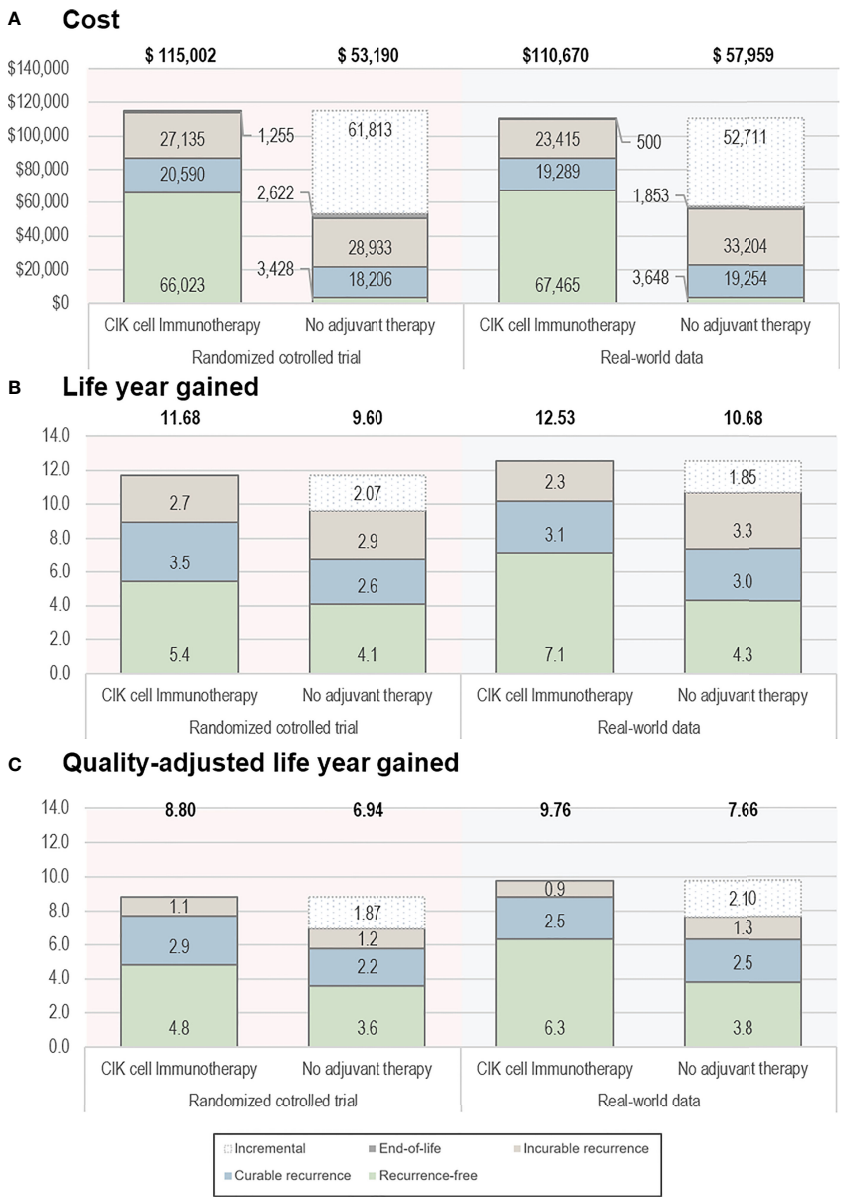

FIGURE 2 | Base-case results. **(A)** Cost, **(B)** life-year gained, and **(C)** quality-adjusted life-year gained. The bold text indicates the total value estimated from the analyses. CIK, cytokine-induced killer.

time horizon. Regarding other parameters, including productivity loss in the analysis (societal perspective) resulted in lower ICER ($ 25,562), whereas applying medical costs from Italy and the USA showed the robustness of the study results with ICER ranging from $34,141–$38,425 (**Supplementary Table 3**). All ICERs based on the RWD were lower than those based on the RCTs. The CEAC calculated from our model showed that the likelihood of CIK cell immunotherapy being cost-effective was 95% and 88% based on RCT and RWD, respectively, with a WTP threshold of $50,000 (**Figure 3**). For WTP values below $42,350, the cost-effectiveness acceptability based on RWD was higher than that based on RCT, but the trend reversed for WTP values beyond $42,350.

DISCUSSION

This study demonstrated that adjuvant CIK cell immunotherapy in patients who received curative treatment for HCC is cost-effective as compared with no adjuvant therapy. By applying data from RCTs and an extended follow-up study, we showed that the higher LYs and QALYs gained from receiving CIK cell

TABLE 3 | Deterministic sensitivity analyses..

Scenario	ICER (US$/QALY)	
	RCT	RWD
Base-case	33,077	25,107
Clinical outcomes		
Survival*		
RFS [Best case; Weibull (RCT), Weibull (RWD)]	31,260	22,948
RFS [Worst case; Log-normal (RCT), Generalized gamma (RWD)]	33,077	31,695
OS [Best case; Weibull (RCT), Generalized gamma (RWD))	31,009	22,587
OS [Worst case; Generalized gamma (RCT), Log-normal (RWD)]	38,831	27,545
Proportion of curable recurrence		
Considering a portion of TACE as a curative treatment (CIK 75.8% vs No Tx 72.6%)	36,293	29,237
Health-related quality of life		
Health state utilities		
Cancer free and incurable recurrence state (Upper bound)	31,876	24,978
Cancer free and incurable recurrence state (Lower bound)	33,971	25,236
Costs		
Medical costs from other healthcare systems		
The USA [derived from Cardier et al., (23)]	38,425	9,505
France [derived from Cardier et al., (23)]	34,617	25,626
Italy [derived from Rognoni et al., (24)]	34,141	22,197
End-of-life cost		
Upper bound (+20%)	32,930	24,695
Lower bound (–20%)	33,223	25,187
Analytic perspective (Societal perspective)		
Including productivity loss cost	25,562	19,858
Model parameters		
Time horizon (15 years)	41,628	32,730
Time horizon (25 years)	28,799	21,263
Annual discount rate (3%)	27,617	20,336
Annual discount rate (7.5%)	40,926	31,973

ICER, incremental cost-effectiveness ratio; RCT, randomized controlled trial; RWD, real-world data; RFS, recurrence-free survival; OS, overall survival; TACE, transarterial chemoembolization.
**To see the uncertainty from the selected survival curve, we carried out a sensitivity analysis that calculated the lowest (best case) and the highest (worst case) ICER by applying each parametric survival distribution to OS and RFS.*

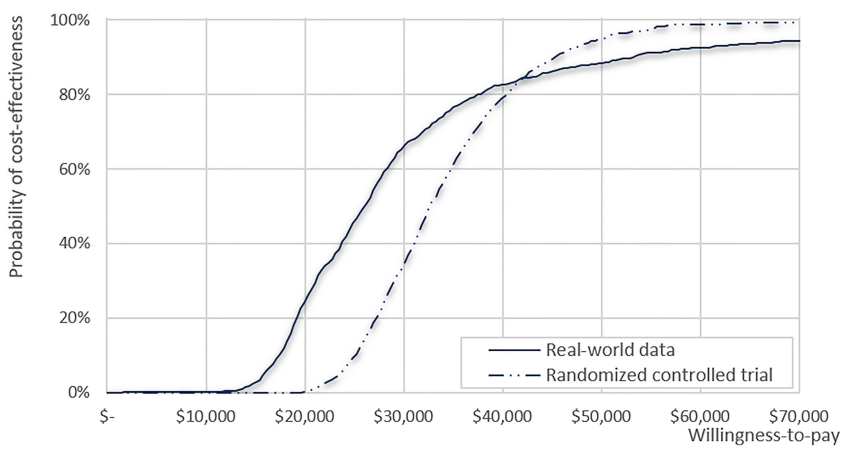

FIGURE 3 | Cost-effectiveness acceptability curve for clinical data from the real-world data and randomized clinical trial.

immunotherapy compared with no adjuvant therapy resulted from prolonged survival, reduced recurrence of HCC, and better prognosis of recurrence (9, 10). Furthermore, decreased medical expenses for the treatment of incurable recurrent HCC partially offset the considerable treatment cost of CIK cell immunotherapy in patient with curable recurrent HCC. Consequently, adjuvant CIK cell immunotherapy could be a cost-effective option based on a WTP threshold of US$ 50,000/QALY.

The simulation results using RWD, where CIK cell immunotherapy prolonged the RFS of patients with HCC, showed further improvement in cost-effectiveness, which was

attributed to more favorable survival for CIK cell immunotherapy than that from the RCT data. The cost-effectiveness model using RWD shows that more patients stayed in recurrence-free health state due to better RFS than that from RCT. Therefore, scenario using RWD incurred less medical expenditure and have more health-related quality of life due to prolonged recurrence-free survival, which means the cost-effectiveness results using RWD were better than that from RCT data.

In the RCT, adjuvant CIK cell immunotherapy was more effective at reducing the rate of early recurrence within the first 24 months (which is mainly associated with residual tumor cells) than late recurrence beyond 24 months (which is mainly related to *de novo* carcinogenesis from diseased liver). Based on this result, the authors of the RWD study suggested that a shorter follow-up duration of RWD (28.0 months) than that of RCT (68.5 months) may be associated with lower HR of tumor recurrence (0.42 vs 0.67) (9–11). However, it should be noticed that the baseline characteristics of patients were worse with higher tumor stage and larger tumor size in RWD than in RCT. These baseline characteristics might be unfavorable to RWD as CIK cell treatment is expected to be more effective in patients with less tumor burden (9). Thus, the lower HR of tumor recurrence or death in RWD is not simply explainable with currently available data and further real-world studies are warranted.

Our findings provide evidence for generalizing the effectiveness of RCTs conducted in controlled populations in the real-world population. The participants in the RCT, who were included following clear inclusion and exclusion criteria and treated following a well-defined schedule, may not represent patients in real-world practice (26). Thus, the validation of the effectiveness of CIK cell adjuvant therapy in RWD is essential, and the benefit of RFS is reproducible. Furthermore, our findings are meaningful in that a more beneficial economic value of CIK cell immunotherapy could be obtained in real-world clinical practice. In addition, the cost-effectiveness results from both RCT and RWD can support decision-making on introducing CIK cell immunotherapy in an adjuvant setting.

The analysis conducted under the societal perspective considering productivity loss was remarkable compared to that conducted from the healthcare system perspective. HCC occurs more frequently in men and is most frequently diagnosed among people aged 55–64 years who are economically active, and also occurs at a younger age, especially in Asia and sub-Saharan Africa, where HBV is endemic, than in other regions where HBV is not a predominant etiology of HCC (27–30). As the socioeconomic burden of disease because of premature death is substantial, preventing recurrence in such patients would reduce productivity loss in society. In South Korea, an HBV-endemic country, HCC was the second-highest cause of cancer-related death (21.5 per 100.000 population) in 2016 following lung cancer but resulted in the highest economic burden (USD 3.144 million) in 2010 among all cancers (31). It is a disappointing outcome considering that the nationwide regular surveillance program is now working well and approximately 40% of new HCC cases are diagnosed at a very early or early stage, where potentially curative treatment can be applied (32). Accordingly, the urgent need for cost-effective adjuvant therapy should be highlighted again.

Our findings on the cost-effectiveness of CIK cell immunotherapy, which prevents the recurrence of HCC, align with the results of previous cost-effectiveness studies on adjuvant therapies. Although there is no guideline-suggested adjuvant therapy for patients with HCC, several RCTs were conducted for adjuvant therapy with an effective drug used in the management of advanced HCC, such as sorafenib (33, 34). Because our study was the first to demonstrate the cost-effectiveness of treatment to prevent recurrence in HCC, there was no previous study to report the cost-effectiveness of adjuvant therapy in patients with HCC who underwent a potentially curative treatment. However, there have been several studies on other types of cancers, in which cost-effectiveness was verified by preventing recurrence or relapse (35–37). Our results emphasize the importance of preventing recurrence after successful primary therapy, which is in line with previously reported findings.

Our research has significant strengths, although decision-analytic models have limitations regarding the input parameters applied in the model. First, our original model was designed to reflect the prognosis of HCC recurrence, which is not generally considered in the conventional three-state model. To reflect the heterogeneous prognosis of recurrence, we conducted a *post-hoc* analysis of subsequent treatments (curative and noncurative treatments) from the phase III clinical trial, followed by the proportion of curable recurrence that we applied to our original model. Therefore, we have improved the model plausibility by reflecting the different prognoses of recurrence and health-related quality of life of patients. In addition, we demonstrated the robustness of cost-effectiveness by performing probabilistic and deterministic sensitivity analyses. Most of the input parameters were derived from the patient-level data of the phase III trial, and the remaining input parameters were verified by clinical experts. Moreover, we applied a wide range of costs and effectiveness to our model to assess inherent uncertainties.

Although our study considered various ranges of uncertainty, there were some limitations. First, the applied costs were obtained from the Korean healthcare system. Therefore, the costs were potentially lower than those in other developed countries, such as the USA. However, cost-effectiveness evaluations focus on the 'incremental' costs and effectiveness of CIK cell immunotherapy, and because the unit medical costs affected both the intervention and comparator in our model, the impact of lower costs in South Korea on the results would be limited. Even if the local cost data were replaced with those in other developed countries, including the USA, France, and Italy, the estimated ICERs from those scenarios ($34,000–$38,000/QALY) were similar to our base-case analysis results and were similar to or lower than each country's gross domestic product (GDP) per capita. Because the cost-effectiveness threshold for anticancer drugs is generally accepted as approximately twice the

GDP per capita, CIK cell immunotherapy would be a cost-effective alternative in all of these countries as well. In addition, the discount rate applied to our model was 5%, which was slightly higher than that in other developed countries; thus, the cost-effectiveness of CIK cell immunotherapy was analyzed conservatively because the long-term effectiveness and offset treatment costs of incurable recurrent HCC were underestimated in the base-case setting.

Second, survival data from RWD study has a relatively shorter observation period than RCTs, and there were some differences in the baseline characteristics among RWD and RCTs. This may increase the uncertainty of modeled survival output using RWD. Therefore, we simulated various parametric survival functions in sensitivity analyses to alleviate the uncertainty caused by short observation periods and different patient characteristics from RCTs, and presented the minimum and maximum values of ICER according to various survival functions in the tornado diagram (**Supplementary Figure 3**). As a result, our model showed robust results even when using RWD data. Finally, the proportion of curable recurrent HCC was calculated based on operational definitions using the subsequent treatment data of patients obtained from RCTs. For example, each recurrence treated with TACE was classified as incurable recurrence. However, there could be a curative TACE for patients who are not eligible for other curative treatments, which could lead to an underestimation of the proportion of curable recurrence. Even if we adopted the most generous criteria for classifying the curability of recurrence, the ICER increased by only 7% from the base-case analysis, and CIK cell immunotherapy was still cost-effective.

In conclusion, we showed that receiving CIK immunotherapy was more cost-effective than no adjuvant therapy in patients with HCC who underwent a potentially curative treatment, attributed to the prolonged survival, reduced recurrence of HCC, and better prognosis of recurrence, and it could be even more cost-effective in the real-world clinical practice.

DATA AVAILABILITY STATEMENT

The raw data supporting the conclusions of this article will be made available by the authors, without undue reservation.

AUTHOR CONTRIBUTIONS

H-LK, E-KL, and J-HL contributed to conception and design of the study. J-HL organized the database. H-LK, S-HK, and J-YC performed the statistical analyses and interpreted results. J-YC and S-HK contributed equally to this work and deserve co-first authorship. H-LK and J-HL are co-corresponding authors. All authors contributed to the article and approved the submitted version.

FUNDING

This study was supported by GC Cell Corp (Yongin, Korea). The sponsor was not involved in the study design, collection, analysis, interpretation of data, the writing of this article or the decision to submit it for publication.

ACKNOWLEDGMENTS

We would like to thank Editage (www.editage.co.kr) for English language editing.

SUPPLEMENTARY MATERIAL

The Supplementary Material for this article can be found online at: https://www.frontiersin.org/articles/10.3389/fonc.2021.728740/full#supplementary-material

REFERENCES

1. Bray F, Ferlay J, Soerjomataram I, Siegel RL, Torre LA, Jemal A. Global Cancer Statistics 2018: GLOBOCAN Estimates of Incidence and Mortality Worldwide for 36 Cancers in 185 Countries. *CA Cancer J Clin* (2018) 68 (6):394–424. doi: 10.3322/caac.21492
2. Park JW, Chen M, Colombo M, Roberts LR, Schwartz M, Chen PJ, et al. Global Patterns of Hepatocellular Carcinoma Management From Diagnosis to Death: The BRIDGE Study. *Liver Int* (2015) 35(9):2155–66. doi: 10.1111/liv.12818
3. European Association for the Study of the Liver EASL Clinical Practice Guidelines: Management of Hepatocellular Carcinoma. *J Hepatol* (2018) 69 (1):182–236. doi: 10.1016/j.jhep.2018.03.019
4. Llovet JM, Di Bisceglie AM, Bruix J, Kramer BS, Lencioni R, Zhu AX, et al. Design and Endpoints of Clinical Trials in Hepatocellular Carcinoma. *J Natl Cancer Inst* (2008) 100(10):698–711. doi: 10.1093/jnci/djn134
5. Shah SA, Cleary SP, Wei AC, Yang I, Taylor BR, Hemming AW, et al. Recurrence After Liver Resection for Hepatocellular Carcinoma: Risk Factors, Treatment, and Outcomes. *Surgery* (2007) 141(3):330–9. doi: 10.1016/j.surg.2006.06.028
6. Sempokuya T, Wong LL. Ten-Year Survival and Recurrence of Hepatocellular Cancer. *Hepatoma Res* (2019) 5:38. doi: 10.20517/2394-5079.2019.013
7. Schmidt-Wolf IG, Negrin RS, Kiem HP, Blume KG, Weissman IL. Use of a SCID Mouse/Human Lymphoma Model to Evaluate Cytokine-Induced Killer Cells With Potent Antitumor Cell Activity. *J Exp Med* (1991) 174(1):139–49. doi: 10.1084/jem.174.1.139
8. Zhang Y, Schmidt-Wolf IGH. Ten-Year Update of the International Registry on Cytokine-Induced Killer Cells in Cancer Immunotherapy. *J Cell Physiol* (2020) 235(12):9291–303. doi: 10.1002/jcp.29827
9. Lee JH, Lee JH, Lim YS, Yeon JE, Song TJ, Yu SJ, et al. Adjuvant Immunotherapy With Autologous Cytokine-Induced Killer Cells for Hepatocellular Carcinoma. *Gastroenterology* (2015) 148(7):1383–91.e6. doi: 10.1053/j.gastro.2015.02.055
10. Lee JH, Lee JH, Lim YS, Yeon JE, Song TJ, Yu SJ, et al. Sustained Efficacy of Adjuvant Immunotherapy With Cytokine-Induced Killer Cells for Hepatocellular Carcinoma: An Extended 5-Year Follow-Up. *Cancer Immunol Immunother* (2019) 68(1):23–32. doi: 10.1007/s00262-018-2247-4
11. Yoon JS, Song BG, Lee JH, Lee HY, Kim SW, Chang Y, et al. Adjuvant Cytokine-Induced Killer Cell Immunotherapy for Hepatocellular Carcinoma: A Propensity Score-Matched Analysis of Real-World Data. *BMC Cancer* (2019) 19(1):523. doi: 10.1186/s12885-019-5740-z
12. Woods BS, Sideris E, Palmer S, Latimer N, Soares M. Partitioned Survival and State Transition Models for Healthcare Decision Making in Oncology: Where Are We Now? *Value Health* (2020) 23(12):1613–21. doi: 10.1016/j.jval.2020.08.2094
13. Marrero JA, Kulik LM, Sirlin CB, Zhu AX, Finn RS, Abecassis MM, et al. Diagnosis, Staging, and Management of Hepatocellular Carcinoma: 2018

Practice Guidance by the American Association for the Study of Liver Diseases. *Clin Liver Dis (Hoboken)* (2019) 13(1):1. doi: 10.1002/cld.802
14. The Health Insurance Review and Assessment Service (HIRA) *Guidelines for Economic Evaluation of Pharmaceuticals in Korea*. Wonju: Health Insurance Review & Assessment Service (2011).
15. Husereau D, Drummond M, Petrou S, Carswell C, Moher D, Greenberg D, et al. Consolidated Health Economic Evaluation Reporting Standards (CHEERS)–Explanation and Elaboration: A Report of the ISPOR Health Economic Evaluation Publication Guidelines Good Reporting Practices Task Force. *Value Health* (2013) 16(2):231–50. doi: 10.1016/j.jval.2013.02.002
16. Pollom EL, Lee K, Durkee BY, Grade M, Mokhtari DA, Wahl DR, et al. Cost-Effectiveness of Stereotactic Body Radiation Therapy Versus Radiofrequency Ablation for Hepatocellular Carcinoma: A Markov Modeling Study. *Radiology* (2017) 283(2):460–8. doi: 10.1148/radiol.2016161509
17. Ock M, Lim SY, Lee HJ, Kim SH, Jo MW. Estimation of Utility Weights for Major Liver Diseases According to Disease Severity in Korea. *BMC Gastroenterol* (2017) 17(1):103. doi: 10.1186/s12876-017-0660-3
18. Yang SY, Park SK, Kang HR, Kim HL, Lee EK, Kwon SH. Haematological Cancer Versus Solid Tumour End-of-Life Care: A Longitudinal Data Analysis. *BMJ Support Palliat Care* (2020). doi: 10.1136/bmjspcare-2020-002453
19. Hoyle MW, Henley W. Improved Curve Fits to Summary Survival Data: Application to Economic Evaluation of Health Technologies. *BMC Med Res Methodol* (2011) 11:139. doi: 10.1186/1471-2288-11-139
20. Peabody JW, Lee SW, Bickel SR. Health for All in the Republic of Korea: One Country's Experience With Implementing Universal Health Care. *Health Policy* (1995) 31(1):29–42. doi: 10.1016/0168-8510(94)00669-6
21. Kim L, Kim JA, Kim S. A Guide for the Utilization of Health Insurance Review and Assessment Service National Patient Samples. *Epidemiol Health* (2014) 36:e2014008. doi: 10.4178/epih/e2014008
22. Weinstein MC, Torrance G, McGuire A. QALYs: The Basics. *Value Health* (2009) 12(Suppl 1):S5–9. doi: 10.1111/j.1524-4733.2009.00515.x
23. Cadier B, Bulsei J, Nahon P, Seror O, Laurent A, Rosa I, et al. Early Detection and Curative Treatment of Hepatocellular Carcinoma: A Cost-Effectiveness Analysis in France and in the United States. *Hepatol (Baltimore Md)* (2017) 65 (4):1237–48. doi: 10.1002/hep.28961
24. Rognoni C, Ciani O, Sommariva S, Tarricone R. Real-World Data for the Evaluation of Transarterial Radioembolization Versus Sorafenib in Hepatocellular Carcinoma: A Cost-Effectiveness Analysis. *Value Health* (2017) 20(3):336–44. doi: 10.1016/j.jval.2016.09.2397
25. Tangka FK, Subramanian S, Sabatino SA, Howard DH, Haber S, Hoover S, et al. End-Of-Life Medical Costs of Medicaid Cancer Patients. *Health Serv Res* (2015) 50(3):690–709. doi: 10.1111/1475-6773.12259
26. May GS, DeMets DL, Friedman LM, Furberg C, Passamani E. The Randomized Clinical Trial: Bias in Analysis. *Circulation* (1981) 64(4):669–73. doi: 10.1161/01.CIR.64.4.669
27. White DL, Thrift AP, Kanwal F, Davila J, El-Serag HB. Incidence of Hepatocellular Carcinoma in All 50 United States, From 2000 Through 2012. *Gastroenterology* (2017) 152(4):812–20.e5. doi: 10.1053/j.gastro.2016.11.020
28. Kennedy K, Graham SM, Arora N, Shuhart MC, Kim HN. Hepatocellular Carcinoma Among US and Non-US-Born Patients With Chronic Hepatitis B: Risk Factors and Age at Diagnosis. *PloS One* (2018) 13(9):e0204031. doi: 10.1371/journal.pone.0204031
29. National Cancer Institute Surveillance, Epidemiology, and End Results Program. *Cancer Stat Facts: Liver and Intrahepatic Bile Duct Cancer*. (2020). Available at: https://seer.cancer.gov/statfacts/html/livibd.html [November 24. 2021].
30. Zhu RX, Seto WK, Lai CL, Yuen MF. Epidemiology of Hepatocellular Carcinoma in the Asia-Pacific Region. *Gut Liver* (2016) 10(3):332–9. doi: 10.5009/gnl15257
31. Korean Liver Cancer Association; National Cancer Center. 2018 Korean Liver Cancer Association-National Cancer Center Korea Practice Guidelines for the Management of Hepatocellular Carcinoma. *Gut Liver* (2019) 13(3):227–99. doi: 10.5009/gnl19024
32. Chon YE, Lee HA, Yoon JS, Park JY, Kim BH, Lee IJ, et al. Hepatocellular Carcinoma in Korea Between 2012 and 2014: An Analysis of Data From the Korean Nationwide Cancer Registry. *J Liver Cancer* (2020) 20(2):135–47. doi: 10.17998/jlc.20.2.135
33. Bruix J, Takayama T, Mazzaferro V, Chau GY, Yang J, Kudo M, et al. Adjuvant Sorafenib for Hepatocellular Carcinoma After Resection or Ablation (STORM): A Phase 3, Randomised, Double-Blind, Placebo-Controlled Trial. *Lancet Oncol* (2015) 16(13):1344–54. doi: 10.1016/S1470-2045(15)00198-9
34. Zhu XD, Li KS, Sun HC. Adjuvant Therapies After Curative Treatments for Hepatocellular Carcinoma: Current Status and Prospects. *Genes Dis* (2020) 7 (3):359–69. doi: 10.1016/j.gendis.2020.02.002
35. Seferina SC, Ramaekers BLT, de Boer M, Dercksen MW, van den Berkmortel F, van Kampen RJW, et al. Cost and Cost-Effectiveness of Adjuvant Trastuzumab in the Real World Setting: A Study of the Southeast Netherlands Breast Cancer Consortium. *Oncotarget* (2017) 8(45):79223–33. doi: 10.18632/oncotarget.16985
36. Millar JA, Millward MJ. Cost Effectiveness of Trastuzumab in the Adjuvant Treatment of Early Breast Cancer: A Lifetime Model. *Pharmacoeconomics* (2007) 25(5):429–42. doi: 10.2165/00019053-200725050-00006
37. Hisashige A, Sasako M, Nakajima T. Cost-Effectiveness of Adjuvant Chemotherapy for Curatively Resected Gastric Cancer With S-1. *BMC Cancer* (2013) 13:443. doi: 10.1186/1471-2407-13-443

Conflict of Interest: E-KL report receiving grants from Green Cross Cell Corp during the conduct of the study. J-HL reports a research grant and lecture fee from Green Cross Cell Corp. H-LK has received research grant and lecture fee from Green Cross Cell Corp.

The remaining authors declare that the research was conducted in the absence of any commercial or financial relationships that could be construed as a potential conflict of interest.

Publisher's Note: All claims expressed in this article are solely those of the authors and do not necessarily represent those of their affiliated organizations, or those of the publisher, the editors and the reviewers. Any product that may be evaluated in this article, or claim that may be made by its manufacturer, is not guaranteed or endorsed by the publisher.

frontiers in Oncology

ORIGINAL RESEARCH
published: 13 December 2021
doi: 10.3389/fonc.2021.754240

Loss of Hyaluronan and Proteoglycan Link Protein-1 Induces Tumorigenesis in Colorectal Cancer

Yao Wang[1,2†], Xiaoyue Xu[3†], Jacqueline E. Marshall[4,5], Muxue Gong[6], Yang Zhao[7], Kamal Dua[4,8], Philip M. Hansbro[4,5], Jincheng Xu[9,10] and Gang Liu[4,5]*

[1] College of Biology and Food Engineering, Anyang Institute of Technology, Anyang, China, [2] Hangzhou Xunyao Biotechnology Pty. Ltd., Hangzhou, China, [3] School of Population Health, University of New South Wales, Sydney, NSW, Australia, [4] Centre for Inflammation, Centenary Institute, Sydney, NSW, Australia, [5] School of Life Sciences, Faculty of Science, University of Technology, Sydney, NSW, Australia, [6] School of Clinical Medicine, Bengbu Medicine College, Bengbu, China, [7] Department of Biochemistry and Molecular Biology, School of Medicine, Nanjing University of Chinese Medicine, Nanjing, China, [8] Discipline of Pharmacy, Graduate School of Health, University of Technology Sydney, Sydney, NSW, Australia, [9] Stomatology Department, The First Affiliated Hospital of Bengbu Medical College, Bengbu, China, [10] School of Dental Medicine, Bengbu Medical College, Bengbu, China

Colorectal cancer (CRC) is the third most common diagnosed cancer worldwide, but there are no effective cures for it. Hyaluronan and proteoglycan link protein-1 (HAPLN1) is a component of the extracellular matrix (ECM) proteins and involved in the tumor environment in the colon. Transforming growth factor (TGF)-β is a key cytokine that regulates the deposition of ECM proteins in CRC. However, the role of HAPLN1 in TGF-β contributions to CRC remains unknown. We found that the mRNA expression of *HAPLN1* was decreased in tumors from CRC patients compared with healthy controls and normal tissue adjacent to the tumor using two existing microarray datasets. This was validated at the protein level by tissue array from CRC patients (n = 59). HAPLN1 protein levels were also reduced in human CRC epithelial cells after 24 h of TGF-β stimulation, and its protein expression correlated with type I collagen alpha-1 (COL1A1) in CRC. Transfection of *HAPLN1* overexpression plasmids into these cells increased protein levels but reduced COL1A1 protein, tumor growth, and cancer cell migration. TGF-β stimulation increased Smad2/3, p-Smad2/3, Smad4, and E-adhesion proteins; however, *HAPLN1* overexpression restored these proteins to baseline levels in CRC epithelial cells after TGF-β stimulation. These findings suggest that HAPLN1 regulates the TGF-β signaling pathway to control collagen deposition *via* the TGF-β signaling pathway and mediates E-adhesion to control tumor growth. Thus, treatments that increase HAPLN1 levels may be a novel therapeutic option for CRC.

Keywords: HAPLN1, extracellular matrix protein, microenvironment, TGF-β, CRC

OPEN ACCESS

Edited by:
Vita Golubovskaya, ProMab Biotechnologies, United States

Reviewed by:
Ravindra Deshpande, Wake Forest School of Medicine, United States
Ila Pant, Icahn School of Medicine at Mount Sinai, United States

***Correspondence:**
Gang Liu
gang.liu@uts.edu.au

[†]These authors have contributed equally to this work

Specialty section:
This article was submitted to Gastrointestinal Cancers: Gastric and Esophageal Cancers, a section of the journal Frontiers in Oncology

Received: *06 August 2021*
Accepted: *08 November 2021*
Published: *13 December 2021*

Citation:
Wang Y, Xu X, Marshall JE, Gong M, Zhao Y, Dua K, Hansbro PM, Xu J and Liu G (2021) Loss of Hyaluronan and Proteoglycan Link Protein-1 Induces Tumorigenesis in Colorectal Cancer. Front. Oncol. 11:754240. doi: 10.3389/fonc.2021.754240

INTRODUCTION

Colorectal cancer (CRC) is the third most commonly diagnosed cancer worldwide and the second most lethal with more than 900,000 deaths annually (1). The number of new cases is predicted to reach 2.5 million in 2035 (1). With early diagnosis, the 5-year survival rate of CRC is ~65%, but this drops to less than 10% at later stages (2). The cause of tumor formation in CRC remains unknown. Polyps induce long-term inflammation in the colon and may contribute to tumor development of CRC (3). Tissue microenvironment changes also result in tumor formation in CRC. Therefore, it is important to understand the processes that lead to the development and growth of tumors in CRC.

Extracellular matrix (ECM) proteins are a group of macromolecules that provide structural support to cells. Alterations in ECM protein deposition result in aberrant structural changes in tissues, and ECM protein levels need to be balanced to maintain a normal microenvironment in the colon. Hyaluronan and proteoglycan link protein-1 (HAPLN1) is an ECM component that stabilizes other ECM proteins (4). Studies show that a loss of HAPLN1 proteins promotes metastasis of melanoma in patients, and tumor growth is inhibited by reconstitution of HAPLN1 (5). Also, HAPLN1 has important roles in maintaining endothelial permeability, and its loss promotes metastasis *via* blood vessels (6). However, the role of HAPLN1 in CRC has not been widely studied and remains unclear.

Transforming growth factor (TGF)-β is an important cytokine that has major beneficial functions in wound repair, but is also involved in tumor cell survival, invasion, and metastasis in many cancers, including CRC (7). Indeed, previous studies show that increased TGF-β promotes tumor cell proliferation in CRC patients (8, 9). TGF-β is also a central factor in regulating ECM genes and proteins in many diseases (10). Previous studies showed that TGF-β challenge reduced *HAPLN1* mRNA expression in human brain cells after 24 h (11). Another study found amplified *HAPLN1* mRNA levels in CRC patients ($n = 15$) (12), but protein levels have not been assessed in CRC. Links between TGF-β signaling and HAPLN1 in CRC remain unknown.

We hypothesized that HAPLN1 is a key ECM protein that regulates tumor growth and development in CRC. In this study, HAPLN1 mRNA and protein levels were measured in tumor, normal tissue adjacent to tumors, and healthy control tissue in existing microarray datasets and protein tissue arrays. TGF-β challenge reduced HAPLN1 protein levels in human CRC epithelial cells. We also found that decreased HAPLN1 negatively correlated with collagen expression and contributes to tumor development in CRC. *HAPLN1* overexpression restored protein levels in human CRC cells after TGF-β challenge and reduced collagen and tumor cell growth in CRC. Thus, we propose that TGF-β signaling reduces HAPLN1 levels that leads to collagen production and CRC. These data highlight the role of HAPLN1 as an important suppressor of tumor growth in CRC.

MATERIALS AND METHODS

Gene Expression in Human CRC Microarray Datasets

HAPLN1 gene expression in colorectal tumor and normal tissue adjacent to tumors from CRC patients and healthy controls was assessed in two existing microarray datasets (GSE128449 and GSE110224) in the Gene Expression Omnibus (GEO). Normal tissues adjacent to tumors were described to be those normal samples dissected from adjacent tumors (>4 cm from the tumor) from the same CRC patients (13). The data were analyzed using Bioconductor in R as previously described (14–16).

In the GSE128449 dataset, gene microarray from colorectal tissues was obtained from healthy controls ($n = 5$) and CRC patients ($n = 31$). Data were profiled by Agilent-014850 Whole Human Genome Microarray 4x44K G4112F. In the GSE110224 dataset, gene microarray from colorectal tissues and normal tissues adjacent to tumors was obtained from 17 CRC patients of similar age during surgery (17). mRNAs were profiled by Affymetrix Human Genome U133 Plus 2.0 array. The Benjamini–Hochberg method for adjusted *P*-value/false discovery rate (FDR) was used to analyze differences between groups. Statistical significance was set at FDR <0.05. All target gene expression was calculated as $\log_2$ intensity robust multi-array average signals ($\log_2$-transformed intensity value) (18).

Human Subjects

Human colon cancer tumor (CD4, SuperBioChips Laboratories, Seoul, South Korea) and normal tissues adjacent to tumor samples (CDN4, SuperBioChips Laboratories, Seoul, South Korea) were obtained from 59 stage I–IV CRC patients in tissue array slides (**Table 1**). The tumor and normal tissues adjacent to tumor tissues were collected during colorectal surgery and fixed with formalin. The tissues were dehydrated with gradient ethanol (70%, 90%, 95%, 99%, and 100%) for 1 h for each progressive step and paraffin embedded at 60°C for 3 h. The tissue blocks were sectioned in 4 μm thickness on new silane III slides (Cat # 5116-20F, Muto Pure Chemicals).

Survival Analysis

CRC samples with *HAPLN1* low ($n = 176$) and high ($n = 242$) gene expression were obtained from the colons of CRC patients (stages I–IV, **Supplementary Table S1**) based on The Cancer Genome Atlas Program (TCGA, https://ww.cancer.gov/tcga) (19). The Kaplan–Meier survival curve was produced using R packages survival and survminer by OncoLnc (http://www.oncolnc.org) (20). The relationship between *HAPLN1* gene expression and overall patient survival time was verified using a log-rank test.

Single-Cell Analysis of Human CRC Dataset

HAPLN1 gene expression from different cell clusters in CRC was assessed in previously published single-cell RNA-sequencing dataset (21). Single cells were obtained from tumor tissues that were resected from CRC patients ($n = 31$) as previously

TABLE 1 | Patient characteristics (n = 59).

	No. of patients	%
Sex		
Male	15	25.5
Female	44	74.5
Age mean = 60.6 ± SD 10.58 (range 35–86 years old)		
Stage		
I	2	3.3
II	33	55.9
III	20	33.9
IV	4	6.9

described (21). RNA-sequencing was performed using a Chromium system (10x Genomics) across eight lanes on a HiSeq 4000 platform. Cells were clustered and visualized using *t*-distributed stochastic neighbor embedding (tSNE) plots as previously described (16, 21). The cellular sources of *HAPLN1* mRNA in CRC were identified using the UCSC cell browser.

Immunohistochemistry

Slides of human colon cancer and normal tissues adjacent to tumor tissue were incubated at 60°C for 30 min, deparaffinized with xylene (5 min twice), and dehydrated in 100%, 95%, 90%, and 75% ethanol for 2 min (twice each). They were then incubated in citrate buffer (pH 6.0) at 100°C (35 min) for antigen retrieval and blocked with 5% bovine serum albumin (A9418, Sigma-Aldrich) at room temperature for 1 h. Slides were then incubated with HAPLN1 (1:100, sc-46826, Santa Cruz Biotechnology), p-Smad2/3 (1:100, SAB454208, Merck), and type I collagen alpha-1 (COL1A1, 1:100, ab21286, Abcam) antibodies at 4°C overnight, and then with anti-rabbit horseradish peroxidase-conjugated secondary antibody (HAF008, R&D Systems, USA) at room temperature for 1 h. They were washed in PBS-Tween 20 (three times, 5 min) with shaking, and sections were incubated with 3,3′-diaminobenzidine (DAB) chromogen solution at room temperature for 10 min according to the instruction of the manufacturer (GV825, Agilent). Slides were counterstained with hematoxylin at room temperature for 5 min. Images were taken under ×5 and ×20 magnifications using a light microscope. The area of HAPLN1 proteins was calculated using ImageJ with a color deconvolution plug-in (ImageJ) as previously described (22). The percentage of HAPLN1 protein in each image (at least 20 random images) was calculated by the area of positive staining divided by the total area of the view under ×20 magnification.

Cell Culture

Human CRC epithelial cells (Caco-2, HTB-37, ATCC, Manassas, VA, USA) were maintained in Eagle's minimum essential medium (EMEM) containing 2.5 mM L-glutamine, 10 mM HEPES, and 10% fetal bovine serum (FBS) at 37°C with 5% CO_2. Cells (1×10^5 cells/well) were seeded in a six-well plate and cultured in EMEM medium with 0.1% FBS at 37°C with 5% CO_2 for 24 h. Human recombinant TGF-β protein (50 μg/ml, 7666-MB-005/CF, R&D Systems) was added to the cell media, and control cells received an equal volume of EMEM medium. Cell lysates were collected after 6, 12, 24, and 48 h for immunoblot. Some cells were seeded on coverslips in a 24-well plate overnight and treated with TGF-β recombinant protein for 6, 12, 24, and 48 h, and cells were collected for immunofluorescence assays.

Protein Extraction

Cell lysates were obtained using radioimmunoprecipitation assay buffer (RIPA; Sigma-Aldrich, St. Louis, USA) supplemented with protease and phosphatase inhibitors (Thermo Fisher Scientific, MA, USA). Lysed cell samples were centrifuged (8,000×*g*, 10 min, 4°C) and supernatants were collected for protein assays. Total protein concentrations in cell lysates were determined using a Pierce bicinchoninic acid (BCA) protein assay kit (Thermo Fisher Scientific, MA, USA) according to the instructions of the manufacturer.

Immunoblot

Proteins from cell lysates were separated by electrophoresis under 110 V for 1.5 h and transferred onto polyvinylidene difluoride (PVDF) membranes. Membranes were blocked with 5% BSA for 2 h at room temperature, and then incubated with anti-HAPLN1 (1:100, sc-46826, Santa Cruz Biotechnology), COL1A1 (1:2,000, ab21286, Abcam), E-cadherin (1:2,000, 3195S, Cell Signaling), Smad2/3 (1:2,000, 8685S, Cell Signaling), Smad4 (1:2,000, 46535S, Cell Signaling), p-Smad2/3 (1:1,000, SAB454208, Merck), and anti-β-actin (1:10,000, ab8226, Abcam, Cambridge, UK) antibodies at 4°C overnight. Blots were washed with TBS-Tween 20 (three times, 10 min) and incubated with anti-rabbit or anti-mouse IgG HRP-conjugated antibodies (R&D Systems, MN, USA) at room temperature for 2 h. Substrate (SuperSignal™ West Femto Maximum Sensitivity Substrate, Thermo Fisher Scientific, MA, USA) was added to the membrane and images of immunoblots were captured using a ChemiDoc MP System (Bio-Rad, Hercules, USA). Some blots were stripped (15 g glycine, 1 g SDS, 10 ml Tween 20, pH 2.2) but only once to avoid background effects. Densitometry analysis was performed relative to the housekeeping protein β-actin using ImageJ (NIH, Bethesda, USA) as previously described (23, 24). The fold change of normalized area in each challenge/treatment group was compared with the control group.

Immunofluorescence

Caco-2 cells were fixed with cold methanol (−20°C) and 3% paraformaldehyde in PBS (pH 7.4) both at room temperature for 10 min each, permeabilized with 0.2% Triton X-100, and blocked with 5% BSA at room temperature for 1 h. Cells were incubated with anti-human HAPLN1 (1:100, sc-46826, Santa Cruz Biotechnology), COL1A1 (1:100, ab21286, Abcam), or p-Smad2/3 (1:100, SAB454208, Merck) antibodies at 4°C overnight. After three washes with PBS-Tween 20, cells were incubated with FITC-conjugated anti-rabbit secondary antibody (1:100, ab6717, Abcam) or AF594 anti-rabbit secondary antibody (1:200, ab150080, Abcam) at room temperature for 1 h. Nuclei were counterstained with DAPI at room temperature for 5 min. Ten random images per section were visualized using an Axio Imager M2 microscope and analyzed using an imaging

software (Zen, Zeiss) as previously described (24, 25). The percentage of HAPLN1-positive cells was calculated as the percentage of the total cell number (DAPI-positive cells).

HAPLN1 Overexpression Treatment

HAPLN1 overexpression plasmids within a pCMV3-C-GFPSpark® vector (HG10323-ACG, Sino Biological, China) or negative control (CV026, Sino Biological, China) plasmids (200 pg/μl) were transformed into SIG10 chemically competent cells (CMC0001, Sigma-Aldrich) according to the instructions of the manufacturer. Cells were cultured in LB broth at 37°C for 3 h with 200 rpm shaking. Cells were then cultured on LB agar plates (L3147, Sigma-Aldrich, St. Louis, USA) containing kanamycin sulfate (200 μg/ml, 60615, Sigma-Aldrich, St. Louis, USA) at 37°C overnight. A single colony was collected and cultured in LB broth at 37°C for 6 h with 200 rpm shaking, and bacterial cells were collected by centrifugation (6,000 rpm at room temperature for 10 min). Plasmids were isolated and purified using a PureLink HiPure Plasmid Midiprep kit (Thermo Fisher Scientific, Waltham, USA) according to the instructions of the manufacturer (25). Caco-2 cells (2×10^5 cells/well) were seeded in EMEM media (0.1% BSA and without antibiotics) on a 24-well plate at 37°C overnight. *HAPLN1* or negative control plasmids (1,000 ng) were transfected into Caco-2 cells using Lipofectamine 3000 transfection reagent (L3000008, Thermo Fisher Scientific, Waltham, USA) according to the instructions of the manufacturer. Cell lysates were collected after 12, 24, and 48 h for immunoblot analysis. Some cells were seeded on coverslips for immunofluorescence assays.

Cell Proliferation Assay

To investigate cell proliferation, Caco-2 cells (1×10^4 cells/well) were seeded in a 96-well plate and then transfected with *HAPLN1* overexpression or negative control plasmids. Cells were incubated with TGF-β recombinant protein (50 μg/ml) for 24 h and control cells received media only. Cells were stained with crystal violet (10%) at room temperature for 20 min and incubated with methanol at room temperature for 10 min. At least 10 random images were taken using a light microscope under ×40 magnification. Crystal violet-positive cells were enumerated using ImageJ as previously described (26).

Wound Healing Assay

Caco-2 cells were cultured on a 24-well plate with serum-free media for 24 h. The cells were scratched with a p200 pipette tip to generate a straight line across the center of each well as previously described (26), and then gently washed three times with PBS. Fresh serum-free EMEM media with TGF-β recombinant protein (50 μg/ml) were added to each well and control cells received media only. Cells were incubated at 37°C for 24 h with 5% CO_2. Images were taken using a phase-contrast microscope at 0, 6, 12, and 24 h after scratching. The area of each scratch at each time point was compared to images from 0 h using ImageJ software.

Cell Migration Assay

CRC cell migration was assessed using Boyden's chamber assay as previously described (27). Caco-2 cells (2×10^4 cells/ml) were seeded in upper chambers (Transwell) with 200 μl of DMEM media (1% FBS). Chambers were cultured in wells of 24-well plates containing 750 μl of DMEM overnight. Some cells were transfected with *HAPLN1* overexpression or negative control plasmids for 24 h using Lipofectamine 3000. Controls received equal volumes of media. Cells were then incubated with recombinant TGF-β protein for 24 h. Non-migrated cells remaining on the top surface of Transwell membrane were removed using cotton swabs. Cells that migrated to the lower surface of the membranes were fixed with 10% formalin (15 min) and permeabilized with methanol (5 min). Cells were then stained with crystal violet. Migrated cells were visualized and counted in at least five random fields per well under ×20 magnification using an inverted microscope.

Tissue Atlas Protein Analysis

Representative immunohistochemistry images of Smad2, Smad3, Smad4, and COL1A1 proteins in human healthy control colon and tumors from CRC patients were obtained from the Human Atlas database (version 19.3) as previously described (16).

Statistical Analysis

Results are presented as mean ± standard error of the mean (SEM). Each *in-vitro* experiment was performed in triplicate and repeated in three to four independent experiments. Unpaired Student's *t*-tests were used to compare two groups, and one-way analysis of variance (ANOVA) with Bonferroni comparisons was used to compare the results of more than two groups. All statistical analyses were performed using GraphPad Prism Software (San Diego, CA, USA). Statistical differences were accepted at $P < 0.05$.

RESULTS

HAPLN1 Gene Is Decreased in CRC Patients

Previous studies showed that HAPLN1 was involved in tissue remodeling (6), but its role in CRC remains unknown. We assessed the *HAPLN1* mRNA levels in CRC patients and colons from healthy controls using an existing microarray dataset (GSE128449). We found that *HAPLN1* mRNA was significantly decreased in CRC patients compared with healthy tissues (**Figure 1A**). To further assess the level of *HAPLN1* in CRC patients, we measured *HAPLN1* mRNA in tumor tissues and their normal tissues adjacent to the tumor in CRC patients using another microarray dataset (GSE110224). *HAPLN1* mRNA levels were also decreased in tumor compared with normal tissues adjacent to tumor tissues in the same CRC patients (**Figure 1B**). We also found that low expression of the *HAPLN1* gene in CRC patients correlated with shorter survival periods than those with high *HAPLN1* expression ($P = 0.035$, **Figure 1C**). To define the cellular source of HAPLN1 in CRC, tumors were collected from 31 CRC patients (21) and single-cell RNA-sequencing analysis was preformed (**Figure 1D**). *HAPLN1* mRNA was found in epithelial, stromal, and endothelial cells and myofibroblasts (**Figure 1E**).

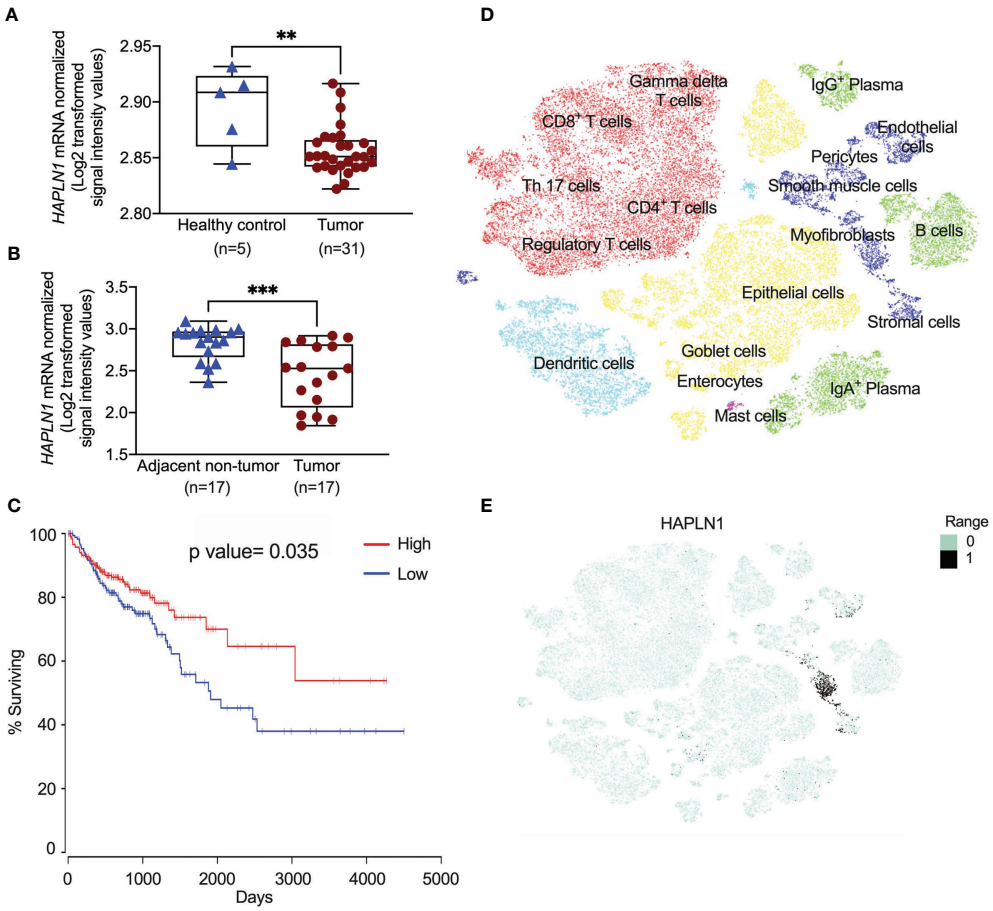

FIGURE 1 | *HAPLN1* gene expression is decreased in colorectal cancer (CRC) patients. **(A)** *HAPLN1* gene expression was analyzed in colon tissues from healthy (n = 5) and CRC patients (n = 31) in the GSE128449 dataset. **(B)** *HAPLN1* gene expression was analyzed in colon tissues from tumor and normal tissue adjacent to the tumor from the same CRC patients (n = 17) in the GSE110224 dataset. **(C)** The Kaplan–Meier survival curve of the correlations between the mRNA expression of the *HAPLN1* gene and survival days, and the cutoff value of RNA expression was 27.8. **(D)** Single cells were isolated from tumors in CRC patients (n = 31) after surgery. Cells were clustered using a graph-based shared nearest neighbor clustering approach and visualized in a *t*-distributed stochastic neighbor embedding (tSNE) plot in UCSC cell browser. **(E)** mRNA expression of *HAPLN1* in different cells in CRC patients. Results are mean ± SEM. $^{**}P < 0.01$, $^{***}P < 0.001$ compared with healthy control or non-tumor adjacent tissues.

Decreased HAPLN1 Protein in CRC Patients

To confirm that the decrease of *HAPLN1* mRNA translates to reduced protein levels in CRC patients, we assessed the HAPLN1 protein in tumor and normal tissues adjacent to tumor tissues from 59 CRC patients using immunohistochemistry (**Figure 2A**), and the HAPLN1 protein was mainly produced by CRC epithelial cells. The HAPLN1 protein was decreased in tumor (stage I–IV cancer) compared with normal tissues adjacent to tumor tissues (mean = 35.56 vs. 22.73, **Figure 2B**). The level of HAPLN1 protein was further reduced in severe stage (III–IV) CRC compared with early stages (mean 13.48 vs. 10.5, **Figure 2C**).

TGF-β Reduces HAPLN1 Proteins in Cancer Cells

Many studies have shown that CRC is associated with increased TGF-β protein and its downstream signaling is the key driver of tumor development (28). Previous studies also showed that TGF-β-induced ECM proteins led to the changes in the tissue microenvironment and tumor formation (26). COL1A1 is the most abundant ECM proteins in human (10). We examined the presence of abnormal ECM deposition and microenvironment change in CRC using TGF-β challenge of human CRC epithelial cells and assessing the levels of COL1A1 proteins over a time course (6, 12, 24, and 48 h, **Figure 3A** and **Supplementary Figure S1A**). TGF-β challenge resulted in significantly increased COL1A1 protein in the cell lysates reaching a peak after 24 h (**Figure 3B**).

To assess the role of HAPLN1 in CRC, we then measured its protein levels in cell lysates by immunoblot (**Figure 3A**). TGF-β challenge reduced HAPLN1 proteins in CRC epithelial cells from the 6-h time point with the maximal decrease after 24 h compared with controls (**Figure 3C**).

To further assess HAPLN1 in CRC, we challenged human CRC epithelial cells with TGF-β and assessed downstream

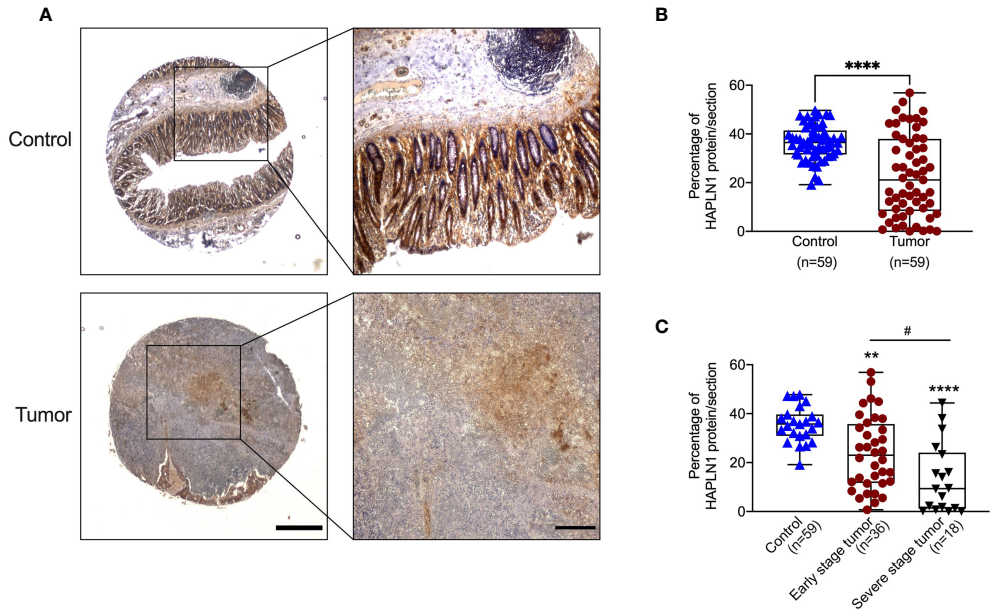

FIGURE 2 | Colorectal cancer (CRC) patients have decreased HAPLN1 protein in tumors. **(A)** Colon tissues were collected from tumors and normal tissue adjacent to the tumor from CRC patients (n = 59). Tissues were sectioned and stained with HAPLN1 antibody by immunohistochemistry (low magnification scale bar = 200 μm; high magnification scale bar = 50 μm). **(B)** The area of HAPLN1 staining in all stages of CRC patients was normalized to the total area of the colon section. **(C)** The area of HAPLN1 staining in early (stages I and II, n = 36) and severe stages (stages III and IV, n = 18) of CRC patients was normalized to the total area of the colon section. Results are mean ± SEM. $^{**}P < 0.01$, $^{****}P < 0.0001$ compared with a normal tissue adjacent to the tumors from CPC patients. $^{\#}P < 0.05$ compared with early stage tumour of CPC patients.

signaling and HAPLN1 by immunofluorescence (**Figure 3D**). p-Smad2/3 (active version of Smad2/3) is an important downstream mediator in the TGF-β signaling pathway. p-Smad2/3-positive cells increased after 6 h of TGF-β compared with controls, were then maintained at the same level up to 24 h, but then decreased at further time points (48 h, **Figure 3E**). TGF-β reduced the percentage of HAPLN1-positive cells, with the greatest effect after 24 h (**Figure 3F**), and this confirmed our result in cell lysates.

Overexpression of *HAPLN1* Gene in CRC Epithelial Cells Reduces Tumor Growth

Given that CRC development was associated with a decrease in HAPLN1 protein levels, to further understand its role, we transfected *HAPLN1* overexpression or negative control plasmid into human CRC epithelial cells. We assessed *HAPLN1* overexpression plasmid transfection efficiency by enumerating GFP-positive cells at different time points (6, 12, 24, and 48 h) after plasmid transfection as the plasmid contained the *GFP* gene (**Figure 4A**). The number of GFP-positive cells peaked 24 h after transection (**Figure 4B**) with a decrease after 48 h. We also measured HAPLN1 proteins in cell lysates during the transfection time course by immunoblot (**Figure 4C** and **Supplementary Figure S1B**). HAPLN1 proteins were significantly increased 24 h after transfection, but the levels decreased thereafter (**Figure 4D**), which confirmed the immunofluorescence data (**Figure 4A**). Therefore, we chose 24 h as the optimized transfection time point.

We also found that COL1A1 proteins were decreased in CRC epithelial cells after *HAPLN1* overexpression plasmid transfection (**Figure 4E**). COL1A1 proteins were the lowest after 24 h corresponding with the highest level of HAPLN1 proteins, indicating a correlation between HAPLN1 and COL1A1 proteins.

HAPLN1 Changes the Tumor Microenvironment by Regulating Collagen Production in CRC

To better understand the role of HAPLN1 in regulating CRC growth, we transfected *HAPLN1* overexpression plasmid with and without TGF-β recombinant protein and examined the effects after 24 h. Human CRC epithelial cell growth significantly increased with concomitant TGF-β protein challenge, with an ~3-fold increase of cells after 24 h compared with controls (**Figure 5A**). *HAPLN1* overexpression reduced CRC growth compared with cells transfected with the negative control plasmid and media controls with concomitant TGF-β (**Figures 5A–C**). We further assessed the role of HAPLN1 in CRC using migration assays (**Figure 5D**). TGF-β recombinant protein significantly increased CRC epithelial cell migration; however, *HAPLN1* overexpression substantially reduced the number of migrated cells (**Figure 5E**). We then assessed the role of HAPLN1 in CRC growth using wound healing assays (**Figure 5F**). The wounds in the CRC epithelial cells started to recover 6 h after TGF-β challenge and resolved after 24 h in cells treated with media control or negative control plasmid (**Figure 5G**). However, cells overexpressing *HAPLN1* had reduced wound healing speed, even slower than in control cells without TGF-β challenge,

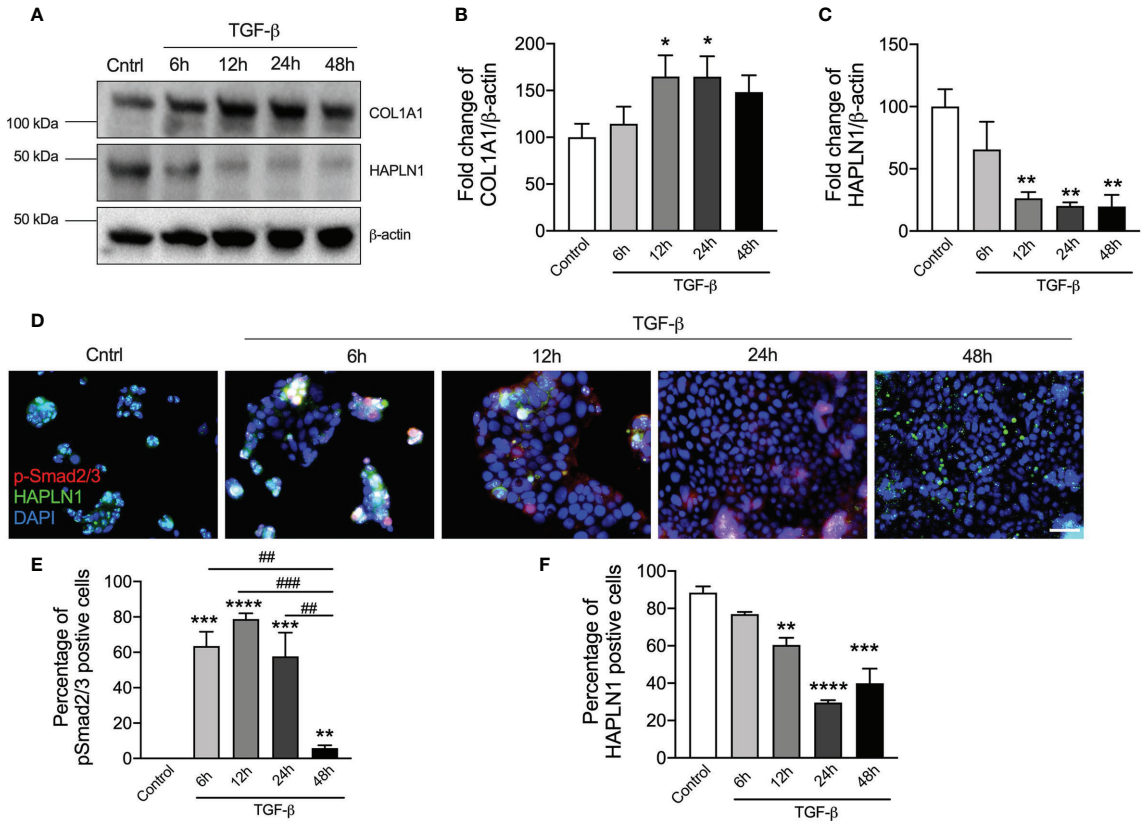

FIGURE 3 | TGF-β stimulation reduces HAPLN1 protein in human colorectal cancer (CRC) cells. Human CRC epithelial cells (Caco-2) were challenged with recombinant TGF-β protein (5 ng/μl), and controls cells received media. **(A)** HAPLN1 and COL1A1 protein levels were assessed in cell lysates over a time course (6, 12, 24, and 48 h) of TGF-β challenge by immunoblot. Fold change of densitometry of HAPLN1 **(B)** and COL1A1 **(C)** was normalized to β-actin. **(D)** Caco-2 cells were stained with HAPLN1 and nuclei were stained with DAPI and assessed using immunofluorescence (n = 4, scale bar = 100 μm). p-Smad2/3 **(E)** and HAPLN1 **(F)**-positive cells were normalized to total cells to determine the percentage of HAPLN1-positive cells. Results are mean ± SEM. $^{*}P < 0.05$, $^{**}P < 0.01$, $^{***}P < 0.001$, $^{****}P < 0.0001$ compared with control cells that received media. $^{\#\#}P < 0.01$, $^{\#\#\#}P < 0.001$ compared with TGF-β-challenged cells after 48 h.

indicating that the HAPLN1 protein reduces CRC epithelial cell growth.

HAPLN1 Regulates Collagen *via* the TGF-β Signaling Pathway in CRC

To assess the mechanisms of how HAPLN1 regulates CRC epithelial cell growth, we transfected these cells with *HAPLN1* overexpression plasmid with and without TGF-β for 24 h. TGF-β significantly reduced the numbers of HAPLN1-positive cells but increased collagen proteins (COL1A1) in those cells (**Figure 6A**). *HAPLN1* overexpression restored the numbers of HAPLN1-positive cells but reduced collagen deposition after TGF-β challenge.

To confirm that HAPLN1 regulates collagen in CRC, we also collected cell lysates 24 h after *HAPLN1* overexpression with or without 24 h TGF-β challenge. TGF-β reduced the HAPLN1 protein in CRC epithelial cells, and *HAPLN1* overexpression increased the HAPLN1 proteins after TGF-β challenge compared with control cells (**Figures 6B, C** and **Supplementary Figure S2A**). *HAPLN1* overexpressing cells also had reduced collagen after TGF-β challenge (**Figure 6D**).

Given that reduced HAPLN1 was associated with increased collagen in CRC, we investigated the mechanism of how HAPLN1 regulates collagen in CRC. Previous studies showed that the TGF-β signaling pathway regulates collagen deposition (10, 22); thus, we assessed the key downstream proteins (Smad2, Smad3, Smad4, and COL1A1) in this signaling pathway in normal colon tissue and tumors from CRC patients. Smad2, Smad3, Smad4, and COL1A1 proteins were strongly expressed in tumor tissues from CRC patients compared with normal colon controls (**Figure 6E**). We also measured Smad2/3, p-Smad2/3, and Smad4 proteins in an *in-vitro* model of CRC. We found that Smad2/3, p-Smad2/3 and Smad4 proteins were significantly increased in CRC epithelial cells after TGF-β challenge, but were decreased with *HAPLN1* over-expression (**Figures 6E–I** and **Supplementary Figure S2B**).

To further understand how HAPLN1 regulates CRC growth, we assessed E-cadherin protein in our *in-vitro* model of CRC. E-cadherin is an important molecule involved in cell adhesion and tumor development (29). TGF-β challenge increased E-cadherin protein levels in CRC epithelial cells; however, the levels were

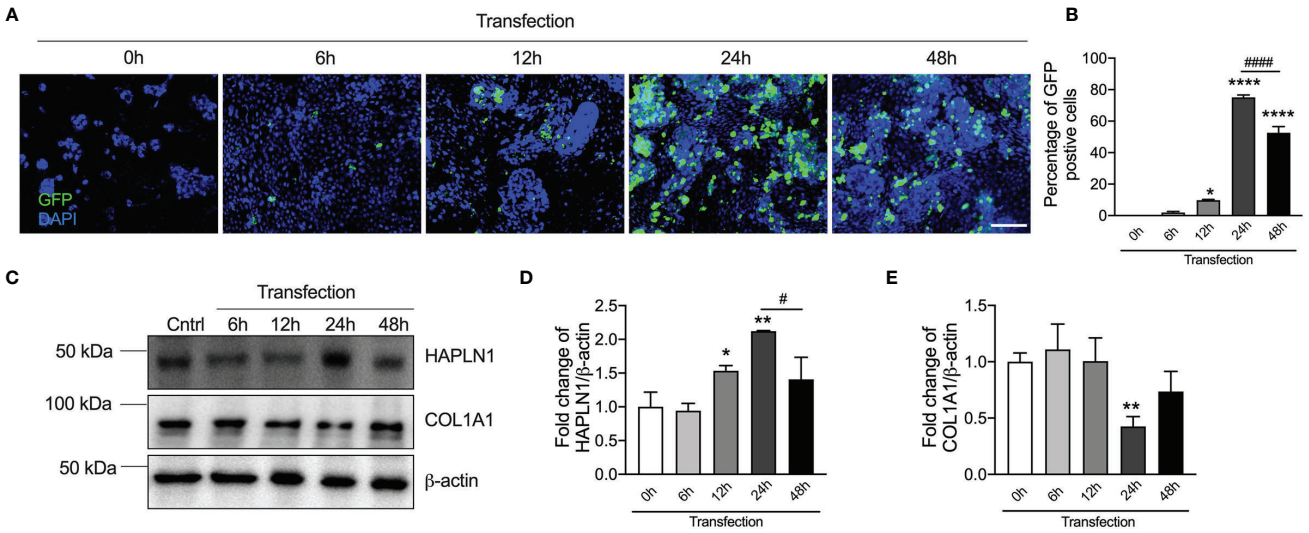

FIGURE 4 | *HAPLN1* overexpression increases HAPLN1 but decreases COL1A1 proteins in human colorectal cancer (CRC) epithelial cells. *HAPLN1* overexpression plasmids conjugated with GFP were transfected into human CRC epithelial (Caco-2) cells. **(A)** GFP-positive cells were assessed over a time course of transfection (0, 6, 12, 24, and 48 h) by immunofluorescence (n = 4, scale bar = 100 μm), and **(B)** GFP-positive cells were normalized to total cells (per view). **(C)** HAPLN1 and COL1A1 proteins were assessed in cell lysates over a time course of *HAPLN1* overexpression plasmid transfection (0, 6, 12, 24, and 48 h) by immunoblot. Fold changes of densitometry of HAPLN1 **(D)** and COL1A1 **(E)** were normalized to β-actin. n = 4. Results are mean ± SEM. $^{*}P < 0.05$, $^{**}P < 0.01$, $^{****}P < 0.0001$ compared with cells 0 h after HAPLN1 overexpression plasmid transfection. $^{\#}P < 0.05$, $^{\#\#\#\#}P < 0.0001$ compared with cells 48 h after *HAPLN1* overexpression plasmid transfection.

significantly decreased with *HAPLN1* overexpression compared with cells transfected with the negative control plasmid (**Figure 6J**).

DISCUSSION

HAPLN1 is an ECM protein that contributes to cell proliferation, cell–cell interactions, and tumor development. In this study, we found that the *HAPLN1* gene and proteins are decreased in tumors from CRC patients compared with colon healthy controls and normal colon regions of CRC patients. We also show that decreases in HAPLN1 proteins are associated with increased COL1A1 protein levels in CRC epithelial cells after TGF-β challenge and control tumor growth. A potential mechanism is that HAPLN1 regulates tumor cell proliferation *via* the TGF-β (Smad2/3, p-Smad2/3, and Smad4) signaling pathway. HAPLN1 also mediates E-cadherin to regulate tumor cell attachment in CRC. However, *HAPLN1* overexpression restored COL1A1, TGF-β signaling, and E-cadherin proteins in CRC epithelial cells.

Studies have shown that *HAPLN1* mRNA is downregulated in chondrocytes in endoplasmic reticulum stress-induced cartilage damage (30). *HAPLN1* expression is significantly reduced by interleukin-1 alpha stimulation and further results in decreased cell proliferation in cartilage injury (31). Previous studies showed that *HAPLN1* mRNA was decreased in brain cells 24 h after TGF-β-induced brain damage (11). These studies indicate that HAPLN1 is associated with cell growth, but HAPLN1 levels vary in different cancers. *HAPLN1* gene expression is increased in lung tissues from patients with pleural mesothelioma compared with healthy controls (32), while some other studies showed HAPLN1 levels decreased during aging, and this is potentially involved in cancer invasion (6). The decrease in HAPLN1 protein results in the disruption of the vascular basement membrane and induces vessel permeability, and this enhances melanoma metastasis (6). To our knowledge, only one other study has assessed the *HAPLN1* gene in a small cohort (n = 15) of CRC patients and it was found to be elevated in CRC (12). However, previous studies indicated that *HAPLN1* expression may be altered during colorectal carcinogenesis (33). In our study, we observed a decreased gene expression of *HAPLN1* in CRC patients compared with healthy controls and normal tissue adjacent to the tumor. The decreased in HAPLN1 protein has also been confirmed in CRC patients by histological analysis in a larger cohort (n = 59). The HAPLN1 protein is further decreased in severe CRC patients, indicating a correlation between HAPLN1 and CRC severity. Low levels of *HAPLN1* gene in the colon are associated with a lower survival rate of CRC patients, indicating that factor downregulation of HAPLN1 may drive CRC development. We have also shown that epithelial, stromal, and endothelial cells and myofibroblasts express *HAPLN1* gene in the colon by RNA-sequencing, but only epithelial cells are associated with tumor formation in CRC.

Abnormal deposition of ECM leads to tissue stiffening and is associated with the tumor microenvironment in CRC (34). Collagen is the most abundant component of ECM protein and increased collagen deposition results in tissue remodeling and tumor formation (10). We previously showed that collagen (COL1A1 and COL3A1) mRNAs are increased in tumor tissues

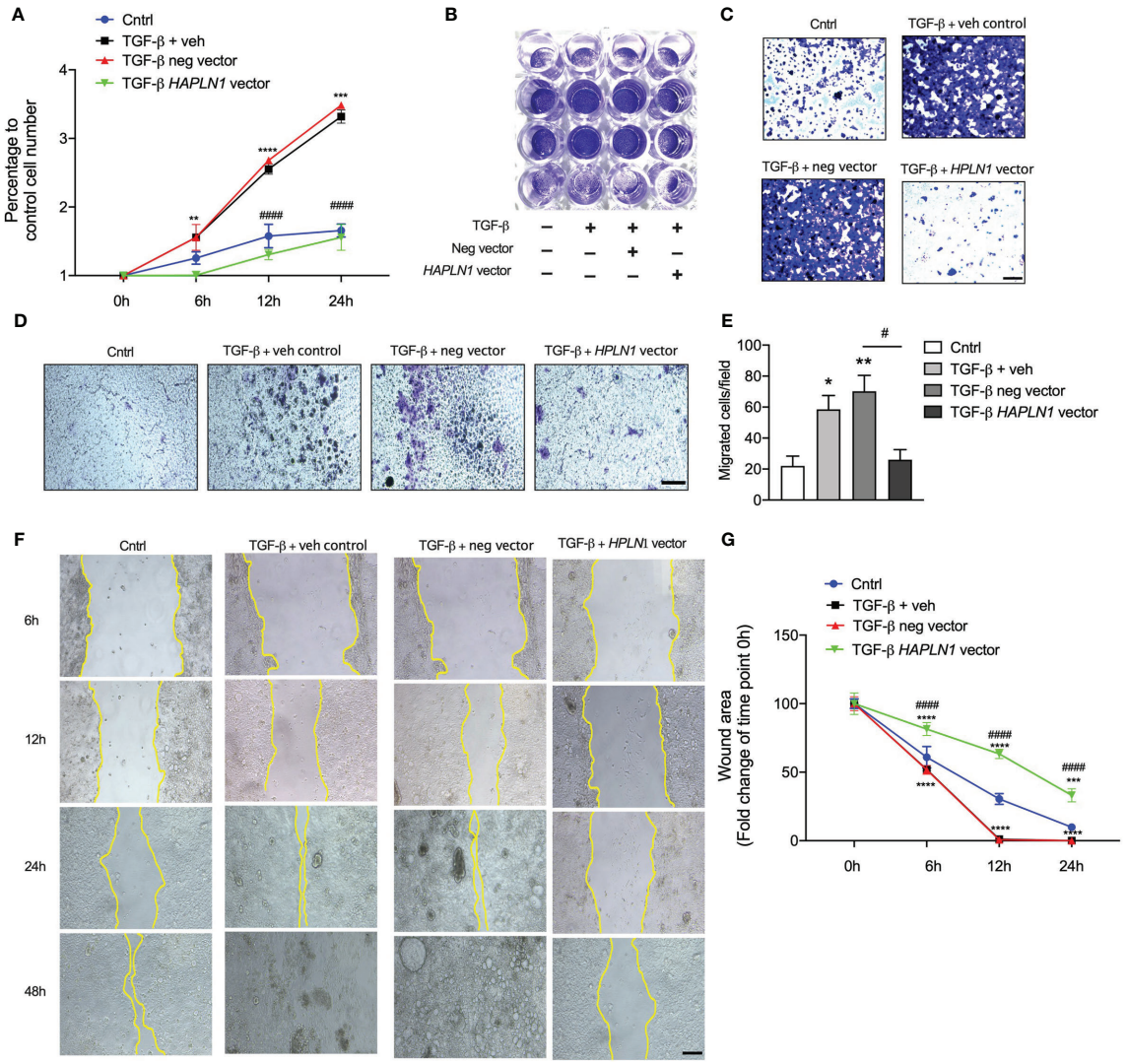

FIGURE 5 | *HAPLN1* overexpression reduces tumor cell growth in colorectal cancer (CRC). Human CRC epithelial (Caco-2) cells were transfected with *HAPLN1* overexpression or negative control plasmid, and vehicle controls received media. Cells were then challenged with human recombinant TGF-β protein. **(A)** Live cells were enumerated during the time course of TGF-β challenge (0, 6, 12, and 24 h) using a cell viability assay. **(B)** Cells were stained with crystal violet after 24 h of TGF-β challenge and **(C)** visualized using light microscopy (scale bar = 100 um). **(D)** Cell migration was assessed by boyden's chamber assay after 24 hours TGF-β challenge that Caco-2 cells were stained with crystal violet (scale bar = 100 um) and **(E)** migrated were counted in at least 5 random fields per well under 20x magnification lens by an inverted microscope. **(F)** Cell Scratch assays were performed in wells cultured with Caco-2 cells, and cancer cell invasion and migration were assessed by wound healing (scale bar = 200 um). **(G)** Wound area was assessed by measuring wound closure size after 0, 6, 12, and 24 h post-scratch. n = 4. Results are mean ± SEM. $^{*}P < 0.05$, $^{**}P < 0.01$, $^{***}P < 0.001$, $^{****}P < 0.0001$ compared with control cells. $^{\#}P < 0.05$, $^{\#\#\#\#}P < 0.0001$ compared with cells transfected with negative control plasmid.

from CRC patients compared with normal tissue adjacent to the tumor (26). In this study, we show that COL1A1 protein is significantly increased in CRC epithelial cells after TGF-β challenge. We also show that HAPLN1 correlated with collagen in CRC, indicating that HAPLN1 may regulate collagen in the tumor microenvironment. Increased collagen deposition in tissues results in cancer cell proliferation and tumor growth (35). However, increased collagen is associated with decreased HAPLN1 in CRC epithelial cells after TGF-β challenge. We also observed an increase of HAPLN1 protein in CRC epithelial cells after 24 h of *HAPLN1* overexpression compared with earlier time points. This leads to a decrease of collagen in the cancer cells, indicating that HAPLN1 may regulate collagen formation in CRC.

TGF-β is an important cytokine in the regulation of cell proliferation, differentiation, adhesion, and migration in many cell types (36). It is a key regulator of ECM products and the microenvironment in cancers (36). The TGF-β signaling pathway is involved in cancer development and tumor growth in CRC, and Smad family members are important downstream molecules in the TGF-β signaling pathway (37). Studies show that *Smad2* knockout

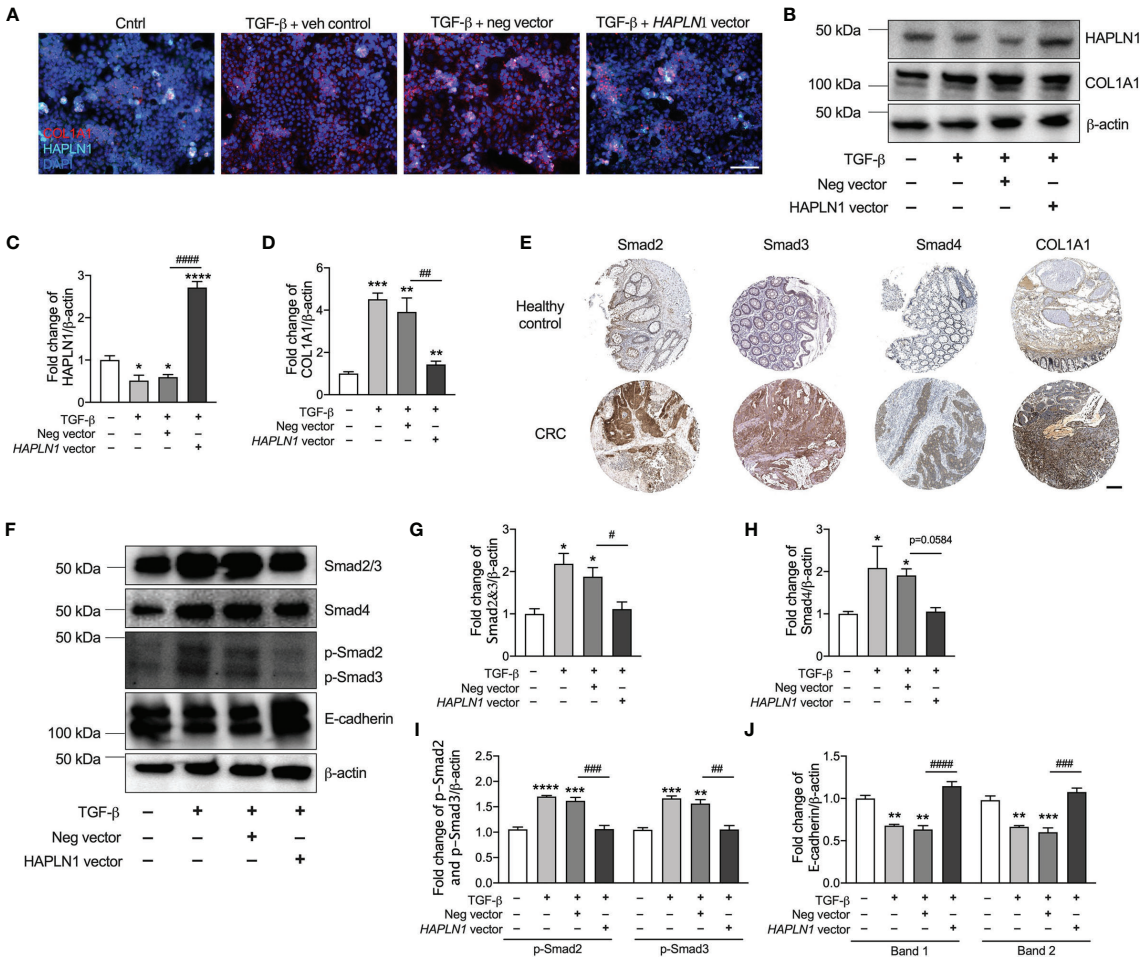

FIGURE 6 | HAPLN1 regulates collagen *via* the TGF-β signaling pathway and E-cadherin to control tumor growth in colorectal cancer (CRC). Human CRC epithelial (Caco-2) cells were transfected with *HAPLN1* overexpression or negative control plasmid, and vehicle controls received media. Cells were then challenged with human recombinant TGF-β protein. **(A)** Cells were stained with HAPLN1 and COL1A1 fluorescent antibody after 24 h of TGF-β and assessed by immunofluorescence (scale bar = 100 μm). **(B)** HAPLN1 and COL1A1 proteins were assessed in cell lysates by immunoblot. Fold change of densitometry of HAPLN1 **(C)** and COL1A1 **(D)** was normalized to β-actin. **(E)** Smad2, Smad3, Smad4, and COL1A1 proteins in human colon healthy controls and tumors from CRC patients by immunohistochemistry in the Pathology Atlas database (scale bar = 200 μm). **(F)** Smad2/3, Smad4, p-Smad2/3, and E-cadherin proteins were assessed in cell lysates by immunoblot. Fold change of densitometry of Smad2/3 **(G)**, Smad4 **(H)**, p-Smad2/3 **(I)**, and E-cadherin **(J)** was normalized to β-actin. $n = 4$. Results are mean ± SEM. $^{*}P < 0.05$, $^{**}P < 0.01$, $^{***}P < 0.001$, $^{****}P < 0.0001$ compared with control cells receiving media. $^{\#}P < 0.05$, $^{\#\#}P < 0.01$, $^{\#\#\#}P < 0.001$, $^{\#\#\#\#}P < 0.0001$ compared with cells transfected with negative control plasmid.

mice are embryonic lethal (38). Smad3 protects against the development of colorectal tumors, and specifically, knockout of exon 2 in *Smad3* promotes metastasis of large bowel cancer (39). However, knockout of exon 8 in *Smad3* results in autoimmunity with abnormally activated T cells, and this induces colon inflammation and adenocarcinomas (40). *Smad4* knockout mice are prone to embryonic lethality due to defects in gastrulation (41). Depletion of Smad4 from T cells in mice leads to epithelial carcinomas in the gut (42). We show that TGF-β stimulation increases both Smad2/3 and p-Smad2/3 proteins in CRC epithelial cells, and this confirmed the findings of a previous study (43). This demonstrates that the balance of Smad proteins is critical in tumor formation in CRC. We have shown that *HAPLN1* overexpression in cancer cells restored p-Smad2/3 to control levels, indicating that HAPLN1 may regulate the TGF-β signaling pathway.

Changes in the tissue microenvironment contribute to cell–cell adhesion, and loss of adhesion is a key mechanism of cancer invasion and progression (44). E-cadherin is a key adhesion protein that promotes cell–cell adhesion and maintains epithelial morphology (45). Studies have identified that low levels of E-cadherin expression are associated with colon cancer invasiveness (44). The expression of E-cadherin in cancer patients with metastasis is lower than that in normal tissue adjacent to the tumor (45). Patients with cancer had decreased E-cadherin expression and this led to a lower survival time (44). This indicates that E-cadherin is associated with tumor differentiation,

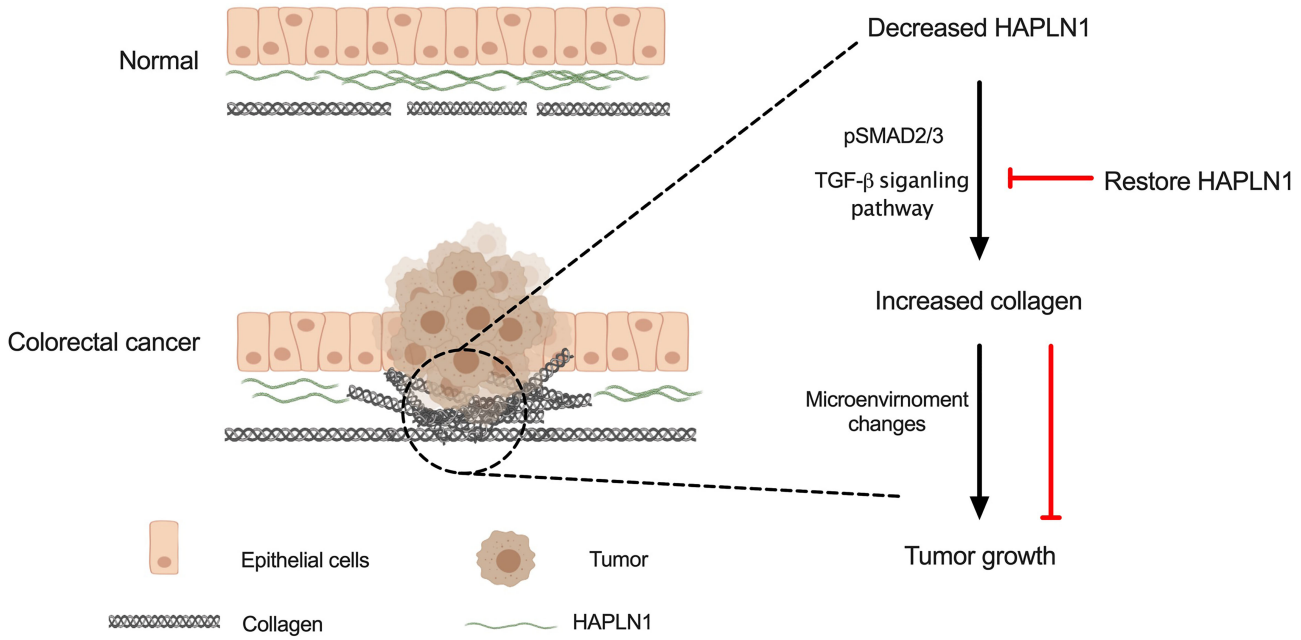

FIGURE 7 | Schematic of HAPLN1 regulation of collagen and tumor growth. Decreased HAPLN1 expression leads to increased collagen deposition *via* pSmad2/3 in the TGF-β signaling pathway, resulting in tumor growth. Restoring HAPLN1 levels can reduce collagen and inhibit tumor growth.

invasion, lymph node metastasis, and severity of cancer (46). In this study, we have shown that TGF-β challenge reduces E-cadherin protein in CRC cells, and this confirmed previous observations (47). However, overexpression of *HAPLN1* in CRC cells increased E-cadherin proteins after TGF-β stimulation, indicating that HAPLN1 regulates E-cadherin and reduces tumor cell growth.

Taken together, our data show that low levels of HAPLN1 induces collagen deposition in the colon *via* p-Smad2/3 involved in the TGF-β signaling pathway. Increased collagen leads to cell microenvironment changes and tumor cell proliferation, migration, and invasion in CRC. *HAPLN1* overexpression restored HAPLN1 protein and reduced cancer cell growth (**Figure 7**). This provides a new therapeutic approach by restoring HAPLN1 in CRC patients.

DATA AVAILABILITY STATEMENT

The datasets presented in this study can be found in online repositories. The names of the repository/repositories and accession number(s) can be found below: https://www.ncbi.nlm.nih.gov/geo/, GSE128449 and https://www.ncbi.nlm.nih.gov/geo/, GSE110224.

ETHICS STATEMENT

The studies involving human participants were reviewed and approved by Bengbu Committee of Bengbu Medical College. Written informed consent for participation was not required for this study in accordance with the national legislation and the institutional requirements. Written informed consent was obtained from the individual(s) for the publication of any potentially identifiable images or data included in this article.

AUTHOR CONTRIBUTIONS

YW performed the *in-vitro* experiments and data analysis. XX performed the statistical analysis and revised the manuscript. MG and JM assisted in the experimentation. YZ, KD, PH, and JX revised the manuscript. GL designed the study, performed some *in-vitro* experiments, and prepared the manuscript. All authors contributed to the article and approved the submitted version.

FUNDING

This work was supported by TSANZ and the Australian Lung Foundation (GL). XX is supported by the Australia National Heart Foundation post-doctoral fellowship and the University of New South Wales Scientia Program. PH is funded by a fellowship and grants from the National Health and Medical Research Council (NHMRC) of Australia (1175134), University of Technology Sydney (UTS), and Cancer Council of NSW (1099119, 1157073).

ACKNOWLEDGMENTS

The results here are part based on data generated by the TCGA Research Network (https://ww.cancer.gov/tcga).

SUPPLEMENTARY MATERIAL

The Supplementary Material for this article can be found online at: https://www.frontiersin.org/articles/10.3389/fonc.2021.754240/full#supplementary-material

REFERENCES

1. Dekker E, Tanis PJ, Vleugels JLA, Kasi PM, Wallace MB. Colorectal Cancer. *Lancet* (2019) 394(10207):1467–80. doi: 10.1016/S0140-6736(19)32319-0
2. Hakami Z, Raposo T, Alsulaiman A, Dalleywater W, Otifi H, Horobin C, et al. N-Glycosylation of CD24 Mediates Cell Motility But Inhibits Cell Proliferation in Colorectal Cancer. *bioRxiv* (2021). doi: 10.1101/2021.05.02.442315
3. Mattar MC, Lough D, Pishvaian MJ, Charabaty A. Current Management of Inflammatory Bowel Disease and Colorectal Cancer. *Gastrointest Cancer Res* (2011) 4(2):53–61.
4. Long KR, Newland B, Florio M, Kalebic N, Langen B, Kolterer A, et al. Extracellular Matrix Components HAPLN1, Lumican, and Collagen I Cause Hyaluronic Acid-Dependent Folding of the Developing Human Neocortex. *Neuron* (2018) 99(4):702–19.e6. doi: 10.1016/j.neuron.2018.07.013
5. Kaur A, Ecker BL, Douglass SM, Kugel CH3rd, Webster MR, Almeida FV, et al. Remodeling of the Collagen Matrix in Aging Skin Promotes Melanoma Metastasis and Affects Immune Cell Motility. *Cancer Discov* (2019) 9(1):64–81. doi: 10.1158/2159-8290.CD-18-0193
6. Ecker BL, Kaur A, Douglass SM, Webster MR, Almeida FV, Marino GE, et al. Age-Related Changes in HAPLN1 Increase Lymphatic Permeability and Affect Routes of Melanoma Metastasis. *Cancer Discov* (2019) 9(1):82–95. doi: 10.1158/2159-8290.CD-18-0168
7. Massague J. TGFbeta in Cancer. *Cell* (2008) 134(2):215–30. doi: 10.1016/j.cell.2008.07.001
8. Buckhaults P, Rago C, St Croix B, Romans KE, Saha S, Zhang L, et al. Secreted and Cell Surface Genes Expressed in Benign and Malignant Colorectal Tumors. *Cancer Res* (2001) 61(19):6996–7001.
9. Schroy P, Rifkin J, Coffey RJ, Winawer S, Friedman E. Role of Transforming Growth Factor Beta 1 in Induction of Colon Carcinoma Differentiation by Hexamethylene Bisacetamide. *Cancer Res* (1990) 50(2):261–5.
10. Liu G, Philp AM, Corte T, Travis MA, Schilter H, Hansbro NG, et al. Therapeutic Targets in Lung Tissue Remodelling and Fibrosis. *Pharmacol Ther* (2021) 225:107839. doi: 10.1016/j.pharmthera.2021.107839
11. Kim SY, Senatorov VVJr., Morrissey CS, Lippmann K, Vazquez O, Milikovsky DZ, et al. TGFbeta Signaling Is Associated With Changes in Inflammatory Gene Expression and Perineuronal Net Degradation Around Inhibitory Neurons Following Various Neurological Insults. *Sci Rep* (2017) 7(1):7711. doi: 10.1038/s41598-017-07394-3
12. Ashktorab H, Schaffer AA, Daremipouran M, Smoot DT, Lee E, Brim H. Distinct Genetic Alterations in Colorectal Cancer. *PLoS One* (2010) 5(1):e8879. doi: 10.1371/journal.pone.0008879
13. Aran D, Camarda R, Odegaard J, Paik H, Oskotsky B, Krings G, et al. Comprehensive Analysis of Normal Adjacent to Tumor Transcriptomes. *Nat Commun* (2017) 8(1):1077. doi: 10.1038/s41467-017-01027-z
14. Bhattacharya S, Srisuma S, Demeo DL, Shapiro SD, Bueno R, Silverman EK, et al. Molecular Biomarkers for Quantitative and Discrete COPD Phenotypes. *Am J Respir Cell Mol Biol* (2009) 40(3):359–67. doi: 10.1165/rcmb.2008-0114OC
15. Christenson SA, van den Berge M, Faiz A, Inkamp K, Bhakta N, Bonser LR, et al. An Airway Epithelial IL-17A Response Signature Identifies a Steroid-Unresponsive COPD Patient Subgroup. *J Clin Invest* (2019) 129(1):169–81. doi: 10.1172/JCI121087
16. Xu J, Xu X, Jiang L, Dua K, Hansbro PM, Liu G. SARS-CoV-2 Induces Transcriptional Signatures in Human Lung Epithelial Cells That Promote Lung Fibrosis. *Respir Res* (2020) 21(1):182. doi: 10.1186/s12931-020-01445-6
17. Vlachavas EI, Pilalis E, Papadodima O, Koczan D, Willis S, Klippel S, et al. Radiogenomic Analysis of F-18-Fluorodeoxyglucose Positron Emission Tomography and Gene Expression Data Elucidates the Epidemiological Complexity of Colorectal Cancer Landscape. *Comput Struct Biotechnol J* (2019) 17:177–85. doi: 10.1016/j.csbj.2019.01.007
18. Kaiko GE, Chen F, Lai CW, Chiang IL, Perrigoue J, Stojmirovic A, et al. PAI-1 Augments Mucosal Damage in Colitis. *Sci Transl Med* (2019) 11(482):eaat0852. doi: 10.1126/scitranslmed.aat0852
19. Cancer Genome Atlas Research N, Weinstein JN, Collisson EA, Mills GB, Shaw KR, Ozenberger BA, et al. The Cancer Genome Atlas Pan-Cancer Analysis Project. *Nat Genet* (2013) 45(10):1113–20. doi: 10.1038/ng.2764
20. Zheng H, Zhang G, Zhang L, Wang Q, Li H, Han Y, et al. Comprehensive Review of Web Servers and Bioinformatics Tools for Cancer Prognosis Analysis. *Front Oncol* (2020) 10:68. doi: 10.3389/fonc.2020.00068
21. Lee HO, Hong Y, Etlioglu HE, Cho YB, Pomella V, Van den Bosch B, et al. Lineage-Dependent Gene Expression Programs Influence the Immune Landscape of Colorectal Cancer. *Nat Genet* (2020) 52(6):594–603. doi: 10.1038/s41588-020-0636-z
22. Liu G, Cooley MA, Nair PM, Donovan C, Hsu AC, Jarnicki AG, et al. Airway Remodelling and Inflammation in Asthma Are Dependent on the Extracellular Matrix Protein Fibulin-1c. *J Pathol* (2017) 243(4):510–23. doi: 10.1002/path.4979
23. Liu G, Cooley MA, Jarnicki AG, Hsu ACY, Nair PM, Haw TJ, et al. Fibulin-1 Regulates the Pathogenesis of Tissue Remodeling in Respiratory Diseases. *JCI Insight* (2016) 1(9):e86380. doi: 10.1172/jci.insight.86380
24. Liu G, Cooley MA, Jarnicki AG, Borghui T, Nair PM, Tjin G, et al. Fibulin-1c Regulates Transforming Growth Factor-β Activation in Pulmonary Tissue Fibrosis. *JCI Insight* (2019) 4(16):e124529. doi: 10.1172/jci.insight.124529
25. Liu G, Baird AW, Parsons MJ, Fan K, Skerrett-Byrne DA, Nair PM, et al. Platelet Activating Factor Receptor Acts to Limit Colitis-Induced Liver Inflammation. *FASEB J* (2020) 34(6):7718–32. doi: 10.1096/fj.201901779R
26. Li J, Xu X, Jiang Y, Hansbro NG, Hansbro PM, Xu J, et al. Elastin Is a Key Factor of Tumor Development in Colorectal Cancer. *BMC Cancer* (2020) 20(1):217. doi: 10.1186/s12885-020-6686-x
27. Schanin J, Gebremeskel S, Korver W, Falahati R, Butuci M, Haw TJ, et al. A Monoclonal Antibody to Siglec-8 Suppresses Non-Allergic Airway Inflammation and Inhibits IgE-Independent Mast Cell Activation. *Mucosal Immunol* (2021) 14(2):366–76. doi: 10.1038/s41385-020-00336-9
28. Calon A, Espinet E, Palomo-Ponce S, Tauriello DV, Iglesias M, Cespedes MV, et al. Dependency of Colorectal Cancer on a TGF-Beta-Driven Program in Stromal Cells for Metastasis Initiation. *Cancer Cell* (2012) 22(5):571–84. doi: 10.1016/j.ccr.2012.08.013
29. Jeanes A, Gottardi CJ, Yap AS. Cadherins and Cancer: How Does Cadherin Dysfunction Promote Tumor Progression? *Oncogene* (2008) 27(55):6920–9. doi: 10.1038/onc.2008.343
30. Yang L, Carlson SG, McBurney D, Horton WEJr. Multiple Signals Induce Endoplasmic Reticulum Stress in Both Primary and Immortalized Chondrocytes Resulting in Loss of Differentiation, Impaired Cell Growth, and Apoptosis. *J Biol Chem* (2005) 280(35):31156–65. doi: 10.1074/jbc.M501069200
31. Aida Y, Maeno M, Ito-Kato E, Suzuki N, Shiratsuchi H, Matsumura H. Effect of IL-1alpha on the Expression of Cartilage Matrix Proteins in Human Chondrosarcoma Cell Line OUMS-27. *Life Sci* (2004) 75(26):3173–84. doi: 10.1016/j.lfs.2004.06.011
32. Ivanova AV, Goparaju CM, Ivanov SV, Nonaka D, Cruz C, Beck A, et al. Protumorigenic Role of HAPLN1 and Its IgV Domain in Malignant Pleural Mesothelioma. *Clin Cancer Res* (2009) 15(8):2602–11. doi: 10.1158/1078-0432.CCR-08-2755
33. Naishiro Y, Yamada T, Idogawa M, Honda K, Takada M, Kondo T, et al. Morphological and Transcriptional Responses of Untransformed Intestinal Epithelial Cells to an Oncogenic Beta-Catenin Protein. *Oncogene* (2005) 24(19):3141–53. doi: 10.1038/sj.onc.1208517
34. Bauer J, Emon MAB, Staudacher JJ, Thomas AL, Zessner-Spitzenberg J, Mancinelli G, et al. Increased Stiffness of the Tumor Microenvironment in Colon Cancer Stimulates Cancer Associated Fibroblast-Mediated Prometastatic Activin A Signaling. *Sci Rep* (2020) 10(1):50. doi: 10.1038/s41598-019-55687-6

35. Winkler J, Abisoye-Ogunniyan A, Metcalf KJ, Werb Z. Concepts of Extracellular Matrix Remodelling in Tumour Progression and Metastasis. *Nat Commun* (2020) 11(1):5120. doi: 10.1038/s41467-020-18794-x
36. Jung B, Staudacher JJ, Beauchamp D. Transforming Growth Factor Beta Superfamily Signaling in Development of Colorectal Cancer. *Gastroenterology* (2017) 152(1):36–52. doi: 10.1053/j.gastro.2016.10.015
37. Hata A, Chen YG. TGF-Beta Signaling From Receptors to Smads. *Cold Spring Harb Perspect Biol* (2016) 8(9):a022061. doi: 10.1101/cshperspect.a022061
38. Liu L, Liu X, Ren X, Tian Y, Chen Z, Xu X, et al. Smad2 and Smad3 Have Differential Sensitivity in Relaying TGFbeta Signaling and Inversely Regulate Early Lineage Specification. *Sci Rep* (2016) 6:21602. doi: 10.1038/srep21602
39. Sodir NM, Chen X, Park R, Nickel AE, Conti PS, Moats R, et al. Smad3 Deficiency Promotes Tumorigenesis in the Distal Colon of ApcMin/+ Mice. *Cancer Res* (2006) 66(17):8430–8. doi: 10.1158/0008-5472.CAN-06-1437
40. Yang X, Letterio JJ, Lechleider RJ, Chen L, Hayman R, Gu H, et al. Targeted Disruption of SMAD3 Results in Impaired Mucosal Immunity and Diminished T Cell Responsiveness to TGF-Beta. *EMBO J* (1999) 18 (5):1280–91. doi: 10.1093/emboj/18.5.1280
41. Sirard C, de la Pompa JL, Elia A, Itie A, Mirtsos C, Cheung A, et al. The Tumor Suppressor Gene Smad4/Dpc4 Is Required for Gastrulation and Later for Anterior Development of the Mouse Embryo. *Genes Dev* (1998) 12(1):107–19. doi: 10.1101/gad.12.1.107
42. Kim BG, Li C, Qiao W, Mamura M, Kasprzak B, Anver M, et al. Smad4 Signalling in T Cells Is Required for Suppression of Gastrointestinal Cancer. *Nature* (2006) 441(7096):1015–9. doi: 10.1038/nature04846
43. Walsh MF, Ampasala DR, Hatfield J, Vander Heide R, Suer S, Rishi AK, et al. Transforming Growth Factor-Beta Stimulates Intestinal Epithelial Focal Adhesion Kinase Synthesis *via* Smad- and P38-Dependent Mechanisms. *Am J Pathol* (2008) 173(2):385–99. doi: 10.2353/ajpath.2008.070729
44. Christou N, Perraud A, Blondy S, Jauberteau MO, Battu S, Mathonnet M. E-Cadherin: A Potential Biomarker of Colorectal Cancer Prognosis. *Oncol Lett* (2017) 13(6):4571–6. doi: 10.3892/ol.2017.6063
45. Petrova YI, Schecterson L, Gumbiner BM. Roles for E-Cadherin Cell Surface Regulation in Cancer. *Mol Biol Cell* (2016) 27(21):3233–44. doi: 10.1091/mbc.E16-01-0058
46. Gao M, Zhang X, Li D, He P, Tian W, Zeng B. Expression Analysis and Clinical Significance of Eif4e, VEGF-C, E-Cadherin and MMP-2 in Colorectal Adenocarcinoma. *Oncotarget* (2016) 7(51):85502–14. doi: 10.18632/oncotarget.13453
47. Vogelmann R, Nguyen-Tat MD, Giehl K, Adler G, Wedlich D, Menke A. TGFbeta-Induced Downregulation of E-Cadherin-Based Cell-Cell Adhesion Depends on PI3-Kinase and PTEN. *J Cell Sci* (2005) 118(Pt 20):4901–12. doi: 10.1242/jcs.02594

Conflict of Interest: Author YW was employed by Hangzhou Xunyao Biotechnology Pty. Ltd.

The remaining authors declare that the research was conducted in the absence of any commercial or financial relationships that could be construed as a potential conflict of interest.

Publisher's Note: All claims expressed in this article are solely those of the authors and do not necessarily represent those of their affiliated organizations, or those of the publisher, the editors and the reviewers. Any product that may be evaluated in this article, or claim that may be made by its manufacturer, is not guaranteed or endorsed by the publisher.

frontiers in Oncology

ORIGINAL RESEARCH
published: 14 December 2021
doi: 10.3389/fonc.2021.797426

Neoadjuvant Immunotherapy Combined Chemotherapy Followed by Surgery Versus Surgery Alone for Locally Advanced Esophageal Squamous Cell Carcinoma: A Propensity Score-Matched Study

Zhi-Nuan Hong[1†], Kai Weng[1†], Kaiming Peng[1†], Zhen Chen[1†], Jihong Lin[1,2,3,4‡] and Mingqiang Kang[1,2,3,4*‡]*

[1] Department of Thoracic Surgery, Fujian Medical University Union Hospital, Fuzhou, China, [2] Key Laboratory of Cardio-Thoracic Surgery, Fujian Medical University, Fujian Province University, Fuzhou, China, [3] Key Laboratory of Ministry of Education for Gastrointestinal Cancer, Fujian Medical University, Fuzhou, China, [4] Fujian Key Laboratory of Tumor Microbiology, Fujian Medical University, Fuzhou, China

Background: Combination of neoadjuvant immunotherapy and chemotherapy (nICT) is a novel treatment for locally esophageal cancer squamous cell carcinoma (ESCC). This study aimed to evaluate the potential effect of nICT on surgery safety by comparing short-term outcomes between the surgery alone group and the nICT followed by surgery group.

Methods: A retrospective analysis was performed to identify patients (from January 2017 to July 2021) who underwent surgery for ESCC with or without nICT. A propensity score matching (PSM) comparison (1:1) was conducted to reduce selection biases and balance the demographic and oncologic characteristics between groups.

Results: After PSM, the nICT group (n = 38) was comparable to the surgery alone group (n = 38) in the following characteristics: age, sex, BMI, ASA status, smoking, tumor location, lymph node resection, clinical stage, anastomotic location, surgical approach, and surgical approach. The operation time and incidence of postoperative pneumonia in the nICT group were higher than those in the control group ($p < 0.05$). However, other complications and major complications were comparable between the two groups. There was no significant difference between the two groups in intraoperative blood loss, ICU stay time, postoperative hospital stay, and hospitalization cost. The 30-day mortality, 30-day readmission, and ICU readmission rates were also similar in the nICT and control groups. In the nICT group, the pathological complete response rate in primary tumor was 18.4%, and the major pathological response rate in tumor was 42.1%.

OPEN ACCESS

Edited by:
Vita Golubovskaya, ProMab Biotechnologies, United States

Reviewed by:
Helei Hou, The Affiliated Hospital of Qingdao University, China
John Morton, University of Colorado, United States

****Correspondence:***
Mingqiang Kang
kangmingqiang0799@163.com
Jihong Lin
ljh060@qq.com

†These authors have contributed equally to this work and share first authorship

‡These authors have contributed equally to this work

Specialty section:
This article was submitted to Gastrointestinal Cancers: Gastric & Esophageal Cancers, a section of the journal Frontiers in Oncology

Received: *18 October 2021*
Accepted: *19 November 2021*
Published: *14 December 2021*

Citation:
Hong Z-N, Weng K, Peng K, Chen Z, Lin J and Kang M (2021) Neoadjuvant Immunotherapy Combined Chemotherapy Followed by Surgery Versus Surgery Alone for Locally Advanced Esophageal Squamous Cell Carcinoma: A Propensity Score-Matched Study. Front. Oncol. 11:797426. doi: 10.3389/fonc.2021.797426

Conclusions: Based on our preliminary experience, nICT followed by surgery is safe and effective with acceptable increased operation risk, manageable postoperative complications, and promising pathological response. Further multicenter prospective trials are needed to validate our results.

Keywords: esophagectomy, neoadjuvant immunotherapy, surgery, esophageal cancer squamous cell carcinoma, operation difficulty

BACKGROUND

Esophageal cancer (EC) is one of the most prevalent types of cancer and a major cause of death with 572,000 new diagnosis cases and 500,000 deaths annually. Esophageal cancer squamous cell carcinoma (ESCC) is the main sub-type in Asians (1, 2). Esophagectomy plays an important role in treatment for locally advanced ESCC (3). However, surgery alone is often associated with high recurrence and metastasis rates up to 43.3%–50.0% (4).

Compared to surgery alone, neoadjuvant chemotherapy (nCT) and neoadjuvant chemoradiotherapy (nCRT) have been proven to improve long-term survival without additional postoperative morbidity and mortality (5). In Asia, nCT followed by surgery has been advocated as standard treatment for locally advanced ESCC (6). Kamarajah et al. reported that compared to nCT, overall survival benefit was evident for nCRT (HR 0.78, 0.62 to 0.97), and recommended nCRT followed by surgery for ESCC (6). A meta-analysis including 4,529 patients (nCT: 2,035; nCRT: 2,494) found that compared to the nCT group, deaths caused by tumor progression or recurrence were significantly less in the nCRT group than in the nCT group; however, there was not an increase in 5-year survival (7). Optimal neoadjuvant treatment strategy for locally advanced ESCC is still controversial and not promising. It is necessary to explore novel treatment regiments to achieve better long-term prognosis (8).

Antibodies against the immune inhibitory pathway of programmed death 1 (PD-1) protein or PD-1 ligand 1 (PD-L1) checkpoint inhibitors is a milestone in treatment of ESCC. In CheckMate 577 trails, Kelly et al. reported that nivolumab adjuvant therapy could prolong 11.4 months disease-free survival among patients with resected esophageal or gastroesophageal junction cancer who had received nCRT (9). Recently, pembrolizumab plus chemotherapy has been recommended as first-line treatment for advanced EC (10). Considering the promising results in advanced EC, it is reasonable to explore the efficacy and safety of neoadjuvant immunotherapy combined chemotherapy (nICT) (11, 12).

Recently, Shen et al. reported a cohort of 27 patients who received surgery after 2 cycles of nICT with a low-toxicity profile, a high R0 resection rate, and a promising pathological complete response (pCR) rate (13). Although the nICT has become popular, there were still concerns that immune therapy may affect surgical safety, complications, and mortality. To date, there was only a handful of study focusing on the above concerns and there remains a need for further evidence. This study aimed to evaluate the potential effect of nICT on surgery by comparing short-term outcomes in the surgery alone group and esophagectomy followed by nICT.

METHODS

Patient Selection and Study Design

This study was approved by the Ethics Committee of Fujian Medical University Union Hospital. Patients' written informed consent was obtained. Consecutive patients were recruited retrospectively who underwent esophagectomy with or without nICT for ESCC at Fujian Medical University Union Hospital from January 2017 to July 2021. The inclusion criteria were as follows: (1) thoracic ESCC; (2) receiving minimally invasive esophagectomy (MIE); and (3) with complete clinical data. Patients with nonresectable tumors or metastases during exploratory surgery or who received either neoadjuvant chemotherapy or chemoradiotherapy were excluded.

A propensity score matched analysis (1:1) was conducted to balance the demographic and oncologic characteristics. Propensity score was measured based on 4 factors: age, BMI, clinical tumor-lymph node-metastasis (cTNM) stage (for nICT group: cTNM stage after neoadjuvant therapy), and American Society of Anesthesiologists (ASA) status. We chose cTNM stage after neoadjuvant therapy due to two reasons: First, before treatment, most patients in the nICT group were diagnosed with III or IV cTNM stage, and it is hard to conduct a balanced match with the surgery alone group. Second, compared with using cTNM stage before neoadjuvant therapy, using cTNM stage after neoadjuvant therapy could better reflect the clinical reality, and further confirm the safety and efficacy of nICT followed by surgery. The 8th edition American Joint Committee on Cancer/Union for International Cancer Control staging system was used in clinicopathologic staging.

Treatment Protocols

Patients who meet the following inclusions received nICT: (1) aged between 18 and 75 years old; (2) staged as $cT_{1\text{-}2}N_{1\text{-}3}M_0$ or $cT_{3\text{-}4a}N_{0\text{-}3}M_0$; (3) with normal hematologic, hepatic, and renal function; and (4) ECOG status ranged 0–2. The patients received 2–4 cycles of intravenous PD-1 inhibitor (sintilimab at a dose of 200 mg, pembrolizumab at a dose of 200 mg, and camrelizumab at a dose of 200 mg) every 3 weeks (day 1). Chemotherapy mainly consisted of simultaneous treatment with platinum-based drugs and paclitaxel [TP regimen, with cisplatin (60 mg/m^2) on day 1, and albumin-bound paclitaxel (125 mg/m^2) on days 1 and 8]. Surgery was performed within 4–8 weeks after the end of the

last neoadjuvant treatment. All patients received MIE with standard 2-field or 3-field lymphadenectomy and gastric reconstruction. We regularly conducted standard 2-field lymphadenectomy. Neck lymphadenectomy was conducted when patients were suspected with swollen lymph nodes in the neck.

Outcome Measures

Postoperative complications in hospital were coded using the Clavien-Dindo classification; major complications were defined as Clavien-Dindo classification grade ≧ 3 (14). The primary end point was 30-day complications. Secondary end points were interval to surgery, operation time, thoracic drainage tube stay, 30-day readmission rate, and 30-day mortality. Interval to surgery was defined as the last measured from the end of last neoadjuvant treatment to the date of surgery. Operative time was measured from incision to wound closure. ICU stay was defined as from the day of entry into the ICU to the day of leaving the ICU.

Statistical Analysis

Patients were classified into two groups, the surgery alone group and the nICT group. The propensity score (PS) matched analysis was used to reduce the bias. PS was calculated with a logic model to fit the following variables: age, sex, BMI, and tumor-node-metastasis (TNM) stage. Setting caliper = 0.05, matching ratio = 1:1, and two comparable groups of patients were created with 38 patients in each group. The continuous variable of normal distribution was expressed as mean ± standard deviation, the continuous variable of abnormal distribution was expressed as median (quartile range), and the classified variable was expressed as number (percentage). For equivalent variables with a normal distribution, an independent Student's *t*-test was used. The Mann–Whitney *U* test was used to compare the abnormal distribution variables between the two groups. The frequency of the classification variables was determined by using Pearson 2 or Fisher's exact test, where appropriate. Statistical analysis was conducted in R version 4.0.4 (R Foundation for Statistical Computing, Vienna, Austria). A two-sided p-value < 0.05 was considered as significant.

RESULTS

Patient Selection and Baseline Characteristics

To reduce the confounding bias, we conducted a 1:1 PSM cohort between the nICT group (n = 38) and surgery alone group (n = 38). After PSM, the clinical and demographic characteristics of the two groups were well balanced, including age, gender, BMI, ASA status, hypertension history, smoking, tumor location, lymphadenectomy, pathological stage, anastomotic position, route of gastric conduit, procedure type, and operative approach. The baseline characteristics are summarized in **Table 1**.

Complications and Short-Term Outcomes

All patients successfully received MIE. No patients converted to open surgery. The nICT group had a significantly longer operation time (311.7 ± 74.5 min), compared to that in the surgery alone group (273.4 ± 51.5 min). The number of removed lymph nodes were more in the nICT group, with a median 35.5 and 30 in the nICT group and surgery alone group, respectively (p = 0.039). The intraoperative blood loss was comparable. The nICT group had more thoracic drainage volume (p = 0.25). Furthermore, the thoracic drainage tube stay was significantly longer in the nICT group (p < 0.001). The ICU stay, hospital stay, postoperative hospital stays, hospital cost, 30-day mortality, 30-day readmission, and ICU readmission were similar in both groups. Perioperative outcomes before and after PSM are summarized in **Table 2**.

Complications within 30 days after PSM are summarized in **Table 3**. Incidences of anastomotic leakage, pleural effusion, palsy of recurrent laryngeal nerve, chylothorax, bleeding, and postoperative blood transfusion were similar in nICT group and surgery alone group. The incidence of pneumonia was significantly higher in the nICT group (24/38, 63.2%) than that in the surgery alone group (11/38, 28.9%). Frequency of 30-day major complications after PSM is listed in **Figure 1**.

Efficacy

R0 resection was achieved in all patients in the nICT group and control group. In the nICT cohort, 21 patients achieved clinical partial recovery, and 17 patients achieved clinical stable disease. In the surgery alone group, 1 patient achieved clinical partial advance; others achieved clinical stable disease during the period of waiting for surgery. In the nICT group, seven patients (7/38, 18.4%) achieved pCR in primary tumors, and sixteen patients (16/38, 42.1%) achieved major pathological response (MPR) in primary tumors. Two patients still had cancer residual in lymph node, while achieving pCR in primary tumors. The median tumor regression rate was 72.5%. The details of tumor regression are shown in **Figure 2**.

DISCUSSION

In this study, there were no significant postponement of surgery after completion of neoadjuvant therapy. Although the operation time in the nICT group was longer than that in control, which contributed to a higher incidence of pneumonia in nICT group, other major complications were comparable between the nICT group and control group after PSM. Furthermore, there was no significantly increased risk of 30-day mortality, 30-day readmission, and ICU readmission due to neoadjuvant immunotherapy. The postoperative hospital stay and hospital cost were similar in the nICT group and control group. From our preliminary experience, nICT followed by surgery is safe and effective with acceptable increased operation risk and manageable postoperative complications.

Operation time, especially duration of one-lung ventilation (OLV), is a risk factor for postoperative pneumonia. OLV is

TABLE 1 | Baseline characteristics after propensity score matching.

Characteristics	nICT group	Control group	*p*
Number	38	38	NA
Age	58.8 ± 7.6	59.1 ± 7.91	0.9
Male	22	21	0.74
BMI	22.4 ± 1.9	22.9 ± 3.1	0.57
ASA			0.60
1	1	0	
2	35	36	
3	2	2	
Diabetes	2	1	0.60
Hypertension	4	6	0.50
Smoking history	24	22	0.64
FEV1	2.8 ± 0.6	2.5 ± 0.6	0.28
EF%	67.8 ± 6.2	67.7 ± 5.9	0.94
Neoadjuvant cycle	2 (2, 2)	NA	NA
Interval to surgery	46.5 ± 19.1	NA	NA
Tumor location			0.17
Upper	1	3	
Middle	21	26	
Lower	16	9	
cTNM Stage (nICT Group: stage after neoadjuvant therapy)			0.21
I	19	16	
II	4	10	
III	15	12	
IV	0	0	
Lymphadenectoy			0.08
2-field	35	38	
3-field	3	0	
Anastomotic position			NA
Cervical	38	38	
Thoracic	0	0	
Route of gastric conduit			0.08
Posterior mediastinal	38	35	
Restro-sternal	0	3	
Procedure type			0.64
Robot-assisted	35	36	
Thoracoscopy	3	2	

ASA, American Society of Anesthesiologists; BMI, body mass index; FEV1, Forced expiratory volume in one second; EF, Ejection Fractions. NA, Not available.

necessary to help achieve optimal surgical exposure during thoracic surgery and reduce the contralateral lung contamination (15). However, OLV can cause serious physiological disorders. Then, the ventilated lung is exposed to hyperperfusion and ventilator-induced lung injury, whereas the collapsed lung is mainly affected by ischemia-reperfusion injury (16). Lai et al. found that OLV ≥150 min is an important risk factor for postoperative pneumonia after McKeown esophagectomy and recommended that lung protection should be taken when OLV prolongation is expected (17). We found

TABLE 2 | Perioperative outcomes after propensity score matching.

Outcomes	nICT group	Control group	*p*
Operative time (min)	311.7 ± 74.5	273.4 ± 51.5	0.01
Converted to open surgery	0	0	NA
Intraoperative blood loss (ml)	100 (50, 100)	100 (80, 100)	0.77
Lymph nodes moved number	35.5 (28.3, 42)	30(21.8, 37.8)	0.039
Thoracic drainage tube stay (days)	7 (8, 12.5)	4 (3, 5.3)	<0.001
Thoracic drainage volume (ml)	1,895 (1,150, 2,675)	1,500 (1,173.5, 1,086.5)	0.25
ICU stay (days)	0 (0, 0.5)	0 (0, 0)	0.38
ICU readmission (*n*)	2	1	0.39
30-day mortality (*n*)	0	0	NA
30-day readmission (*n*)	2	2	1.00
Postoperative hospital stay (days)	9 (9, 14.3)	10 (8, 14.5)	1.00
Hospital stay (days)	21.5 (15.8, 28.5)	19 (16, 25)	0.49
Hospital cost (10,000 RMB)	8.8 (7.9, 11.3)	8.9 (8.4, 10.9)	0.82

Hb, hemoglobin; ICU, intensive care unit; CCI, comprehensive complications index. NA, Not available.

TABLE 3 | Postoperative complications within 30-day after operation coded by the Clavien-Dindo classification.

Complications	nICT group	Control group	*p*
Pneumonia			0.005
Grade 0	14	27	
Grade 2	6	5	
Grade 3	11	6	
Grade 4	7	0	
Anastomotic leakage			0.18
Grade 0	35	31	
Grade 1	0	0	
Grade 2	3	7	
Grade 3	0	0	
Pleural effusion			0.16
Grade 0	19	23	
Grade 1	13	9	
Grade 2	3	0	
Grade 3	3	6	
Palsy of recurrent laryngeal nerve			1.00
Grade 0	36	36	
Grade 1	2	2	
Cardiac events			0.06
Grade 0	29	36	
Grade 1	2	0	
Grade 2	7	2	
Chylothorax			0.16
Grade 0	36	37	
Grade 1	2	1	
Bleeding			0.33
Grade 0	37	38	
Grade 1	0	0	
Grade 2	1	0	
Postoperative blood transfusion			1.00
Grade 0	37	37	
Grade 2	1	1	

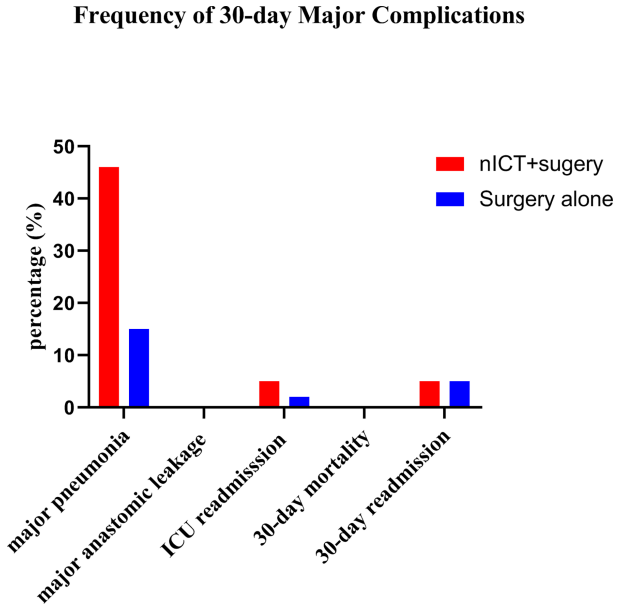

FIGURE 1 | Frequencies of 30-day major complications (defined as Clavien-Dindo classification grade ≧ 3) after propensity score matching in the neoadjuvant immunotherapy combined chemotherapy (nICT) group and the surgery alone group.

that incidence of major pneumonia was similar in the nICT group and control group. The possible reason is that early intervention could treat pneumonia. In our institution, we positively managed preoperative comorbidities, such as diabetes and chronic obstructive pulmonary disease (18), and advise patients to do respiratory function exercise. Sputum suction was conducted during operation and after operation. Early diagnosis of pneumonia and antibiotic treatment can prevent progression to respiratory failure and an increased risk of death. For patients who received nICT, pneumonitis may occur after operation, and sometimes it is difficult to diagnose based on CT scan. One patient underwent pneumonitis on the 7th day after operation, and this patient finally recovered with methylprednisolone treatment. Thus, for patients who have received nICT, pneumonitis should be considered when postoperative pneumonia does not respond to antibiotic treatment. Totally, the postoperative complications in nICT group were manageable.

In this study, we attributed the higher incidence of postoperative pneumonia to the longer operation time in the nICT group. From our experience, the thoracic surgery led to a longer operation time. Previous studies on the safety and feasibility of surgical resection after neoadjuvant immunotherapy for non-small cell lung cancer have shown increased surgical difficulty and technical challenges. Chaft et al. reported that response to immunotherapy in patients with non-small cell lung cancer may lead to high-density fibrosis. For patients with dense fibrosis (19), dissection of the mediastinum and hilum is technically challenging. Bott et al. reported the possibility of an unexpected transition from thoracoscopic lobectomy after immunotherapy (20), although there was still no report of an unexpected transformation from thoracoscopic surgery to open surgery in patients receiving nICT. However, the adhesions at the site of tumor retreat would result in unclear interstitial boundaries, especially if the tumor is located in the middle thoracic region adjacent to the trachea. Thus, when there is an adhesion between the esophagus and surrounding tissue, the surgeon needs to carefully distinguish the tissue boundaries to avoid damage to trachea, thoracic duct, and important nerve and vessels. For surgeons still on a learning curve, esophagectomy on patients who received nICT is not recommended. Fortunately, there were no dense adhesions that would require unexpected thoracotomy. Sihag et al. conducted a PSM to compare the short-term outcomes between the neoadjuvant immunotherapy and chemoradiotherapy, and the chemoradiotherapy alone group. Based on their preliminary experience, esophagectomy is safe and feasible following combined neoadjuvant immunotherapy and standard chemoradiotherapy for locally advanced esophageal cancer (21). Thus, from our opinions, the operation risk and technical challenge from immune therapy were acceptable.

Hao Wang et al. reported the pCR rate of resected tumors of 35.7% in the nCRT group and 3.8% in the nCT group (22). In this study, the anti-tumor effect of nICT were promising, with a pCR rate of 18.4% in primary tumor and a MPR rate in tumor

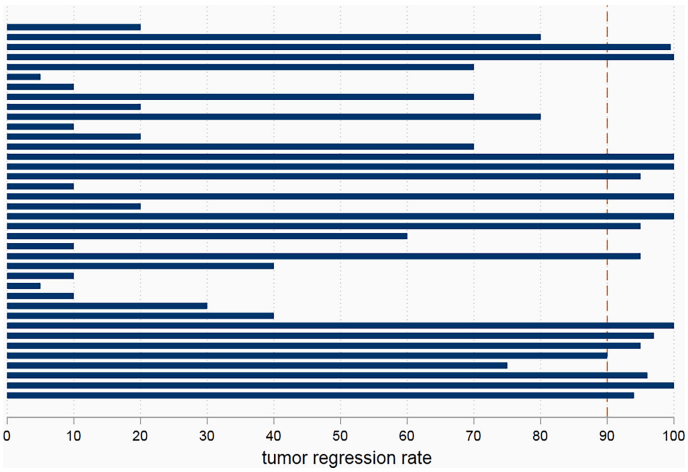

FIGURE 2 | The pathological tumor regression rate in patients receiving neoadjuvant immunotherapy combined chemotherapy.

42.1%. Pathological response to neoadjuvant therapy is significantly associated with long-term survival in patients with ESCC (23). It seems that a combination of immune therapy appears to be superior to that with nCT only and inferior to that in nCRT. Considering that most patients in this study were at the clinical III or IVA stage, there is a need to conduct long-term follow-up to evaluate the efficacy of nICT pattern.

The current study is known to have limitations. Its retrospective design introduces the inevitable risk of selection and information bias. Although propensity score matching was used to minimize indication confusion, potential bias can never be completely eliminated. All operations were performed by specialized, experienced thoracic surgeons in high-volume centers with surgery volume over 300 cases per year to ensure the treatment standardization. The sample size is relatively limited, and a multi-center large-sample study is needed to further verify the current results.

CONCLUSION

Compared with the control group, esophagectomy followed by nICT would increase operation time and incidence of pneumonia. However, the nICT group and control group were similar in major postoperative complications and mortality. Based on our preliminary experience, nICT followed by surgery is safe and effective with acceptable increased operation risk and promising pathological response.

DATA AVAILABILITY STATEMENT

The raw data supporting the conclusions of this article will be made available by the authors, without undue reservation.

AUTHOR CONTRIBUTIONS

Z-NH and MK conceived the concept and coordinated the design. Z-NH drafted the manuscript with significant contributions from KP and KW. All authors contributed to the article and approved the submitted version.

FUNDING

This study was sponsored by Key Laboratory of Cardio-Thoracic Surgery (Fujian Medical University), Fujian Province University.

ACKNOWLEDGMENTS

We deeply appreciate advice from Liqin Huang.

REFERENCES

1. Lin Y, Totsuka Y, He Y, Kikuchi S, Qiao Y, Ueda J, et al. Epidemiology of Esophageal Cancer in Japan and China. *J Epidemiol* (2013) 23(4):233–42. doi: 10.2188/jea.je20120162
2. He F, Wang J, Liu L, Qin X, Wan Z, Li W, et al. Esophageal Cancer: Trends in Incidence and Mortality in China From 2005 to 2015. *Cancer Med* (2021) 10 (5):1839–47. doi: 10.1002/cam4.3647
3. Lagergren J, Smyth E, Cunningham D, Lagergren P. Oesophageal Cancer. *Lancet* (2017) 390(10110):2383–96. doi: 10.1016/S0140-6736(17)31462-9
4. Ajani JA, D'Amico TA, Bentrem DJ, Chao J, Corvera C, Das P, et al. Esophageal and Esophagogastric Junction Cancers, Version 2.2019, NCCN Clinical Practice Guidelines in Oncology. *J Natl Compr Cancer Netw* (2019) 17:855–83. doi: 10.6004/jnccn.2019.0100
5. Yang H, Liu H, Chen Y, Zhu C, Fang W, Yu Z, et al. Neoadjuvant Chemoradiotherapy Followed by Surgery Versus Surgery Alone for Locally Advanced Squamous Cell Carcinoma of the Esophagus (NEOCRTEC5010): A Phase III Multicenter, Randomized, Open-Label Clinical Trial. *J Clin Oncol* (2018) 36(27):2796–803.
6. Ando N, Kato H, Igaki H, Shinoda M, Ozawa S, Shimizu H, et al. A Randomized Trial Comparing Postoperative Adjuvant Chemotherapy With

Cisplatin and 5-Fluorouracil Versus Preoperative Chemotherapy for Localized Advanced Squamous Cell Carcinoma of the Thoracic Esophagus (JCOG9907). *Ann Surg Oncol* (2012) 19:68–74. doi: 10.1245/s10434-011-2049-9
7. Han J, Wang Z, Liu C. Survival and Complications After Neoadjuvant Chemotherapy or Chemoradiotherapy for Esophageal Cancer: A Meta-Analysis. *Future Oncol* (2021) 17(17):2257–74. doi: 10.2217/fon-2021-0021
8. Yarchoan M, Johnson BA 3rd, Lutz ER, Laheru DA, Jaffee EM. Targeting Neoantigens to Augment Antitumour Immunity. *Nat Rev Canc* (2017) 17 (4):209e22. doi: 10.1038/nrc.2016.154
9. Kelly RJ, Ajani JA, Kuzdzal J, Zander T, Van Cutsem E, Piessen G, et al. Adjuvant Nivolumab in Resected Esophageal or Gastroesophageal Junction Cancer. *N Engl J Med* (2021) 384(13):1191–203. doi: 10.1056/NEJMoa2032125
10. Smyth EC, Gambardella V, Cervantes A, Fleitas T. Checkpoint Inhibitors for Gastroesophageal Cancers: Dissecting Heterogeneity to Better Understand Their Role in First-Line and Adjuvant Therapy. *Ann Oncol* (2021) 32(5):590–9. doi: 10.1016/j.annonc.2021.02.004
11. Zheng Y, Liu XB, Sun HB, Xu J, Shen S, Ba YF, et al. A Phase III Study on Neoadjuvant Chemotherapy Versus Neoadjuvant Toripalimab Plus Chemotherapy for Locally Advanced Esophageal Squamous Cell Carcinoma: Henan Cancer Hospital Thoracic Oncology Group 1909 (Hchtog1909). *Ann Transl Med* (2021) 9(1):73. doi: 10.21037/atm-20-5404
12. Xing W, Zhao L, Fu X, Liang G, Zhang Y, Yuan D, et al. A Phase II Single-Centre Trial of Neoadjuvant Toripalimab Plus Chemotherapy in Locally Advanced Esophageal Squamous Cell Carcinoma. *J Thorac Dis* (2020) 12 (11):6861–7. doi: 10.21037/jtd-20-2198
13. Shen D, Chen Q, Wu J, Li J, Tao K, Jiang Y, et al. The Safety and Efficacy of Neoadjuvant PD-1 Inhibitor With Chemotherapy for Locally Advanced Esophageal Squamous Cell Carcinoma. *J Gastrointest Oncol* (2021) 12(1):1–10. doi: 10.21037/jgo-20-599
14. Dindo D, Demartines N, Clavien PA. Classification of Surgical Complications: A New Proposal With Evaluation in a Cohort of 6336 Patients and Results of a Survey. *Ann Surg* (2004) 240(2):205–13. doi: 10.1097/01.sla.0000133083.54934.ae
15. Karzai W, Schwarzkopf K. Hypoxemia During One-Lung Ventilation: Prediction, Prevention, and Treatment. *Anesthesiology* (2009) 110:1402–11. doi: 10.1097/ALN.0b013e31819fb15d
16. Lohser J, Slinger P. Lung Injury After One-Lung Ventilation: A Review of the Pathophysiologic Mechanisms Affecting the Ventilated and the Collapsed Lung. *Anesth Analg* (2015) 121:302–18. doi: 10.1213/ANE.0000000000000808
17. Lai G, Guo N, Jiang Y, Lai J, Li Y, Lai R, et al. Duration of One-Lung Ventilation as a Risk Factor for Postoperative Pulmonary Complications After McKeown Esophagectomy. *Tumori* (2020) 106(1):47–54. doi: 10.1177/0300891619900805
18. Avila AC, Fenili R. Incidence and Risk Factors for Postoperative Pulmonary Complications in Patients Undergoing Thoracic and Abdominal Surgeries. *Rev Col Bras Cir* (2017) 44:284–92. doi: 10.1590/0100-69912017003011
19. Naidoo J, Wang X, Woo KM, Iyriboz T, Halpenny D, Cunningham J, et al. Pneumonitis in Patients Treated With Anti-Programmed Death-1/Programmed Death Ligand 1 Therapy. *J Clin Oncol* (2017) 35(7):709–17. doi: 10.1200/JCO.2016.68.2005
20. Bott MJ, Cools-Lartigue J, Tan KS, Dycoco J, Bains MS, Downey RJ, et al. Safety and Feasibility of Lung Resection After Immunotherapy for Metastatic or Unresectable Tumors. *Ann Thorac Surg* (2018) 106(1):178–83. doi: 10.1016/j.athoracsur.2018.02.030
21. Sihag S, Ku GY, Tan KS, Nussenzweig S, Wu A, Janjigian YY, et al. Safety and Feasibility of Esophagectomy Following Combined Immunetherapy and Chemoradiotherapy for Esophageal Cancer. *J Thorac Cardiovasc Surg* (2021) 161(3):836–43. doi: 10.1016/j.jtcvs.2020.11.106
22. Wang H, Tang H, Fang Y, Tan L, Yin J, Shen Y, et al. Morbidity and Mortality of Patients Who Underwent Minimally Invasive Esophagectomy After Neoadjuvant Chemoradiotherapy vs Neoadjuvant Chemotherapy for Locally Advanced Esophageal Squamous Cell Carcinoma: A Randomized Clinical Trial. *JAMA Surg* (2021) 156(5):444–51. doi: 10.1001/jamasurg.2021.0133
23. Berger AC, Farma J, Scott WJ, Freedman G, Weiner L, Cheng JD, et al. Complete Response to Neoadjuvant Chemoradiotherapy in Esophageal Carcinoma Is Associated With Significantly Improved Survival. *J Clin Oncol* (2005) 23(19):4330–7. doi: 10.1200/JCO.2005.05.017

Conflict of Interest: The authors declare that the research was conducted in the absence of any commercial or financial relationships that could be construed as a potential conflict of interest.

frontiers in Oncology

SYSTEMATIC REVIEW
published: 21 December 2021
doi: 10.3389/fonc.2021.777686

Efficacy and Safety of Immune Checkpoint Inhibitor in Advanced Esophageal Squamous Cell Carcinoma: A Meta-Analysis

Yi-Min Gu[1†], Qi-Xin Shang[1†], Yue Zhuo[2], Jian-Feng Zhou[1], Bo-Wei Liu[1], Wen-Ping Wang[1], Guo-Wei Che[1] and Long-Qi Chen[1]*

[1] Department of Thoracic Surgery, West China Hospital of Sichuan University, Chengdu, China, [2] West China School of Medicine, Sichuan University, Chengdu, China

OPEN ACCESS

Edited by:
Sripathi Sureban, University of Oklahoma Health Sciences Center, United States

Reviewed by:
Takahiro Tsushima, Shizuoka Cancer Center, Japan
Wencheng Zhang, Tianjin Medical University Cancer Institute and Hospital, China

****Correspondence:***
Long-Qi Chen
drchenlq@scu.edu.cn

[†]These authors have contributed equally to this work and share first authorship

Specialty section:
This article was submitted to Gastrointestinal Cancers: Gastric and Esophageal Cancers, a section of the journal Frontiers in Oncology

Received: *15 September 2021*
Accepted: *06 December 2021*
Published: *21 December 2021*

Citation:
Gu Y-M, Shang Q-X, Zhuo Y, Zhou J-F, Liu B-W, Wang W-P, Che G-W and Chen L-Q (2021) Efficacy and Safety of Immune Checkpoint Inhibitor in Advanced Esophageal Squamous Cell Carcinoma: A Meta-Analysis. Front. Oncol. 11:777686. doi: 10.3389/fonc.2021.777686

Background: The published evidence from several randomized controlled clinical trials of immunotherapy for advanced esophageal squamous cell carcinoma has shown promising results. This study aimed to investigate the efficacy and safety of immune checkpoint inhibitor treatment in esophageal squamous cell carcinoma.

Methods: PubMed, Web of Science, Cochrane Library, and Embase databases were searched for relevant articles published before December 30, 2020. The data for efficacy and safety of immune checkpoint inhibitor treatment were subjected to meta-analysis.

Results: Seven clinical trials comprising 1733 patients were included. The results showed that immune checkpoint inhibitor treatment as second- or later-line treatment was associated with an increased risk of the objective response rate (relative risk: 1.82, 95% confidence interval: 0.82–4.04; P=0.002) and median overall survival (hazard ratio: 0.75, 95% confidence interval: 0.67–0.85; P<0.001) compared with chemotherapy in locally advanced or metastatic esophageal squamous cell carcinoma. Moreover, immune checkpoint inhibitor treatment was associated with significant improvement in median overall survival (hazard ratio: 0.61, 95% confidence interval: 0.48–0.77, P<0.001) compared with chemotherapy in the programmed death-ligand 1 (PD-L1)-positive population. However, immune checkpoint inhibitor treatment was also effective in all patients independent of PD-L1 expression. The most common grade ≥3 treatment-related adverse events with immune checkpoint inhibitor therapy were anemia, asthenia, rash, fatigue, decreased appetite, diarrhea, pneumonia, decreased neutrophil count, and vomiting. Patients undergoing immune checkpoint inhibitor therapy was associated with a decreased risk of treatment-related adverse events (relative risk: 0.82, 95% confidence interval: 0.62–1.08; P<0.001) and grade ≥3 treatment-related adverse events (relative risk: 0.50, 95% confidence interval: 0.42–0.60; P<0.001) compared with those undergoing chemotherapy.

Conclusions: Immune checkpoint inhibitors as second- or later-line therapy may improve overall response rate and overall survival but not all oncological outcomes for patients with

locally advanced or metastatic esophageal squamous cell carcinoma. Patients treated with immune checkpoint inhibitors might experience fewer treatment-related adverse events of any grade, but specifically grade ≥3, compared with those treated with chemotherapy.

Keywords: esophageal squamous cell carcinoma, immune checkpoint inhibitor, anti-tumor activity, survival, adverse event

INTRODUCTION

Esophageal cancer is the seventh most common malignant tumor and the sixth leading cause of cancer death worldwide (1). To date, the optimal therapy for local advanced esophageal cancer has consisted of multidisciplinary therapy involving neoadjuvant chemotherapy or chemoradiotherapy plus surgery. Despite improvements in treatment, the long-term survival for patients with advanced esophageal cancer is still unsatisfactory (2, 3).

Immunotherapy, with agents such as immune checkpoint inhibitors (ICIs), cancer vaccines, and adoptive T-cell therapy, has recently increased hope for improved survival outcomes in patients with esophageal cancer (4–7). ICI therapy has dramatically changed the treatment of melanoma and advanced non-small cell lung cancer (8–12). In the past few years, published evidence from randomized controlled clinical trials (RCTs) has shown promise for treatment of esophageal squamous cell carcinoma (ESCC) (13–15). The two most common types of esophageal cancer are ESCC and esophageal adenocarcinoma (EAC), the incidence of which can vary by region, with the highest rate of EAC occurring in Western countries and of ESCC occurring in East Asian countries. There are clear differences between the etiology, molecular biological features, and prognosis of ESCC and EAC (16, 17). ESCC with a high level of tumor mutations appeared to be more sensitive to treatment than EAC (18). The randomized phase 3 trial KEYNOTE-181 showed that patients with ESCC treated with anti-programmed death-ligand 1 (PD-L1) antibody therapy tended to survive longer than the overall patient population but did not make a direct comparison between treatments (13). Given the high prevalence of ESCC in East Asia and the shortage of effective treatment options for advanced ESCC, conventional chemotherapy is far from satisfactory. Thus, there is an urgent need for the development of novel and effective treatments for advanced ESCC.

This study aimed to perform a meta-analysis to assess the efficacy and safety of ICI treatments for patients with advanced ESCC. Findings from this meta-analysis may be helpful in guiding ICI treatment for patients with ESCC.

METHODS

Study Search

We conducted a systematic literature review according to the Preferred Reporting Items for Systematic Reviews and Meta-Analyses (PRISMA) 2009 guidelines (19). Two authors independently searched PubMed, Web of Science, Cochrane Library, and Embase for relevant clinical trials published before December 31, 2020. The search keyword terms were as follows: ((esophageal neoplasm [MeSH Terms]) OR ((((((esophageal squamous cell carcinoma) OR (oesophageal squamous cell carcinoma)) OR (squamous cell carcinoma of esophagus)) OR (squamous cell carcinoma of oesophagus)) OR (esophageal cancer)) OR (oesophageal cancer))) AND (immunotherapy [MeSH Terms]) OR ((((((((((immune checkpoint inhibitor) OR (PD-1)) OR (PD-L1)) OR (Nivolumab) OR (Pembrolizumab)) OR (Camrelizumab)) OR (SHR-1210) OR (Toripalimab)) OR (Ipilimumab)) OR (Avelumab) OR (Atezolizumab)) OR (Durvalumab))).

Study Selection, Data Extraction, and Quality Assessment

The inclusion criteria were clinical trials that included ICI monotherapy as second- or later-line treatment for patients with advanced or metastatic ESCC. Hazard ratio (HR) and relative risk (RR) for antitumor activity, survival outcomes, and safety indicators were available. Two researchers independently selected studies and extracted data; if there were any questions, another senior researcher was invited to discuss these. The following information was extracted from the selected articles: author, year, study name, study design, participant characteristics, sample size, and interventions. A quality appraisal of three randomized trials was performed using the Cochrane Risk of Bias tool (20).

Statistical Analysis

HR, RR, and their associated 95% confidence interval (CI) were extracted from each article and combined to estimate the prognostic value. HR or RR <1 indicated a better oncologic outcome in patients with esophageal cancer treated with ICI than in those treated with chemotherapy. The Q test and I-squared statistic were used to assess the heterogeneity of the included studies. Pooled estimates of HR or RR were calculated initially using a fixed-effect model. If significant heterogeneity existed ($P<0.10$ or $I2>50\%$), a random-effect model was used. Publication bias was evaluated by both Begg's and Egger's tests. All P-values were two-sided and significant publication bias was defined as $P<0.05$. Subgroup analyses were performed on the basis of which anti-PD-L1 antibody was used. All statistical analyses were performed using Stata/SE 12.0 software (StataCorp. LLC, version 12.0, College Station, TX, USA).

RESULTS

Study Identification and Study Characteristics

Our search screened 1452 eligible studies and identified nine clinical trials; one study by Kato et al., 2020 (21) used the same dataset as that reported by Kudo et al., 2017 (22). In another trial by Zhang et al., 2020 (23) the study arm applied ICI combined with chemotherapy, which did not meet the inclusion criteria. Finally, a total of seven articles (13–15, 22, 24–26) were included in this meta-analysis. The flow diagram for identifying relevant studies is shown in **Figure 1A**.

All the included studies were published in peer-reviewed journals between 2010 and 2019 and were performed in eight countries (Japan, China, France, South Korea, USA, France, United Kingdom, and Germany). Of these clinical trials, three were multicenter, open-label, phase 3 RCTs (13–15) comparing ICI monotherapy vs. chemotherapy, and four were single-arm, prospective, phase 1–2 trials (22, 24–26) applying ICI monotherapy. Four trials enrolled patients with ESCC, three enrolled patients with both ESCC and EAC. All trials investigated anti-PD-L1 antibody therapy (three with pembrolizumab, two with camrelizumab, and two with nivolumab). A comprehensive outline of the characteristics of the included clinical trials are presented in **Table 1**. Three randomized trials reported the sample size assessment and follow-up time, but the method used for study allocation concealment in one study was unclear (**Figure 1B**). Because of a lack of appropriate evaluation tools, the risk of bias in the four single-arm trials was not estimated.

Objective Response Rate (ORR) and Disease Control Rate (DCR)

The pooled ORR and DCR of ICI treatment and a subgroup analysis are summarized in **Table 2**. The pooled ORR of ICI treatment was 18.3%. The ORRs of the pembrolizumab, camrelizumab, and nivolumab ICI subgroups were 16.3%, 24.2%, and 18.5%, respectively. The pooled DCR of ICI treatment was 38.4%. The DCRs of the pembrolizumab, camrelizumab, and nivolumab subgroups were 28.0%, 46.1%, and 33.0%, respectively.

Three RCTs including 1268 patients demonstrated that ICI treatment was significantly associated with improvement of ORR compared with chemotherapy, with an estimated RR of 1.82 (95% CI: 0.82–4.04, P=0.002) with significant heterogeneity (I2 = 85.7%, P=0.001) (**Figure 2A**). These results suggested that ICI as second- or later-line treatment for patients with locally advanced or metastatic ESCC was associated with an increased risk of response compared with chemotherapy.

However, two studies comprising 867 patients compared the DCR between two groups, ICI versus chemotherapy. Pooled data from the two studies showed no significant difference between ICI treatment and chemotherapy, with an estimated RR of 0.88 (95% CI: 0.41–1.88, P=0.739) without apparent heterogeneity (I2 = 95.4%, P<0.001) (**Figure 2B**).

Overall Survival Rate, Median Overall Survival (OS) and Median Progression-Free Survival (PFS)

The results of analysis of pooled 6-month and 12-month OS rate of ICI treatment and the associated subgroup analysis are also summarized in **Table 2**. The pooled 6-month OS rate of ICI treatment was 57.1%. The 6-month OS rate of the pembrolizumab and camrelizumab ICI subgroups was 50.8% and 63.0%, respectively. The pooled 12-month OS rate of ICI treatment was 37.5%. The 12-month OS rate of the pembrolizumab, camrelizumab, and nivolumab ICI subgroups was 34.9%, 34.0%, and 47.0%, respectively. The highest 6-month OS rate (63.0%) was observed in the camrelizumab subgroup and the highest 12-month OS rate (47%) in the nivolumab subgroup.

Meta-analysis of three RCTs comprising 1268 patients revealed that ICI treatment improved median OS compared with chemotherapy when used as second- or later-line treatment of locally advanced or metastatic ESCC. This

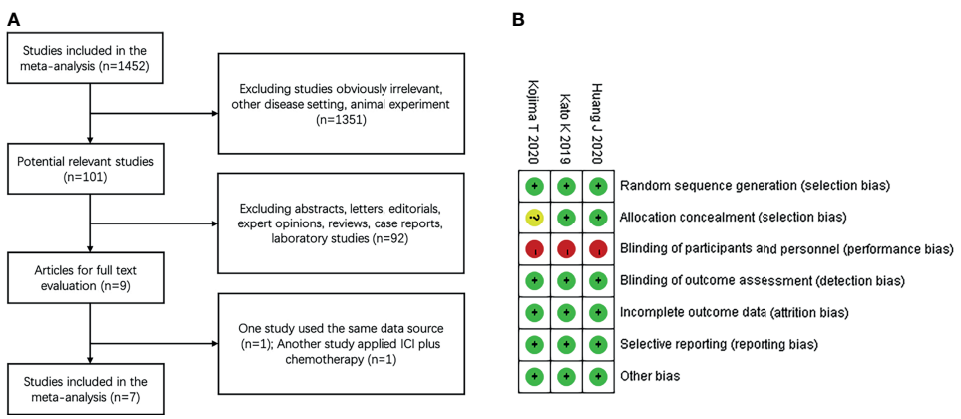

FIGURE 1 | Study identification and risk of bias **(A)** Flow diagram of identification of relevant studies; **(B)** Summary of risk of bias summary of randomized controlled trials. + low risk,? unclear risk, – high risk.

TABLE 1 | Baseline characteristics of included studies.

Author	Study name	Study design	Participants characteristics	Sample size	Study arm (N)	Control arm (N)
Kojima T, (13)	KEYNOTE-181	RCT phase 3	Advanced/metastatic ESCC or EAC that progressed after one prior therapy	628 (401 ESCC & 227EAC)	Pembrolizumab 200 mg/3 weeks i.v. (314)	Chemotherapy with paclitaxel, docetaxel, or irinotecan (314)
Huang J, (14)	ESCORT	RCT phase 3	Advanced/metastatic ESCC; ECOG 0-1; and had progressed on, or were intolerant to, first-line standard therapy	448	Camrelizumab 200 mg/2 weeks i.v. (228)	Chemotherapy with docetaxel 75 mg/m2/3 weeks or irinotecan 180 mg/m2/2 weeks (220)
Kato K, (15)	ATTRACTION-3	RCT phase 3	Unresectable advanced or recurrent ESCC; ≥20 years old; ECOG 0–1; and who were refractory or intolerant to previous chemotherapy and had a life expectancy of ≥ 3 months	419	Nivolumab 240 mg/2 weeks i.v. (210)	Chemotherapy with paclitaxel 100 mg/m2/week or docetaxel 75 mg/m2/3 weeks (209)
Shah MA, (24)	KEYNOTE-180	Single-arm phase 2	Advanced/metastatic esophageal cancer that progressed after 2 or more lines of therapy	121 (63 ESCC & 58 EAC)	Pembrolizumab 200mg/3 weeks i.v. (121)	NA
Huang J, (25)	NCT02742935	Single-arm phase 1	Advanced ESCC who were refractory or intolerant to previous chemotherapy	30	SHR-1210 60 mg, with escalation to 200 mg and 400 mg/2 weeks i.v. (30)	NA
Doi T, (26)	KEYNOTE-028	Single-arm phase 1b	ESCC or EAC of the esophagus or gastroesophageal junction in whom standard therapy failed	23 (18 ESCC & 5 EAC)	Pembrolizumab 10 mg/kg/2 weeks i.v. (23)	NA
Kudo T, (22)	ATTRACTION-1	Single-arm phase 2	Advanced ESCC refractory or intolerant to fluoropyrimidine-based, platinum-based, and taxane-based chemotherapy	64	Nivolumab 3 mg/kg/2 weeks i.v. (64)	NA

ESCC, esophageal squamous cell carcinoma; EAC, esophageal adenocarcinoma; ECOG, Eastern Cooperative Oncology Group; NA, not available.

corresponded to a pooled HR of 0.75 (95% CI: 0.67–0.85; P<0.001) without obvious heterogeneity (I2 = 0.0%, P=0.801) (**Figure 3A**).

However, no significant difference was found in the median PFS of patients treated with ICI or chemotherapy (HR: 0.88, 95% CI: 0.68–1.14, P=0.330) with significant heterogeneity (I2 = 76.7%, P=0.014) (**Figure 3B**).

PD-L1-Positive Tumors

Three studies compared the antitumor activity of treatment in patients with PD-L1 positive (≥1%) and negative (<1%) tumors. The ORR and DCR of patients with PD-L1 positive tumors were 22.2% and 48.0%, while those of patients with PD-L1 negative tumors were 6.7% and 26.9% (**Table 2**). Meta-analysis of three RCTs comprising 561 patients revealed that in patients with high

TABLE 2 | ORR, DCR and OS rate in different subgroups.

Source[a]	Outcome	Heterogeneity	Rate (95% CI) %
13-15,22,24-26	ICI ORR	Fixed	18.3 (15.8-20.9)
13,24,26	Pembrolizumab ORR	Fixed	16.3 (12.3-20.2)
14,26	Camrelizumab ORR	Random	24.2 (12.4-36.0)
15,22	Nivolumab ORR	Fixed	18.5 (13.9-23.1)
14,15,22,25,26	ICI DCR	Random	38.4 (30.1-46.8)
26	Pembrolizumab DCR	——	28.0 (35.2-43.2)
14,26	Camrelizumab DCR	Fixed	46.1 (40.0-52.2)
15,22	Nivolumab DCR	Random	33.0 (23.4-42.6)
14,24,26	ICI 6-month OS rate	Random	57.1 (46.6-67.7)
24,26	Pembrolizumab 6-month OS rate	Fixed	50.8 (42.7-59.0)
14	Camrelizumab 6-month OS rate	——	63.0 (56.7-69.3)
13-15,24,26	ICI 12-month OS rate	Random	37.5 (30.6-44.4)
13,24,26	Pembrolizumab 12-month OS rate	Random	34.9 (26.0-43.7)
14	Camrelizumab 12-month OS rate	——	34.0 (27.0-40.1)
15	Nivolumab 12-month OS rate	——	47.0 (40.2-53.8)
13,24,25	PD-L1+ ORR	Random	22.2 (10.5-34.0)
13,24,25	PD-L1+ DCR	Random	48.0 (34.2-61.9)
24,25	PD-L1- ORR	Fixed	6.7 (0.9-12.4)
24,25	PD-L1- DCR	Fixed	26.9 (12.0-41.7)

[a]*Source appertain to corresponding references; ORR, objective response rate; DCR, disease control rate; OS, overall survival; ICI, immune checkpoint inhibitor.*

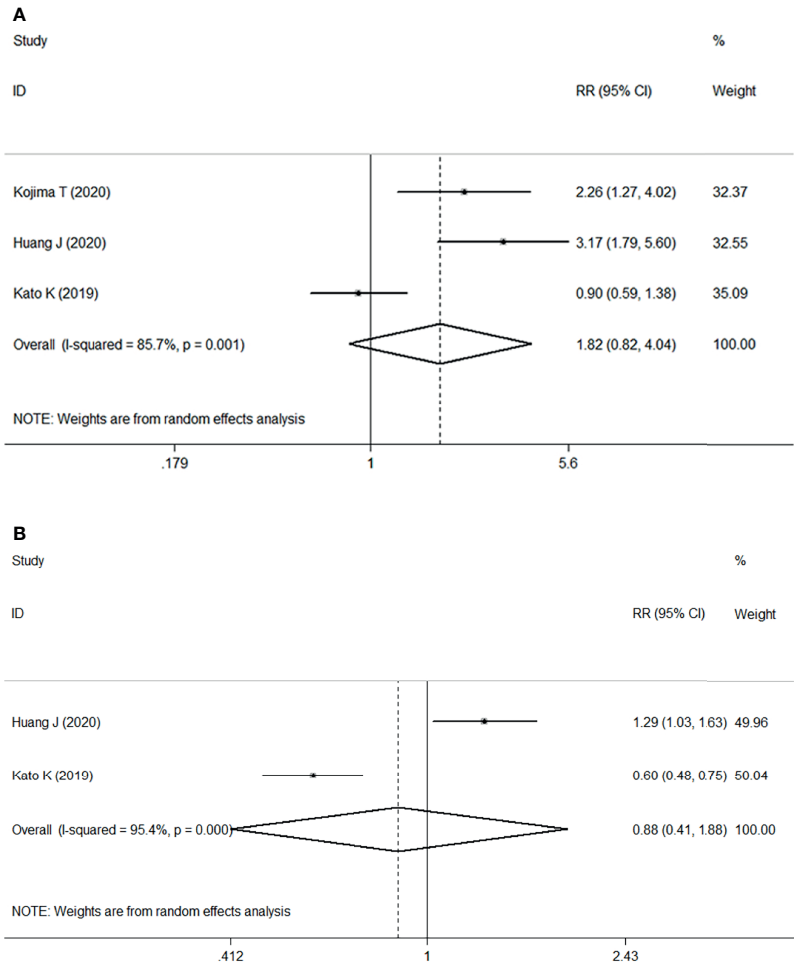

FIGURE 2 | Forest plots. **(A)** Forest plots of RR comparing the objective response rate between patients treated with ICI and chemotherapy; **(B)** Forest plots of RR comparing disease control rate between patients treated with ICI and chemotherapy. RR, relative risk; CI, confidence interval; ICI, immune checkpoint inhibitor.

PD-L1 expression, median OS was improved with ICI treatment versus chemotherapy. This corresponded to a pooled HR of 0.61 (95% CI: 0.48–0.77; P<0.001) without obvious heterogeneity (I2 = 0.0%, P=0.681) (**Figure 4**).

Treatment-Related Adverse Events (TRAEs)

We investigated the pooled incidence of any-grade TRAEs and grade ≥3 TRAEs (both total and specific events) (**Table 3**). The overall incidence of TRAEs in patients treated with ICI was 61.9%. The incidence of TRAEs in the pembrolizumab and nivolumab subgroups was 50.7% and 85.0%, respectively. However, the incidence of grade ≥3 TRAE in patients treated with ICI was 16.7%. The incidence of grade ≥3 TRAE in the pembrolizumab, nivolumab, and camrelizumab subgroups was 16.2%, 19.5%, and 15.0%, respectively. The patients in camrelizumab subgroup had the least incidence (15%).

The most common TRAEs with ICI therapy of locally advanced or metastatic ESCC were rash (10.8%), hypothyroidism (10.1%), fatigue (9.3%), asthenia (7.0%), decreased appetite (7.0%), diarrhea (6.0%), anemia (4.7%), nausea (3.0%), pneumonia (2.7%), vomiting (2.0%), decreased neutrophil count (1.1%), and alopecia (0.7%). The most common grade ≥3 TRAEs with ICI therapy were anemia (1.8%), asthenia (1.2%), rash (1.1%), fatigue (0.8%), decreased appetite (0.8%), diarrhea (0.8%), pneumonia (0.5%), decreased neutrophil count (0.5%), and vomiting (0.3%).

The meta-analysis of the three RCTs indicated that patients undergoing ICI therapy was associated with a decreased risk of overall TRAEs (RR: 0.82, 95% CI 0.62–1.08; *P*<0.001) (**Figure 5A**) and grade ≥3 TRAEs (RR=0.50, 95% CI 0.42–0.60; *P*<0.001) (**Figure 5B**) compared with those undergoing chemotherapy.

Publication Bias

Publication bias was evaluated by both Begg's and Egger's tests (**Table 4**). All outcomes had P>0.05, except for the Egger's test of ICI vs. chemotherapy TRAEs (P<0.05). Overall, no obvious publication bias was observed.

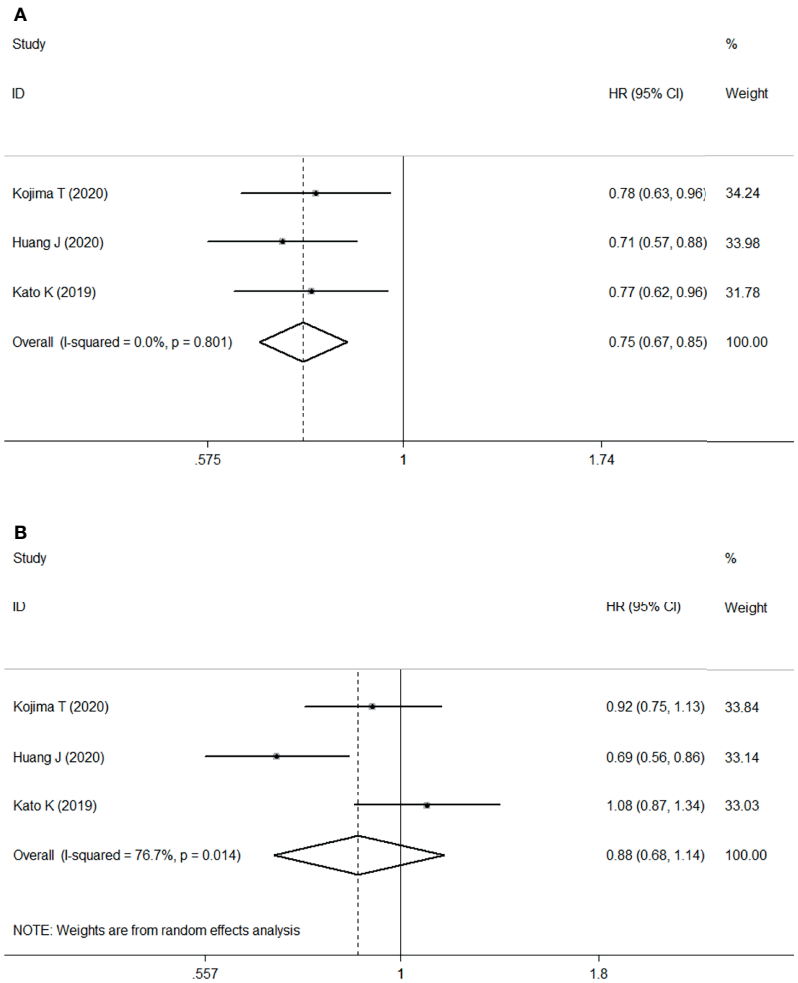

FIGURE 3 | Forest plots. **(A)** Forest plots of HR comparing overall survival between patients treated with ICI and chemotherapy; **(B)** Forest plots of HR comparing progression-free survival between patients treated with ICI and chemotherapy. HR, hazard ratio; CI, confidence interval; ICI, immune checkpoint inhibitor.

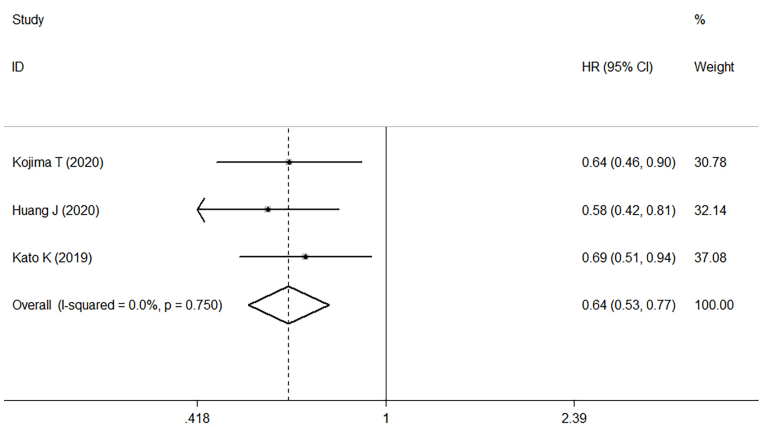

FIGURE 4 | Forest plots of HR comparing overall survival between patients with PD-L1-positive tumors treated with ICI treatment and chemotherapy. HR, hazard ratio; CI, confidence interval; ICI, immune checkpoint inhibitor.

TABLE 3 | The incidence of specific TRAEs, grade ≥3 TRAEs.

TRAE Name	Subgroup	Source[a]	TRAE		Grade ≥3 TRAE	
			Heterogeneity	Rate (95% CI) %	Heterogeneity	Rate (95% CI) %
Total TRAE	Anti-PD-1	13-15,22,24-26	Random	61.9 (37.9-85.9)	Fixed	16.7 (14.4-19.0)
	Pembrolizumab	13,24,26	Random	50.7 (32.6-68.7)	Fixed	16.2 (12.9-19.6)
	Nivolumab	15,22	——	85.0 (76.3-93.7)	Fixed	19.5 (14.8-24.2)
	Camrelizumab	14,25	——	——	Fixed	15.0 (10.7-19.4)
Rash	Anti-PD-1	15,22,25,26	Fixed	10.8 (7.5-14.2)	Fixed	1.1 (-0.2-2.4)
	Pembrolizumab	26	——	13.0 (-0.7-26.7)	——	0.4 (-0.4-12.0)
	Nivolumab	15,22	Fixed	10.8 (7.1-14.5)	——	1.0 (-0.3-2.3)
	Camrelizumab	25	——	10 (-0.7-20.7)	——	0
Hypothyroidism	Anti-PD-1	13,14,24-26	Random	10.1 (5.4-14.7)	——	0
	Pembrolizumab	13,24,26	Random	7.6 (3.6-11.5)	——	0
	Camrelizumab	14,25	Fixed	16.5 (12.0-21.0)	——	0
Fatigue	Anti-PD-1	13,15,22,24-26	Fixed	9.3 (7.3-11.4)	Fixed	0.8 (0.1-1.5)
	Pembrolizumab	13,24,26	Fixed	10.6 (7.8-13.4)	——	0.6 (-0.3-1.5)
	Nivolumab	15,22	Fixed	8.0 (4.8-11.2)	Fixed	1.1 (-0.1-2.4)
	Camrelizumab	25	——	6.7 (-2.2-15.6)	——	0
Asthenia	Anti-PD-1	13,14,26	Fixed	7.0 (4.2-9.8)	Fixed	1.2 (0.3-2.1)
	Pembrolizumab	13,26	Fixed	6.7 (4.0-9.3)	——	1.3 (0.0-2.6)
	Camrelizumab	14	——	9.0 (5.3-9.6)	——	1.0 (-0.3-2.3)
Decreased appetite	Anti-PD-1	13-15,22,26	Fixed	7.0 (5.2-8.7)	Fixed	0.8 (0.1-1.5)
	Pembrolizumab	13,26	Fixed	8.0 (5.1-10.9)	——	0.6 (-0.3-1.5)
	Nivolumab	15,22	Fixed	8.2 (5.0-11.5)	Fixed	1.2 (-0.1-2.5)
	Camrelizumab	14	——	5.0 (2.2-7.8)	——	0
Diarrhea	Anti-PD-1	13-15,22,24-25	Fixed	6.0 (4.5-7.6)	Fixed	0.8 (0.2-1.4)
	Pembrolizumab	13,24	Fixed	5.3 (3.2-7.3)	Fixed	0.6 (-0.1-1.4)
	Nivolumab	15	——	11.0 (6.8-15.2)	——	1.0 (-0.3-2.3)
	Camrelizumab	14,25	Fixed	5.3 (2.6-8.1)	——	1.0 (-0.3-2.3)
Anemia	Anti-PD-1	13-15,24-25	Random	4.7 (1.4-8.1)	Fixed	1.8 (0.8-2.7)
	Pembrolizumab	13	——	2.5 (0.8-4.2)	——	1.3 (0.0-2.6)
	Nivolumab	15	——	3.0 (0.7-5.3)	——	2.0 (0.1-3.9)
	Camrelizumab	14,25	Random	7.6 (0.1-15.1)	——	3.0 (0.8-5.2)
Nausea	Anti-PD-1	13-15,25	Random	3.0 (1.8-4.1)	——	0
	Pembrolizumab	13	——	7.0 (4.2-9.8)	——	0
	Nivolumab	15	——	2.0 (0.1-3.9)	——	0
	Camrelizumab	15,22	Fixed	2.2 (0.4-4.0)	——	0
Pneumonia	Anti-PD-1	14,22,24-26	Random	2.7 (-0.5-5.9)	Random	0.5 (-0.2-1.2)
	Pembrolizumab	24,26	Fixed	6.5 (2.5-10.5)	——	2.4 (-0.3-5.1)
	Nivolumab	22	——	2.0 (-1.4-5.4)	——	0
	Camrelizumab	14,25	——	0.3 (-0.4-1.0)	Fixed	0.3 (-0.4-1.0)
Vomiting	Anti-PD-1	13,14	Random	2.0 (-0.2-4.1)	——	0.3 (-0.3-0.9)
	Pembrolizumab	13	——	3.2 (1.3-5.1)	——	0.3 (-0.3-0.9)
	Camrelizumab	14	——	1.0 (-0.2-4.1)	——	0
Neutrophil count decreased	Anti-PD-1	13-15,22	Random	1.1 (0.4-1.9)	Fixed	0.5 (-0.1-1.0)
	Pembrolizumab	13	——	0.6 (-0.3-1.5)	——	0.3 (-0.3-0.9)
	Nivolumab	15,22	——	2.0 (0.1-3.9)	Fixed	1.1 (-0.1-2.4)
	Camrelizumab	14	——	4.0 (1.5-6.5)	——	0
Alopecia	Anti-PD-1	13-15,24,26	Fixed	0.7 (-0.0-1.4)	——	0
	Pembrolizumab	13,24,26	——	0.6 (-0.3-1.5)	——	0
	Nivolumab	15	——	1.0 (-0.3-2.3)	——	0
	Camrelizumab	14	——	0	——	0

TRAE, treatment-related adverse event; [a]Source appertain to corresponding references.

DISCUSSION AND CONCLUSIONS

To our knowledge, this is the first meta-analysis to evaluate the efficacy and safety of ICIs (anti-PD-L1 antibody) as second- or later-line treatment for unresectable locally advanced or recurrent/metastatic ESCC. This study included seven published clinical trials including three RCTs and four single-arm trials published before December 31, 2020. The main outcomes showed that ICI therapy used as second- or later-line treatment for advanced or metastatic ESCC could increase ORR, improve OS, and decrease the incidence of any-grade TRAEs and grade ≥3 TRAEs compared with chemotherapy.

Several RCTs of ICIs have reported the clinical outcomes in patients with ESCC. The randomized phase 3 trial KEYNOTE-181 (13) reported that patients with ESCC treated with anti-PD-L1 antibody therapy showed a trend toward longer survival compared with the overall population of patients with ESCC

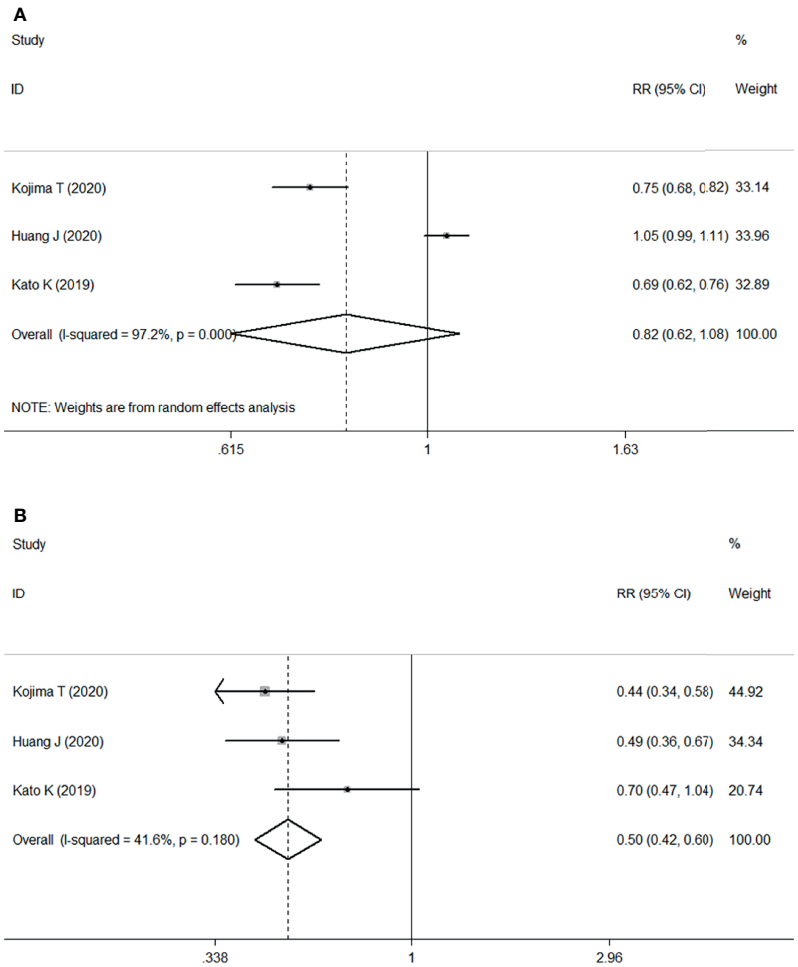

FIGURE 5 | Forest plots. **(A)** Forest plots of RR comparing TRAEs between patients treated with ICI and chemotherapy; **(B)** Forest plots of RR comparing grade ≥3 TRAEs between patients treated with ICI and chemotherapy. RR, relative risk; CI, confidence interval; ICI, immune checkpoint inhibitor; TRAEs, treatment-related adverse events.

but did not make a direct comparison. The randomized trial ATTRACTION-3 reported by Kato et al. (15) also demonstrated that median OS was significantly improved in patients treated with nivolumab compared with those treated with chemotherapy (10.9 months vs 8.4 months; HR: 0.77, 95% CI: 0.62–0.96; P=0.019). However, the effects of ICI on PFS and its antitumor activity differ between studies. The ESCORT randomized phase 3 study (14) showed that camrelizumab improved OS compared with chemotherapy as second-line therapy in Chinese patients with advanced ESCC.

Patients with PD-L1-positive tumors may derive more survival benefit with ICI therapy than with chemotherapy.

TABLE 4 | Publication bias of different outcomes.

Outcomes	Included study numbers	Effect size	*P*	
			Begg	Egger
ICI ORR	3	logRR	1.000	0.171
ICI DCR	2	logRR	1.000	——
ICI OS	3	lnHR	1.000	0.815
ICI PFS	3	lnHR	1.000	0.967
ICI TRAEs	3	logRR	0.296	0.000
ICI grade≥3 TRAEs	3	logRR	0.296	0.077
PD-L1+ ICI OS	3	lnHR	1.000	0.505

ICI, immune checkpoint inhibitor; ORR, objective response rate; DCR, disease control rate; OS, overall survival; PFS, progression-free survival; TRAEs, treatment-related adverse events; PD-L1+, PD-L1 positive; RR, relative risk; HR, hazard ratio.

However, ICI therapy was also reported to be effective in all patients independent of PD-L1 expression (14). The RCT reported by Kato et al. also observed no significant interaction between the effectiveness of ICI therapy and PD-L1 status (15). This suggests that PD-L1 might not be sufficiently specific to serve as the optimal biomarker for ICI treatment of ESCC. In advanced gastric or gastroesophageal junction cancer, high microsatellite instability and tumor mutational burden has been shown to be associated with the ORR of patients (27, 28). Studies have found that the tumor mutation burden is usually higher in ESCC than in EAC (18, 29). Further investigation of candidate biomarkers for ICI treatment is warranted.

The three randomized trials included in this meta-analysis all involved monotherapy with ICI vs. chemotherapy as a second- or later-line treatment. There are a number of unpublished clinical trials with an accessible conference abstract that evaluated the efficacy of ICI as first-line therapy and adjuvant therapy, such as the KEYNOTE-590 randomized phase 3 study (30); this showed that the median OS of patients with ESCC was longer with first-line treatment with pembrolizumab plus chemotherapy than with chemotherapy alone (12.6 months vs. 9.8 months; HR: 0.72, 95% CI: 0.60–0.88, P=0.0006). In the CheckMate 577 randomized phase 3 study (31), median DFS in patients treated with nivolumab after surgery was twice that in the placebo population (22.4 months vs. 11.0 months; HR: 0.69; 96.4% CI: 0.56–0.86; P=0.0003). The optimal timing, dosing, and combination of ICI regimens for treatment of esophageal cancer require further study.

The safety profile of ICIs showed a lower incidence of any-grade TRAEs and grade ≥3 TRAEs compared with chemotherapy. In this meta-analysis, 61.9% patients receiving ICI treatment reported TRAEs, but the probability of developing grade ≥3 TRAEs was 16.7%. Notably, the incidence of reactive cutaneous capillary endothelial proliferation after receiving camrelizumab was high (14, 23). However, no similar adverse event was noted in patients receiving pembrolizumab or nivolumab. Moreover, the incidence of treatment leading to death was almost zero. Accordingly, ICI treatment can be considered a relatively safe option.

This meta-analysis has some limitations that should be acknowledged. First, it included only seven studies comprising three RCTs and four single-arm trials. Even though no obvious publication bias was detected in the included RCTs by Begg's or Egger's test, the single-arm studies without a control group might introduce a potential bias. The low number of trials may limit the accuracy of the test. However, the number of 1733 included patients is relatively high, indicating reliability. Second, three studies included both patients with ESCC and those with EAC. Specific information about squamous cell carcinoma patients was provided by Kojima et al. (13), but was not available for two single-arm studies (24, 26) that included 81 ESCC patients and 63 EAC patients. Unfortunately, we do not have access to their raw data. These confounding factors may limit the interpretation of our results.

In conclusion, ICI treatment in patients with locally advanced or metastatic ESCC may improve the ORR and median OS but not all oncological outcomes, and result in a lower incidence of TRAEs compared with chemotherapy. Although ICI treatment was more effective in patients with PD-L1-positive tumors, it was also effective in all patients with ESCC independent of their PD-L1 expression. Further investigation of the optimal timing, dosing, combination of drug regimens, and candidate biomarkers for ICI treatment of esophageal cancer is warranted.

DATA AVAILABILITY STATEMENT

The original contributions presented in the study are included in the article/supplementary material. Further inquiries can be directed to the corresponding author.

AUTHOR CONTRIBUTIONS

L-QC and G-WC conceptualized the study, revised the manuscript and supervised the study. Y-MG and Q-XS conceptualized the study, drafted the manuscript and made the figures. Y-MG, YZ, J-FZ, B-WL and W-PW collected the literature and revised the manuscript. All authors contributed to the article and approved the submitted version.

REFERENCES

1. Torre LA, Bray F, Siegel RL, Ferlay J, Lortet-Tieulent J, Jemal A. Global Cancer Statistics, 2012. *CA Cancer J Clin* (2015) 65(2):87–108. doi: 10.3322/caac.21262
2. van Hagen P, Hulshof MC, van Lanschot JJ, Steyerberg EW, van Berge Henegouwen MI, Wijnhoven BP, et al. Preoperative Chemoradiotherapy for Esophageal or Junctional Cancer. *N Engl J Med* (2012) 366(22):2074–84. doi: 10.1056/NEJMoa1112088
3. Yang H, Liu H, Chen Y, Zhu C, Fang W, Yu Z, et al. Neoadjuvant Chemoradiotherapy Followed by Surgery Versus Surgery Alone for Locally Advanced Squamous Cell Carcinoma of the Esophagus (NEOCRTEC5010): A Phase III Multicenter, Randomized, Open-Label Clinical Trial. *J Clin Oncol* (2018) 36(27):2796–803. doi: 10.1200/jco.2018.79.1483
4. Baba Y, Nomoto D, Okadome K, Ishimoto T, Iwatsuki M, Miyamoto Y, et al. Tumor Immune Microenvironment and Immune Checkpoint Inhibitors in Esophageal Squamous Cell Carcinoma. *Cancer Sci* (2020) 111(9):3132–41. doi: 10.1111/cas.14541
5. Akin Telli T, Bregni G, Camera S, Deleporte A, Hendlisz A, Sclafani F. PD-1 and PD-L1 Inhibitors in Oesophago-Gastric Cancers. *Cancer Lett* (2020) 469:142–50. doi: 10.1016/j.canlet.2019.10.036
6. Iwahashi M, Katsuda M, Nakamori M, Nakamura M, Naka T, Ojima T, et al. Vaccination With Peptides Derived From Cancer-Testis Antigens in Combination With CpG-7909 Elicits Strong Specific CD8+ T Cell Response in Patients With Metastatic Esophageal Squamous Cell Carcinoma. *Cancer Sci* (2010) 101(12):2510–7. doi: 10.1111/j.1349-7006.2010.01732.x
7. Yamamoto TN, Kishton RJ, Restifo NP. Developing Neoantigen-Targeted T Cell-Based Treatments for Solid Tumors. *Nat Med* (2019) 25(10):1488–99. doi: 10.1038/s41591-019-0596-y
8. Larkin J, Chiarion-Sileni V, Gonzalez R, Grob JJ, Rutkowski P, Lao CD, et al. Five-Year Survival With Combined Nivolumab and Ipilimumab in Advanced Melanoma. *N Engl J Med* (2019) 381(16):1535–46. doi: 10.1056/NEJMoa1910836
9. Chesney J, Puzanov I, Collichio F, Singh P, Milhem MM, Glaspy J, et al. Randomized, Open-Label Phase II Study Evaluating the Efficacy and Safety of

Talimogene Laherparepvec in Combination With Ipilimumab Versus Ipilimumab Alone in Patients With Advanced, Unresectable Melanoma. *J Clin Oncol* (2018) 36(17):1658–67. doi: 10.1200/jco.2017.73.7379
10. Ribas A, Hamid O, Daud A, Hodi FS, Wolchok JD, Kefford R, et al. Association of Pembrolizumab With Tumor Response and Survival Among Patients With Advanced Melanoma. *Jama* (2016) 315(15):1600–9. doi: 10.1001/jama.2016.4059
11. Hellmann MD, Paz-Ares L, Bernabe Caro R, Zurawski B, Kim SW, Carcereny Costa E, et al. Nivolumab Plus Ipilimumab in Advanced Non-Small-Cell Lung Cancer. *N Engl J Med* (2019) 381(21):2020–31. doi: 10.1056/NEJMoa1910231
12. Borghaei H, Paz-Ares L, Horn L, Spigel DR, Steins M, Ready NE, et al. Nivolumab Versus Docetaxel in Advanced Nonsquamous Non-Small-Cell Lung Cancer. *N Engl J Med* (2015) 373(17):1627–39. doi: 10.1056/NEJMoa1507643
13. Kojima T, Shah MA, Muro K, Francois E, Adenis A, Hsu CH, et al. Randomized Phase III KEYNOTE-181 Study of Pembrolizumab Versus Chemotherapy in Advanced Esophageal Cancer. *J Clin Oncol* (2020) 38 (35):4138–48. doi: 10.1200/jco.20.01888
14. Huang J, Xu J, Chen Y, Zhuang W, Zhang Y, Chen Z, et al. Camrelizumab Versus Investigator's Choice of Chemotherapy as Second-Line Therapy for Advanced or Metastatic Oesophageal Squamous Cell Carcinoma (ESCORT): A Multicentre, Randomised, Open-Label, Phase 3 Study. *Lancet Oncol* (2020) 21(6):832–42. doi: 10.1016/s1470-2045(20)30110-8
15. Kato K, Cho BC, Takahashi M, Okada M, Lin CY, Chin K, et al. Nivolumab Versus Chemotherapy in Patients With Advanced Oesophageal Squamous Cell Carcinoma Refractory or Intolerant to Previous Chemotherapy (ATTRACTION-3): A Multicentre, Randomised, Open-Label, Phase 3 Trial. *Lancet Oncol* (2019) 20(11):1506–17. doi: 10.1016/s1470-2045(19)30626-6
16. Jones JO, Smyth EC. Gastroesophageal Cancer: Navigating the Immune and Genetic Terrain to Improve Clinical Outcomes. *Cancer Treat Rev* (2020) 84:101950. doi: 10.1016/j.ctrv.2019.101950
17. Ku GY. The Current Status of Immunotherapies in Esophagogastric Cancer. *Surg Oncol Clin N Am* (2017) 26(2):277–92. doi: 10.1016/j.soc.2016.10.012
18. Kelly RJ. The Emerging Role of Immunotherapy for Esophageal Cancer. *Curr Opin Gastroenterol* (2019) 35(4):337–43. doi: 10.1097/mog.0000000000000542
19. Moher D, Liberati A, Tetzlaff J, Altman DG. Preferred Reporting Items for Systematic Reviews and Meta-Analyses: The PRISMA Statement. *Bmj* (2009) 339:b2535. doi: 10.1136/bmj.b2535
20. Higgins JP, Altman DG, Gøtzsche PC, Jüni P, Moher D, Oxman AD, et al. The Cochrane Collaboration's Tool for Assessing Risk of Bias in Randomised Trials. *Bmj* (2011) 343:d5928. doi: 10.1136/bmj.d5928
21. Kato K, Doki Y, Ura T, Hamamoto Y, Kojima T, Tsushima T, et al. Long-Term Efficacy and Predictive Correlates of Response to Nivolumab in Japanese Patients With Esophageal Cancer. *Cancer Sci* (2020) 111(5):1676–84. doi: 10.1111/cas.14380
22. Kudo T, Hamamoto Y, Kato K, Ura T, Kojima T, Tsushima T, et al. Nivolumab Treatment for Oesophageal Squamous-Cell Carcinoma: An Open-Label, Multicentre, Phase 2 Trial. *Lancet Oncol* (2017) 18(5):631–9. doi: 10.1016/s1470-2045(17)30181-x
23. Zhang B, Qi L, Wang X, Xu J, Liu Y, Mu L, et al. Phase II Clinical Trial Using Camrelizumab Combined With Apatinib and Chemotherapy as the First-Line Treatment of Advanced Esophageal Squamous Cell Carcinoma. *Cancer Commun (Lond)* (2020) 40(12):711–20. doi: 10.1002/cac2.12119
24. Shah MA, Kojima T, Hochhauser D, Enzinger P, Raimbourg J, Hollebecque A, et al. Efficacy and Safety of Pembrolizumab for Heavily Pretreated Patients With Advanced, Metastatic Adenocarcinoma or Squamous Cell Carcinoma of the Esophagus: The Phase 2 KEYNOTE-180 Study. *JAMA Oncol* (2019) 5 (4):546–50. doi: 10.1001/jamaoncol.2018.5441
25. Huang J, Xu B, Mo H, Zhang W, Chen X, Wu D, et al. Safety, Activity, and Biomarkers of SHR-1210, an Anti-PD-1 Antibody, for Patients With Advanced Esophageal Carcinoma. *Clin Cancer Res* (2018) 24(6):1296–304. doi: 10.1158/1078-0432.Ccr-17-2439
26. Doi T, Piha-Paul SA, Jalal SI, Saraf S, Lunceford J, Koshiji M, et al. Safety and Antitumor Activity of the Anti-Programmed Death-1 Antibody Pembrolizumab in Patients With Advanced Esophageal Carcinoma. *J Clin Oncol* (2018) 36(1):61–7. doi: 10.1200/jco.2017.74.9846
27. Tsao MS, Kerr KM, Kockx M, Beasley MB, Borczuk AC, Botling J, et al. PD-L1 Immunohistochemistry Comparability Study in Real-Life Clinical Samples: Results of Blueprint Phase 2 Project. *J Thorac Oncol* (2018) 13(9):1302–11. doi: 10.1016/j.jtho.2018.05.013
28. Ma C, Patel K, Singhi AD, Ren B, Zhu B, Shaikh F, et al. Programmed Death-Ligand 1 Expression Is Common in Gastric Cancer Associated With Epstein-Barr Virus or Microsatellite Instability. *Am J Surg Pathol* (2016) 40(11):1496–506. doi: 10.1097/pas.0000000000000698
29. Bockorny B, Pectasides E. The Emerging Role of Immunotherapy in Gastric and Esophageal Adenocarcinoma. *Future Oncol* (2016) 12(15):1833–46. doi: 10.2217/fon-2016-0103
30. Kato K SJ, Shah MA. Pembrolizumab Plus Chemotherapy Versus Chemotherapy as First-Line Therapy in Patients With Advanced Esophageal Cancer: The Phase 3 KEYNOTE-590 Study. *Ann Oncol* (2020) 31(Suppl 4):S1192–S3. doi: 10.1016/j.annonc.2020.08.2298
31. Kelly RJ AJ, Kuzdzal J. Adjuvant Nivolumab in Resected Esophageal or Gastroesophageal Junction Cancer (EC/GEJC) Following Neoadjuvant Chemoradiation Therapy (CRT): First Results of the CheckMate 577 Study. *Ann Oncol* (2020) 31(Suppl 4):S1193– S4. doi: 10.1016/j.annonc.2020.08.2299

Conflict of Interest: The authors declare that the research was conducted in the absence of any commercial or financial relationships that could be construed as a potential conflict of interest.

Publisher's Note: All claims expressed in this article are solely those of the authors and do not necessarily represent those of their affiliated organizations, or those of the publisher, the editors and the reviewers. Any product that may be evaluated in this article, or claim that may be made by its manufacturer, is not guaranteed or endorsed by the publisher.

frontiers in Oncology

ORIGINAL RESEARCH
published: 18 February 2022
doi: 10.3389/fonc.2021.798415

A Composite Biomarker of Derived Neutrophil–Lymphocyte Ratio and Platelet–Lymphocyte Ratio Correlates With Outcomes in Advanced Gastric Cancer Patients Treated With Anti-PD-1 Antibodies

Yuting Pan[1,2], *Haiyan Si*[2], *Guochao Deng*[1,2], *Shiyun Chen*[1,2], *Nan Zhang*[1,2], *Qian Zhou*[1,2], *ZhiKuan Wang*[2*] and *Guanghai Dai*[2*]

[1] Chinese People's Liberation Army Medical School, Beijing, China, [2] Medical Oncology Department, The First Medical Center, Chinese People's Liberation Army General Hospital, Beijing, China

OPEN ACCESS

Edited by:
Sripathi Sureban,
University of Oklahoma Health Sciences Center, United States

Reviewed by:
Simone Scagnoli,
Sapienza University of Rome, Italy
Antonella Argentiero,
National Cancer Institute Foundation (IRCCS), Italy

***Correspondence:**
ZhiKuan Wang
wangzkme@sohu.com
Guanghai Dai
daigh301@vip.sina.com

Specialty section:
This article was submitted to Gastrointestinal Cancers: Gastric & Esophageal Cancers, a section of the journal Frontiers in Oncology

Received: 20 October 2021
Accepted: 29 December 2021
Published: 18 February 2022

Citation:
Pan Y, Si H, Deng G, Chen S, Zhang N, Zhou Q, Wang Z and Dai G (2022) A Composite Biomarker of Derived Neutrophil–Lymphocyte Ratio and Platelet–Lymphocyte Ratio Correlates With Outcomes in Advanced Gastric Cancer Patients Treated With Anti-PD-1 Antibodies. Front. Oncol. 11:798415. doi: 10.3389/fonc.2021.798415

Background: The highly heterogeneous characteristics of GC may limit the accuracy of a single biomarker for screening populations benefiting from immunotherapy. However, the combination of multiple indicators can provide more directed information for the detection of potential immune benefit subgroups. At present, there are no recognized complex indexes to identify advanced GC (AGC) in patients who likely benefited from immunotherapy. The objective of this research is to explore whether the composite biomarker of derived neutrophil–lymphocyte ratio (dNLR) and platelet–lymphocyte ratio (PLR) can be used as a reliable prognostic factor for the survival of AGC patients receiving immunotherapy.

Methods: From December 2014 to May 2021, a total 238 AGC patients at a single Center were included in this retrospective cohort research study. The cutoff value of dNLR was obtained by the ROC curves to predict the disease progression rate at the 8th month and the cutoff value of PLR was estimated by the median value. The cutoff values of dNLR and PLR were 1.95 and 163.63, respectively. The high levels of dNLR (≥1.95) and PLR (≥163.63) were considered to be risk factors. Based on these two risk factors, patients were categorized into 3 groups: the risk factor number for the "good" group was 0, that for the "intermediate" group was 1, and that for the "poor" group was 2. The subjects were divided into two groups: dNLR/PLR-good and dNLR/PLR-intermediate/poor.

Results: Of the 238 patients, the median overall survival (mOS) and progression-free survival (mPFS) were 12.5 and 4.7 months, respectively. Multivariate analysis revealed that the good dNLR/PLR group was independently associated with better prognosis. The intermediate/poor dNLR/PLR group was independently correlated with an over 1.4 times greater risk of disease progression (4.1 months vs. 5.5 months; $p = 0.016$) and an over 1.54 times greater risk of death (11.1 months vs. 26.3 months; $p = 0.033$) than the good

dNLR/PLR group. However, no clear differences in the disease control rate (DCR) and overall response rate (ORR) were observed between the intermediate/poor dNLR/PLR group and the good dNLR/PLR group (51.5% vs. 56.3%, 26.3% vs. 29.6%; $p = 0.494$, $p = 0.609$).

Conclusion: Our study firstly verifies that the composite biomarker of dNLR and PLR is an independent prognostic factor affecting survival of advanced AGC patients receiving immunotherapy. It may be difficult for patients with the intermediate/poor dNLR/PLR group to benefit from immunotherapy.

Keywords: immunotherapy, advanced gastric cancer, dNLR, PLR, efficacy, prognosis

INTRODUCTION

Gastric cancer (GC) is one type of very common gastrointestinal tumors around the world. The incidence rate of GC ranks fifth globally and second domestically in China (1). The progress of GC treatment is relatively slow, and traditional chemotherapy, such as surgery, chemotherapy, and targeted therapy, is therefore limited. The emergence of immunotherapy brings a new option for GC; nevertheless, its application in GC is still difficult. Researchers have been trying both back line and front line, as well as single-drug and different combinations. The "ATTRACTION-2" study confirms the efficacy of nivolumab for the back line of GC (2, 3). The results of the "KEYNOTE-061" study were negative, and pembrolizumab failed in the second-line chemotherapy challenge (4–6). The "CheckMate 649" study explored whether the nivolumab-based first-line immunotherapy was suitable for advanced GC (AGC) (7). Moehler et al. found that patients treated with a combination of nivolumab and chemotherapy showed consistent overall survival (OS) benefits in the whole population and the Chinese subgroup, regardless of the expression status of programmed death ligand-1 (*PD-L1*) (8). The first result of the "KEYNOTE-811" study showed that *HER2*-positive metastatic gastric or gastroesophageal junction cancer could benefit from using the combination of pembrolizumab, trastuzumab, and chemotherapy (9). However, the current evaluation of biomarkers for immunotherapy has been limited. There is a lack of effective biomarkers that can be used as prognostic factors for AGC-treated patients with immune checkpoint inhibitors (ICIs). In recent years, the expression of *PD-L1* and microsatellite steady-state (MSI) in AGC patients can be effectively assessed for the efficacy of immunotherapy (10, 11).

Peripheral inflammatory blood complex index such as neutrophil–lymphocyte ratio (NLR), platelet–lymphocyte ratio (PLR), and hemoglobin (Hb) levels have demonstrated a promising and suitable biomarker prognostic for GC (12–15). However, the highly heterogeneous characteristics of GC may limit the accuracy of a single biomarker for screening populations benefiting from immunotherapy. In contrast, the combination of multiple indicators can provide more targeted information for the detection of potential immune benefit subgroups. Dharmapuri S et al. established a statistical model by NLR/PLR groups and found that the high-NLR/ low-PLR group in advanced hepatocellular carcinoma patients treated with anti–PD-1 therapy has shorter OS and progression free survival (PFS) than the low-NLR/ low-PLR group (16). However, as a biomarker of poor prognosis in AGC patients undergoing immunotherapy, the role of NLR is quite well defined in some studies (17–19). Furthermore, in May 2021, a study conducted by Lim et al. showed that non-small-cell lung cancer (NSCLC) patients with a high level of derived neutrophil–lymphocyte ratio (dNLR) baseline value were associated with poor outcomes, when they were treated with ICIs (20).

Our research found that patients with an elevated dNLR value (≥ the best cutoff value) were associated with shorter OS and PFS too. However, patients with high levels of PLR (≥ the median value) were only associated with shorter OS, but not PFS. Thus, we combined dNLR and PLR to stratify risk factors. The high levels of dNLR (≥1.95) and PLR (≥163.63) were considered to be risk factors. Based on these two risk factors, patients were categorized into 3 groups: the risk factor number for the "good" group was 0, that for the "intermediate" group was 1, and that for the "poor" group was 2. The subjects were divided into two groups: dNLR/PLR-good and dNLR/PLR-intermediate/poor. We then began to evaluate the differences in prognosis and survival of AGC patients after immunotherapy between the good and the intermediate/poor groups.

Abbreviations: GC, Gastric cancer, AGC, advanced gastric cancer; ICIs, immune checkpoint inhibitors; OS, overall survival; PD-L1, programmed death ligand-1; MSI, microsatellite steady-state; NLR, neutrophil–lymphocyte ratio; dNLR, derived neutrophil-to-lymphocyte; PLR, platelet–lymphocyte ratio; Hb, hemoglobin; PFS, progression-free survival; ROC, receiver operating characteristic; ECOG PS, Eastern Cooperative Oncology Group performance status scores; ANC, absolute neutrophil count; ALC, absolute lymphocyte count; PLT, platelet count; DCR, disease control rate; CR, complete response; SD, stable disease; PR, partial response; ORR, overall response rate; PD, progressive disease; LDH, lactate dehydrogenase.

MATERIALS AND METHODS

Study Population

From December 2014 to May 2021, all patients involved were diagnosed with GC at stage IV and received ICI treatment in the Senior Department of Oncology at Chinese PLA General

Hospital. We set the inclusion criteria as follows: (1) patients detected with measurable lesions, (2) patients who underwent blood routine and blood biochemistry tests within 1 week before ICI administration, and (3) patients who have received at least two rounds of ICI treatment continuously. Patients failing to provide imaging data for comparing the efficacy of ICIs before and after treatment were excluded. As a result, a total of 238 patients were considered eligible for this cohort study. Clinical parameters of those AGC patients from their medical records were collected, including sex, age, Eastern Cooperative Oncology Group performance status scores (ECOG PS), smoking history, smoking exposure, history of diabetes, tumor type, the status of *HER-2* expression, the dose of ICIs, the status of bone metastasis, the status of liver metastasis, response to line before immunotherapy, the status of pleural fluid, the status of ascites, the number of metastatic sites, lines of treatment with ICIs, ICIs agent, and immunotherapy scheme. Meanwhile, blood parameters were analyzed routinely, including absolute neutrophil count (ANC), absolute lymphocyte count (ALC), white blood count cells (WBC), and platelet count (PLT) 7 days before immunotherapy implementing to obtain dNLR and PLR values.

Treatment Regimens

Five treatment methods were used in this research study: (1) ICI monotherapy, (2) ICIs combined with chemotherapy, (3) ICIs combined with anti-angiogenic therapy, (4) ICIs combined with DNA-derived humanized monoclonal antibodies (trastuzumab) and chemotherapy, and (5) ICIs combined with chemotherapy and anti-angiogenic therapy. The types and doses of ICIs were as follows: (1) Sintilimab was injected intravenously 200 mg once every 3 weeks. (2) Toripalimab was injected intravenously 240 mg once every 3 weeks. (3) The recommended dose of pembrolizumab injection for intravenous infusion was a dose of 3 mg/kg, administered once every 3 weeks. (4) The recommended dose of nivolumab injection for intravenous infusion was a dose of 2 mg/kg, administered once every 2 weeks. The first imaging evaluation of nivolumab was carried out 2–4 weeks after the 3rd intravenous injection; nevertheless, the evaluation of toripalimab, sintilimab, and pembrolizumab was carried out 3–5 weeks after the 2nd intravenous injection. The trastuzumab course was administered for 3 weeks. For the first course, the dose was 8 mg/kg, applied by intravenous injection for 90 min. Starting from the 2nd course, the dose was lowered to 6 mg/kg. For the infusion time, if the patients tolerate trastuzumab well in the first course, the 2nd course was applied by intravenous injection for 30 min. course. Anti-angiogenic drugs involved were apatinib (850 mg, orally administrated 30 min after a meal, once a day) and bevacizumab (5 mg/kg body weight, once every 2 weeks; or 7.5 mg/kg body weight, once every 3 weeks). The chemotherapy regimens include (1) XELOX regimen: capecitabine (1,000 mg/m^2) was used 2 times a day orally after breakfast and dinner for 14 consecutive days with 7 days of rest as a treatment cycle. Oxaliplatin (130 mg/m^2) was added on the first day of each cycle by intravenous injection. (2) SOX regimen: tiggio (40–60 mg) was used 2 times a day orally after breakfast and dinner for 14 consecutive days with 7 days of rest as a treatment cycle. Oxaliplatin (130 mg/m^2) was added on the first day of each cycle by intravenous injection. (3) DCF regimen: docetaxel (75 mg/m^2), cisplatin (75 mg/m^2), and fluorouracil (750 mg/m^2) were applied by intravenous injection. On the first day of every course, each course lasted 21 days. (4) The combined regimen of irinotecan and oxaliplatin: irinotecan (180 mg/m^2) and oxaliplatin (130 mg/m^2) were applied by intravenous injection. On the first day of every course, each course lasted 14 days. (5) The combined regimen of irinotecan and raltitrexed: irinotecan (180 mg/m^2) and raltitrexed (3 mg/m^2) were applied by intravenous injection. On the first day of every course, each course lasted 14 days. (6) Others. The choice of the above regimens was based on the patient's pathological stage and general health conditions.

Assessment

For effectiveness evaluation, the disease control rate (DCR) and the overall response rate (ORR) is termed as the percentage of patients with complete response (CR), partial response (PR), and stable disease (SD) and the percentage of patients with CR and PR, respectively. For prognosis analysis, OS and PFS are counted from the time of the immunotherapy beginning to death and the time between the onset of ICIs and the progression or death of the tumor, respectively.

dNLR, PLR, and Statistical Models by dNLR/PLR Groups

We analyzed the value of PLR (platelet/lymphocyte ratio) and NLR (neutrophil/lymphocyte ratio) 7 days before immunotherapy was implemented. With dNLR before treatment as the test variable, and the disease progression rate at the 8th month as the state variable, the receiver operating characteristic (ROC) curve of immunotherapy effect and dNLR level before treatment was drawn. The area under the ROC curve was 0.584, which indicated a statistically significant difference (p = 0.037). The best cutoff value of dNLR was 1.95, and its corresponding sensitivity and specificity were 61.1% and 60.5%, respectively (**Figure 1**). The cutoff value of PLR was estimated by the median value. The high levels of dNLR (≥ the best cutoff value) and PLR (≥ the median value) were considered to be risk factors. Based on these two risk factors, patients were categorized into 3 groups: the risk factor number for the "good" group was 0, and that for the "poor" group was 1 or 2. The risk factor number for the "good" group was 0, that for the "intermediate" group was 1, and that for the "poor" group was 2. Due to the similar efficacy and survival outcomes of patients in the intermediate and good groups (**Supplementary Table 1** and **Supplementary Figure 1**), we integrated the intermediate group into the poor group, forming the intermediate/poor group.

Statistical Analysis

SPSS 26.0 software was used to perform all statistical analyses. Data were summarized as the median values for non-normally distributed continuous variables. Based on the values of α (α = 0.05) and β (β = 0.2), the expected median OS (mOS) of the good group and the intermediate/poor group, we evaluated the

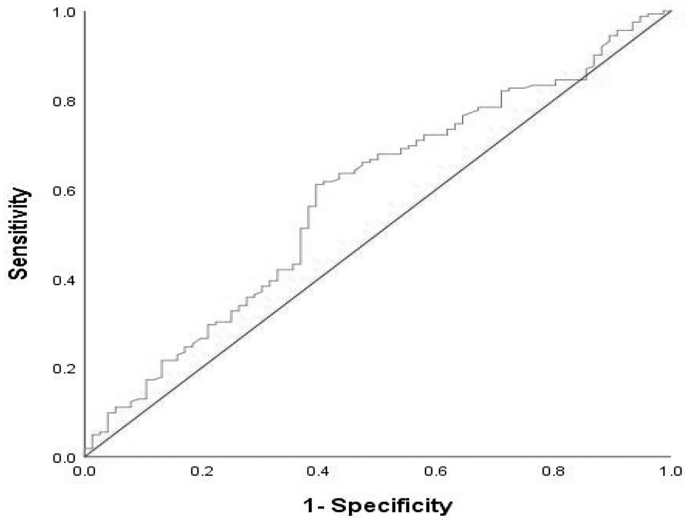

FIGURE 1 | ROC curve of pretreatment dNLR in assessment of the disease progression rate at the 8th month. Sensitivity:61.1%; Specificity:60.5%; AUC:0.584; $p = 0.037$. dNLR, derived neutrophil–lymphocyte ratio; ROC, receive operating characteristic; AUC, areaunder the curve.

number of the sample size of our retrospective cohort study. the expected mOS of the good group and the intermediate/poor group were 17 and 11 months, respectively. Data were reported as percentages and counts for categorical variables. The ROC curves were applied to clarify the best cutoff value of dNLR. χ^2 or Fisher's exact test was carried out to evaluate the relationship between clinical response and dNLR/PLR groups of AGC patients. The survival curve was depicted by Kaplan–Meier analysis. Logistic regression models and Cox proportional hazard were applied to assess the prognostic values of dNLR/PLR groups for DCR and survival, respectively. *p*-values less than 0.05 ($p < 0.05$) were considered statistically significant.

RESULTS

Baseline Characteristics

A total of 238 AGC patients receiving ICIs were reviewed in the retrospective cohort study. The clinical features of patients are provided below (**Table 1**). The median age was 58 years. Among these patients, 121 patients were elders (≥58 years); 188 patients were male, 63 patients had Cardia, 99 had body/fundus, and 76 patients had pylorus cancer; 223 patients had ECOG PS scores of 0–1; 33 patients had positive *HER-2* expression, 163 patients had a negative expression, and 42 patients were untested; 118 patients had poor tumor differentiation, 101 patients had moderate tumor differentiation, 4 patients had good tumor differentiation, and tumor differentiation was unknown for 15 patients; 12 patients had pleural fluid; 54 patients had ascites; 22 patients had bone metastases before immunotherapy. After grouping, 71 patients were in the good dNLR/PLR group and 167 patients were in the intermediate/poor dNLR/PLR group.

Treatment Characteristics

Of 238 patients, 158 (66.8%) patients had previously progressed before using ICIs; 84 (35.3%) patients received nivolumab, 30 (12.6%) patients were treated with pembrolizumab, and 124 (52.1%) patients received other immunotherapy drugs; 130 (54.6%) patients used the 1st line ICIs and 108 (45.4%) patients used ICIs after the 1st line; 186 (78.2%) patients were treated with ICIs combined with other therapies; 52 (21.8%) patients were treated with ICI monotherapy (**Table 1**).

A Composite Biomarker of dNLR and PLR for Response to ICIs

The optimal efficacy of all AGC patients was evaluated in the study, and the results were as follows: 112 (47.1%) patients had progressive disease (PD), 4 (1.7%) patients had CR, 62 (26.1%) patients had PR, and 60 (25.2%) patients had SD. The ORR was 27.7% and DCR was 52.9% (**Table 2**). No clear differences in DCR and ORR were observed between the intermediate/poor dNLR/PLR group and the good dNLR/PLR group (51.5% vs. 56.3%, 26.3% vs. 29.6%; $p = 0.494$, $p = 0.609$) (**Table 2**).

dNLR and PLR for Survival of AGC Patients

The cutoff value of dNLR and PLR were 1.95 and 163.63, respectively. For patients with an elevated dNLR value (≥1.95) and with a lower dNLR value (<1.95), the mPFS was 3.6 (95% CI, 2.855–4.345) and 6.2 (95% CI, 4.488–7.912) months, respectively, and the mOS was 9 (95% CI, 6.032–11.968) and 26 (95% CI, 14.286–37.714) months, respectively. Patients with an elevated dNLR value were associated with an over 1.8 times greater risk of disease progression (HR = 1.807; 95% CI, 1.356–2.407; $p < 0.001$) and an over 2.1 times greater risk of death (HR = 2.161; 95% CI, 1.542–3.028; $p < 0.001$) than those with a

TABLE 1 | General data and clinical features.

Characteristics	Number of Patients (%)		
	Overall (*n* = 238)	The good group (*n* = 71)	The intermediate/poor group (*n* = 167)
Median age (range), years	58 (18–86)	58 (27–82)	58 (18–86)
Sex			
Female	62 (26.1)	21 (29.6)	41 (24.6)
Male	176 (73.9)	50 (70.4)	126 (75.4)
Smoking history			
Yes	88 (37)	26 (36.6)	62 (37.1)
No	150 (63)	45 (63.4)	105 (62.9)
Smoking exposure			
>30 packs per year	44 (18.5)	14 (19.7)	30 (18.0)
≤30 packs per year	194 (81.5)	57 (80.3)	137 (82.0)
Drinking history			
Yes	85 (35.7)	26 (36.6)	59 (35.3)
No	153 (64.3)	45 (63.4)	108 (64.7)
Tumor location			
Cardia	60 (25.2)	18 (25.4)	42 (25.1)
Body/Fundus	89 (37.4)	23 (32.4)	66 (39.5)
Pylorus	86 (36.1)	30 (42.3)	56 (33.5)
Unknown	3 (1.3)	0 (0)	3 (1.8)
Response to line before immunotherapy			
PD	159 (66.8)	40 (56.3)	119 (71.3)
Others	79 (33.2)	31 (43.7)	48 (28.7)
Liver metastasis			
Present	100 (42)	30 (42.3)	70 (41.9)
Absent	138 (58)	41 (57.7)	97 (58.1)
Pleural fluid			
Present	12 (5.0)	3 (4.2)	9 (5.4)
Absent	226(95)	68 (95.8)	158 (94.6)
Ascites			
Present	54 (22.7)	8 (11.3)	46 (27.5)
Absent	184 (77.3)	63 (88.7)	121 (72.5)
Bone metastasis			
Present	22 (9.2)	8 (11.3)	14(8.4)
Absent	216 (90.8)	63 (88.7)	153(91.6)
Number of metastatic sites			
≥3	58 (24.4)	11 (15.5)	47 (28.1)
<3	180 (75.6)	60 (84.5)	120 (71.9)
Dosage of immunotherapy			
≥200 mg	147 (61.8)	49 (69.0)	98 (58.7)
<200 mg	91 (38.2)	22 (31.0)	69 (41.3)
Tumor differentiation			
Poorly	176 (73.9)	50 (70.4)	126 (75.4)
Moderately	42 (17.6)	14 (19.7)	28 (16.8)
Well	4 (1.7)	3 (4.2)	1 (0.6)
Unknown	16 (6.7)	4 (5.6)	12 (7.2)
Lines of immunotherapy			
≥2	130 (54.6)	33 (46.5)	97 (58.1)
<2	108 (45.4)	38 (53.5)	70 (41.9)
ECOG PS			
≥2	15 (6.3)	1 (1.4)	14 (8.4)
0-1	223 (93.7)	70 (98.6)	153 (91.6)
PD-1 inhibition agent			
Nivolumab	84 (35.3)	25 (35.2)	59 (35.3)
Pembrolizumab	30 (12.6)	6 (8.5)	24 (14.4)
Others	124 (52.1)	40 (56.3)	84 (50.3)
Therapies			
ICIs monotherapy	52 (21.8%)	14 (19.7)	38 (22.8)
ICIs combined with other therapies	186 (78.2%)	57 (80.3)	129 (18.6)

PD, progressive disease; PD-1, programmed cell death-1; ECOG PS, Eastern Cooperative Oncology Group performance status scores; ICIs, immune checkpoint inhibitors.

lower dNLR value (**Table 3** and **Figures 2A, B**). For patients with an elevated PLR value (≥163.63) and with a lower PLR value (<163.63), the median PFS was 4.6 (95% CI, 3.549–6.251) and 4.9 (95% CI, 2.983–6.017) months, respectively, and the mOS was 10.4 (95% CI, 7.386–13.414) and 15.8 (95% CI, 4.400–27.200) months, respectively. Patients with an elevated PLR value were associated with an over 1.4 times greater risk of death than those with a lower PLR value (<163.63) (HR = 1.416; 95% CI, 1.026–

TABLE 2 | Relationship between the good group and the intermediate/poor group and response to ICIs treatment.

Best Overall Response	Number of Patients (%)			*p*-value
	Overall, *n* = 238	The good group, *n* =71	The intermediate/poor group, *n* = 167	
CR	4 (1.7)	2 (2.8)	2 (1.2)	0.388
PR	62 (26.1)	20 (28.2)	42 (25.1)	0.627
SD	60 (25.2)	18 (25.4)	42 (25.1)	0.974
PD	112 (47.1)	31 (43.7)	81 (48.5)	0.494
ORR	65 (27.3)	21 (29.6)	44 (26.3)	0.609
DCR	126 (52.9)	40 (56.3)	86 (51.5)	0.494

ICIs, immune checkpoint inhibitors; CR, complete response; PR, partial response; SD, stable disease; PD, progressive disease; DCR, disease control rate; ORR, overall response rate.

1.956; p = 0.033). However, no clear difference of PFS was observed between the two groups of patients (HR = 1.237; 95% CI, 0.936–1.636; p = 0.132) (**Table 3**; **Figures 2C, D**).

The Composite Biomarker of dNLR and PLR for PFS of AGC Patients

Among 238 AGC patients, 203 (85.3%) patients had tumor progression by the last follow-up date of July 1, 2021. The median PFS was 4.7 (95% CI: 3.686–5.714) months (**Table 4**). After we checked for hazard proportionality, Cox regression multivariable approach was performed (**Supplementary Figure 2A**). Univariate and multivariate analyses of factors associated with PFS were shown in **Table 5**. In univariate analysis, patients with a good dNLR/PLR score, with fewer organ metastases (<3), with a good PS (ECOG PS of 0–1), with no ascites, or with no pleural fluid showed improved PFS. Moreover, patients who did not reach PD before immunotherapy, who were treated with the 1st line ICIs, who were treated with more doses of ICIs (≥200 mg), or who were treated with ICIs combined with other therapies were also associated with improved PFS. Patients in the good dNLR/PLR group were closely related to longer PFS, compared to those in the poor dNLR/PLR group (5.5 months vs. 4.1 months; p = 0.005) (**Figure 3A** and **Table 4**). Multivariate analysis revealed that patients in the intermediate/poor dNLR/PLR group were independently correlated with an over 1.4 times greater risk of disease progression (HR = 1.499; 95% CI, 1.078–2.086; p = 0.016) than those in the good dNLR/PLR group. In addition, we also noticed that patients in the intermediate dNLR/PLR group were closely related to longer PFS, compared to those in the poor dNLR/PLR group (5.8 months vs. 3.8 months). In other words, the intermediate group was correlated with an over 1.3 times greater risk of disease progression (HR = 1.394; 95% CI, 1.009–1.926; p = 0.044) than the poor group (**Table 6**). Multivariate analysis revealed that patients in the intermediate/poor dNLR/PLR group were independently correlated with an over 1.4 times greater risk disease progression (HR = 1.499; 95% CI, 1.078–2.086; p = 0.016) than those in the good NLR/PLR group. Moreover, patients who had fewer organ metastases (<3) and treated with the 1st line ICIs were independently associated with improved PFS. Additionally, patients who had more organ metastases (≥3) were independently correlated with an over 1.5 times greater risk of disease progression (HR = 1.581; 95% CI, 1.108–2.256; p = 0.011) than those that had fewer organ metastases (<3). Moreover, patients treated with ICIs after 1st line were independently correlated with an over 2.3 times greater risk of disease progression (HR = 2.355; 95% CI, 1.645–3.370; p < 0.001) than those treated with the 1st line ICIs.

The Composite Biomarker of dNLR and PLR for OS of AGC Patients

Among 238 AGC patients, 150 (63%) patients died by the last follow-up date of July 1, 2021. The mOS was 12.5 (95% CI, 10.278–14.722) months (**Table 4**). After we checked for hazard proportionality, Cox regression multivariable approach was performed (**Supplementary Figure 2B**). Univariate and multivariate analyses of factors associated with OS are shown in **Table 5**. In univariate analysis, patients with a good dNLR/PLR score, with fewer organ metastases (<3), with a good PS (ECOG PS of 0–1), with no bone metastasis, with no ascites, or with no pleural fluid showed improved OS. Moreover, patients who did not reach PD before immunotherapy, and those who were treated with ICIs combined with other therapies, who were treated with the 1st line ICIs, who were treated with more doses of ICIs (≥200 mg), or who treated with ICIs combined with other therapies were also associated with improved OS. Patients in the

TABLE 3 | Survival of dNLR and PLR.

Classification	PFS (months)			OS (months)		
	Median (95% CI)	HR (95% CI)	*p*	Median (95% CI)	HR (95% CI)	*p*
dNLR<1.95	6.2 (4.488–7.912)	1 [the reference]		26.0 (14.286–37.714)	1 [the reference]	
dNLR≥1.95	3.6 (2.855–4.345)	1.807 (1.356–2.407)	<0.001	9.0 (6.032–11.968)	2.161 (1.542–3.028)	<0.001
PLR<163.63	4.9 (2.983–6.017)	1 [the reference]		15.8 (4.400–27.200)	1 [the reference]	
PLR≥163.63	4.6 (3.549–6.251)	1.237 (0.936–1.636)	0.132	10.4 (7.386–13.414)	1.416 (1.026–1.956)	0.033

PFS, progression-free survival; OS, overall survival; HR, hazard ratio; dNLR, derived neutrophil-to-lymphocyte, PLR, platelet–lymphocyte ratio.

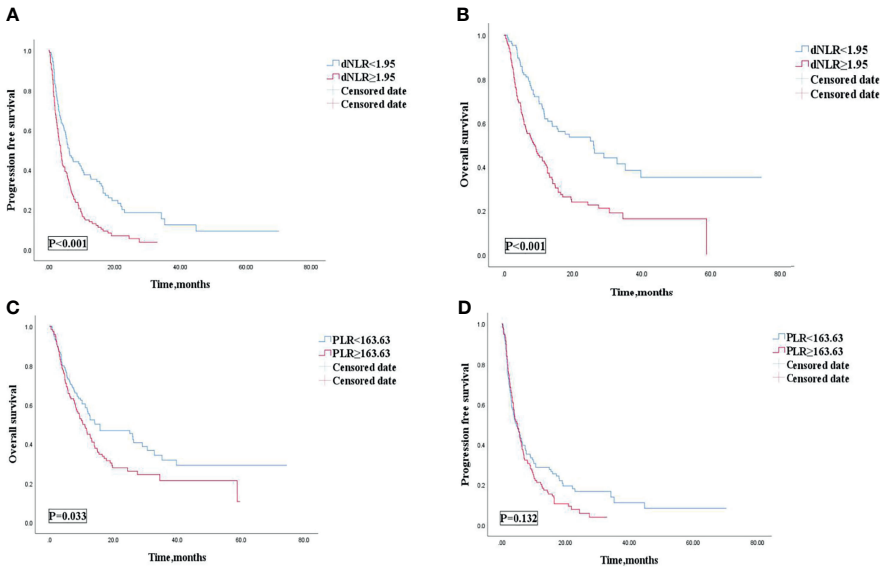

FIGURE 2 | PFS **(A)** and OS **(B)** of the dNLR of patients with AGC receiving ICIs cohort, and OS **(C)** and PFS **(D)** of the PLR of patients with AGC, receiving ICIs cohort. PFS, progression free survival; OS, overall survival; AGC, advanced gastric cancer; ICIs, immune checkpoint inhibitors; dNLR, derived neutrophil-to-lymphocyte; PLR, platelet–lymphocyte ratio.

good dNLR/PLR group were closely related to longer OS, compared to those in the intermediate/poor dNLR/PLR group (26.3 months vs. 11.1 months; p = 0.001) (**Figure 3B** and **Table 4**). In addition, we also noticed that patients in the intermediate dNLR/PLR group were closely related to longer OS, compared to those in the poor dNLR/PLR group (12.1 months vs. 8.2 months). In other words, the intermediate group was correlated with an over 1.56 times greater risk of death (HR = 1.562; 95% CI, 1.083–2.253; p = 0.017) than the poor group (**Table 6**). Multivariate analysis revealed that patients in the intermediate/poor dNLR/PLR group were independently correlated with an over 1.54 times greater risk of death (HR = 1.540; 95% CI, 1.036–2.288; p = 0.033) than those in the good dNLR/PLR group. Moreover, patients with fewer organ metastases (<3) or with a good PS (ECOG PS of 0–1) were independently associated with improved OS. Furthermore, patients who were treated with the 1st line ICIs or who were treated with more doses of ICIs (≥200 mg) were also independently associated with improved OS. Firstly, patients who had more organ metastases (≥3) were independently correlated with an over 1.5 times greater risk of death (HR = 1.581; 95% CI, 1.108–2.256; p = 0.011) than those who had fewer organ metastases (<3). Moreover, patients who had a good PS (ECOG PS of 0–1) were independently correlated with an over 1.9 times greater risk of death (HR = 1.937; 95% CI, 1.075–3.489; p = 0.028) than those had a poor PS (ECOG PS of ≥2). Furthermore, patients treated with ICIs after 1st line were independently correlated with an over 2.3 times greater risk of death (HR = 2.355; 95% CI, 1.645–3.370; p < 0.001) than those treated with the 1st line ICIs. Patients treated with less doses of ICIs (<200 mg) were independently correlated with an over 1.6 times greater risk of death (HR = 1.625; 95% CI, 1.156–2.286; p = 0.005) than those treated with more doses of ICIs (≥200 mg).

Association of the Composite Biomarker of dNLR and PLR With Outcomes in Lines of Immunotherapy of 1 or a Large Number of Lines of Immunotherapy (≥2): Subgroup Analysis

Multivariate analysis revealed that patients treated with the 1st line ICIs were independently correlated with improved OS and PFS.

TABLE 4 | Efficacy and prognosis based on the good and the intermediate/poor groups.

dNLR combined with PLR score classification		Response rate		OS (months)		PFS (months)	
		DCR (n, %)	OR (95% CI)	Median	HR (95% CI)	Median	HR (95% CI)
Overall	(n = 238)	126 (52.9)		12.5 (10.278–14.722)		4.7 (3.686–5.714)	
The good group	(n = 71)	40 (56.3)	1 [the reference]	26.3 (18.895–33.705)	1 [the reference]	5.5 (3.787–7.213)	1 [the reference]
The intermediate/poor group	(n = 167)	86 (51.5)	0.823 (0.471–1.439)	11.1 (8.823–13.377)	1.909 (1.299–2.805)	4.1 (2.961–5.239)	1.582 (1.147–2.181)
p-value		0.494		0.001		0.005	

PFS, progression-free survival; OS, overall survival; HR, hazard ratio; DCR, disease control rate; OR, odds ratio.

TABLE 5 | Univariate and multivariate analyses of factors associated with PFS and OS.

Patient Characteristics	Univariate Analysis		Multivariate Analysis	
PFS	**HR (95% CI)**	***p***	**HR (95% CI)**	***p***
Lines of immunotherapy				
<2	1 [the reference]	<0.001	1 [the reference]	<0.00
≥2	2.402 (1.798–3.208)		2.387 (1.783–3.196)	1
Pleural fluid				
Absent	1 [the reference]	0.017	1 [the reference]	0.055
Present	2.062 (1.140–3.727)		1.792 (0.987–3.252)	
Ascites				
Absent	1 [the reference]	0.012	1 [the reference]	0.674
Present	1.511 (1.094–2.087)		1.081 (0.753–1.550)	
ECOG PS				
0–1	1 [the reference]	0.002	1 [the reference]	0.376
≥ 2	2.316 (1.363–3.936)		1.310 (0.721–2.379)	
Dosage of immunotherapy, median				
<200 mg	1 [the reference]	0.026	1 [the reference]	0.557
≥200 mg	1.375 (1.040–1.817)		1.098 (0.804–1.499)	
Response to line before immunotherapy				
Others	1 [the reference]	0.007	1 [the reference]	0.857
PD	1.518 (1.120–2.058)		0.968 (0.684–1.372)	
Number of metastatic sites				
<3	1 [the reference]	0.020	1 [the reference]	0.027
≥3	1.458 (1.061–2.003)		1.439 (1.042–1.987)	
ICIs combined with other therapies				
Yes	1 [the reference]	0.024	1 [the reference]	0.541
No	1.495 (1.050–2.000)		1.116 (0.785–1.584)	
dNLR combined with PLR score				
The good group	1 [the reference]	0.005	1 [the reference]	0.016
The intermediate/poor group	1.582 (1.147–2.181)		1.499 (1.078–2.086)	
Patient Characteristics	**Univariate Analysis**		**Multivariate Analysis**	
OS	**HR (95% CI)**	***p***	**HR (95% CI)**	***p***
ECOG PS				
0–1	1 [the reference]	<0.001	1 [the reference]	0.028
≥ 2	4.251 (2.471–7.312)		1.937 (1.075–3.489)	
Lines of immunotherapy				
<2	1 [the reference]	<0.001	1 [the reference]	<0.00
≥2	2.668(1.881–3.785)		2.355 (1.645–3.370)	1
Bone metastasis				
Absent	1 [the reference]	0.019	1 [the reference]	0.186
Present	1.782(1.100–2.887)		1.453 (0.835–2.527)	
Ascites				
Absent	1 [the reference]	0.031	1 [the reference]	0.785
Present	1.485 (1.037–2.125)		1.056 (0.715–1.560)	
Pleural fluid				
Absent	1 [the reference]	0.035	1 [the reference]	0.315
Present	2.002(1.050–3.815)		1.445 (0.705–2.961)	
Number of metastatic sites				
<3	1 [the reference]	0.002	1 [the reference]	0.011
≥3	1.765 (1.242–2.507)		1.581 (1.108–2.256)	
Response to line before immunotherapy				
Others	1 [the reference]	0.001	1 [the reference]	0.404
PD	1.896 (1.302–2.760)		1.204 (0.779–1.862)	
Dosage of immunotherapy, median (range)				
≥200 mg	1 [the reference]	<0.001	1 [the reference]	0.005
<200 mg	1.984 (1.440–2.734)		1.625 (1.156–2.286)	
ICIs combined with other therapies				
Yes	1 [the reference]	0.001	1 [the reference]	0.760
No	1.825 (1.280–2.603)		1.064 (0.713–1.588)	
dNLR combined with PLR score				
The good group	1 [the reference]	0.001	1 [the reference]	0.033
The intermediate/poor group	1.909 (1.299–2.805)		1.540 (1.036–2.288)	

PFS, progression-free survival; OS, overall survival; AGC, advanced gastric cancer; ICIs, immune checkpoint inhibitors; HR, hazard ratio; dNLR, derived neutrophil-to-lymphocyte, PLR, platelet–lymphocyte ratio; PD, progressive disease; ECOG PS, Eastern Cooperative Oncology Group performance status scores.

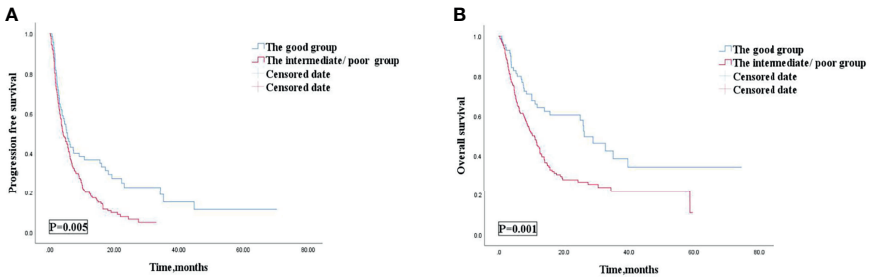

FIGURE 3 | PFS **(A)** and OS **(B)** according to the good group and the intermediate/poor group of patients with AGC receiving ICIs cohort. PFS, progression free survival; OS, overall survival; AGC, advanced gastric cancer; ICIs, immune checkpoint inhibitors.

Our study then conducted subgroup analysis based on different lines of immunotherapy. Univariate analyses of association of the dNLR/PLR group with outcomes in a large number of lines of immunotherapy (≥2) are shown in **Table 7**. For 130 patients treated with ICIs in subsequent lines, 97 (58.1%) patients were in the intermediate/poor dNLR/PLR group and 33 (46.5%) patients were in the good group. The median PFS and OS were 8.4 and 3 months, respectively. Patients of the intermediate/poor dNLR/PLR group had shorter PFS and OS than the good dNLR/PLR group (2.9 months vs. 3.3 months, 8.1 months vs. 11.2 months; $p = 0.007$, $p = 0.014$) (**Figures 4A, B**, and **Table 7**). Moreover, Kaplan–Meier analysis show that patients using ICIs in multilines with an elevated dNLR value (≥1.95) had shorter PFS and OS than those with a lower dNLR value (2.8 months vs. 4.2 months, 5.8 months vs. 11.6 months; $p < 0.001$, $p = 0.001$) (**Figures 4C, D**). However, no clear differences in PFS and OS were observed between the patients with an elevated PLR value (≥163.63) and those with a lower PLR value (<163.63) (2.8 months vs. 3.2 months, 8.2 months vs. 9.7 months; $p = 0.308$, $p = 0.210$) (**Figures 4E, F**).

Univariate analyses of association of the dNLR/PLR group with outcomes in lines of immunotherapy of 1 are shown in **Table 8**. For the 108 patients treated with ICIs in the 1st line, 70 (41.9%) patients were in the intermediate/poor dNLR/PLR group and 38 (53.5%) patients were in the good dNLR/PLR group. The median PFS and OS were 9.1 and 29 months, respectively. No clear differences in PFS and OS were observed between the intermediate/poor dNLR/PLR group and the good dNLR/PLR group (9.1 months vs. 9.1 months, 24.4 months vs. 32.8 months; $p = 0.414$, $p = 0.128$) (**Figures 5A, B**, and **Table 8**). Moreover, Kaplan–Meier analysis show that patients implementing ICIs in the 1st line with an elevated dNLR value (≥1.95) had shorter OS than those with a lower dNLR value (17.1 months vs. 35.2 months; $p = 0.016$) (**Figure 5C**). However, no clear difference of PFS was observed between the patients with an elevated dNLR value and with a lower dNLR value (7.6 months vs. 10.5 months; $p = 0.090$) (**Figure 5D**). Furthermore, there were no statistical differences in PFS and OS between the patients with an elevated PLR value (≥163.63) and with a lower PLR value (<163.63) (7.6 months vs. 9.1 months, 24.4 months vs. 32.8 months; $p = 0.766$, $p = 0.391$) (**Figures 5E, F**).

Association of the Composite Biomarker of dNLR and PLR With Outcomes in ICIs Combined With Other Therapies or ICIs Monotherapy: Subgroup Analysis

Univariate analysis revealed that patients treated with ICIs combined with other therapies were correlated with improved

TABLE 6 | Efficacy and prognosis based on the good, the intermediate, and the poor groups.

dNLR combined with PLR score classification		Response rate		OS (months)		PFS (months)	
		DCR (*n*, %)	OR (95% CI)	Median	HR (95% CI)	Median	HR (95% CI)
Overall	(*n* = 238)	126 (52.9)		12.5 (10.278–14.722)		4.7 (3.686–5.714)	
The good group	(*n* = 71)	40 (56.3)	1 [the reference]	26.3 (19.029–33.571)	1 [the reference]	5.5 (3.787–7.213)	1 [the reference]
The intermediate group	(*n* = 86)	43 (50.0)	1.290 (0.686–2.426)	12.1 (10.687–13.513)	1.540 (0.999–2.373)	5.8 (3.437–8.163)	1.355 (0.944–1.944)
The poor group	(*n* =81)	43 (53.1)	1.140 (0.601–2.164)	8.2 (4.966–11.434)	2.406 (1.579–3.665)	3.8 (3.017–4.583)	1.889 (1.319–2.704)
P-value		0.730		<0.001		0.002	
The intermediate group	(*n* = 86)	43 (50.0)	1 [the reference]	12.1 (10.687–13.513)	1 [the reference]	5.8 (3.437–8.163)	1 [the reference]
The poor group	(*n* =81)	43 (53.1)	0.884 (0.481–1.622)	8.2 (4.966–11.434)	1.562 (1.083–2.253)	3.8 (3.017–4.583)	1.394 (1.009–1.926)
p-value		0.690		0.017		0.044	
The good group	(*n* = 71)	40 (56.3)	1 [the reference]	26.3 (19.029–33.571)	1 [the reference]	5.5 (3.787–7.213)	1 [the reference]
The intermediate group	(*n* = 86)	43 (50.0)	1.290 (0.686–2.426)	12.1 (10.687–13.513)	1.540 (0.999–2.373)	5.8 (3.437–8.163)	1.355 (0.944–1.944)
p-value				0.050		0.099	
The good group	(*n* = 71)	40 (56.3)	1 [the reference]	26.3 (19.029–33.571)	1 [the reference]	5.5 (3.787–7.213)	1 [the reference]
The poor group	(*n* =81)	43 (53.1)	1.140 (0.601–2.164)	8.2 (4.966–11.434)	2.406 (1.579–3.665)	3.8 (3.017–4.583)	1.889 (1.319–2.704)
p-value				<0.001		0.001	

PFS, progression-free survival; OS, overall survival; HR, hazard ratio; DCR, disease control rate; OR, odds ratio.

TABLE 7 | Univariate analyses of the good group and the intermediate/poor group associated with OS and PFS of AGC patients treated with ICIs in the multi-line.

dNLR combined with PLR score classification	Patients treated with ICIs in the multi-line			
	OS (months)		PFS (months)	
	Median	HR (95%CI)	Median	HR (95%CI)
The good	11.2	1 [Reference]	3.3	1 [Reference]
The intermediate/ poor group	8.1	1.811 (1.117-2.935)	2.9	1.844 (1.168-2.909)
P value		0.014		0.007

PFS, progression free survival; OS, overall survival; AGC, advanced gastric cancer; ICIs, immune checkpoint inhibitors; HR, hazard ratio; dNLR, derived neutrophil-to-lym- phocyte: PLR, platelet-lymphocyte ratio.

OS and PFS. Our study then conducted subgroup analysis based on ICIs combined with other therapies or ICI monotherapy. Univariate analyses of association of the dNLR/PLR group with outcomes in patients treated with ICIs combined with other therapies are shown in **Table 9**. For 186 patients in whom ICIs are combined with other therapies, 129 (69.4) patients were in the intermediate/poor dNLR/PLR group and 57 (30.6%) patients were in the good group. The median PFS and OS were 5.1 and 14.2 months, respectively. Patients of the intermediate/poor dNLR/PLR group had shorter PFS and OS than the good dNLR/PLR group (4.7 months vs. 5.5 months, 24.4 months vs. 32.8 months; $p = 0.026$, $p = 0.002$) (**Table 9**). Patients in the intermediate/poor dNLR/PLR group were correlated with an over 2 times greater risk of death (HR = 2.063; 95% CI, 1.305–

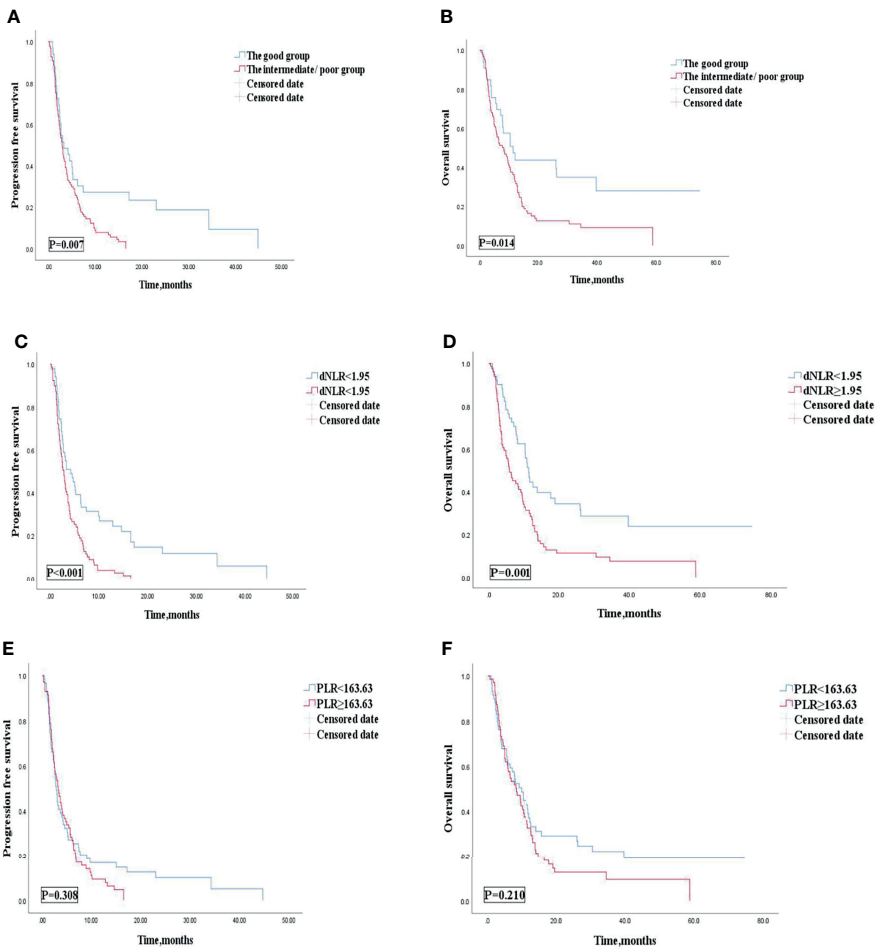

FIGURE 4 | PFS **(A)** and OS **(B)** of the good group and the intermediate/poor group of the multi-line of patients with AGC, receiving ICIs cohort, PFS **(C)** and OS **(D)** of the dNLR of the multi-line of patients with AGC, receiving ICIs cohort, and PFS **(E)** and OS **(F)** of the PLR of the multi-line of patients with AGC, receiving ICIs cohort. PFS, progression-free survival; OS, overall survival; ICIs, immune checkpoint inhibitors; dNLR, derived neutrophil-to-lymphocyte; PLR, platelet–lymphocyte ratio.

TABLE 8 | Univariate analyses of the good group and the intermediate/poor group associated with OS and PFS of AGC patients treated with 1st line ICIs.

dNLR combined with PLR score classification	Patients treated with the 1st line ICIs			
	OS (months)		PFS (months)	
	Median	HR (95%CI)	Median	HR (95%CI)
The good	32.8	1 [Reference]	9.1	1 [Reference]
The intermediate/ poor group	24.4	1.641 (0.861-3.127)	9.1	1.219 (0.756-1.963)
P value		0.128		0.414

PFS, progression free survival; OS, overall survival; AGC, advanced gastric cancer; ICIs, immune checkpoint inhibitors; HR, hazard ratio.

3.260; $p = 0.002$) and with an over 1.5 times greater risk disease progression (HR = 1.507; 95% CI, 1.046–2.170; $p = 0.028$) than those in the good NLR/PLR group (**Figures 6A, B**, and **Table 9**). Moreover, Kaplan–Meier analysis shows that patients using ICIs combined with other therapies with an elevated dNLR value (≥1.95) had shorter PFS and OS than those with a lower dNLR value (3.9 months vs. 5.8 months, 9.5 months vs. 29.0 months; $p = 0.002$, $p < 0.001$) (**Figures 6C, D**). Furthermore, patients with an elevated PLR value (≥163.63) had shorter OS than those with a lower PLR value (<163.63) (11.6 months vs. 29.0 months;

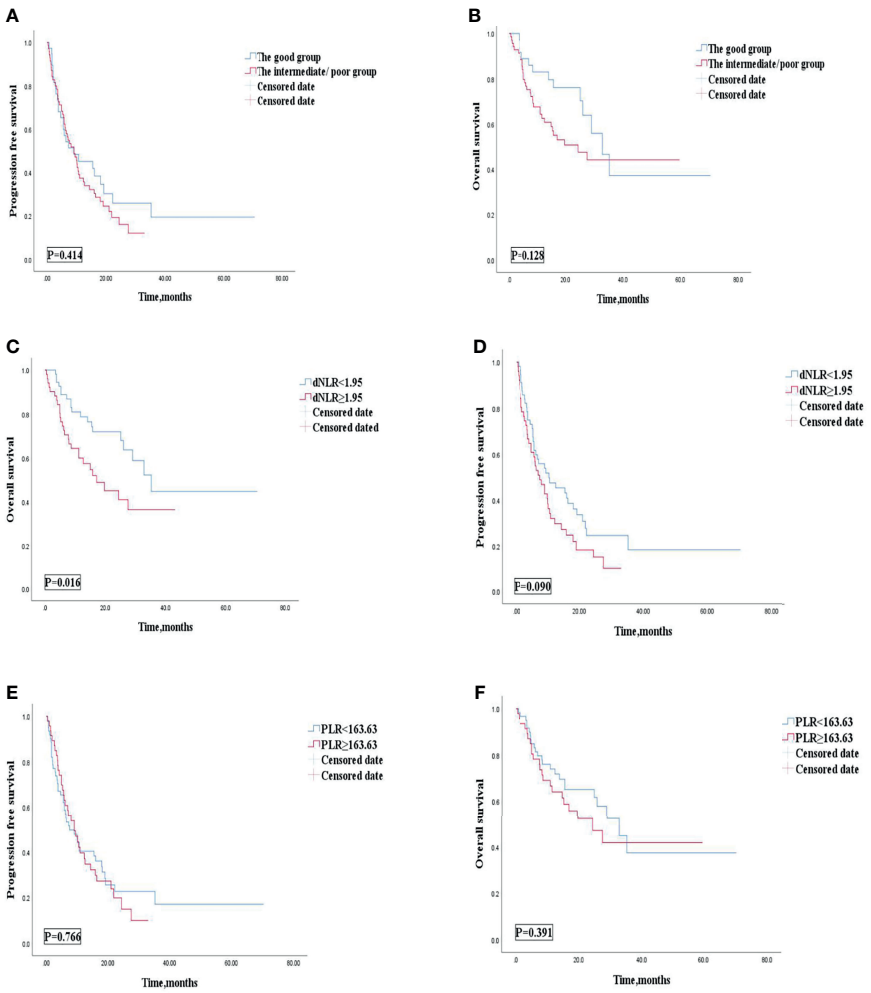

FIGURE 5 | PFS **(A)** and OS **(B)** of the good group and the intermediate/poor group of the 1st line of patients with AGC, receiving ICIs cohort, OS **(C)** and PFS **(D)** of the dNLR of the 1st line of patients with AGC, receiving ICIs cohort, and OS **(E)** and PFS **(F)** of the PLR of the 1st line of patients with AGC, receiving ICIs cohort. PFS, progression-free survival; OS, overall survival; ICIs, immune checkpoint inhibitors; dNLR, derived neutrophil-to-lymphocyte; PLR, platelet–lymphocyte ratio.

TABLE 9 | Univariate analyses of the good group and the intermediate/poor group associated with OS and PFS of AGC patients treated with ICIs combined with other therapies.

dNLR combined with PLR score classification	Patients treated with ICIs combined with other therapies.				
	Overall *n* = 186	OS (months)		PFS (months)	
		Median	HR (95% CI)	Median	HR (95% CI)
The good	57 (30.6)	32.8	1 [Reference]	5.5	1 [Reference]
The intermediate/poor group	129 (69.4)	11.8	2.063 (1.305–3.260)	4.7	1.507 (1.046–2.170)
p-value		0.002		0.028	

PFS, progression-free survival; OS, overall survival; AGC, advanced gastric cancer; ICIs, immune checkpoint inhibitors; HR, hazard ratio; dNLR, derived neutrophil-to-lymphocyte, PLR, platelet–lymphocyte ratio.

$p = 0.005$) (**Figure 6E**). However, no clear difference in PFS was observed between the patients with an elevated PLR value and with a lower PLR value (4.7 months vs. 5.5 months; $p = 0.068$) (**Figure 6F**).

Univariate analyses of association of the dNLR/PLR group with outcomes in patients treated with ICIs monotherapy are shown in **Table 10**. For the 52 patients treated with ICI monotherapy, 38 (73.1%) patients were in the intermediate/

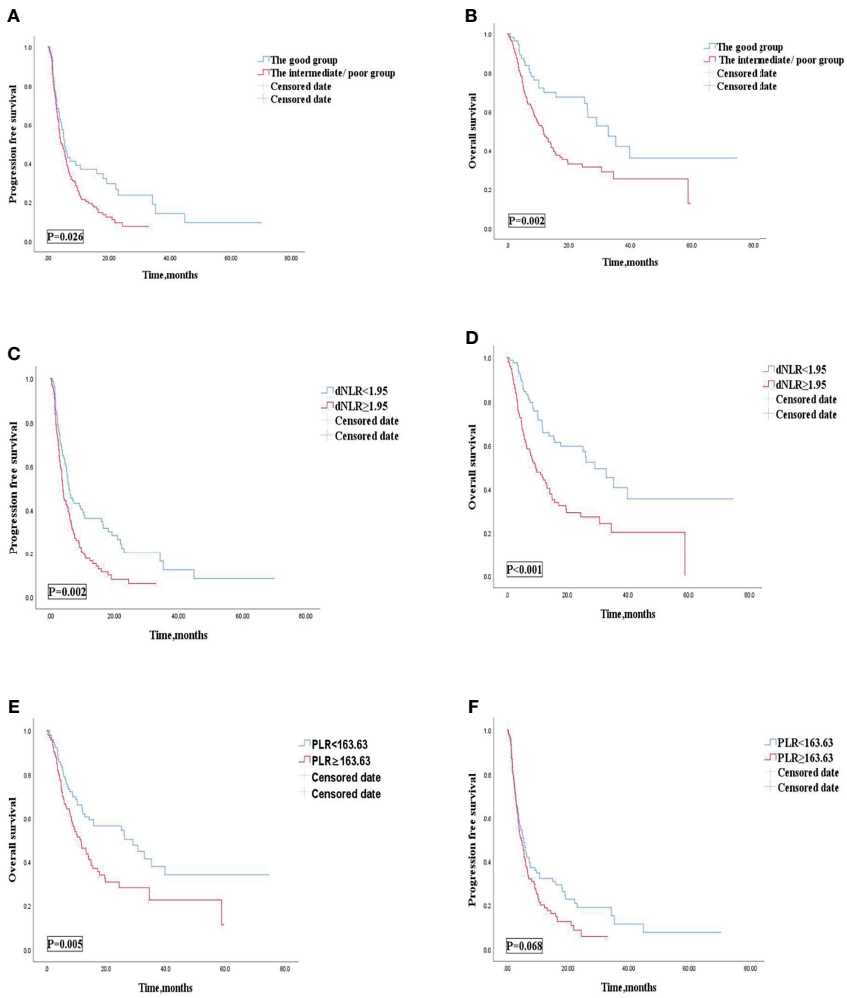

FIGURE 6 | PFS **(A)** and OS **(B)** of the good group and the intermediate/poor group of patients with AGC, receiving ICIs combined with other therapies cohort, OS **(C)** and PFS **(D)** of the dNLR of patients with AGC, receiving ICIs combined with other therapies cohort, and OS **(E)** and PFS **(F)** of the PLR of patients with AGC, receiving ICIs combined with other therapies cohort. PFS, progression-free survival; OS, overall survival; ICIs, immune checkpoint inhibitors; dNLR, derived neutrophil-to-lymphocyte; PLR, platelet–lymphocyte ratio.

TABLE 10 | Univariate analyses of the good group and the intermediate/poor group associated with OS and PFS of AGC patients treated with ICIs monotherapy.

dNLR combined with PLR score classification	Patients treated with ICIs combined without chemotherapy				
	Overall *n* = 52	OS (months)		PFS (months)	
		Median	HR (95% CI)	Median	HR (95% CI)
The good	14 (26.9)	7.9	1 [Reference]	2.7	1 [Reference]
The intermediate/poor group	38 (73.1)	8.1	1.448 (0.711–2.948)	2.2	1.887 (0.953–3.738)
p-value		0.307		0.069	

PFS, progression-free survival; OS, overall survival; AGC, advanced gastric cancer; ICIs, immune checkpoint inhibitors; HR, hazard ratio; dNLR, derived neutrophil-to-lymphocyte; PLR, platelet–lymphocyte ratio.

poor dNLR/PLR group and 14 (26.9%) patients were in the good dNLR/PLR group. The median PFS and OS were 2.4 and 8.1 months, respectively. No clear differences in PFS and OS were observed between the intermediate/poor dNLR/PLR group and the good dNLR/PLR group (2.2 months vs. 2.7 months, 8.1 months vs. 7.9 months; $p = 0.061$ $p = 0.302$) (**Figures 7A, B**, and **Table 10**). Moreover, Kaplan–Meier analysis shows that patients in whom ICIs were implemented in the multiline with an elevated dNLR value (≥1.95) had shorter PFS and OS than those with a lower dNLR value (1.9 months vs. 7.4 months, 5.7 months vs. 11.2 months; $p = 0.008$, $p = 0.028$) (**Figures 7C, D**). However, no clear differences in PFS and OS were observed

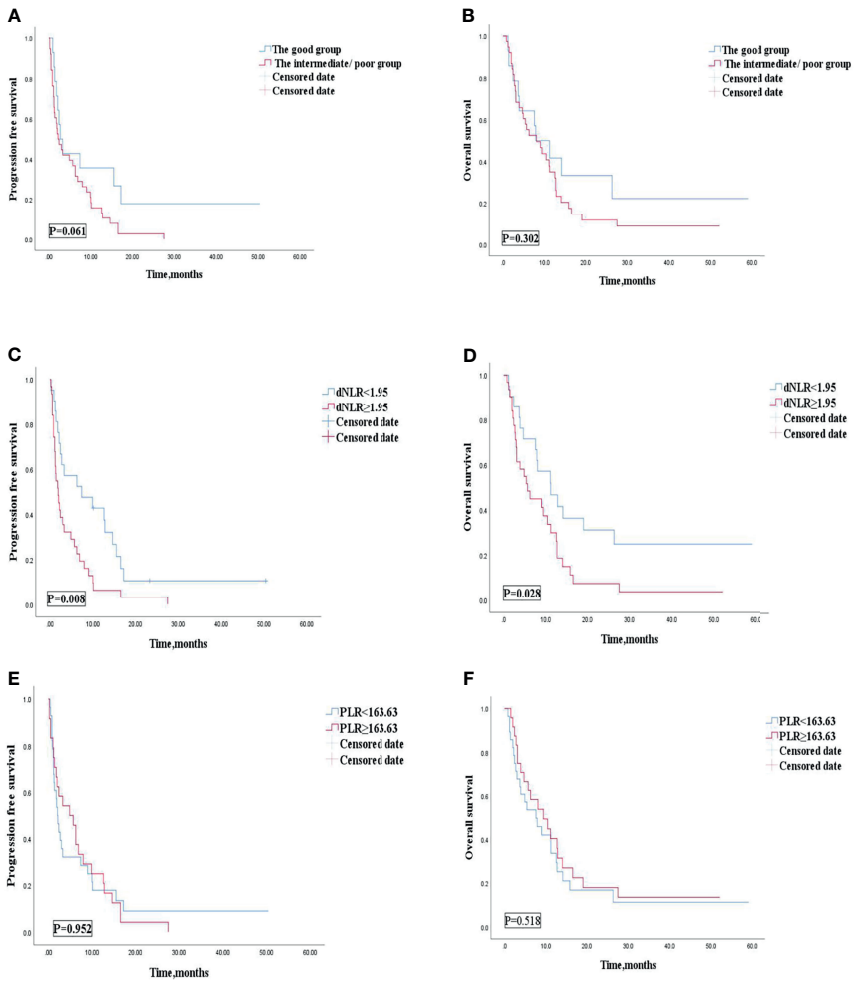

FIGURE 7 | PFS **(A)** and OS **(B)** of the good group and the intermediate/poor group of patients with AGC, receiving ICIs monotherapy cohort, OS **(C)** and PFS **(D)** of the dNLR of patients with AGC, receiving ICIs monotherapy cohort, and OS **(E)** and PFS **(F)** of the PLR of patients with AGC, receiving ICIs monotherapy cohort. PFS, progression-free survival; OS, overall survival; ICIs, immune checkpoint inhibitors; dNLR, derived neutrophil-to-lymphocyte; PLR, platelet–lymphocyte ratio.

between the patients with an elevated PLR value (≥163.63) and those with a lower PLR value (<163.63) (2.1 months vs. 4.9 months, 7.6 months vs. 9.4 months; $p = 0.952$, $p = 0.518$) (**Figures 7E, F**).

DISCUSSION

The usage of immunotherapy in the field of GC treatment has increased annually worldwide (7, 21). Based on the current clinical trial results, the positive effect of immune checkpoint inhibitors is very apparent (22). Comparatively, immunotherapy drugs are expensive and prone to drug resistance and even super-progress (23, 24). Therefore, finding an effective predictive marker is an urgent matter to be solved. These indicators can predict immune curative effect, so as to achieve precise treatment. However, the current evaluation of biomarkers for immunotherapy is relatively limited (15). The highly heterogeneous characteristics of GC may limit the accuracy of a single biomarker for screening populations benefiting from immunotherapy (25). In contrast, the combination of multiple indicators can provide more targeted information for the detection of potential immune benefit subgroups. Peripheral inflammatory blood indexes such as NLR, dNLR, and PLR are independent prognostic biomarkers for patients receiving immunotherapy (13, 14, 20). A prognostic correlation analysis of patients with advanced non-small cell lung cancer treated with peripheral blood biomarkers and anti-PD-1 antibody treatment by Soyano et al. showed that patients with an elevated PLR value were correlated independently with poor prognosis (26). When the fluctuations of PLR are interpreted along with other complementary hematologic indices, its value as an inflammatory marker will increase. One typical example of the complementary hematologic index is NLR, which provides additional information about neutrophilic inflammation and infectious complications (27). Consequently, Dharmapuri et al. established a statistical model by NLR/PLR groups and found that there were significant differences in survival between the high-NLR/low-PLR group and the low-NLR/low-PLR group in advanced hepatocellular carcinoma patients treated with ICIs (16). The efficiency of dNLR as useful biomarkers, predicting ICI response, has been proved by Lim et al. (20). Our research also found that patients with an elevated dNLR value (≥ the best cutoff value) were associated with shorter OS and PFS. Patients with an elevated dNLR value were associated with an over 1.8 times greater risk of disease progression (HR = 1.807; 95% CI, 1.356–2.407; $p < 0.001$) and an over 2.1 times greater risk of death (HR = 2.161; 95% CI, 1.542–3.028; $p < 0.001$) than those with a lower dNLR value. However, patients with high levels of PLR (≥ the median value) were only associated with shorter OS, but not PFS. Patients with an elevated PLR value were associated with an over 1.4 times greater risk of death than those with a lower PLR value (<163.63) (HR = 1.416; 95% CI, 1.026–1.956; $p = 0.033$). On the other hand, Baicun Hou et al. noticed that the Lung immune prognostic index (LIPI), consisting of lactate dehydrogenase (LDH) levels and dNLR, was correlated with the outcomes of AGC patients receiving immunotherapy (28). As such, we combined dNLR and PLR to stratify risk factors. The high levels of dNLR (≥1.95) and PLR (≥163.63) were considered to be risk factors. Based on these two risk factors, patients were categorized into 3 groups: the risk factor number for the "good" group was 0, that for the "intermediate" group was 1, and that for the "poor" group was 2. Due to the similar efficacy and survival outcomes of patients in intermediate and good groups, the subjects were divided into two groups: dNLR/PLR-good and dNLR/PLR-intermediate/poor. We then began to evaluate the differences in prognosis and survival of AGC patients after immunotherapy between the good and the intermediate/poor groups. The cutoff value of dNLR was obtained by the ROC curves to predict the disease progression rate at the 8th month and the cutoff value of PLR was estimated by the median value. The cutoff values of dNLR and PLR were 1.95 and 163.63, respectively. Dharmapuri et al. found that the high-NLR/low-PLR group has shorter OS and PFS than the low-NLR/low-PLR group. We also found that the good dNLR/PLR group was independently associated with better prognosis. The intermediate/poor dNLR/PLR group was independently correlated with an over 1.4 times greater risk of disease progression (4.1 months vs. 5.5 months; $p = 0.016$) and an over 1.54 times greater risk of death (11.1 months vs. 26.3 months; $p = 0.033$) than the good dNLR/PLR group. However, no clear differences in the disease control rate (DCR) and overall response rate (ORR) were observed between the intermediate/poor dNLR/PLR group and the good dNLR/PLR group (51.5% vs. 56.3%, 26.3% vs. 29.6%; $p = 0.494$, $p = 0.609$). Baicun Hou et al. noticed that patients with a good PS (ECOG PS of 0–1) were also independently associated with PFS and OS for AGC patients treated with ICIs (28). However, in our study, patients who had a good PS (ECOG PS of 0–1) were independently associated with improved OS, but without improved PFS. Baicun Hou et al. noticed that patients treated with combination of immunotherapy and other therapies were associated with longer OS, with HRs of 0.58 (95% CI, 0.37–0.93; $p = 0.024$), and PFS, with HRs of 0.49 (95% CI, 0.30–0.81; $p = 0.005$) (28). However, in our study, there were no statistical differences for OS and PFS between patients treated with ICIs, ICI plus chemotherapy, ICI plus antiangiogenic and chemotherapy group, and ICI plus antiangiogenic or target agents. We found that patients treated with the 1st line ICIs were independently associated with improved PFS and OS. However, no clear differences in OS and PFS were observed between patients treated with the 1st line ICIs and those treated with ICIs after the 1st line in the study of Baicun Hou et al. (28). We also found that patients who had fewer organ metastases (<3) were independently associated with improved PFS and OS. However, Baicun Hou et al. found that patients who had fewer organ metastases (< 2) were not independently associated with improved PFS and OS than those who had more organ metastases (≥2) (28). In addition, our study firstly found that patients treated with more doses of ICIs (≥200 mg) were independently associated with improved OS, but without improved PFS. However, the mechanism of the correlation

between this peripheral blood inflammatory complex index and the tumor prognosis is relatively complicated, and it still needs to be further explored through basic experiments and clinical trials. Some studies suggested that this may be related to the tumor-immune microenvironment of patients (29, 30). In addition to direct immune killing effects on tumor cells, these biomarkers are also related to tumor immunostimulatory signals and the activation of effector cells. Neutrophils are derived from bone marrow hematopoietic stem cells and have chemotaxis, phagocytosis, and bactericidal effect (31). Moreover, not only can it enhance the growth of tumor cells under the effect of tumor, its microenvironment reproduction and invasion can also promote angiogenesis and mediate tumor immunosuppression (32).

Lymphocyte is an important component for the body's immune response function (33). Elevated neutrophils can inhibit the immune attack ability of lymphocytes (34). Consequently, NLR, defined as the ratio of neutrophils to lymphocytes, can comprehensively reflect the immune status and inflammation of the tumor patients (35). dNLR is defined as the ratio between the neutrophil and white blood cell minus neutrophil. The dNLR can reflect changes in the body's immune system, so it is more meaningful than NLR (36). Platelets are produced by mature megakaryocytes in bone marrow hematopoietic tissue (37). It can release inflammatory factors such as thrombospondin and vascular endothelial growth factor, and participates in tumor cell adhesion, extravasation, invasion, immune escape, and tumor angiogenesis (38). Moreover, tumors grow and evolve through constant crosstalk with the surrounding microenvironment, and emerging evidence indicates that angiogenesis and immunosuppression frequently occur simultaneously in response to this crosstalk (39). Accordingly, strategies combining anti-angiogenic therapy and immunotherapy seem to have the potential to tip the balance of the tumor microenvironment and improve treatment response (39). Therefore, based on the value of PLR, we may be able to roughly assess whether patients can benefit from the therapy of ICI combined with antiangiogenic agents. dNLR and PLR are composite indicators of lymphocyte, neutrophil, and platelet, so they can reflect the balance of the body's tumor inflammatory response to a certain extent. Therefore, the higher dNLR and PLR tumor patients get, the worse their prognosis will be.

As a retrospective data collection, this study might have some reporting errors. Due to these, positive results could be exaggerated, and some false positives could appear on research results. However, these errors were inevitable in research design. Moreover, this study had some limitations, including a relatively small sample size with a mixed population of GC of cardia, GC of body/fundus, and GC of pylorus, as well as a lack of comparison of the two groups among the three cancers.

CONCLUSION

This retrospective cohort study has demonstrated that a composite biomarker of dNLR and PLR is independently correlated with the survival of AGC patients implementing immunotherapy. It may be difficult for patients with the intermediate/poor dNLR/PLR group to benefit from immunotherapy. However, the possibility of using the complex index as an effective and economic prognostic biomarker to select patients who are best suited to receiving ICIs needs further investigation in a larger prospective study.

DATA AVAILABILITY STATEMENT

The raw data supporting the conclusions of this article will be made available by the authors, without undue reservation.

ETHICS STATEMENT

This study was approved by the Ethics Committee of Chinese PLA General Hospital and was conducted according to the principles of the Declaration of Helsinki.

AUTHOR CONTRIBUTIONS

YP was in charge of writing and analysis. GD and ZW provided the guide and idea. HS, GCD, SC, NZ, and QZ contributed to analysis. All authors contributed to the article and approved the submitted version.

ACKNOWLEDGMENTS

The authors gratefully acknowledge the advice and insights of GD and ZW, whose work is supported (or supported in part) by the Department of Medical Oncology, Chinese PLA General Hospital.

SUPPLEMENTARY MATERIAL

The Supplementary Material for this article can be found online at: https://www.frontiersin.org/articles/10.3389/fonc.2021.798415/full#supplementary-material

Supplementary Table 1 | Relationship between the good, the intermediate, and the poor groups and response to ICIs treatment. :response rate.

Supplementary Figure 1 | PFS **(A)** and OS **(B)** according to the good,the intermediate, and the poor groups of patients with AGC receiving ICIs cohort. PFS, progression free survival; OS,overall survival; AGC,advanced gastric cancer; ICIs, immune checkpoint inhibitors.

Supplementary Figure 2 | Cox proportional hazard of PFS **(A)** and OS **(B)**. PFS, progression free survival; OS, overall survival; AGC, advanced gastric cancer; ICIs, immune checkpoint inhibitors.

REFERENCES

1. Siegel RL, Miller KD, Jemal A. Cancer Statistics, 2020. *CA Cancer J Clin* (2020) 70(1):7–30. doi: 10.3322/caac.21590
2. Chen LT, Satoh T, Ryu MH, Chao Y, Kato K, Chung HC, et al. A Phase 3 Study of Nivolumab in Previously Treated Advanced Gastric or Gastroesophageal Junction Cancer (ATTRACTION-2): 2-Year Update Data. *Gastric Cancer* (2020) 23(3):510–9. doi: 10.1007/s10120-019-01034-7
3. Kato K, Satoh T, Muro K, Yoshikawa T, Tamura T, Hamamoto Y, et al. A Subanalysis of Japanese Patients in a Randomized, Double-Blind, Placebo-Controlled, Phase 3 Trial of Nivolumab for Patients With Advanced Gastric or Gastro-Esophageal Junction Cancer Refractory to, or Intolerant of, at Least Two Previous Chemotherapy Regimens (ONO-4538-12, ATTRACTION-2). *Gastric Cancer* (2019) 22(2):344–54. doi: 10.1007/s10120-018-0899-6
4. Shitara K, Özgüroğlu M, Bang YJ, Di Bartolomeo M, Mandalà M, Ryu MH, et al. KEYNOTE-061 Investigators. Pembrolizumab Versus Paclitaxel for Previously Treated, Advanced Gastric or Gastro-Oesophageal Junction Cancer (KEYNOTE-061): A Randomised, Open-Label, Controlled, Phase 3 Trial. *Lancet* (2018) 392(10142):123–33. doi: 10.1016/S0140-6736(18)31257-1
5. Liang F. The KEYNOTE-061 Trial. *Lancet* (2019) 393(10176):1098. doi: 10.1016/S0140-6736(18)33073-3
6. Smyth EC, Petty RD. Pembrolizumab Versus Paclitaxel in Gastro-Oesophageal Adenocarcinoma. *Lancet* (2018) 392(10142):97–8. doi: 10.1016/S0140-6736(18)31277-7
7. Janjigian YY, Shitara K, Moehler M, Garrido M, Salman P, Shen L, et al. First-Line Nivolumab Plus Chemotherapy Versus Chemotherapy Alone for Advanced Gastric, Gastro-Oesophageal Junction, and Oesophageal Adenocarcinoma (CheckMate 649): A Randomised, Open-Label, Phase 3 Trial. *Lancet* (2021) 398(10294):27–40. doi: 10.1016/S0140-6736(21)00797-2
8. Moehler M, Dvorkin M, Boku N, Özgüroğlu M, Ryu MH, Muntean AS, et al. Phase III Trial of Avelumab Maintenance After First-Line Induction Chemotherapy Versus Continuation of Chemotherapy in Patients With Gastric Cancers: Results From JAVELIN Gastric 100. *J Clin Oncol* (2021) 39(9):966–77. doi: 10.1200/JCO.20.00892
9. Chung HC, Bang YJ S, Fuchs C, Qin SK, Satoh T, Shitara K, et al. First-Line Pembrolizumab/Placebo Plus Trastuzumab and Chemotherapy in HER2-Positive Advanced Gastric Cancer: KEYNOTE-811. *Future Oncol* (2021) 17 (5):491–501. doi: 10.2217/fon-2020-0737
10. Kelly RJ. Immunotherapy for Esophageal and Gastric Cancer. *Am Soc Clin Oncol Educ Book* (2017) 37:292–300. doi: 10.1200/EDBK_175231
11. Kono K, Nakajima S, Mimura K. Current Status of Immune Checkpoint Inhibitors for Gastric Cancer. *Gastric Cancer* (2020) 23(4):565–78. doi: 10.1007/s10120-020-01090-4
12. Wei Q, Yuan X, Xu Q, Li J, Chen L, Ying J. Correlation Between Hemoglobin Levels and the Prognosis of First-Line Chemotherapy in Patients With Advanced GC. *Cancer Manag Res* (2020) 12:7009–19. doi: 10.2147/CMAR.S256074
13. Kim EY, Lee JW, Yoo HM, Park CH, Song KY. The Platelet-To-Lymphocyte Ratio Versus Neutrophil-To-Lymphocyte Ratio: Which Is Better as a Prognostic Factor in GC. *Ann Surg Oncol* (2015) 22(13):4363–70. doi: 10.1245/s10434-015-4518-z
14. Matsuoka T, Yashiro M. Biomarkers of GC: Current Topics and Future Perspective. *World J Gastroenterol* (2018) 24(26):2818–32. doi: 10.3748/wjg.v24.i26.2818
15. Gou M, Zhang Y, Liu T, Qu T, Si H, Wang Z, et al. The Prognostic Value of Pre-Treatment Hemoglobin (Hb) in Patients With Advanced or Metastatic GC Treated With Immunotherapy. *Front Oncol* (2021) 11:655716. doi: 10.3389/fonc.2021.655716
16. Dharmapuri S, Özbek U, Lin JY, Sung M, Schwartz M, Branch AD, et al. Predictive Value of Neutrophil to Lymphocyte Ratio and Platelet to Lymphocyte Ratio in Advanced Hepatocellular Carcinoma Patients Treated With Anti-PD-1 Therapy. *Cancer Med* (2020) 9(14):4962–70. doi: 10.1002/cam4.3135
17. Namikawa T, Yokota K, Tanioka N, Fukudome I, Iwabu J, Munekage M, et al. Systemic Inflammatory Response and Nutritional Biomarkers as Predictors of Nivolumab Efficacy for Gastric Cancer. *Surg Today* (2020) 50(11):1486–95. doi: 10.1007/s00595-020-02048-w
18. Ohta A, Komatsu S, Tsuji R, Tanaka S, Kumano T, Imura K, et al. [Clinical Evaluation of the Efficacy and Adverse Effects of Nivolumab Treatment for Patients With Advanced Gastric Cancer]. *Gan To Kagaku Ryoho* (2020) 47 (4):725–7.
19. Nakamura N, Kinami S, Fujita J, Kaida D, Tomita Y, Miyata T, et al. Chronological Changes in Neutrophil/lymphocyte Ratio in Advanced Gastric Cancer Patients Treated With Nivolumab: A Report of Nine Cases. *Asian Pac J Cancer Prev* (2020) 21(10):2955–60. doi: 10.31557/APJCP.2020.21.10.2955
20. Lim JU, Kang HS, Yeo CD, Kim JS, Park CK, Kim JW, et al. Predictability of Early Changes in Derived Neutrophil-to-Lymphocyte Ratio and Neutrophil-to-Lymphocyte Ratio in Patients With Advanced Non-Small Cell Lung Cancer Treated With Immune Checkpoint Inhibitors. *J Thorac Dis* (2021) 13(5):2824–32. doi: 10.21037/jtd-20-3416
21. Xie J, Fu L, Jin L. Immunotherapy of Gastric Cancer: Past, Future Perspective and Challenges. *Pathol Res Pract* (2021) 218:153322. doi: 10.1016/j.prp.2020.153322
22. Tan S, Li D, Zhu X. Cancer Immunotherapy: Pros, Cons and Beyond. *BioMed Pharmacother* (2020) 124:109821. doi: 10.1016/j.biopha.2020.109821
23. Chen S, Gou M, Yan H, Fan M, Pan Y, Fan R, et al. Hyperprogressive Disease Caused by PD-1 Inhibitors for the Treatment of Pan-Cancer. *Dis Markers* (2021) 2021:6639366. doi: 10.1155/2021/6639366
24. Kim RD, Chung V, Alese OB, El-Rayes BF, Li D, Al-Toubah TE, et al. A Phase 2 Multi-Institutional Study of Nivolumab for Patients With Advanced Refractory Biliary Tract Cancer. *JAMA Oncol* (2020) 6(6):888–94. doi: 10.1001/jamaoncol.2020.0930
25. Huang X, Zhang J, Zheng Y. ANTXR1 Is a Prognostic Biomarker and Correlates With Stromal and Immune Cell Infiltration in Gastric Cancer. *Front Mol Biosci* (2020) 7:598221:598221. doi: 10.3389/fmolb.2020.598221
26. Soyano AE, Dholaria B, Marin-Acevedo JA, Diehl N, Hodge D, Luo Y, et al. Peripheral Blood Biomarkers Correlate With Outcomes in Advanced Non-Small Cell Lung Cancer Patients Treated With Anti-PD-1 Antibodies. *J Immunother Cancer* (2018) 6(1):129. doi: 10.1186/s40425-018-0447-2
27. Gasparyan AY, Ayvazyan L, Mukanova U, Yessirkepov M, Kitas GD. The Platelet-To-Lymphocyte Ratio as an Inflammatory Marker in Rheumatic Diseases. *Ann Lab Med* (2019) 39(4):345–57. doi: 10.3343/alm.2019.39.4.345
28. Hou B, Wang P, Liu T, Chen S, Li T, Zhang S, et al. Association of the Pretreatment Lung Immune Prognostic Index With Survival Outcomes in Advanced Gastric Cancer Patients Treated With Immune Checkpoint Inhibitors. *Clin Res Hepatol Gastroenterol* (2021) 45(5):101748. doi: 10.1016/j.clinre.2021.101748
29. Balkwill F, Mantovani A. Inflammation and Cancer: Back to Virchow? *Lancet* (2001) 357(9255):539–45. doi: 10.1016/S0140-6736(00)04046-0
30. Coussens LM, Werb Z. Inflammation and Cancer. *Nature* (2002) 420 (6917):860–7. doi: 10.1038/nature01322
31. Garwicz D, Lennartsson A, Jacobsen SE, Gullberg U, Lindmark A. Biosynthetic Profiles of Neutrophil Serine Proteases in a Human Bone Marrow-Derived Cellular Myeloid Differentiation Model. *Haematologica* (2005) 90(1):38–44.
32. Li TJ, Jiang YM, Hu YF, Huang L, Yu J, Zhao LY, et al. Interleukin-17-Producing Neutrophils Link Inflammatory Stimuli to Disease Progression by Promoting Angiogenesis in Gastric Cancer. *Clin Cancer Res* (2017) 23 (6):1575–85. doi: 10.1158/1078-0432.CCR-16-0617
33. Manson J, Hoffman R, Chen S, Ramadan MH, Billiar TR. Innate-Like Lymphocytes Are Immediate Participants in the Hyper-Acute Immune Response to Trauma and Hemorrhagic Shock. *Front Immunol* (2019) 10:1501:1501. doi: 10.3389/fimmu.2019.01501
34. Wu L, Saxena S, Singh RK. Neutrophils in the Tumor Microenvironment. *Adv Exp Med Biol* (2020) 1224:1–20. doi: 10.1007/978-3-030-35723-8_1
35. Guo C, Ding P, Xie C, Ye C, Ye M, Pan C, et al. Potential Application of the Oxidative Nucleic Acid Damage Biomarkers in Detection of Diseases. *Oncotarget* (2017) 8(43):75767–77. doi: 10.18632/oncotarget.20801
36. Mezquita L, Auclin E, Ferrara R, Charrier M, Remon J, Planchard D, et al. Association of the Lung Immune Prognostic Index With Immune Checkpoint Inhibitor Outcomes in Patients With Advanced NSCLC. *JAMA Oncol* (2018) 4(3):351–7. doi: 10.1001/jamaoncol

37. Leiva O, Leon C, Kah Ng S, Mangin P, Gachet C, Ravid K. The Role of Extracellular Matrix Stiffness in Megakaryocyte and Platelet Development and Function. *Am J Hematol* (2018) 93(3):430–41. doi: 10.1002/ajh.25008
38. Mege D, Aubert M, Lacroix R, Dignat-George F, Panicot-Dubois L, Dubois C. Involvement of Platelets in Cancers. *Semin Thromb Hemost* (2019) 45(6):569–75. doi: 10.1055/s-0039-1693475
39. Solimando AG, Summa S, Vacca A, Ribatti D. Cancer-Associated Angiogenesis: The Endothelial Cell as a Checkpoint for Immunological Patrolling. *Cancers (Basel)* (2020) 12(11):3380. doi: 10.3390/cancers12113380

Conflict of Interest: The authors declare that the research was conducted in the absence of any commercial or financial relationships that could be construed as a potential conflict of interest.

Publisher's Note: All claims expressed in this article are solely those of the authors and do not necessarily represent those of their affiliated organizations, or those of the publisher, the editors and the reviewers. Any product that may be evaluated in this article, or claim that may be made by its manufacturer, is not guaranteed or endorsed by the publisher.

frontiers | Frontiers in Oncology

REVIEW
published: 07 April 2022
doi: 10.3389/fonc.2022.734581

Neoadjuvant Therapy for Locally Advanced Esophageal Cancers

Runkai Huang[1†], Zhenbin Qiu[1†], Chunwen Zheng[1], Ruijie Zeng[1], Wanxian Chen[1], Simeng Wang[1], Enmin Li[1] and Yiwei Xu[2,3*]*

[1] Department of Biochemistry and Molecular Biology, Shantou University Medical College, Shantou, China, [2] Department of Clinical Laboratory Medicine, the Cancer Hospital of Shantou University Medical College, Shantou, China, [3] Guangdong Esophageal Cancer Research Institute, Shantou University Medical College, Shantou, China

Esophageal carcinoma is one of the most aggressive malignant diseases. At present, neoadjuvant chemotherapy and neoadjuvant chemoradiotherapy are regarded as the standard modalities for the treatments of locally advanced esophageal cancers based on several landmark trials. However, the optimal regimen, radiation dose, and surgical intervals are uncertain and the rate of recurrence after neoadjuvant therapy is high. Patients receiving neoadjuvant therapy and reaching a pathological complete response have been reported to have a better survival benefit and a fewer recurrence risk than those non-pathological complete responses. Nevertheless, less than half of patients will reach a pathological complete response after neoadjuvant therapy, and the methods to evaluate the efficacy after neoadjuvant therapy accurately are limited. Immune checkpoint inhibitors have been recommended for the treatments of advanced esophageal cancers. Recently, research has been beginning to evaluate the safety and efficacy of immunotherapy combined with neoadjuvant therapy. Here, we will review and discuss the development of the neoadjuvant therapy of locally advanced esophageal cancers and unsolved clinical problems.

Keywords: locally advanced esophageal cancers, neoadjuvant, chemoradiotherapy, chemotherapy, immunotherapy

OPEN ACCESS

Edited by:
Sripathi Sureban, University of Oklahoma Health Sciences Center, United States

Reviewed by:
Mohamed Rahouma, NewYork-Presbyterian, United States
Dongryul Oh, Sungkyunkwan University, South Korea

****Correspondence:***
Yiwei Xu
yiwei512@126.com
Enmin Li
nmli@stu.edu.cn

[†]These authors have contributed equally to this work and share first authorship

Specialty section:
This article was submitted to Gastrointestinal Cancers: Gastric Esophageal Cancers, a section of the journal Frontiers in Oncology

Received: *01 July 2021*
Accepted: *09 March 2022*
Published: *07 April 2022*

Citation:
Huang R, Qiu Z, Zheng C, Zeng R, Chen W, Wang S, Li E and Xu Y (2022) Neoadjuvant Therapy for Locally Advanced Esophageal Cancers. Front. Oncol. 12:734581. doi: 10.3389/fonc.2022.734581

INTRODUCTION

Esophageal carcinoma has been regarded as the seventh common cancer and the sixth leading cause of cancer death (1). Histologically, esophageal cancers include squamous cancer, which is common in Asian countries, and adenocarcinoma, which is common in western countries. To date, the treatment for esophageal cancers is still a tough clinical problem. For locally advanced esophageal cancers (LAECs), neoadjuvant chemotherapy (nCT) and neoadjuvant chemoradiotherapy (nCRT) have been recommended as standard treatments. Many studies have proved their anti-tumor efficacy, while some unsolved clinical problems also exist (2–4). Immune checkpoint inhibitors (ICIs) are being widely researched in various tumors. For esophageal cancers, ICIs have been recommended for the second/first-line treatment of advanced esophageal cancers. Recently, research regarding immunotherapy combined with conventionally neoadjuvant chemo(radio) therapy is ongoing. Hence, here we review and discuss the development of neoadjuvant therapy for LAECs and potential clinical problems.

NEOADJUVANT CHEMOTHERAPY

The research regarding the efficacy of nCT for LAECs has been conducted since the 1980s. As we summarized in **Table 1**, for adenocarcinoma, the utilization status of neoadjuvant treatments is owed to three randomized controlled trials. The UK Medical Research Council (OE02) trial was the first large-sized study to demonstrate a survival benefit of nCT for patients with esophageal cancer, in which patients were randomly assigned to receive preoperative chemotherapy or surgery alone, showing a 5% increase in 5-year survival for patients with adenocarcinoma (6, 7). Thus, nCT became a standard treatment for local esophageal adenocarcinoma (EAC). Besides, the Medical Research Council Adjuvant Gastric Infusional Chemotherapy (MAGIC) and Fédération Nationales des Centres de Lutte Contre le Cancer/ Fédération Francophone de Cancérologie Digestive trials (FNCLCC-FFCD), which included 26% and 75% LAEC in the group receiving perioperative epirubicin, cisplatin, fluorouracil and cisplatin, fluorouracil respectively, showed that the perioperative chemotherapy group had a higher overall survival as shown by a hazard ratio (HR) reduction from 25% to 31% and a 5-year survival increase from 13% to 14% (8, 9). Since the benefit of survival, perioperative chemotherapy has become a standard treatment for locally gastroesophageal carcinoma. Recently, results from the trial 5-FU, Leucovorin, Oxaliplatin and Docetaxel (FLOT) Versus Epirubicin, Cisplatin and 5-FU (ECF) in Patients With Locally Advanced Resectable Gastric Cancer (FLOT4-AIO) revealed that the regimen with docetaxel, oxaliplatin, leucovorin, and fluorouracil showed better survival and disease control. Compared with perioperative epirubicin, cisplatin, and fluorouracil/capecitabine, the median overall survival (mOS) in patients administered with the FLOT regimen increased by 15 months (P=0.012) and the median disease-free survival (mDFS) increased by 12 months (P=0.0036) (10, 11). Thus, the FLOT has been one of the standard regimens for perioperative chemotherapy.

For esophageal squamous carcinoma (ESCC), in the OE02 trial, 247 patients with ESCC were randomly assigned to receive nCT or surgery alone (6). Long-term results showed a benefit survival outcome (25.5% vs. 17.0% in 5-year OS) (7). The standard preoperative chemotherapy for locally advanced ESCC is cisplatin-fluorouracil based, which improved the R0 resection and overall survival (OS) in the Japan Clinical Oncology Group (JCOG) 9907 trial showing a 5-year OS of 55% in the nCT group while 43% in the postoperative treatment group (P=0.04). Based on this trial, the nCT based on cisplatin–fluorouracil (CF) has become the standard treatment for locally ESCC in Japan (2).

In summary, compared with surgery alone, adding chemotherapy before surgery has been proved to improve R0 resection rate and survival for patients with LAEC. For adenocarcinoma, the 5-year OS increased by 13%–15% by adding nCT. For ESCC, evidence from large-scale clinical trials is limited. The efficacy of nCT was confirmed in the JCOG9907 trial by comparing it with postoperative therapy (2). Nevertheless, the efficacy of nCT remains unsatisfactory as shown by a low pathological complete response (pCR) rate after nCT. For adenocarcinoma, thanks to the FLOT regimen, the pCR rate has been significantly improved, showing an increase of up to 16% (10). For ESCC, the pCR rate after a preoperative CF-based treatment was only 5%. Furthermore, although the JCOG9907 trial showed an OS benefit after nCT compared with postoperative therapy, there were no differences in progression-free survival (PFS; HR 0.84, 95%CI 0.63–1.11) indicating no improvement in the quality of life. Subgroup analysis reported that patients at stage III had less benefit than those at stage II. Thus, a more effective regimen is needed (2). Recent research has shown the promising efficacy of the regimen with docetaxel, cisplatin, and 5-FU (DCF). Results from a phase II trial reported a 90.5% completion rate and 17% pCR rate suggesting the feasibility of the DCF regimen (12). For disease control, the DCF regimen showed a higher 5-year PFS than that in the CF regimen (38.2% vs. 58.3%, P=0.006) (13). For security, the DCF regimen had no effects on surgical outcomes (14). However, the incidence of blood adverse events (AEs) was high (grade ≥3 neutropenia: 83%) (12). A propensity score-matched analysis reported that the DCF showed better efficacy for patients with locally advanced squamous carcinoma at stage III [objective response rate (ORR): 61.0% vs. 43.2%, P=0.021; HR for death 0.49, 95%CI 0.24–0.999, P=0.050] (15). Most recently, the JCOG1109 NExT trial (UMIN000009482), aiming to compare the efficacy between the CF regimen, the DCF regimen, and CF combined with radiotherapy in patients with locally advanced ESCC, reported its results in the 2022 American Society of Clinical Oncology Gastrointestinal Cancers Symposium (ASCO-GI) meeting, demonstrating that the DCF regimen was superior to the CF regimen in both OS and PFS with a high pCR rate of 19.8% and a manageable toxicity profile (mOS: 4.6 years versus not reach; median progression-free survival (mPFS): 2.7 years versus not reach). Based on this result, the DCF might be a new standard neoadjuvant treatment for locally advanced ESCC (16). In addition, there are other regimens for nCT (**Table 2**). However, it should be pointed out that there is a lack of large size, head-to-head clinical trials to compare the efficacy between nCT regimens. Besides exploring new regimens, the exploration of new modalities has also attracted much attention, like the combination of chemotherapy and immunotherapy, which will be shown below.

NEOADJUVANT CHEMORADIOTHERAPY

Preoperative chemoradiotherapy plus surgery has been widely used for LAECs (**Table 3**). At the early stage, the results from clinical research were controversial since the heterogeneity between the studies included chemoradiotherapy regimens, surgical technique, tumor histology, sample size, and less advanced diagnostic methods. Until the ChemoRadiotherapy for Oesophageal cancer followed by Surgery Study (CROSS) trial and the Phase III Study of Neo-adjuvant Chemoradiotherapy Followed by Surgery for Squamous Cell Esophageal Cancer

TABLE 1 | Characteristics and main outcomes of clinical trials regarding neoadjuvant chemotherapy.

Trials	Histology	Interventions	Size	R0 (%)	P value	pCR (%)	mOS (m)	P value	x-year OS (x,%)	P value
RTOG8911 (5) (1998)	ESCC, AC of esophgus, GEJ	Pre and Post: 3 and 2 cycles of cisplatin, 5-FU	213	62	NS	2.5	14.9	0.53	3, 23	NA
		Surgery	227	59			16.1		3, 26	
OE02 (6, 7) (2002)	ESCC, EAC	Pre: 2 cycles of cisplatin, 5-FU	390	60	<0.0001	4	16.8	0.004	5, 23	0.03
		Surgery	397	53			13.3		5, 17	
MAGIC (8) (2006)	AC of esophgus, GEJ, stomach	Pre and Post: 3 cycles of epirubicin, cisplatin, 5-FU	250	79.3	0.03	NA	NA	0.009	5, 36	NA
		Surgery	253	70.3			NA		5, 23	
FNCLCC-FFCD (9) (2011)	AC of esophgus, GEJ, stomach	Pre and Post: 2/3 and 3/4 cycles of cisplatin, 5-FU	113	87	0.04	NA	NA	NA	5, 38	0.02
		Surgery	111	74			NA		5, 24	
FLOT4-AIO (10, 11) (2016,2019)	AC of stomach or GEJ	Pre and Post: 4 cycles of docetaxel, oxaliplatin, leucovorin, and 5-FU	128	85	0.02	16	50	0.012	5, 45	NA
		Pre and Post: 3 cycles of epirubicin, cisplatin, 5-FU/capecitabine	137	74		6	35		5, 30	
JCOG9907 (2) (2015)	ESCC	Pre: 2 cycles of cisplatin, fluorouracil	164	96	0.04	5	NA	0.01	5, 55	0.04
		Post: 2 cycles of cisplatin, fluorouracil	166	91			NA		5, 43	

RTOG9811, Radiation Therapy Oncology Group trial 8911 trial; OE02, the UK Medical Research Council OE02 trial; MAGIC, the Medical Research Council Adjuvant Gastric Infusional Chemotherapy trial; FNCLCC-FFCD, the Fédération Nationales des Centres de Lutte Contre le Cancer/Fédération Francophone de Cancérologie Digestive trial; JCOG9907, the Japan Clinical Oncology Group 9907 trial; FLOT4-AIO 5-FU, leucovorin, oxaliplatin, and docetaxel (FLOT) versus epirubicin, cisplatin, and 5-FU (ECF) in patients with locally advanced resectable gastric cancer; EAC, esophageal adenocarcinoma; ESCC, esophageal squamous carcinoma; AC, adenocarcinoma; GEJ, gastroesophageal junction; Pre, preoperative; Post, postoperative; 5-FU, 5-fluorouracil; pCR, pathological complete response; mOS, median overall survival; m, months; NA, not available.

(NEOCRTEC5010) trial, the standard treatment status of nCRT for LAEC was established.

For adenocarcinoma, in the CROSS trial, 336 patients, in which EAC accounted for 75%, were enrolled to receive nCRT or surgery alone. Initial results showed that after nCRT, the resection specimen demonstrated that a pCR was 23% and there were no differences in postoperative complications and in-hospital mortality between the nCRT group and the surgery group, which meant the feasibility and acceptable toxicity of the CROSS regimen (3). Long-term results revealed a benefit of OS [mOS: 43.2 vs. 21.7 months (m)] and PFS (mPFS: 29.9 vs. 17.7 m), and the effect of OS was up to 10 years of follow-up, indicating that compared with surgery, the nCRT based on the CROSS regimen significantly prolonged lifespans and improved disease control (27, 28). Thus, nCRT was regarded as the standard treatment for locally EAC and the regimen; 5 cycles of paclitaxel (50 mg/m^2) and 3 cycles of carboplatin (2 mg/AUC) concurrent with 41.4Gy became the standard regimen for nCRT.

For ESCC, however, although the CROSS trial reported a much better efficacy of nCRT (pCR rate: 49%; mOS: 81.6 m:21.1 m; mPFS: 74.7 m: 11.6 m; 10-year OS rate: 46% vs. 23%), it should be noted that only 23% tumor types were ESCC, which might make it hard to convince the benefit of ESCC (3, 27, 28). Most recently, the results from the NEOCRTEC5010 trial demonstrated the better efficacy of nCRT (vinorelbine, cisplatin, 40.0 Gy) versus surgery alone. The R0 rate was significantly higher in the nCRT group than that in the surgery group. Resection specimens showed that the pCR rate was 43.2%. With a median follow-up of 41.0 months, significant differences in mOS and 3-year OS were found in favor of nCRT (mOS: 100.1 vs. 66.5 m, *P*=0.025; 3-year OS: 69.1% vs. 58.9%). Furthermore, disease-free survival (DFS) was also significantly improved in the nCRT group compared with the surgery group (100.1 vs. 41.7 m, P<0.001) (4). Based on these two trials, nCRT also became the standard treatment modality for locally ESC and the regimen, 2 cycles of vinorelbine (25 mg/m^2) and cisplatin (75 mg/m^2) concurrent with 40.0 Gy became the standard regimen for nCRT in China.

In summary, most of the studies comparing the efficacy of nCRT to surgery alone obtained negative results before the 2000s. After the 2000s, many studies showed that nCRT was better than surgery alone. Based on the results from the landmark trials, CROSS and NEOCRTEC5010, nCRT has become the standard treatment for LAECs. The CROSS regimen has been widely used around the world. Current evidence shows that compared with surgery alone treatment, nCRT can ameliorate R0, pCR, OS, and recurrence. After nCRT, R0, pCR, and OS range from 81% to 98%, 25% to 43%, and 16 to 100.1 months, respectively.

NEOADJUVANT CHEMORADIOTHERAPY VS. NEOADJUVANT CHEMOTHERAPY

As mentioned above, nCT and nCRT are two main modalities for the treatment of LAECs. In Japan, based on its own research,

TABLE 2 | Main outcomes of studies regarding different regimens used in neoadjuvant chemotherapy.

Regimen	Phase	Target	Interventions	Size	Rate of completion (%)	pCR (%)	Major adverse events (Grades 3–4)
CF (2)	III	ESCC	2 cycles cisplatin, 5-FU	164	85.4	5	Leukopenia 3% Thrombocytopenia 1% Diarrhea 1% Mucositis 3%
DCF (12)	II	ESCC	3 cycles of docetaxel, cisplatin,5-FU	42	90.5	17	Leukopenia 45.2% Neutropenia 83.3% Anorexia 7.1%
ACF (17)	II	ESCC	2 cycles of adriamycin, cisplatin, and 5-FU	81	88	0.00	Neutropenia 69% Leukopenia 58% Febrile neutropenia 17%
DOS (18)	I	Locally advanced AEG; advanced AEG, without distant metastasis	Level 1: 2 cycles of docetaxel, cisplatin,S-1 Level 2: 2 cycles of docetaxel, cisplatin, S-1	12	100	25	level 1: Neutropenia 50% Leukopenia 17% Febrile neutropenia 17% Level 2: Neutropenia 83% Leukopenia 50%
DCS (19)	II	ESCC of the thoracic esophagus	3 cycles of docetaxel, cisplatin, S-1	58	90	10	Leukopenia 50% Neutropenia: 68% Fbrile neutropenia: 18% hyponatremia 23%
DNF (20)	II	ESCC	3 cycles of docetaxel, nedaplatin, 5-FU	28	89.30	32	Neutropenia 39.3% Leukocytopenia 32.1% Febrile neutropenia 10.7%
ECX (21)	III	EAC	4 cycles of epirubicin, cisplatin, capecitabine	446	81	Local pathology assessment: 11 Central pathology assessment: 7	Neutropenia 23% Diarrhea: 8% Nausea: 6% Vomiting: 6%
DNS (22)	II	ESCC	2 cycles of docetaxel, nedaplatin, S-1	32	96.90%	15.60%	Neutropenia 25% Leukopenia 18.8% Mucositis 15.6% Hyponatremia 15.6%

pCR, pathological complete response; ESCC, esophageal squamous carcinoma; AEG, adenocarcinoma of esophagogastric junction; EAC, esophageal adenocarcinoma.

nCT was the standard modality for LAECs. In some western countries, nCRT was the preferred treatment modality based on the results of the CROSS trial. Based on the NEOCRTEC5010, nCRT also has become the standard treatment for locally ESCC in China. Whether nCRT or nCT brings better efficacy for patients with LAECs is still uncertain so far. Research regarding the comparison between nCT versus nCRT directly is limited and the current evidence is inconclusive. Current research demonstrated that whether in ESCC or EAC, patients receiving nCRT are more likely to reach pCR. The pCR rate in nCRT is higher than that in nCT. However, there are no differences between these two modalities in survival outcomes.

For EAC, only three prospective studies directly compared the advantages and disadvantages of the two modalities. In the PreOperative therapy in Esophagogastric Adenocarcinoma (POET) trial, patients after nCRT showed a significantly higher pCR rate of 14.3% compared with 1.9% after nCT. For OS, there was a trend in favor of nCRT as shown by a longer mOS and higher rate of long-term survival (29, 30). In the Neoadjuvant Chemotherapy Versus Radiochemotherapy for Cancer of the Esophagus or Cardia (NeoRes) trial, which enrolled over 70% of patients with EAC, the authors demonstrated a significant increase of 19% of pCR in the nCRT setting but no differences for OS compared with nCT (31, 32). Also, Burmeister et al. reported similar results that the pCR rate in nCRT significantly increased, while mOS and the long-term survival rate were only higher numerically (33).

The research about the efficacy of nCRT versus nCT in ESCC is limited (**Table 4**). The results from the NeoRes trial containing less than 30% of patients with ESSC could not find benefit in long-term survival although the pCR rate after nCRT was significantly higher than after nCT. The trial, Comparison Between NCRT and NCT Followed by MIE for Treatment of Locally Advanced Resectable ESCC (CMISG1701), reported its initial results, which were to compare the efficacy of four cycles of paclitaxel (50 mg/m^2)/cisplatin(25 mg/m^2) as nCRT regimen, followed by minimally invasive esophagectomy (MIE) versus two cycles of paclitaxel (135 mg/m^2)/cisplatin(75 mg/m^2) as nCT regimen followed MIE in ESCC. The study showed that patients undergoing nCRT had better pathologic outcomes including higher pCR (35.7% vs. 3.8% P<0.01) and less lymph nodes involved (66.1% vs. 46.2%, P = 0.03). However, 1-year OS was not different between the two groups (34).

As the lack of evidence of direct comparison, meta-analyses were conducted. A network meta-analysis including 26 studies compared the efficacy of surgery alone, nCT, neoadjuvant radiotherapy, nCRT, surgery followed by adjuvant chemotherapy, adjuvant radiotherapy, or adjuvant chemoradiotherapy. A ranking

TABLE 3 | Characteristics and main outcomes of clinical trials regarding neoadjuvant chemoradiotherapy versus surgery.

Trials	Histology	Regimen	Size	R0 (%)	P-value	pCR (%)	mOS (m)	P-value	x-year OS (x,%)	P-value
Walsh (23) (1996)	EAC	2 cycles of cisplatin, 5-FU+40 Gy	58	NA	NA	25	16	0.01	3, 32	0.01
		Surgery	55	NA			11		3, 6	
Bosset (24) (1997)	ESCC	2 cycles of cisplatin+37 Gy	143	81.2	0.017	26	18.6	0.78	NA	NA
		Surgery	139	68.6			18.6		NA	
Burmeister (25) (2005)	ESCC, EAC	Cisplatin, 5-FU+35 Gy	128	80	0.0002	16	22.2	0.44	NA	NA
		Surgery	128	59			19.3		NA	
GALGB9781 (26) (2008)	ESCC, EAC, AC of GEJ	Cisplatin+5-FU+50.4 Gy	30	NA	NA	40	4.48 y	0.002	5, 39	NA
		Surgery	26	NA			1.79 y		5, 16	
CROSS (3) (2012)	ESCC, EAC, AC of GEJ	5 cycles of carboplatin, paclitaxel+41.4 Gy	188	92	<0.001	29	49.4	0.003	5, 47	NA
		Surgery	180	69			24		5, 34	
NEOCRTEC 5010 (4) (2018)	ESCC	2 cycles of vinorelbine, cisplatin +40.0 Gy	224	98.4	0.002	43.2	100.1	0.025	3, 69.1	NA
		Surgery	227	91.2			66.5		3, 58.9	

GALGB9781, Cancer and Leukemia Group B 9781; CROSS, the ChemoRadiotherapy for Oesophageal cancer followed by Surgery Study trial; NEOCRTEC5010 Phase III Study of Neo-adjuvant Chemoradiotherapy Followed by Surgery for Squamous Cell Esophageal Cancer; EAC, esophageal adenocarcinoma; ESCC, esophageal squamous carcinoma; AC, adenocarcinoma; GEJ, gastroesophageal junction; pCR, pathologic complete response; mOS, median overall survival; m, months; y, years; NA, not available.

analysis reported that nCRT might be the best option for patients diagnosed with LAECs. When compared to surgery alone, in all the treatments, nCRT yielded the best benefit in terms of OS and PFS/DFS (HR = 0.76, 95%CI 0.67–0.85; HR = 0.8, 95%CI 0.68–0.94, respectively). Also, only nCRT associated with a statistically confident decrease in locoregional recurrence or distant metastasis [odd ratios (OR)=0.48, 95%CI 0.30–0.77; OR = 0.67, 95%CI 0.49–0.93, respectively] (35).

To sum up, currently, it is still unable to define which modality is better for LAECs. Current evidence suggests that despite the histological type, patients with LAECs are more likely to develop pCR after nCRT, whereas in the OS of nCRT, there was no statistical improvement compared to that of nCT. Reasons why the higher rate of pCR after nCRT fails to translate into the benefit of survival, are still a primary concern. The toxicities of treatments and perioperative complications may contribute to the problem. The POET trial showed that the grade 3/4 toxicities were 5% in the nCT group, while grade 3/4 leukocytopenia and thrombocytopenia were 12% and 5%, respectively, in the nCRT group (29). The NeoRes trial demonstrated that the severity of postoperative complications in the nCRT group was significantly higher than that in the nCT group (P=0.001) (31). Long-term results showed that the patients after nCRT had higher risks of postoperative complications (9% vs. 1% P=0.02) (32). Meta-analyses also reported a significantly higher postoperative mortality in nCRT (RR 1.58, 95% CR 1.00–2.49) (36). We hypothesize that in looking for new drugs or treatment modalities that can lead to fewer toxicities, and the improvement of surgery technology, the introduction of early interdisciplinary supportive care (ESC) may help solve the problem. Most recently, a phase III clinical trial explored whether ESC combined with the standard first-line treatment for patients with metastatic esophageal cancers could improve the prognosis. Results showed the mOS in the ESC group was significantly higher than those in the standard care group (14.8 vs. 11.9 m, HR 0.68, 95%CI 0.51–0.9, P=0.021) (37). Another study demonstrated that a multidisciplinary team approach started before neoadjuvant therapy would decrease the risk of AE rate during chemotherapy (P=0.007) and provide safe perioperative conditions(P=0.003) (38). MIE is becoming more and more common in surgical treatments. A new meta-analysis has reported that MIE decreased 18% risk of all-cause 5-year mortality for patients with esophageal cancers compared with open surgery (39). Nowadays, the regimens of neoadjuvant therapy are various. CROSS, MAGIC, and FLOT regimens have been widely used. Here, we summarize the ongoing clinical trials comparing the efficacy of nCRT versus nCT based on these regimens, expecting that more valid and powerful evidence can be provided by these trials (**Table 5**).

PROBLEMS IN NEOADJUVANT CHEMORADIOTHERAPY

For nCRT, however, there are some problems to be solved, which are shown as follows.

Nowadays, the optimal regimen for nCRT is still inconclusive. The excellent efficacy of nCRT showed in clinical trials cannot be reproduced completely in a real-world scenario (**Table 6**). Four studies that evaluated the efficacy of the CROSS regimen in the real-world scenario demonstrated that patients who did not fully meet the CROSS criteria had a lower efficacy than those who fully met them, showing a lower pCR and mOS and possibly higher postoperative morbidity and mortality (40–43). Moreover, even patients eligible for the criteria could not obtain the efficacy as well as that in the CROSS trial. Based on the results of the CROSS trial, the CROSS regimen has replaced the CF-based regimen that was used widely before. However, no prospective head-to-head comparative study was conducted. A propensity score-matched study, comparing the efficacy of the cisplatin/fluorouracil regimen versus the CROSS regimen in patients with locally advanced ESCC, recently reported that there were no differences in the pathological or survival outcome between the two regimens but the study showed a trend in favor of the cisplatin/fluorouracil regimen (44). For adenocarcinoma, one retrospective study (adenocarcinoma: 86%) showed that the CF regimen could increase the pCR rate (P=0.032), improve the recurrence-free survival (HR 0.39, 95%CI 0.21–0.73, P=0.003) and OS (HR 0.46, 95%CI 0.24–0.87, P=0.016) (45). In addition, retrospective research, comparing the NEOCRTECT5010 regimen to the CF regimen, demonstrated the former increased pCR rate (47.4% vs. 28.1%, P=0.034) and contributed to better OS (52.8 vs. 25.2 m, P=0.001) while leading to increasing hematologic toxicities (P=0.03) (46).

The radiation dose is various in nCRT ranging from 37 to 50.4 Gy. A retrospective study evaluated the efficacy of high dose (>45Gy) versus low dose (≤45 Gy) in ESCC, showing no differences in pCR rate and survival (47). Recently, a systematic review incorporated 110 studies, involving ESCC/EAC, where patients receiving nCRT up to a dose of 50.4 Gy, to evaluate the efficacy and safety of different radiation doses and try to find an optimal dose. Results demonstrated that 40.0–41.4 Gy might be a rational dose for nCRT (48). Prospective controlled studies are needed to confirm the optimal dose.

So far, the surgical interval for nCRT is 4–6 weeks. The optimal surgical interval for nCRT is still inconclusive. The proper extension of the surgical interval may increase the pCR rate because of the shrinkage of tumors under the effects of nCRT. Also, it gives patients more time to recover from the preoperative treatments, which may reduce the risk of surgical-related AEs. All these may bring a benefit of survival. However, some research reported the increase in pCR rate profiting from the extending surgical interval failed to translate into a benefit of survival (49, 50). There may be several reasons. First, these studies are retrospective studies where patients delayed surgeries because of their poor body conditions or the AEs from nCRT rather than their preferences. Second, although extending surgical interval increases the pCR rate, its contribution is not enough to reflect on a statistically significant benefit in survival. Subgroup analysis, comparing the efficacy of extension of surgical interval between patients reaching pCR versus non-pCR, showing a significantly better survival benefit supported this point (8.7 years for patients with pCR vs.

TABLE 4 | Characteristics and outcomes of studies regarding neoadjuvant chemotherapy vs. neoadjuvant chemoradiotherapy.

Studies	Target	Regimen	Size	R0 (%)	pCR (%)	OS (m)	3-year OS (%)	5-year OS (%)
Neoadjuvant chemotherapy vs. neoadjuvant chemoradiotherapy								
Michael Stahl (29, 30) (2009, 2017)	AC of GEJ	**nCT:** 2.5 cycles of 5-FU,leucovorin,cisplatin **nCRT:** 2 cycles of 5-FU, leucovorin, cisplatin followed by cisplatin, etoposide+30 Gy	119	69.5 vs. 72 NS	1.9 vs. 14.3 P=0.03	21.1 vs. 30.8 m P=0.055	26.1 vs. 46.7	24.4 vs. 39.5
NeoRes (31, 32) (2016,2018)	ESCC, EAC, AC of GEJ	**nCT:** 3 cycles of cisplatin, 5-FU **nCRT:** 3 cycles of cisplatin, 5-FU+40 Gy	181	74 vs. 87 P=0.04	9.0 vs. 28.0 P=0.002	31.4 vs. 36.0 m	49 vs. 47 P=0.77	39.6% vs. 42.2 P=0.60
Bryan H. Bumeister (33) 2011	EAC, AC of GEJ	**nCT:** 2 cycles of cisplatin, 5-FU **nCRT:** 2 cycles of cisplatin, 5-FU+35 Gy	75	80.5 vs. 84.6 P=0.61	0 vs. 13 P=0.02	29 vs. 32 m P=0.83	49 vs. 52 P=0.97	36 vs. 45 P=0.60
Hao Wang (34) 2021	ESCC	**nCT:** 2 cycles of paclitaxel, cisplatin **nCRT:** 4 cycles of paclitaxel, cisplatin+40 Gy	264	96.2 vs. 97.3 P=0.92	3.8 vs. 35.7 P<0.01	NA	1-year OS 82.6 vs. 87.1 P = .30	NA

NeoRes, the Neoadjuvant Chemotherapy Versus Radiochemotherapy for Cancer of the Esophagus or Cardia trial; AC, adenocarcinoma; GEJ, gastroesophageal junction; EAC, esophageal adenocarcinoma; NA, not available; nCT, neoadjuvant chemotherapy; nCRT, neoadjuvant chemoradiotherapy..

TABLE 5 | Characteristics clinical trials regarding neoadjuvant chemotherapy vs. neoadjuvant chemoradiotherapy.

Clinical trials	Phase	Size	Conditions	Interventions	Endpoints		Status
					Primary	Secondary	
NCT01404156	II/III	60	EAC, AEG	**nCT:** FLOT/ECF/ECX regimen + surgery **nCRT:** CROSS regimen concurrently with 45 Gy + surgery	Compliance to treatment, Treatment response	3-year OS, DFS QoL	Recruiting
NCT02509286	III	438	EAC, AEG	**nCT:** FLOT **nCRT:** CROSS regimen concurrently with 41.4 Gy + surgery	OS	PFS, site of failure, RFS, QoL, complications	Not recruiting
NCT01726452	III	377	EAC, AEG	**nCT:** modified MAGIC/FLOT + surgery **nCRT:** CROSS regimen concurrently with 41.4 Gy + surgery	OS	None	Not recruiting
UMIN000009482	III	600	ESCC	**nCT:** 2 cycles of cisplatin,5-FU or docetaxel, cisplatin, 5-FU +surgery **nCRT:** 2 cycles of cisplatin, 5-FU concurrently with 41.4 Gy + surgery	OS	PFS, R0, pCR, AE, morbidity, toxicity, response rate	No longer recruiting
NCT03001596	NA	264	ESCC	**nCT:** 2 cycles of paclitaxel, cisplatin +MIE **nCRT:** 4 cycles of paclitaxel, cisplatin concurrently with 40 Gy+MIE	OS	PFS, R0, RFS, QoL, pathological response rate, treatment-related complication, positive lymph nodes' number	Completed
NCT04138212	III	456	ESCC	**nCT:** 2 cycles of paclitaxel, cisplatin + surgery **nCRT:** CROSS regimen concurrently with 41.4 Gy + surgery	OS	DFS, pCR, AE, complications	Recruiting
NCT03579004	II	48	ESCC	**nCRT:** 2 cycles of paclitaxel, cisplatin+ paclitaxel, cisplatin concurrently with 44 Gy+surgery	DFS	OS, ORR, pCR, number of treatment-related AEs	Unknown
NCT03013010	III	682	AC of stomach, GEJ	**nCT:** 3 cycles of S-1, oxaliplatin+ surgery **nCRT:** 1 cycle of S-1, oxaliplatin +5 weeks of S-1and oxaliplatin concurrently with 45 Gy+surgery+3 cycles of S-1 and oxaliplatin	DFS	OS, R0, toxicity, complications, pathological response rate	Recruiting

EAC, esophageal adenocarcinoma; AEG, adenocarcinoma of esophagogastric-junction; nCT, neoadjuvant chemotherapy; nCRT, neoadjuvant chemoradiotherapy; AC, adenocarcinoma; GEJ, gastroesophageal junction; ESCC, esophageal squamous carcinoma; MIE, minimally invasive esophagectomy; OS, overall survival; DFS, disease-free survival; PFS, progression-free survival; RFS, recurrence-free survival; pCR, pathological response rate; QoL, quality of life; AE, adverse events; RFS, recurrence-free survival time; ORR, objective response rate; NA, not applicable. FLOT 4 cycles of 5FU (2,600 mg/m^2), leucovorin (200 mg/m^2), oxaliplatin (85 mg/m^2), and docetaxel (50 mg/m^2) on day 1, q2w perioperatively, ECF/ECX 3 cycles of epirubicin (50 mg/m^2) on day 1 cisplatin (60 mg/m^2),5-FU (200 mg/m^2)/capecitabine (625 mg/m^2) for 21 days perioperatively, CROSS 5 cycles of paclitaxel (50 mg/m^2) and carboplatin (2 mg/AUC) on days 1, 8, 15, 22, and 29, modified MAGIC 3 cycles of epirubicin (50 mg/m^2) on day 1, cisplatin (60 mg/m^2) on day1/oxaliplatin (139 mg/m^2) on day 1, 5-FU (200 mg/m^2) for 21 days/ capecitabine (625 mg/m^2) perioperatively.

2.0 years) (49). Recently, one prospective research, avoiding the gap of the first reason, reported that the extension of the surgical interval had no effects on short-term operative outcomes (overall postoperative complication: 63.2% vs. 72.6%, *P*=0,134; severe postoperative complications: 31.6% vs. 34.9%; median length of hospital stays: 15 vs. 17 d, *P*=0.234) (51). More prospective studies are needed to focus on the effect of surgical interval on survival.

Although nCRT improves the recurrences of patients compared with surgery, the recurrent rate after nCRT is still high. The ten-year outcome of the CROSS trial revealed that recurrences occurred in 48% of patients, and 33.7% of patients reported in the NEOCRTEC5010 trial (4, 28). Most recurrences occurred in the first 3 years after surgery. Compared with distant metastases, nCRT mainly improved local or regional recurrences. Data from the ten-year outcome of the CROSS trial demonstrated that the overall local-regional recurrence rate after nCRT reduced significantly from 40% to 21% compared with surgery alone (28). Similarly, in the NEOCRTEC5010 trial, nCRT significantly improved the overall local–regional recurrence rate (14.1% vs. 22.5%, *P*=0.031) while the overall distant metastasis rate had no statistical differences (23.9% vs. 31.7%, *P*=0.08) (52). Thus, distant metastasis is the main failed mode after nCRT. Subgroup analysis showed that patients who reached pCR had a lower recurrence rate than those with non-pCR. Histologically, the patients with ESCC or EAC who did not reach pCR after nCRT showed a different recurrent pattern. The patients with EAC showed a likelihood of recurrence compared with ESCC (43.2% vs. 34.3%, *P*=0.023). The patients with ESCC had a higher risk of regional and supraclavicular recurrences while a lower hematogenous metastasis compared with EAC. In addition, it was reported compared with EAC, patients with ESCC had a significantly higher rate of failure to receive salvage treatments (*P*=0.005) mainly because of poor performance status (53).

The high recurrence rate after nCRT demands a close monitor. Besides, salvage measures are essential when recurrence occurs. The

TABLE 6 | Comparison of efficacy of CROSS regimen in real-world scenario versus clinical trial.

Indexes	CROSS-eligible	Extended-CROSS	P-value	CROSS trial`
R0	95.8%[1]	95.2%[1]	0.406[1]	92%
	83.3% for ESCC[2]	84% for ESCC[2]	0.959[2]	
pCR	16.8% for EAC[1]	16.9 for EAC[1]	0.908 for EAC[1]	29% for overall
	48.2% for ESCC[1]	33.3 for ESCC[1]	0.000 for ESCC[1]	23% for EAC
	33.3% for ESCC[2]	20% for ESCC[2]	0.253[2]	49% for ESCC
	27% for overall[3]	28% for overall[3]	0.76[3]	
mOS	24.2 m for ESCC[2]	12.7 m for ESCC[2]	0.047[2]	48.6 m for overall
	58.5 m for overall[3]	35.0 m for overall[3]	0.90[3]	43.2 m for EAC
	37.3 m for overall[4]	17.2 m for overall[4]	0.004[4]	81.6 m for ESCC
Postoperative mortality	3.2%[1]	4.6%[1]	0.037[1]	2%
(<30 d)	0[2]	0[2]	1.00[3]	
	3%[3]	3%[3]	0.486[4]	
	2.2%[4]	4.2%[4]		
Postoperative morbidity	58.3%[1]	61.8%[1]	0.048[1]	46% for pulmonary complications
	16.7% for anastomotic leakage[2]	12% for anastomotic leakage[2]	NS[2]	21% for cardiac complications
	2.8% for chylothorax[2]	4% for ischemic conduit[2]	0.83[3]	10% for chylothorax
	5.6% for fistula[2]	4% for mediastinitis[2]	NS[4]	3% for mediastinitis
	2.8 for ischemic conduit[2]	24% for cardiac complications[2]		22% for anastomotic leakage
	22.2 for cardiac complications[2]	16% for pulmonary complications[2]		
	19.4% for pulmonary complications[2]	8% for urinary complications[2]		
	2.8% for urinary complications[2]	12% for vocal cord palsy[2]		
	19.4% for vocal cord palsy[2]	63%[3]		
	64%[3]			

pCR, pathological complete response; mOS, median overall survival; ESCC, esophageal squamous carcinoma; EAC, esophageal adenocarcinoma, [1] (40), [2] (41), [3] (42), [4] (43).

differences in recurrence patterns between ESCC and EAC require different strategies based on histological tumor types. For EAC, distant metastasis was the main recurrence pattern, which means the necessity of the systematic treatment after nCRT. The Checkmate577 trial had reported that the addition of nivolumab as an adjuvant therapy could significantly reduce the risk of recurrences for patients with residual disease after nCRT (HR 0.74, 95%CI 0.60–0.92). The DFS in the nivolumab group was twice as long as that in the nCRT alone group (22.4 vs. 11.0 m, P<0.001) (54). For ESCC, local–regional recurrence was the main failed mode, indicating the need for the enhancement of local treatment. Systematic lymph node dissection has been recommended in the surgery alone for patients with esophageal cancers. However, whether patients with nCRT followed by systematic lymph node dissection can obtain a survival benefit is debatable. Most recently, a second analysis from the result of the NEOCRTEC5010 trial revealed that systematic lymph node dissection did not increase the surgical risk and could improve the survival and control of disease for patients with nCRT (mOS: 100.0 vs. 85.5 m, *P*=0.01; 3-year OS: 75.2% vs. 61.5%; 3-year DFS: 70.2% vs. 55.5%, *P*<0.001). Compared with the dissection of lymph node <20, the dissection of lymph node ≥20 brought a lower recurrence rate (25.8% vs. 41.2%, *P*=0.027) and better control of disease (5.2% vs. 18.8%, *P*=0.004) (55). Thus, systematic lymph node dissection should be recommended in nCRT for ESCC.

EVALUATION FOR THE EFFICACY OF NEOADJUVANT SETTING

pCR is a strong predictor of a good prognosis after nCRT. Many studies have shown that patients reaching pCR after nCRT would obtain a longer survival and a lower risk of recurrences compared with those with non-pCR. Current evidence shows that after nCRT, the rate of pCR ranges from 20% to 43%, which means that a lot of patients still cannot benefit from nCRT. Furthermore, treatment-related toxicities and the extension of operation may lead to a poorer physical condition and tumor progression. Thus, the development of methods to evaluate a pathological response after nCRT is essential to improve the efficacy of nCRT and avoid unnecessary treatments.

The accuracy of using a single imaging method to find residual disease after nCRT is limited. Recently, a meta-analysis reported the limited accuracy of endoscopic biopsies, endoscopic ultrasound, and positron emission tomography with 2-deoxy-2-[fluorine-18]fluoro-D-glucose integrated (with computed tomography) (18F-FDG PET(-CT)) as single modalities to detect residual disease after nCRT for patients with LAECs (56).

Magnetic resonance imaging (MRI) has been reported to have a promising accuracy in the evaluation of efficacy after nCRT. A prospective study showed the relative increase of the parameter of diffusion-weighted magnetic resonance imaging (DW-MRI), $\Delta ADC_{during\text{-}pre}$(median apparent diffusion coefficient; during 2–3 weeks during nCRT) was positively correlatively with pCR. A cut-off value of 29% yielded a sensitivity of 100%, specificity of 75%, accuracy of 95%, positive predictive value of 94%, and negative predictive value of 100% (57). The parameters of diffusion contrast-enhanced magnetic resonance imaging (DCE-MRI), ΔAUC (area under the concentration–time curve), were reported to predict pCR. At a cut-off of 24.6%, $\Delta AUC_{post\text{-}pre}$ mostly predicted a pCR, yielding a sensitivity of 83%, specificity of 88%, positive predictive value of 71%, and negative predictive value of 93% (58). Based on these two studies, another study evaluated the accuracy of the combination of DW-MRI and

DCE-MRI and reported their complementary value (59). The addition of MRI into gastroscopy with biopsies and endosonographic ultrasound with fine-needle aspiration has been reported to improve the detection of residual tumor after nCRT, as shown by an increased sensitivity from 47% to 89% (60). A prospective study evaluated the combined value of DW-MRI and 18F-FDG PET/CT to predict pCR in patients after nCRT. Results showed that early changes of the parameter on DW-MRI during nCRT and changes on 18F-FDG PET/CT after nCRT might yield a complementary value in the assessment of pCR (61). The Surgery AS Needed for Oesophageal Cancer (preSANO) trial evaluated the efficiency of the combination of different methods to detect residual disease after nCRT and tried to propose an optimal modality. Results showed that endoscopic ultrasonography, bite-on-bite biopsies, and a fine-needle aspiration of suspicious lymph nodes to detect locoregional residual disease combined with PET-CT for the detection of interval metastases were an effective modality for clinical evaluation (62). Now, a phase III trial (NTR6803) has been conducted to compare the outcome of active surveillance with standard resection in patients who reached pCR by using this strategy. Based on the preSANO trial, Chinese scholars are evaluating this strategy in patients with locally advanced ESCC (NCT03937362). Another ongoing trial is evaluating the combined value of DW-MRI, DCE-MRI, 18F-FDG PET/CT, and circulating tumor DNA (ctDNA) to predict the pathological response (NCT03474341).

Compared with multi-imaging methods, a single-imaging method provides limited information. Moreover, usually, imaging methods like CT and endoscopic ultrasound mainly provide anatomical information. However, there are lots of biological parameters like tumor metabolism, structure, and function of blood vessels in tumor tissues, which are sensitive and change early when the tumor tissues react to clinical interventions. This may explain that the combination of multiple imaging methods and addition of MRI can improve the evaluation of pathological response after nCRT. In the future, more attention should be paid to the application of radiomics in the efficacy evaluation after nCRT.

Biomarkers, related to tumor growth, DNA repair, cell cycle, etc., have been investigated to see the predictive value in histology response after nCRT in LAECs. ERCC1 and p53 were probably studied widely. As results regarding the predictive value of p53 to pCR were debatable, Zhang et al. assembled 28 studies in their meta-analysis and reported that the wild-type form of p53 status was probably a predictive biomarker for pCR after nCRT (63). Other molecular markers like cyclinD, p53R2, COX-2, Gli-1, and miRNA also have been explored. Recently, one meta-analysis analyzed that 56 biomarkersm except for p53 from 46 articles, demonstrated that the low expression of COX2, miR-200c, ERCC1, and TS, or a higher expression of CDC258 and p16, were associated with the prediction of response for patients receiving neoadjuvant chemo(radio)therapy (64). However, there are still no effective biomarkers to predict whether someone will respond to chemoradiotherapy or not. The joining of imaging techniques and specimen detection (tissue and/or liquid) has rarely been reported yet, which may have synergistic effects on the evaluation or prediction of response to the neoadjuvant setting.

IMMUNOTHERAPY IN LOCALLY ADVANCED ESOPHAGEAL CANCER

With the insight of the molecular mechanisms of tumors and highlight of individualized treatment, targeted therapy has emerged as a hot direction. The overexpression of Epidermal Growth Factor Receptor (EGFR), Erb-B2 Receptor Tyrosine Kinase 2 (HER2), and Vascular Endothelial Growth Factor Receptor (VEGFR) has been reported in esophageal cancer, which enhances tumor occurrence, progression, and drug resistance. Adding drugs targeting these molecules to the current treatment may bring a synergistic effect. However, so far, most studies failed to show a satisfactory efficacy (65, 66). In recent years, ICIs have been a new modality used in tumor treatments like none small cell lung cancer and melanoma because of their promising efficacy. For esophageal cancer, some research has reported the anti-tumor activity of ICIs. Three landmark clinical trials, Study of Pembrolizumab (MK-3475) Versus Investigator's Choice Standard Therapy for Participants With Advanced Esophageal/Esophagogastric Junction Carcinoma That Progressed After First-Line Therapy (KEYNOTE181), Study of Nivolumab in Unresectable Advanced or Recurrent Esophageal Cancer (ATTRACTION-3), and Study of SHR-1210 Versus Investigator's Choice Standard Therapy for Participants With Advanced Esophageal Cancer (ESCORT) have confirmed the anti-tumor activity of pembrolizumab, nivolumab, and camrelizumab in second-line treatment for advanced/metastatic esophageal cancer by demonstrating that these drugs improved survival, the ORR, and duration of response (DoR) compared with conventional chemotherapy (67–69). With the success in second-line treatments, the usage as first-line treatment in advanced/metastatic esophageal cancer is already being developed. A KEYNOTE-590 trial reported that pembrolizumab combined with a platinum-based regimen (cisplatin/5-FU) as the first-line treatment for advanced/metastatic esophageal cancers showed better survival outcomes compared with a platinum-based regimen alone. For safety, the two regimens were similar (70). A Checkmate-649 trial firstly compared the efficacy of nivolumab combined with capecitabine/oxaliplatin or leucovorin/fluorouracil/oxaliplatin to chemotherapy alone. Data showed that the ORR in patients receiving the new regimen was more than 50%. Compared with chemotherapy alone, the new regimen prolonged the DoR by 2.5 months, reduced the risk of death by 23%, increased the median OS by 2.2 months (71). The Study of SHR-1210 in Combination With Chemotherapy in Advanced Esophageal Cancer (ESCORT-1st) trial evaluated the efficacy of camrelizumab combined with paclitaxel/cisplatin as the first-line regimen for advanced/metastatic ESCC. Data demonstrated that compared with chemotherapy alone, camrelizumab combined with

chemotherapy reduced the risk of death by 30% and 44% in the risk of progression. The median OS and PFS were prolonged by 2.1 and 1.3 months, respectively. The ORR rate was 72.1% in the new regimen group, and the DoR increased by 2.4 months. Moreover, the addition of camrelizumab did not increase the rate of AEs (72).

All these results revealed that immunotherapy combined with chemotherapy could improve survival with no unacceptable AEs for advanced/metastatic esophageal cancers. Notably, the higher ORR after immunotherapy combined with chemotherapy means more patients can reduce their tumor volume by 30% after the treatment. Tumor shrinking may lead to downstage, which may lay a foundation for the addition of ICIs into neoadjuvant therapy for LAECs (**Supplementary Table 1**).

For EAC, one trial (NCT03044613) evaluated the safety and efficacy of the induction therapy of nivolumab, followed by mivolumab concurrently with nCRT. Data suggested acceptable toxicities without the delay of surgery and a high pCR of 40% (73).

For ESCC, one research reported a promising efficacy with acceptable toxicity of the addition of pembrolizumab to paclitaxel–carboplatin-based perioperative therapy, showing a high pCR rate of 46.1% and a rate of 82.1% in 1-year OS (74). The trial, Preoperative Anti-PD-1 Antibody Combined With Chemoradiotherapy for Locally Advanced Squamous Cell Carcinoma of Esophageus, was conducted to evaluate the safety and efficacy of a combination of pembrolizumab and the CROSS regimen. Of 65% grade ≥3 AEs, the most common were leukopenia, lymphopenia, anemia, esophagitis, alopecia, and fatigue, which were all acceptable in clinical practices. The addition of pembrolizumab did not lead to the delay of surgery. After the treatment, the pCR reached 55.6%, which was higher than 49% in the CROSS trial and 43.2% in the NEOCRTEC5010 trial (75). The trial, PDL-1 Targeting in Resectable esophageal Cancer (PERFECT), reported the feasibility of atezolizumab combined with the CROSS regimen for locally advanced ESCC. The rate of completion was 83% with no effects on operation interval. 40% of grade ≥3 AEs were observed, of which the most common AEs were anorexia, nausea, and syncope. The rate of immune-related AEs was 16% including 2 for grade 3 rash, 2 for grade 2 colitis/proctitis, and 2 for grade 2 thyroiditis. However, PCR, mOS, and mPFS had no statistical differences compared with a CROSS regimen cohort (114 patients) (76).

As shown above, current studies suggested neoadjuvant immunotherapy combined with chemo(radio)therapy was feasible. Patients who received such modality had a comparable or even higher pCR compared with conventionally neoadjuvant therapy. Notability, most current results are from phase I/II trials. Whether neoadjuvant immunotherapy combined with chemo (radio)therapy can bring a long survival benefit for patients with LAEC requires adequately valid evidence from phase III trials. The synergistic effects between immunotherapy, chemotherapy, and radiation have been reported. Chemotherapy can either lead to immunosuppression or immune activation, which is related to the change of the composition of the tumor microenvironment like priming or inhibiting the expression of immunosuppressor genes (77). Radiation can help expose the tumor antigen to enhance immune response, while immunotherapy can increase the sensitivity of tumors to radiation. These interactive actions should inspire scientists to focus on the sequence between immunotherapy and conventional chemo(radio)therapy. So far, a trial (NCT03985670) is exploring the effect of the sequence of toripalimab and chemotherapy (paclitaxel/cisplatin, sequential or concurrent) on pCR. Initial results showed a fivefold discrepancy in DFS between the two settings (78). Moreover, as the synergistic effects between immunotherapy and radiation, the modality of radiation including dose and fraction may be changed since its role is no longer to lead to cytotoxicity alone but also to assist the immune system. The interactive actions between radiation and tumor microenvironment should be paid attention to. In addition, the KEYNOTE181 trial showed different efficacy in different populations. Also, some research demonstrated that patients with a higher expression of PD-L1 obtain more benefits. All these raise another question about how to screen the benefit population.

SUMMARY

At present, neoadjuvant therapy is the mainstay for patients with locally esophageal carcinoma. Based on several landmark trials, nCRT has been confirmed to be superior to surgery alone in R0 resection, survival outcomes, and recurrence. So far, the standard regimens for nCRT are the paclitaxel–carboplatin-based regimen for EAC or ESCC from the CROSS trial and vinorelbine–cisplatin-based regimen for ESCC from the NEOCRTEC5010 trial. nCT is also a kind of strategy for LAECs. Especially in Japan, based on its own studies, nCT with the CF-based regimen is the standard modality for locally advanced ESCC. The DCF regimen may replace the CF regimen as a new standard regimen for nCT based on the results from the JCOG1109 NExT trial recently. For locally advanced EAC, nCT based on the MAGIC regimen or perioperative chemotherapy based on the FLOT regimen are the main strategies. As the evidence from randomized clinical trials is limited, it is not yet clear which of these two treatment modalities is better. Histologically, the OE02 trial demonstrated that the efficacy of nCT based on the CF regimen is irrespective of the histological type as no heterogeneity of treatment effect (P=0.81). However, the results from meta-analyses demonstrated that nCT did not improve the survival of patients with ESCC(P=0.18) but increased the survival of those with EAC (P=0.01) (79). Besides, as mentioned above, the recurrence pattern between these two pathologic tumor types is different. Patients with EAC are more likely to have distant metastasis, while those with ESCC are more prone to local recurrence. Furthermore, compared with EAC, ESCC is more sensitive to radiation. Considering these facts, patients with locally advanced EAC might be prone to receive preoperative or perioperative chemotherapy, while those with locally advanced ESCC might be prone to choose nCRT. However, it is more essential to depend on individual characteristics and the building of hospital technology such as physical conditions, individual tumor characteristics, the prediction of pCR or recurrence, and a multidisciplinary cancer

treatment team. Although nCRT has been regarded as the standard treatment for LAECs, some unsolved clinical problems exist like the optimal regimen, radiation dose, surgical intervals, and a high risk of recurrences. pCR is an important predictor of a good prognosis of patients. However, currently, accurate methods to evaluate pathological response after nCRT are limited. Future studies should focus on the research regarding multiple parameters to predict pCR. Immunotherapy combined with neoadjuvant therapy has shown promising anti-efficacy. For a better synergistic effect, future research should focus on the sequence of immunotherapy and chemo(radio)therapy and biomarkers to the recognized beneficiary population.

AUTHOR CONTRIBUTIONS

Conceptualization: RH, ZQ, and EL. Writing – Original Draft Preparation: RH and ZQ. Writing – Review and Editing: YX and EL. Funding Acquisition: YX and EL. All authors read and approved the final manuscript.

FUNDING

This work was supported by funding from the Guangdong College Students' Scientific and Technological Innovation cultivation special fund subsidy project(pdjhb0195; pdjh2020a0218), Cultivation of Guangdong College Students' Scientific and Technological Innovation ('Climbing Program' Special Funds, pdjh2019a0182), the National Undergraduate Training Program for Innovation and Entrepreneurship (201810560037), 'Young Physician Scientist Cultivation' Program of Shantou University Medical College-Li Ka Shing Foundation, 2017-2020 (SMLYPSC-01), and the National Natural Science Foundation of China (21907063).

SUPPLEMENTARY MATERIAL

The Supplementary Material for this article can be found online at: https://www.frontiersin.org/articles/10.3389/fonc.2022.734581/full#supplementary-material

REFERENCES

1. Sung H, Ferlay J, Siegel RL, Laversanne M, Soerjomataram I, Jemal A, et al. Global Cancer Statistics 2020: GLOBOCAN Estimates of Incidence and Mortality Worldwide for 36 Cancers in 185 Countries. *CA Cancer J Clin* (2021) 71(3):209–49. doi: 10.3322/caac.21660
2. Ando N, Kato H, Igaki H, Shinoda M, Ozawa S, Shimizu H, et al. A Randomized Trial Comparing Postoperative Adjuvant Chemotherapy With Cisplatin and 5-Fluorouracil Versus Preoperative Chemotherapy for Localized Advanced Squamous Cell Carcinoma of the Thoracic Esophagus (JCOG9907). *Ann Surg Oncol* (2012) 19(1):68–74. doi: 10.1245/s10434-011-2049-9
3. van Hagen P, Hulshof MC, van Lanschot JJ, Steyerberg EW, van Berge Henegouwen MI, Wijnhoven BP, et al. Preoperative Chemoradiotherapy for Esophageal or Junctional Cancer. *N Engl J Med* (2012) 366(22):2074–84. doi: 10.1056/NEJMoa1112088
4. Yang H, Liu H, Chen Y, Zhu C, Fang W, Yu Z, et al. Neoadjuvant Chemoradiotherapy Followed by Surgery Versus Surgery Alone for Locally Advanced Squamous Cell Carcinoma of the Esophagus (NEOCRTEC5010): A Phase III Multicenter, Randomized, Open-Label Clinical Trial. *J Clin Oncol* (2018) 36(27):2796–803. doi: 10.1200/JCO.2018.79.1483
5. Kelsen DP, Ginsberg R, Pajak TF, Sheahan DG, Gunderson L, Mortimer J, et al. Chemotherapy Followed by Surgery Compared With Surgery Alone for Localized Esophageal Cancer. *N Engl J Med* (1998) 339(27):1979–84. doi: 10.1056/NEJM199812313392704
6. Medical Research Council Oesophageal Cancer Working G. Surgical Resection With or Without Preoperative Chemotherapy in Oesophageal Cancer: A Randomised Controlled Trial. *Lancet* (2002) 359(9319):1727–33. doi: 10.1016/S0140-6736(02)08651-8
7. Allum WH, Stenning SP, Bancewicz J, Clark PI, Langley RE. Long-Term Results of a Randomized Trial of Surgery With or Without Preoperative Chemotherapy in Esophageal Cancer. *J Clin Oncol* (2009) 27(30):5062–7. doi: 10.1200/JCO.2009.22.2083
8. Cunningham D, Allum WH, Stenning SP, Thompson JN, Van de Velde CJ, Nicolson M, et al. Perioperative Chemotherapy Versus Surgery Alone for Resectable Gastroesophageal Cancer. *N Engl J Med* (2006) 355(1):11–20. doi: 10.1056/NEJMoa055531
9. Ychou M, Boige V, Pignon JP, Conroy T, Bouche O, Lebreton G, et al. Perioperative Chemotherapy Compared With Surgery Alone for Resectable Gastroesophageal Adenocarcinoma: An FNCLCC and FFCD Multicenter Phase III Trial. *J Clin Oncol* (2011) 29(13):1715–21. doi: 10.1200/JCO.2010.33.0597
10. Al-Batran SE, Hofheinz RD, Pauligk C, Kopp HG, Haag GM, Luley KB, et al. Histopathological Regression After Neoadjuvant Docetaxel, Oxaliplatin, Fluorouracil, and Leucovorin Versus Epirubicin, Cisplatin, and Fluorouracil or Capecitabine in Patients With Resectable Gastric or Gastro-Oesophageal Junction Adenocarcinoma (FLOT4-AIO): Results From the Phase 2 Part of a Multicentre, Open-Label, Randomised Phase 2/3 Trial. *Lancet Oncol* (2016) 17(12):1697–708. doi: 10.1016/S1470-2045(16)30531-9
11. Al-Batran SE, Homann N, Pauligk C, Goetze TO, Meiler J, Kasper S, et al. Perioperative Chemotherapy With Fluorouracil Plus Leucovorin, Oxaliplatin, and Docetaxel Versus Fluorouracil or Capecitabine Plus Cisplatin and Epirubicin for Locally Advanced, Resectable Gastric or Gastro-Oesophageal Junction Adenocarcinoma (FLOT4): A Randomised, Phase 2/3 Trial. *Lancet* (2019) 393(10184):1948–57. doi: 10.1016/S0140-6736(18)32557-1
12. Hara H, Tahara M, Daiko H, Kato K, Igaki H, Kadowaki S, et al. Phase II Feasibility Study of Preoperative Chemotherapy With Docetaxel, Cisplatin, and Fluorouracil for Esophageal Squamous Cell Carcinoma. *Cancer Sci* (2013) 104(11):1455–60. doi: 10.1111/cas.12274
13. Yamashita K, Hosoda K, Moriya H, Katada C, Sugawara M, Mieno H, et al. Prognostic Advantage of Docetaxel/Cisplatin/ 5-Fluorouracil Neoadjuvant Chemotherapy in Clinical Stage II/III Esophageal Squamous Cell Carcinoma Due to Excellent Control of Preoperative Disease and Postoperative Lymph Node Recurrence. *Oncology* (2017) 92(4):221–8. doi: 10.1159/000455128
14. Akiyama Y, Iwaya T, Endo F, Chiba T, Takahara T, Otsuka K, et al. Investigation of Operative Outcomes of Thoracoscopic Esophagectomy After Triplet Chemotherapy With Docetaxel, Cisplatin, and 5-Fluorouracil for Advanced Esophageal Squamous Cell Carcinoma. *Surg Endosc* (2018) 32 (1):391–9. doi: 10.1007/s00464-017-5688-5
15. Nomura M, Oze I, Abe T, Komori A, Narita Y, Masuishi T, et al. Impact of Docetaxel in Addition to Cisplatin and Fluorouracil as Neoadjuvant Treatment for Resectable Stage III or T3 Esophageal Cancer: A Propensity Score-Matched Analysis. *Cancer Chemother Pharmacol* (2015) 76(2):357–63. doi: 10.1007/s00280-015-2806-8
16. Kato K, Ito Y, Daiko H, Ozawa S, Ogata T, Hara H, et al. A Randomized Controlled Phase III Trial Comparing Two Chemotherapy Regimen and Chemoradiotherapy Regimen as Neoadjuvant Treatment for Locally Advanced Esophageal Cancer, JCOG1109 NExT Study. *J Clin Oncol* (2022) 40(4_suppl):238–. doi: 10.1200/JCO.2022.40.4_suppl.238
17. Shiraishi O, Yamasaki M, Makino T, Motoori M, Miyata H, Shinkai M, et al. Feasibility of Preoperative Chemotherapy With Docetaxel, Cisplatin, and 5-Fluorouracil Versus Adriamycin, Cisplatin, and 5-Fluorouracil for Resectable Advanced Esophageal Cancer. *Oncology* (2017) 92(2):101–8. doi: 10.1159/000452765

18. Hosoda K, Azuma M, Katada C, Ishido K, Niihara M, Ushiku H, et al. A Phase I Study of Docetaxel/Oxaliplatin/S-1 (DOS) Combination Neoadjuvant Chemotherapy for Patients With Locally Advanced Adenocarcinoma of the Esophagogastric Junction. *Int J Clin Oncol* (2020) 25(6):1090–7. doi: 10.1007/s10147-020-01638-5
19. Hayata K, Ojima T, Nakamori M, Nakamura M, Katsuda M, Kitadani J, et al. Neoadjuvant Chemotherapy With Docetaxel, Cisplatin and S-1 for Resectable Advanced Esophageal Cancer. *Anticancer Res* (2018) 38(9):5267–73. doi: 10.21873/anticanres.12852
20. Ohnuma H, Sato Y, Hayasaka N, Matsuno T, Fujita C, Sato M, et al. Neoadjuvant Chemotherapy With Docetaxel, Nedaplatin, and Fluorouracil for Resectable Esophageal Cancer: A Phase II Study. *Cancer Sci* (2018) 109 (11):3554–63. doi: 10.1111/cas.13772
21. Alderson D, Cunningham D, Nankivell M, Blazeby JM, Griffin SM, Crellin A, et al. Neoadjuvant Cisplatin and Fluorouracil Versus Epirubicin, Cisplatin, and Capecitabine Followed by Resection in Patients With Oesophageal Adenocarcinoma (UK MRC OE05): An Open-Label, Randomised Phase 3 Trial. *Lancet Oncol* (2017) 18(9):1249–60. doi: 10.1016/S1470-2045(17)30447-3
22. Tanaka Y, Yoshida K, Tanahashi T, Okumura N, Matsuhashi N, Yamaguchi K. Phase II Trial of Neoadjuvant Chemotherapy With Docetaxel, Nedaplatin, and S1 for Advanced Esophageal Squamous Cell Carcinoma. *Cancer Sci* (2016) 107(6):764–72. doi: 10.1111/cas.12943
23. Walsh TN, Noonan N, Hollywood D, Kelly A, Keeling N, Hennessy TP. A Comparison of Multimodal Therapy and Surgery for Esophageal Adenocarcinoma. *N Engl J Med* (1996) 335(7):462–7. doi: 10.1056/NEJM199608153350702
24. Bosset JF, Gignoux M, Triboulet JP, Tiret E, Mantion G, Elias D, et al. Chemoradiotherapy Followed by Surgery Compared With Surgery Alone in Squamous-Cell Cancer of the Esophagus. *N Engl J Med* (1997) 337(3):161–7. doi: 10.1056/NEJM199707173370304
25. Burmeister BH, Smithers BM, Gebski V, Fitzgerald L, Simes RJ, Devitt P, et al. Surgery Alone Versus Chemoradiotherapy Followed by Surgery for Resectable Cancer of the Oesophagus: A Randomised Controlled Phase III Trial. *Lancet Oncol* (2005) 6(9):659–68. doi: 10.1016/S1470-2045(05)70288-6
26. Tepper J, Krasna MJ, Niedzwiecki D, Hollis D, Reed CE, Goldberg R, et al. Phase III Trial of Trimodality Therapy With Cisplatin, Fluorouracil, Radiotherapy, and Surgery Compared With Surgery Alone for Esophageal Cancer: CALGB 9781. *J Clin Oncol* (2008) 26(7):1086–92. doi: 10.1200/JCO.2007.12.9593
27. Shapiro J, van Lanschot JJB, Hulshof M, van Hagen P, van Berge Henegouwen MI, Wijnhoven BPL, et al. Neoadjuvant Chemoradiotherapy Plus Surgery Versus Surgery Alone for Oesophageal or Junctional Cancer (CROSS): Long-Term Results of a Randomised Controlled Trial. *Lancet Oncol* (2015) 16 (9):1090–8. doi: 10.1016/S1470-2045(15)00040-6
28. Eyck BM, van Lanschot JJB, Hulshof M, van der Wilk BJ, Shapiro J, van Hagen P, et al. Ten-Year Outcome of Neoadjuvant Chemoradiotherapy Plus Surgery for Esophageal Cancer: The Randomized Controlled CROSS Trial. *J Clin Oncol* (2021) 39(18):1995–2004. doi: 10.1200/JCO.20.03614
29. Stahl M, Walz MK, Stuschke M, Lehmann N, Meyer HJ, Riera-Knorrenschild J, et al. Phase III Comparison of Preoperative Chemotherapy Compared With Chemoradiotherapy in Patients With Locally Advanced Adenocarcinoma of the Esophagogastric Junction. *J Clin Oncol* (2009) 27(6):851–6. doi: 10.1200/JCO.2008.17.0506
30. Stahl M, Walz MK, Riera-Knorrenschild J, Stuschke M, Sandermann A, Bitzer M, et al. Preoperative Chemotherapy Versus Chemoradiotherapy in Locally Advanced Adenocarcinomas of the Oesophagogastric Junction (POET): Long-Term Results of a Controlled Randomised Trial. *Eur J Cancer* (2017) 81:183–90. doi: 10.1016/j.ejca.2017.04.027
31. Klevebro F, Alexandersson von Dobeln G, Wang N, Johnsen G, Jacobsen AB, Friesland S, et al. A Randomized Clinical Trial of Neoadjuvant Chemotherapy Versus Neoadjuvant Chemoradiotherapy for Cancer of the Oesophagus or Gastro-Oesophageal Junction. *Ann Oncol* (2016) 27(4):660–7. doi: 10.1093/annonc/mdw010
32. von Dobeln GA, Klevebro F, Jacobsen AB, Johannessen HO, Nielsen NH, Johnsen G, et al. Neoadjuvant Chemotherapy Versus Neoadjuvant Chemoradiotherapy for Cancer of the Esophagus or Gastroesophageal Junction: Long-Term Results of a Randomized Clinical Trial. *Dis Esophagus* (2019) 32(2):1–11. doi: 10.1093/dote/doy078
33. Burmeister BH, Thomas JM, Burmeister EA, Walpole ET, Harvey JA, Thomson DB, et al. Is Concurrent Radiation Therapy Required in Patients Receiving Preoperative Chemotherapy for Adenocarcinoma of the Oesophagus? A Randomised Phase II Trial. *Eur J Cancer* (2011) 47(3):354–60. doi: 10.1016/j.ejca.2010.09.009
34. Wang H, Tang H, Fang Y, Tan L, Yin J, Shen Y, et al. Morbidity and Mortality of Patients Who Underwent Minimally Invasive Esophagectomy After Neoadjuvant Chemoradiotherapy vs Neoadjuvant Chemotherapy for Locally Advanced Esophageal Squamous Cell Carcinoma: A Randomized Clinical Trial. *JAMA Surg* (2021) 156(5):444–51. doi: 10.1001/jamasurg.2021.0133
35. Yuan M, Bao Y, Ma Z, Men Y, Wang Y, Hui Z. The Optimal Treatment for Resectable Esophageal Cancer: A Network Meta-Analysis of 6168 Patients. *Front Oncol* (2021) 11:628706. doi: 10.3389/fonc.2021.628706
36. Chan KKW, Saluja R, Delos Santos K, Lien K, Shah K, Cramarossa G, et al. Neoadjuvant Treatments for Locally Advanced, Resectable Esophageal Cancer: A Network Meta-Analysis. *Int J Cancer* (2018) 143(2):430–7. doi: 10.1002/ijc.31312
37. Lu Z, Fang Y, Liu C, Zhang X, Xin X, He Y, et al. Early Interdisciplinary Supportive Care in Patients With Previously Untreated Metastatic Esophagogastric Cancer: A Phase III Randomized Controlled Trial. *J Clin Oncol* (2021) 39(7):748–56. doi: 10.1200/JCO.20.01254
38. Shirakawa Y, Noma K, Maeda N, Tanabe S, Sakurama K, Sonoyama-Hanaoka A, et al. Early Intervention of the Perioperative Multidisciplinary Team Approach Decreases the Adverse Events During Neoadjuvant Chemotherapy for Esophageal Cancer Patients. *Esophagus* (2021) 18 (4):797–805. doi: 10.1007/s10388-021-00844-y
39. Gottlieb-Vedi E, Kauppila JH, Mattsson F, Lindblad M, Nilsson M, Lagergren P, et al. Long-Term Survival in Esophageal Cancer After Minimally Invasive Esophagectomy Compared to Open Esophagectomy. *Ann Surg* (2021). doi: 10.1097/SLA.0000000000004645
40. Wang HH, de Heer EC, Hulshoff JB, Kats-Ugurlu G, Burgerhof JGM, van Etten B, et al. Effect of Extending the Original CROSS Criteria on Tumor Response to Neoadjuvant Chemoradiotherapy in Esophageal Cancer Patients: A National Multicenter Cohort Analysis. *Ann Surg Oncol* (2021) 28(7):3951–60. doi: 10.1245/s10434-020-09372-y
41. Wong IYH, Lam KO, Chan W, Wong C, So TH, Chan KK, et al. Real-World Scenario: CROSS Regimen as Preoperative Therapy for Oesophageal Squamous Cell Carcinoma. *J Gastrointest Surg* (2020) 24(9):1937–47. doi: 10.1007/s11605-020-04704-5
42. Toxopeus E, van der Schaaf M, van Lanschot J, Lagergren J, Lagergren P, van der Gaast A, et al. Outcome of Patients Treated Within and Outside a Randomized Clinical Trial on Neoadjuvant Chemoradiotherapy Plus Surgery for Esophageal Cancer: Extrapolation of a Randomized Clinical Trial (CROSS). *Ann Surg Oncol* (2018) 25(8):2441–8. doi: 10.1245/s10434-018-6554-y
43. de Heer EC, Hulshoff JB, Klerk D, Burgerhof JGM, de Groot DJA, Plukker JTM, et al. Effect of Extending the Original Eligibility Criteria for the CROSS Neoadjuvant Chemoradiotherapy on Toxicity and Survival in Esophageal Cancer. *Ann Surg Oncol* (2017) 24(7):1811–20. doi: 10.1245/s10434-017-5797-3
44. Wong IYH, Lam KO, Zhang RQ, Chan WWL, Wong CLY, Chan FSY, et al. Neoadjuvant Chemoradiotherapy Using Cisplatin and 5-Fluorouracil (PF) Versus Carboplatin and Paclitaxel (CROSS Regimen) for Esophageal Squamous Cell Carcinoma (ESCC): A Propensity Score-Matched Study. *Ann Surg* (2020) 272(5):779–85. doi: 10.1097/SLA.0000000000004329
45. Haisley KR, Hart KD, Nabavizadeh N, Bensch KG, Vaccaro GM, Thomas CRJr., et al. Neoadjuvant Chemoradiotherapy With Concurrent Cisplatin/5-Fluorouracil is Associated With Increased Pathologic Complete Response and Improved Survival Compared to Carboplatin/Paclitaxel in Patients With Locally Advanced Esophageal Cancer. *Dis Esophagus* (2017) 30(7):1–7. doi: 10.1093/dote/dox015
46. Liu SL, Yang H, Zhang P, Zhang L, Zhao L, Luo LL, et al. Neoadjuvant Chemoradiotherapy With Cisplatin Plus Vinorelbine Versus Cisplatin Plus Fluorouracil for Esophageal Squamous Cell Carcinoma: A Matched Case-Control Study. *Radiother Oncol* (2015) 116(2):262–8. doi: 10.1016/j.radonc.2015.07.020

47. Yang Y, Xu X, Zhou X, Bao W, Zhang D, Gu F, et al. Impact of Radiation Dose on Survival for Esophageal Squamous Cell Carcinoma Treated With Neoadjuvant Chemoradiotherapy. *Front Oncol* (2020) 10:1431. doi: 10.3389/fonc.2020.01431
48. Li Y, Liu H, Sun C, Yin X, Tong J, Zhang X, et al. Comparison of Clinical Efficacy of Neoadjuvant Chemoradiation Therapy Between Lower and Higher Radiation Doses for Carcinoma of the Esophagus and Gastroesophageal Junction: A Systematic Review. *Int J Radiat Oncol Biol Phys* (2021) 111 (2):405–16. doi: 10.1016/j.ijrobp.2021.04.031
49. Haisley KR, Laird AE, Nabavizadeh N, Gatter KM, Holland JM, Vaccaro GM, et al. Association of Intervals Between Neoadjuvant Chemoradiation and Surgical Resection With Pathologic Complete Response and Survival in Patients With Esophageal Cancer. *JAMA Surg* (2016) 151(11):e162743. doi: 10.1001/jamasurg.2016.2743
50. Shapiro J, van Hagen P, Lingsma HF, Wijnhoven BP, Biermann K, ten Kate FJ, et al. Prolonged Time to Surgery After Neoadjuvant Chemoradiotherapy Increases Histopathological Response Without Affecting Survival in Patients With Esophageal or Junctional Cancer. *Ann Surg* (2014) 260(5):807–13; discussion 13-4. doi: 10.1097/SLA.0000000000000966
51. Nilsson K, Klevebro F, Rouvelas I, Lindblad M, Szabo E, Halldestam I, et al. Surgical Morbidity and Mortality From the Multicenter Randomized Controlled NeoRes II Trial: Standard Versus Prolonged Time to Surgery After Neoadjuvant Chemoradiotherapy for Esophageal Cancer. *Ann Surg* (2020) 272(5):684–9. doi: 10.1097/SLA.0000000000004340
52. Liu S, Wen J, Yang H, Li Q, Chen Y, Zhu C, et al. Recurrence Patterns After Neoadjuvant Chemoradiotherapy Compared With Surgery Alone in Oesophageal Squamous Cell Carcinoma: Results From the Multicenter Phase III Trial NEOCRTEC5010. *Eur J Cancer* (2020) 138:113–21. doi: 10.1016/j.ejca.2020.08.002
53. Xi M, Yang Y, Zhang L, Yang H, Merrell KW, Hallemeier CL, et al. Multi-Institutional Analysis of Recurrence and Survival After Neoadjuvant Chemoradiotherapy of Esophageal Cancer: Impact of Histology on Recurrence Patterns and Outcomes. *Ann Surg* (2019) 269(4):663–70. doi: 10.1097/SLA.0000000000002670
54. Kelly RJ, Ajani JA, Kuzdzal J, Zander T, Van Cutsem E, Piessen G, et al. Adjuvant Nivolumab in Resected Esophageal or Gastroesophageal Junction Cancer. *N Engl J Med* (2021) 384(13):1191–203. doi: 10.1056/NEJMoa2032125
55. Guo X, Wang Z, Yang H, Mao T, Chen Y, Zhu C, et al. Impact of Lymph Node Disscinoma: From the Results of NEOCRTEC5010, a Randomized Multicenter Study. *Ann Surg* (2021). doi: 10.1097/SLA.0000000000004798
56. Eyck BM, Onstenk BD, Noordman BJ, Nieboer D, Spaander MCW, Valkema R, et al. Accuracy of Detecting Residual Disease After Neoadjuvant Chemoradiotherapy for Esophageal Cancer: A Systematic Review and Meta-Analysis. *Ann Surg* (2020) 271(2):245–56. doi: 10.1097/SLA.0000000000003397
57. van Rossum PS, van Lier AL, van Vulpen M, Reerink O, Lagendijk JJ, Lin SH, et al. Diffusion-Weighted Magnetic Resonance Imaging for the Prediction of Pathologic Response to Neoadjuvant Chemoradiotherapy in Esophageal Cancer. *Radiother Oncol* (2015) 115(2):163–70. doi: 10.1016/j.radonc.2015.04.027
58. Heethuis SE, van Rossum PS, Lips IM, Goense L, Voncken FE, Reerink O, et al. Dynamic Contrast-Enhanced MRI for Treatment Response Assessment in Patients With Oesophageal Cancer Receiving Neoadjuvant Chemoradiotherapy. *Radiother Oncol* (2016) 120(1):128–35. doi: 10.1016/j.radonc.2016.05.009
59. Heethuis SE, Goense L, van Rossum PSN, Borggreve AS, Mook S, Voncken FEM, et al. DW-MRI and DCE-MRI are of Complementary Value in Predicting Pathologic Response to Neoadjuvant Chemoradiotherapy for Esophageal Cancer. *Acta Oncol* (2018) 57(9):1201–8. doi: 10.1080/0284186X.2018.1473637
60. Vollenbrock SE, van Dieren JM, Voncken FEM, van Turenhout ST, Kodach LL, Hartemink KJ, et al. Added Value of MRI to Endoscopic and Endosonographic Response Assessment After Neoadjuvant Chemoradiotherapy in Oesophageal Cancer. *Eur Radiol* (2020) 30(5):2425–34. doi: 10.1007/s00330-019-06605-x
61. Borggreve AS, Goense L, van Rossum PSN, Heethuis SE, van Hillegersberg R, Lagendijk JJW, et al. Preoperative Prediction of Pathologic Response to Neoadjuvant Chemoradiotherapy in Patients With Esophageal Cancer Using (18)F-FDG PET/CT and DW-MRI: A Prospective Multicenter Study. *Int J Radiat Oncol Biol Phys* (2020) 106(5):998–1009. doi: 10.1016/j.ijrobp.2019.12.038
62. Noordman BJ, Spaander MCW, Valkema R, Wijnhoven BPL, van Berge Henegouwen MI, Shapiro J, et al. Detection of Residual Disease After Neoadjuvant Chemoradiotherapy for Oesophageal Cancer (preSANO): A Prospective Multicentre, Diagnostic Cohort Study. *Lancet Oncol* (2018) 19 (7):965–74. doi: 10.1016/S1470-2045(18)30201-8
63. Zhang SS, Huang QY, Yang H, Xie X, Luo KJ, Wen J, et al. Correlation of P53 Status With the Response to Chemotherapy-Based Treatment in Esophageal Cancer: A Meta-Analysis. *Ann Surg Oncol* (2013) 20(7):2419–27. doi: 10.1245/s10434-012-2859-4
64. Li Y, Huang HC, Chen LQ, Xu LY, Li EM, Zhang JJ. Predictive Biomarkers for Response of Esophageal Cancer to Chemo(Radio)Therapy: A Systematic Review and Meta-Analysis. *Surg Oncol* (2017) 26(4):460–72. doi: 10.1016/j.suronc.2017.09.003
65. Ruhstaller T, Thuss-Patience P, Hayoz S, Schacher S, Knorrenschild JR, Schnider A, et al. Neoadjuvant Chemotherapy Followed by Chemoradiation and Surgery With and Without Cetuximab in Patients With Resectable Esophageal Cancer: A Randomized, Open-Label, Phase III Trial (SAKK 75/08). *Ann Oncol* (2018) 29(6):1386–93. doi: 10.1093/annonc/mdy105
66. Cunningham D, Stenning SP, Smyth EC, Okines AF, Allum WH, Rowley S, et al. Peri-Operative Chemotherapy With or Without Bevacizumab in Operable Oesophagogastric Adenocarcinoma (UK Medical Research Council ST03): Primary Analysis Results of a Multicentre, Open-Label, Randomised Phase 2-3 Trial. *Lancet Oncol* (2017) 18(3):357–70. doi: 10.1016/S1470-2045(17)30043-8
67. Kojima T, Shah MA, Muro K, Francois E, Adenis A, Hsu CH, et al. Randomized Phase III KEYNOTE-181 Study of Pembrolizumab Versus Chemotherapy in Advanced Esophageal Cancer. *J Clin Oncol* (2020) 38 (35):4138–48. doi: 10.1200/JCO.20.01888
68. Kato K, Cho BC, Takahashi M, Okada M, Lin CY, Chin K, et al. Nivolumab Versus Chemotherapy in Patients With Advanced Oesophageal Squamous Cell Carcinoma Refractory or Intolerant to Previous Chemotherapy (ATTRACTION-3): A Multicentre, Randomised, Open-Label, Phase 3 Trial. *Lancet Oncol* (2019) 20(11):1506–17. doi: 10.1016/S1470-2045(19)30626-6
69. Huang J, Xu J, Chen Y, Zhuang W, Zhang Y, Chen Z, et al. Camrelizumab Versus Investigator's Choice of Chemotherapy as Second-Line Therapy for Advanced or Metastatic Oesophageal Squamous Cell Carcinoma (ESCORT): A Multicentre, Randomised, Open-Label, Phase 3 Study. *Lancet Oncol* (2020) 21(6):832–42. doi: 10.1016/S1470-2045(20)30110-8
70. Kato K, Sun JM, Shah MA, Enzinger PC, Adenis A, Doi T, et al. LBA8_PR Pembrolizumab Plus Chemotherapy Versus Chemotherapy as First-Line Therapy in Patients With Advanced Esophageal Cancer: The Phase 3 KEYNOTE-590 Study. *Ann Oncol* (2020) 31:S1192–S3. doi: 10.1016/j.annonc.2020.08.2298
71. Janjigian YY, Shitara K, Moehler M, Garrido M, Salman P, Shen L, et al. First-Line Nivolumab Plus Chemotherapy Versus Chemotherapy Alone for Advanced Gastric, Gastro-Oesophageal Junction, and Oesophageal Adenocarcinoma (CheckMate 649): A Randomised, Open-Label, Phase 3 Trial. *Lancet* (2021) 398(10294):27–40. doi: 10.1016/S0140-6736(21)00797-2
72. Xu R-h, Luo H, Lu J, Bai Y, Mao T, Wang J, et al. ESCORT-1st: A Randomized, Double-Blind, Placebo-Controlled, Phase 3 Trial of Camrelizumab Plus Chemotherapy Versus Chemotherapy in Patients With Untreated Advanced or Metastatic Esophageal Squamous Cell Carcinoma (ESCC). *J Clin Oncol* (2021) 39(15_suppl):4000–. doi: 10.1200/JCO.2021.39.15_suppl.4000
73. Kelly RJ, Smith KN, Anagnostou V, Thompson E, Hales RK, Battafarano RJJ, et al. Neoadjuvant Nivolumab Plus Concurrent Chemoradiation in Stage II/III Esophageal/Gastroesophageal Junction Cancer. *J Clin Oncol* (2019) 37 (4_suppl):142–. doi: 10.1200/JCO.2019.37.4_suppl.142
74. Hong MH, Kim H, Park SY, Kim DJ, Lee CG, Cho J, et al. A Phase II Trial of Preoperative Chemoradiotherapy and Pembrolizumab for Locally Advanced Esophageal Squamous Cell Carcinoma (ESCC). *J Clin Oncol* (2019) 37 (15_suppl):4027–. doi: 10.1200/JCO.2019.37.15_suppl.4027
75. Li C, Zhao S, Zheng Y, Han Y, Chen X, Cheng Z, et al. Preoperative Pembrolizumab Combined With Chemoradiotherapy for Oesophageal Squamous Cell Carcinoma (PALACE-1). *Eur J Cancer* (2021) 144:232–41. doi: 10.1016/j.ejca.2020.11.039

76. tEnde T, Clercq N, Henegouwen M, Gisbertz SS, Meijer SL, Schokker S, et al. A Phase II Feasibility Trial of Neoadjuvant Chemoradiotherapy Combined With Atezolizumab for Resectable Esophageal Adenocarcinoma: The PERFECT Trial. *J Clin Oncol* (2019) 37(15_suppl):4045–. doi: 10.1200/JCO.2019.37.15_suppl.4045
77. Galluzzi L, Buque A, Kepp O, Zitvogel L, Kroemer G. Immunological Effects of Conventional Chemotherapy and Targeted Anticancer Agents. *Cancer Cell* (2015) 28(6):690–714. doi: 10.1016/j.ccell.2015.10.012
78. Zhao L, Xing W, Yang Y, Zhang Y, Ma B, Fu X, et al. The Sequence of Chemotherapy and Anti-PD-1 Antibody Influence the Efficacy of Neoadjuvant Immunochemotherapy in Locally Advanced Esophageal Squamous Cell Cancer: A Phase II Study. *J Clin Oncol* (2021) 39 (15_suppl):4051–. doi: 10.1200/JCO.2021.39.15_suppl.4051
79. Sjoquist KM, Burmeister BH, Smithers BM, Zalcberg JR, Simes RJ, Barbour A, et al. Survival After Neoadjuvant Chemotherapy or Chemoradiotherapy for Resectable Oesophageal Carcinoma: An Updated Meta-Analysis. *Lancet Oncol* (2011) 12(7):681–92. doi: 10.1016/S1470-2045(11)70142-5

Conflict of Interest: The authors declare that the research was conducted in the absence of any commercial or financial relationships that could be construed as a potential conflict of interest.

GLOSSARY

HR	hazard ratio
FLOT-AIO, 5-FU	leucovorin, oxaliplatin, and docetaxel (FLOT) versus epirubicin, cisplatin, and 5-FU (ECF) in patients with locally advanced resectable gastric cancer
FLOT	5-fluorouracil, leucovorin, oxaliplatin, docetaxel
mOS	median overall survival
mDFS	median disease-free survival
ESCC	esophageal squamous carcinoma
OS	overall survival
JCOG9907 trial	the Japan Clinical Oncology Group 9907 trial
CF	cisplatin/5-fluorouracil
pCR	pathological complete response
DCF	docetaxel, cisplatin, 5-FU
PFS	progression-free survival
JCOG1109 NExT trial	the Japan Clinical Oncology Group NexT trial
ASCO-GI	American Society of Clinical Oncology Gastrointestinal Cancers Symposium
CROSS trial	the ChemoRadiotherapy for Oesophageal cancer followed by Surgery Study trial
NEOCRTEC5010	Phase III Study of Neo-adjuvant Chemoradiotherapy Foloowed by Surgery for Squamous Cell Esophageal Cancer
mPFS	median progression-free survival
DFS	disease-free survival
OR	odd ratios
ESC	interdisciplinary supportive care
AEs	adverse events
ORR	objective response rate
DoR	duration of response
POET	PreOperative therapy in Esophagogastric adenocarcinoma
NeoRes	Neoadjuvant Chemotherapy Versus Radiochemotherapy for Cancer of the Esophagus or Cardia
CMISG1701	Comparison Between NCRT and NCT Followed by MIE for Treatment of Locally Advanced Resectable ESCC
MIE	minimally invasive esophagectomy
18F-FDG PET (-CT)	Positron emission tomography with 2-deoxy-2-[fluorine-18] fluoro-D-glucose integrated (with computed tomography)
MRI	magnetic resonance imaging
DW-MRI	Diffusion-weighted magnetic resonance imaging
DCE-MRI	Dynamic contrast-enhanced magnetic resonance imaging
preSANO trial	the Surgery As Needed for Oesophageal Cancer trial
KEYNOTE 181	Study of(MK-3475) Versus Investigator's Choice Standard Therapy for Participants With Advanced Esophageal/ Esophagogastric Junction Carcinoma That Progressed After First-Line Therapy
KEYNOTE 590	First-line Esophageal Carcinoma Study With Chemo cs. Chemo Plus Pembrolizumab
ATTRACTION-3	Study of Nivolumab in Unresectable Advanced or Recurrent Esophageal Cancer
ESCORT	Study of SHR-1210 Versus Investigator's Choice Standard Therapy for Participants With Advanced Esophageal Cancer
ESCORT-1st	Study of SHR-1210 in Combination With Chemotherapy in Advanced Esophagea Cancer
PALACE-1	Preoperative Anti PD-1 Antibody Combined With Chemoradiotherapy for Locally Advanced Squamous Cell Carcinoma of Esophageus
PERFECT	PDL-1 targeting in resectable esophageal cancer
XELOX	capecitabine, oxaliplatin
FOLFOX	leucovorin, fluorouracil, oxaliplatin

Advantages of publishing in Frontiers

OPEN ACCESS
Articles are free to read for greatest visibility and readership

FAST PUBLICATION
Around 90 days from submission to decision

HIGH QUALITY PEER-REVIEW
Rigorous, collaborative, and constructive peer-review

TRANSPARENT PEER-REVIEW
Editors and reviewers acknowledged by name on published articles

Frontiers
Avenue du Tribunal-Fédéral 34
1005 Lausanne | Switzerland

Visit us: www.frontiersin.org
Contact us: frontiersin.org/about/contact

REPRODUCIBILITY OF RESEARCH
Support open data and methods to enhance research reproducibility

DIGITAL PUBLISHING
Articles designed for optimal readership across devices

FOLLOW US
@frontiersin

IMPACT METRICS
Advanced article metrics track visibility across digital media

EXTENSIVE PROMOTION
Marketing and promotion of impactful research

LOOP RESEARCH NETWORK
Our network increases your article's readership